ZooKeys 939: 1–28 (2020)
doi: 10.3897/zookeys.939.52071
https://zookeys.pensoft.net

RESEARCH ARTICLE

A peer-reviewed open-access journal
ZooKeys
Launched to accelerate biodiversity research

Walaphyllium subgen. nov., the dancing leaf insects from Australia and Papua New Guinea with description of a new species (Phasmatodea, Phylliidae)

Royce T. Cumming[1,2,3], Jessa H. Thurman[4], Sam Youngdale[5], Stephane Le Tirant[6]

1 *Associate researcher, Montréal Insectarium, 4581 rue Sherbrooke, Montreal, Quebec, H1X 2B2, Canada* **2** *PhD Student, Richard Gilder Graduate School, American Museum of Natural History, New York, NY 10024, USA* **3** *PhD Student, City University New York, Graduate Center, Ecology and Evolutionary Biology subprogram, New York, NY, USA* **4** *PhD Student, School of Biological Sciences, University of Queensland, St Lucia, Queensland, Australia* **5** *Los Angeles, California, USA* **6** *Collection manager, Montréal Insectarium, 4581 rue Sherbrooke, Montreal, Quebec, H1X 2B2, Canada*

Corresponding author: Royce T. Cumming (phylliidae.walkingleaf@gmail.com)

Academic editor: M. Gottardo | Received 14 March 2020 | Accepted 7 April 2020 | Published 9 June 2020

http://zoobank.org/D10A5E1A-4977-41F9-9D40-7EA6930EA496

Citation: Cumming RT, Thurman JH, Youngdale S, Tirant SL (2020) *Walaphyllium* subgen. nov., the dancing leaf insects from Australia and Papua New Guinea with description of a new species (Phasmatodea, Phylliidae). ZooKeys 939: 1–28. https://doi.org/10.3897/zookeys.939.52071

Abstract

A new subgenus, *Walaphyllium* **subgen. nov.,** is described within *Phyllium* Illiger, 1798 to accommodate three leaf insect species. One of the species included is newly described herein as *Phyllium* (*Walaphyllium*) *lelantos* **sp. nov.** from Papua New Guinea. This new subgenus of *Phyllium* can be diagnosed by a following combination of features. This new species is compared to the two additional new subgenus members, *Phyllium zomproi* Größer, 2001 and *Phyllium monteithi* Brock & Hasenpusch, 2003. Also for the first time the male morphology of *Phyllium zomproi* is described and illustrated. To conclude, a brief biogeographical view of the leaf insects on either side of the Torres Strait is presented, as well as a key to species and a distribution map to the known species of *Phyllium* (*Walaphyllium*) **subgen. nov.**

Keywords

Biogeography, Djagubay, entomology, Phasmida, Phylliinae, *Phyllium*, Queensland, taxonomy, walking leaf

Introduction

The leaf insects (Phylliidae) are leaf-mimicking phasmids with flattened abdomens and tibial and/or femoral lobes enlarged to resemble leaves. These adaptations give them incredible camouflage, which allows them to blend in amongst their host plants (Fig. 1). Unfortunately, due to this evolutionary advantageous concealment, specimens are often difficult to locate in their dense jungle habitats and many species of leaf insect are only known from small series or single specimens (Fig. 2). Using the few representatives made available, recent phylogenomic analyses place the Phylliidae as monophyletic within the Old World clade Oriophasmata and sister group to the Bacillidae (Simon et al. 2019).

The Phylliidae in their extant range can be found throughout tropical Asia, from India and China, through to Australia, New Caledonia, and Fiji. Many of these regions where leaf insects are more commonly encountered, such as the Philippines, Indonesia, or India, have had well-known specimen records since the 1700 and 1800's (Brock et al. 2020). In contrast, records from Australia have only been noted within the the last century with the first written account of Phylliidae in Australia by McKeown (1940). McKeown (1940) speculated that this little-known insect could be native or an accidental introduction from elsewhere in their range (at the time of McKeown he only knew of two leaf insect specimens collected in Australia; McKeown, 1940). It would

Figure 1. Live *Phyllium monteithi* bred by Jack Hasenpusch in Australia.

Figure 2. Australia, Queensland, Garradunga, Polly Creek, photo courtesy of Jack Hasenpusch. Lowland mesophyll vine forest, habitat where *Phyllium monteithi* has been recorded.

not be for another 63 years that this species from Australia would gain recognition as an Australian endemic species, *Phyllium monteithi* Brock & Hasenpusch, 2003.

As is often the case, if a phasmid specialist has not spent ample time working within a collection, the Phylliidae specimens within are often misidentified or left with no species-specific identification. This is likely due to the pronounced sexual dimorphism of the leaf insects and the difficulty of collecting specimens because of their natural camouflage. These hindrances often lead to small type series and largely incomplete museum collections, which has historically resulted in the higher taxonomy within the Phylliidae being minimally assessed.

An example of this neglect from in-depth review is the case of the Australian *Phyllium monteithi* which was known for 63 years before it was recognized as a valid and unique species endemic to Australia and not simply *Phyllium siccifolium* as so many specimens have erroneously been called over the years (Brock & Hasenpusch, 2003). Only in recent years have morphological features such as wing venation and egg morphology begun to be extensively reviewed within the Phylliidae (Cumming et al. 2020). Review of these historically ignored features has helped to reveal unique clades, which to date have mostly been concealed when only gross adult morphology is reviewed.

Upon review of the Phylliidae collection within the Natural History Museum United Kingdom, while focusing on wing morphology, an undescribed species of leaf insect from Papua New Guinea was discovered. After reviewing congenerics, we found

that not only was this specimen an undescribed species but that there were two other well-known species which formed a unique clade separate from other *Phyllium* (*Phyllium*). We here transfer these two species (*Phyllium monteithi* Brock & Hasenpusch, 2003 and *Phyllium zomproi* Größer, 2001), from the *siccifolium* group of *Phyllium* (*Phyllium*) as described in Hennemann et al. (2009), and include the herein described *Phyllium lelantos* sp. nov. into their own subgenus *Walaphyllium* subgen. nov. characterized by the characteristics discussed below.

Materials and methods

Photographs of the holotype specimen were taken by René Limoges of the Montreal Insectarium using a Nikon D810 DSLR camera with Nikon Micro-Nikkor 200mm f/4 lens on Manfrotto 454 micrometric positioning sliding plate. Lighting was provided by two Nikon SB-25 flash units with a Cameron Digital diffusion photo box. Adobe Photoshop Elements 13 was used as post processing software. Measurements of the holotype were made to the nearest 0.1 mm using digital calipers. The *Phyllium lelantos* sp. nov. holotype specimen is deposited in the Natural History Museum United Kingdom collection. The holotype specimen was loaned to the Montreal Insectarium by the Natural History Museum United Kingdom with the assistance of Judith Marshall and Benjamin Price.

Scanning electron microscope (SEM) images of female *Phyllium monteithi* antennae were produced using a Hitachi Tabletop Microscope (Model: TM4000) at the Centre for Microscopy and Microanalysis (CMM) of the University of Queensland, Australia. All specimens were sputter coated with silver (SPI Module Sputter Coater with Carbon Module, Structure Probe, Inc., West Chester, PA) and mounted on a circular specimen-stage. The specimen in Figure 10B was cleaned using a potassium hydroxide protocol developed by Schneeberg et al. (2017), and allowed to air-dry for 24hours before sputter coating and imaging. This method unfortunately made the antennae brittle and warped after cleaning. The specimens in Figure 10A and C were not cleaned before sputter coating, resulting in subsequent debris.

Egg orientation terminology follows Clark (1978). Wing venation terminology follows Burt (1932) and Ragge (1955).

Abbreviations

The following institutional abbreviations are used:

ANIC	Australian National Insect Collection, Canberra, Australia.
NHMUK	Natural History Museum Natural History, London, United Kingdom.
QMBA	Queensland Museum, Brisbane, Australia.
QDPC	Queensland Department of Primary Industries, Indooroopilly, Australia.
SDEI	Senckenberg Deutsches Entomologisches Institut, Müncheberg, Germany.
UQIC	University of Queensland, Saint Lucia, Australia.

Coll JHT	Jessa H. Thurman private collection, Australia.
Coll RC	Royce T. Cumming private collection, U.S.A.
Coll SLT	Stéphane Le Tirant private collection, Canada.

The following wing venation abbreviations are used in Figure 5 (listed in order from the anterior to the posterior of the wing):

C	costa	**Cu**	cubitus
Sc	subcosta	**CuA**	cubitus anterior
R	radius	**CuP**	cubitus posterior
R1	first radius	**CuP1**	first cubitus posterior
R2	second radius	**CuP2**	second cubitus posterior
Rs	radial sector	**Cu+1AA**	cubitus fused with first anterior anal
R–M	radius to media crossvein		
M	media	**1AA–7AA**	anterior anal veins one through seven
MA	media anterior		
MP	media posterior	**1PA–5PA**	posterior anal veins one through five
MP1	first media posterior		
MP2	second media posterior	**1A**	first anal
M–Cu	media to cubitus crossvein		

Taxonomy

***Phyllium* (*Walaphyllium*) subgen. nov.**
http://zoobank.org/5416BF7D-0ED2-4825-859D-690662F3FC20

Type species here designated. *Phyllium zomproi* Größer, 2001: 96.

Distribution. This new subgenus is restricted to Papua New Guinea (two species; Fig. 3A, B, E) and Queensland, Australia (one species; Fig. 3C, D) (Distribution map: Fig. 4).

Differentiation. This new subgenus is easily separated from the other *Phyllium* subgenera by the following combination of features: [Male] tegmina media vein with an anterior media vein (MA) and two posterior media veins (MP1 and MP2) (Fig. 5B) and a vomer with a single apical hook (Figs 6D, 8D, 14C); [Female] tegmina venation with the posterior cubitus split into an anterior cubitus (CuA), first posterior cubitus (CuP1), and second posterior cubitus (CuP2) (Fig. 5A), fourth antennal segment about as long as the following segment individually (Figs 7C, 10A), not short disk-like, and adult females lacking developed alae; [Egg] capsule lacking pinnae, instead with a brittle sponge-textured surface and the operculum conically raised (Fig. 11).

Features which characterize this new subgenus, but do not necessarily differentiate it from others are: in males well-developed ocelli (Figs 7B, 9B, 14A); adult abdomen margins parallel (in males) or subparallel (in females) (Fig. 3); tibiae lacking exterior lobes (and only protibial interior lobe developed; Figs 6A, B, 8A, B, 14B); profemoral interior lobe with four to five small serrate teeth in both males and females (Figs 6A, B,

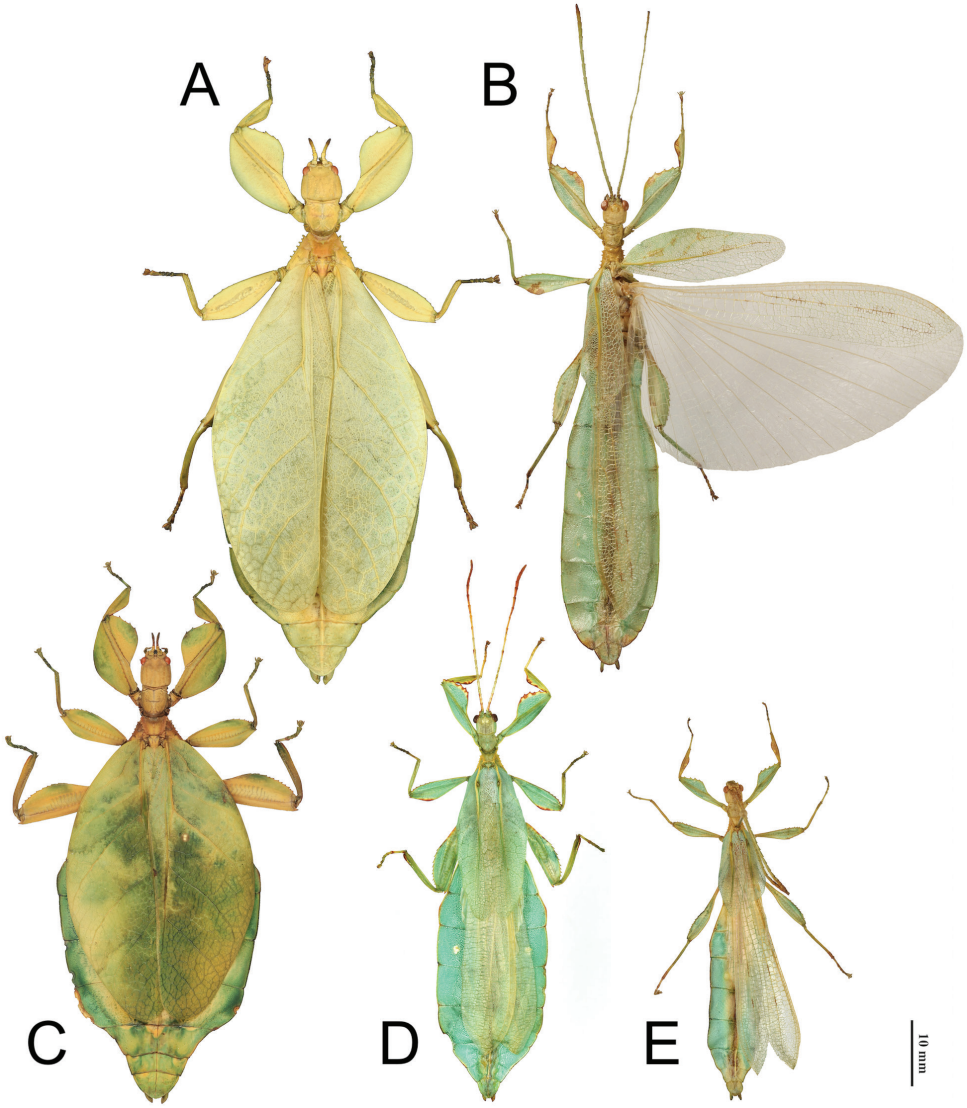

Figure 3. Dorsal view of the known species within the *Phyllium* (*Walaphyllium*), scaled to relative size to show the size differences between species **A** *Phyllium zomproi* female, Coll SLT **B** *Phyllium zomproi* male, Coll RC 17-336 **C** *Phyllium monteithi* female dorsal, Coll RC 16-067 **D** *Phyllium monteithi* male dorsal, Coll SLT **E** *Phyllium lelantos* holotype male, NHMUK. Scale bars: 10 mm.

8A, B, 14B); and mesopleurae with five to seven well developed but not large tubercles which are nearly uniform in size throughout the length of the mesopleurae (Figs 7A, B, 8E, F, 9B, 14A). Comparisons to all the *Phyllium* subgenera can be found in Table 1 to summarize distinctive features.

Of these three species in this new subgenus, only *P. monteithi* has been in the phasmid breeding community to date and therefore this is the only species with the

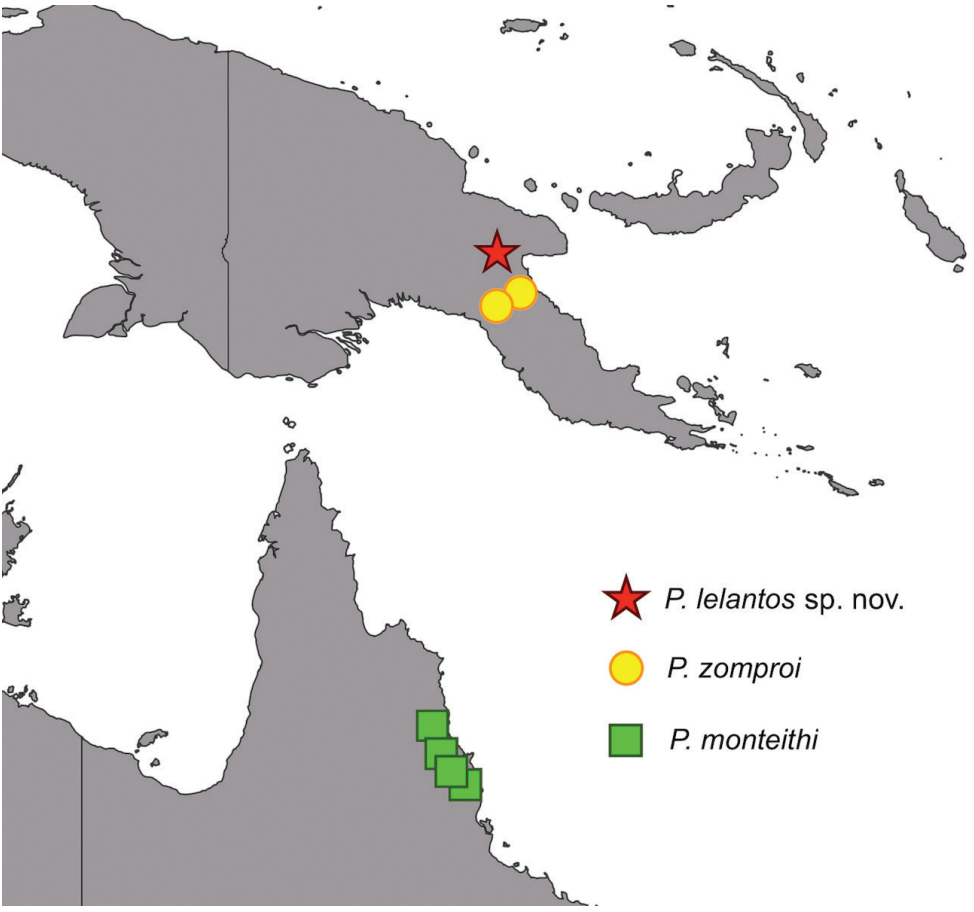

Figure 4. Distribution map for the known species of *Phyllium* (*Walaphyllium*) between Papua New Guinea and Australia.

newly hatched nymph coloration known. Please see the below *P. monteithi* section for a description of the nymph coloration.

Etymology. *Walaphyllium* meaning "Dancing Leaf". This subgeneric epithet is a compound of the Latinized name *Phyllium*, the type genus for the family (from Greek φυλλον, -ου (phyllon, -oy) + -um; Poitout 2007), coupled with the prefix *Wala-* which is derived from the indigenous Australian terms "walawalay" used in the Dyirbal language to describe the shake-a-leg dance (Dixon 1972) and "walayi-y," a verb meaning "to pass by" in the Djagubay language (Patz 1991). Overlapping terms from each of these indigenous languages were investigated as they encompass a large part of the distribution of *Phyllium monteithi*, which is found in the Wet Tropics of far north Queensland, Australia. *Phyllium monteithi* is the most common and well-known species of this new subgenus, thus providing an opportunity to pay respect to the original peoples of this region who may have first appreciated this mysterious insect. This new subgenus is neuter in gender, following *Phyllium*.

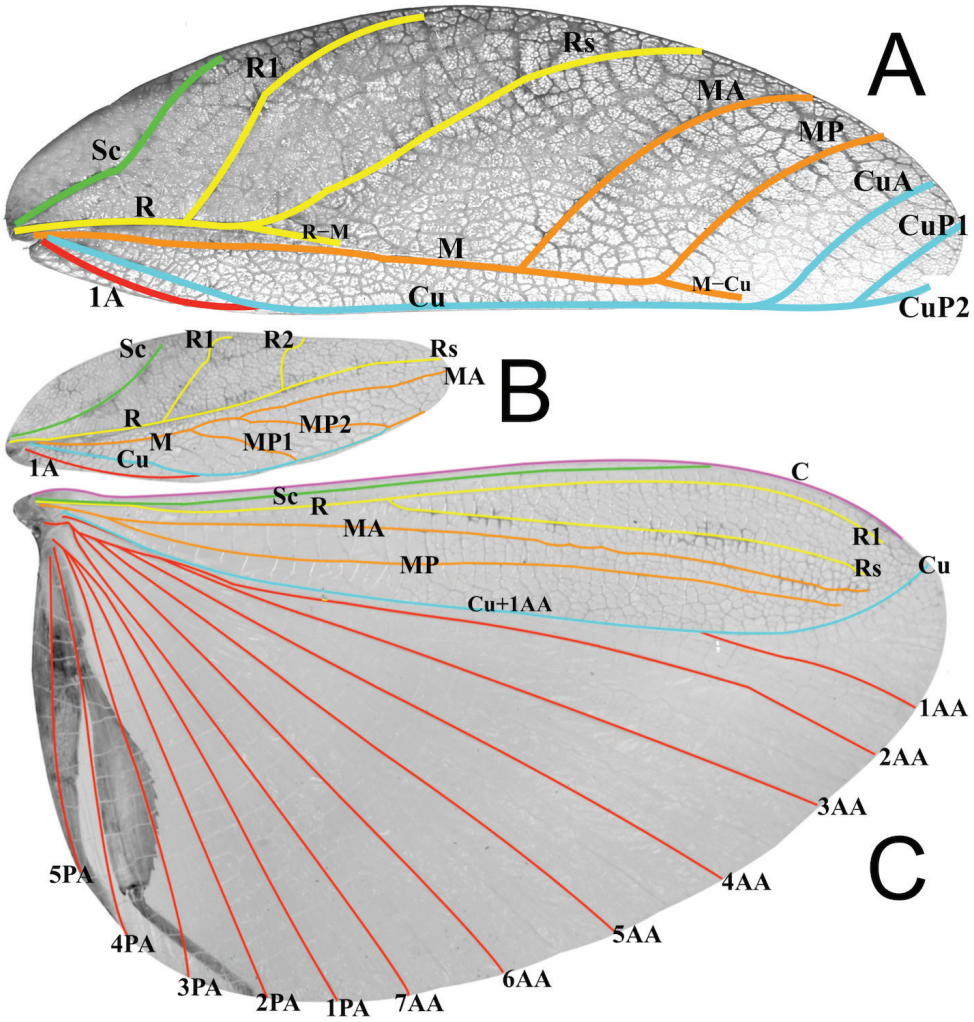

Figure 5. *Phyllium zomproi* wing venation, showing the venation present in the *Phyllium* (*Walaphyllium*) **A** female tegmina, Coll RC 18-175 **B** male tegmina, Coll RC 17-336 **C** male alae, Coll RC 17-336.

Species included.
Phyllium (*Walaphyllium*) *zomproi* Größer, 2001 (Fig. 3A, B)
Phyllium (*Walaphyllium*) *monteithi* Brock & Hasenpusch, 2003 (Fig. 3C, D)
Phyllium (*Walaphyllium*) *lelantos* sp. nov. (Fig. 3E)

Phyllium (*Walaphyllium*) *zomproi* Größer, 2001

Figs 3A, B, 5A–C, 6A–D, 7A–E, 11A–D

Distribution. Papua New Guinea: Morobe Province, Aseki (Winduwe) (NHMUK & Coll RC); Aseki (Wingia) (Holotype: SDEI & Coll RC); Gulf Province (Kaintiba) (Coll RC).

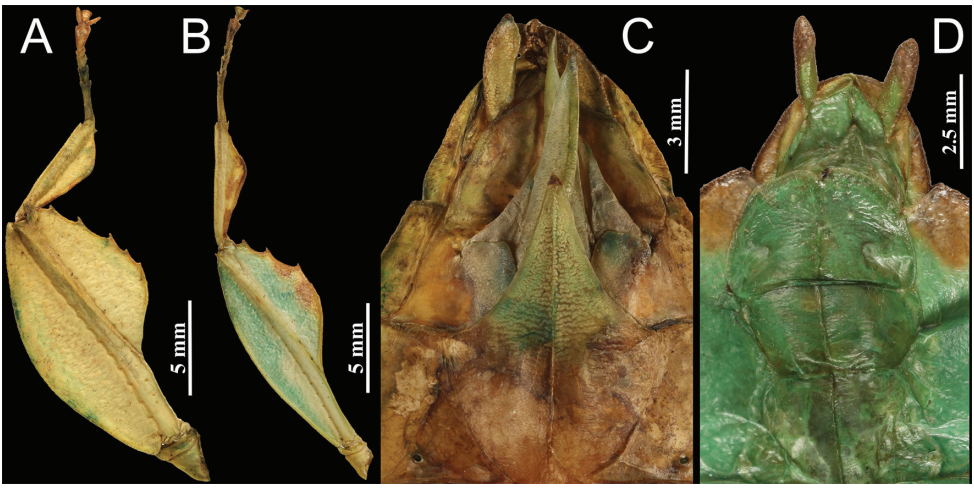

Figure 6. *Phyllium zomproi.* **A** female, profemora and protibia, dorsal, Coll RC 18-277 **B** male, profemora and protibia, dorsal, Coll RC 17-336 **C** female, genitalia, ventral, Coll RC 18-277 **D** male, genitalia, ventral, Coll RC 17-336.

Discussion. Despite being a rarer species in private and museum collections, this is a widespread species, with records from two Papua New Guinea provinces (Morobe and Gulf, Fig. 4). In the original description by Größer (2001) the female and egg were illustrated as well as a subadult male. Since this original description, the adult male has been identified within the NHMUK and within the authors collections. The previously unknown adult male morphology is here described for the first time to help better understand this rarely encountered species.

Body size; females: 80.0–86.0 mm; males: 79.0 mm.

Description. Male. ***Coloration.*** Coloration description based on the limited male specimens from within the authors collections and the NHMUK collection, not on live material. All specimens examined however were with uniform coloration, with little variation between individuals. Overall coloration pale green throughout most of the body. Head through thorax in the preserved specimens is yellow, but this is in all likelihood due to the drying of the specimen and was probably green in life. Compound eyes rusty brown to dark brown color. Antennae pale green or tan, with the terminal segments darker brown. Protibial interior lobe, profemoral interior lobe, and mesofemoral exterior lobe with variable brown patches interrupting the green base color. Tegmina with variable patches of light brown on the green base color, the majority of the tegmina is green. Sclerotized section of the alae can have small patches of brown along the veins, but these are fainter than the brown patches on the tegmina. Abdominal segments V and VI with a small faintly formed clear eyespot of similar width on both the segments. Abdominal segment IX with moderate brown markings on the green, with approximately one third to one half of the segment with brown coloration.

Morphology. *Head.* Head capsule slightly longer than wide, vertex is lumpy with a smooth texture, not overly granular. Frontal convexity stout with a broad point, apex marked with five to seven thin setae. The posteromedial tubercle is not prominent, only

slightly raised from the posterior of the head capsule. *Antennae*. Antennae consist of 22–23 segments (including the scapus and pedicellus), all segments except the scapus and pedicellus and terminal six are covered in moderately dense tan setae that are as long as the antennae segment is wide. The terminal six segments are covered in tan setae that are about as dense as the setae on the other segments but much shorter (some only slightly raised above the segment surface), and the scapus and pedicellus are without setae. Compound eyes large (taking up about half of the head capsule length) but not notably protruding away from the head (Fig. 7B). Three well-developed ocelli are between the compound eyes and slightly raised above the head capsule (Fig. 7B). Antennal fields slightly wider than the scapus width, not notably large (Fig. 7B). *Thorax*. Pronotum with an anterior margin that is clearly but not strongly concave; lateral margins that are straight for the anterior two-thirds and then clearly angled toward the posterior margin which is slightly more than half of the width of the anterior margin and slightly convex (Fig. 7B). Anterior and lateral margins of the pronotum with distinct rims, and the posterior margin lacks a well-developed rim. Face of the pronotum has a lumpy texture and is marked by a distinct sagittal furrow and crescent shaped pit in the center (Fig. 7B). Prosternum is moderately granulose with nodes throughout of relatively even size. Mesosternum surface mostly wrinkled, not as much granulation as the prosternum. Prescutum about as wide as long, with lateral margins slightly converging to the posterior. Lateral rims with six to seven tubercles of slightly varying size and uneven spacing, with most tubercles prominent. Prescutum crest along the sagittal plane with four or five small nodes. The surface of the prescutum is mostly wrinkled in texture and not prominently raised along the sagittal plane. Prescutum anterior margin marked with a prominent slightly recurved tubercle rising above the surface of the pronotum (Fig. 7E). Mesopleurae narrow, nearly parallel for most of their length, only starting to more strongly diverge after about two thirds of the way through with the posterior the broadest portion (Fig. 7B). Lateral margin with five major tubercles throughout the length, and generally two or three small minor tubercles interspersed (Fig. 7B). Face of the mesopleurae smooth except for two distinct pits, one on the anterior third and one on the posterior third. *Wings*. Tegmina moderate in length, extending about one quarter of the way into abdominal segment IV. Tegmina wing venation (Fig. 5B): the subcosta (Sc) is the first vein, running smoothly to the margin and is the first to terminate on the wing margin, about two fifths of the way through the overall tegmina length. The radius (R) spans the entire length of the tegmina with the first radius (R1) branching approximately one third through the length, then a second radius (R2) branches approximately two thirds of the way through the length, and the radial sector (Rs) terminates at the wing apex. The media (M) also spans the entire length of the tegmina (as the media anterior MA, terminating at the wing apex). There are two posterior media veins, the first posterior media (MP1) branches near the middle and meets the cubitus at the wing margin and terminates. The second posterior media (MP2) branches after the first posterior media at about the midline and meets with the cubitus near the wing margin. The cubitus (Cu) runs along most of the tegmina margin and terminates past the midline upon meeting the second media posterior. The first anal

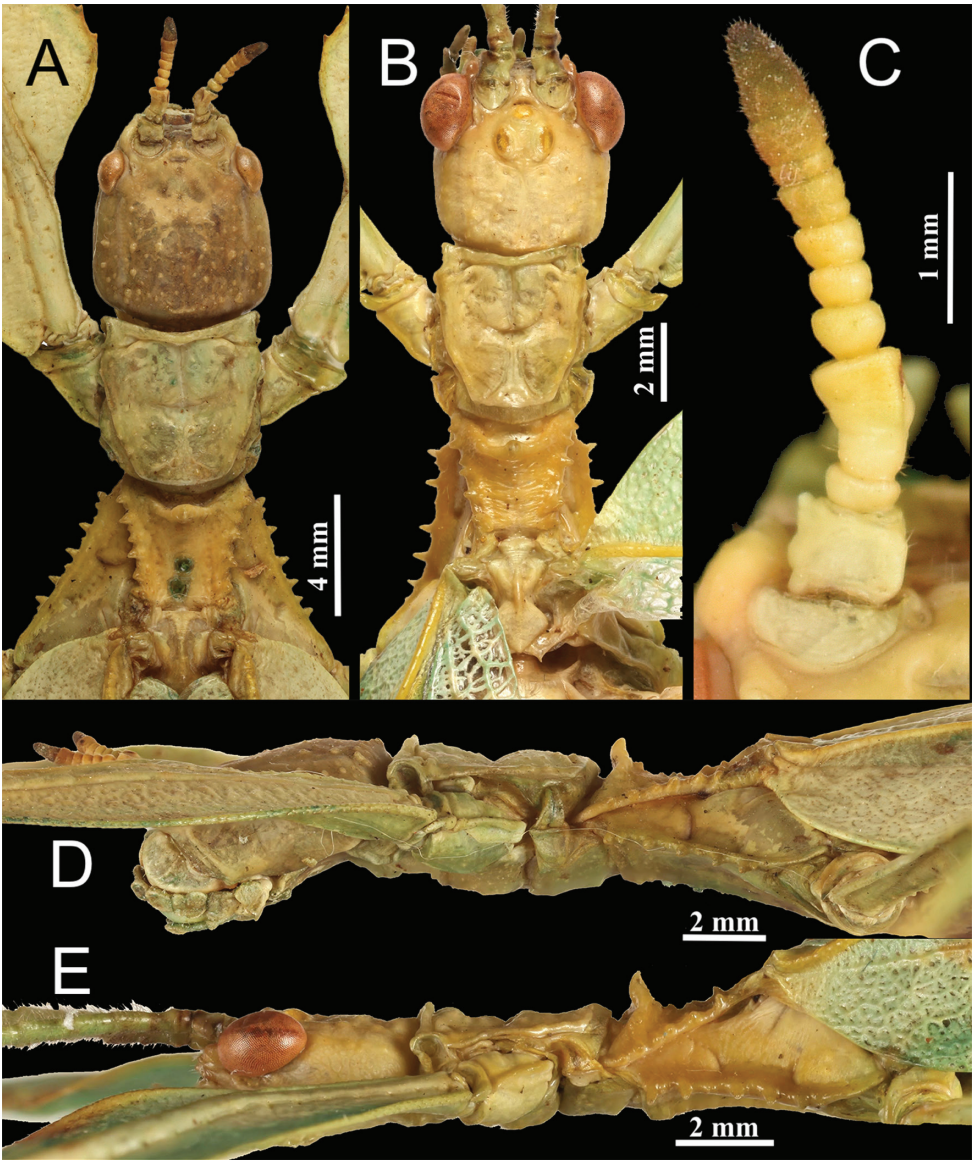

Figure 7. *Phyllium zomproi*. **A** female, head through thorax, dorsal, Coll RC 18-277 **B** male, head through thorax, dorsal, Coll RC 17-336 **C** female, antennae, dorsal, Coll SLT **D** female, lateral, head through thorax, Coll RC 18-277 **E** male, lateral, head through thorax, Coll RC 17-336.

(1A) vein terminates upon reaching the cubitus proximal to the midline. Alae well developed in an oval fan configuration, long, almost reaching to the posterior margin of abdominal segment VIII. Alae wing venation (Fig. 5C): the costa (C) is present throughout the entire foremargin giving stability to the wing. The subcosta (Sc) spans approximately three quarters of the wing length running alongside the costa vein the entire length. The radius (R) spans nearly the entire wing length and branches approximately

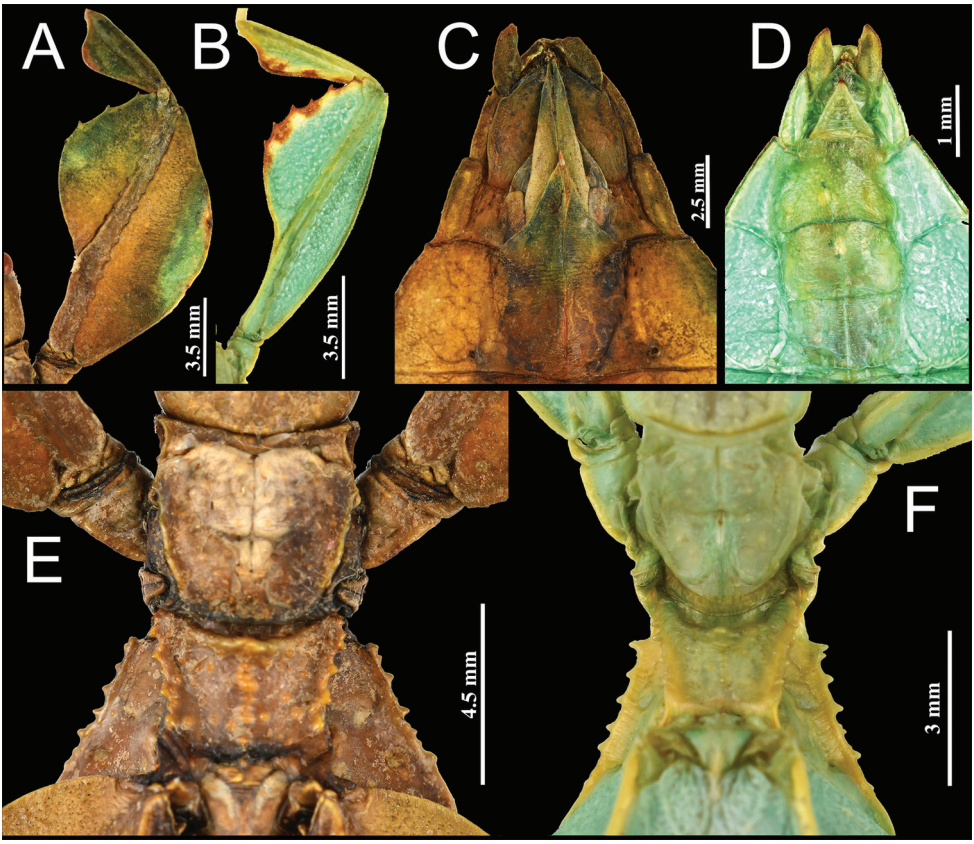

Figure 8. *Phyllium monteithi*. **A** female, profemora and protibia, dorsal **B** male, profemora and protibia, dorsal **C** female, genitalia, ventral **D** male, genitalia, ventral **E** female, thorax, dorsal **F** male, thorax, dorsal. All specimens, Coll SLT.

two fifths of the way through into the first radius (R1) and radial sector (Rs). These run gently diverging through about half of their length after which they become parallel and start to bend toward the media vein. Instead of terminating at the wing apex or meeting the media vein, they simply thin out and end individually just shy of the apex. The media (M) branches almost immediately into the media anterior (MA) and the media posterior (MP) which run parallel or subparallel with each other throughout their entire lengths. Neither the media anterior or posterior terminate at the wing apex and like the radial veins the media veins simply thin out and terminate just shy of the apex near where the radial veins terminated. The cubitus (Cu) runs unbranched and terminates at the wing apex bending towards the terminated radial and media veins but not fusing with any. Of the anterior anals, the first anterior anal (1AA) fuses with the cubitus at the wing base and does not diverge from the cubitus until three quarters of the way through the wing length where it diverges away from the curving cubitus until the first anterior anal terminates at the wing margin. The anterior anals two through seven (2AA–7AA) have a common origin and run unbranched in a folding fan pattern of relatively uni-

Figure 9. Live male *Phyllium monteithi*, Coll JHT. **A** full body, dorsal **B** detail of profemora, head, and thorax, dorsal view **C** detail of antennae and head, lateral view **D** genitalia detail, ventral view.

form spacing to the wing margin. The posterior anals (1PA–5PA) share a common origin separate from the anterior anals and run unbranched to the wing margin with slightly narrower spacing between them than the anterior anals. *Abdomen*. Abdominal segments II through III only slightly diverging, IV through VII about half as long as wide and with parallel margins giving the abdomen a long boxy appearance. Segments VIII and IX with smoothly rounded margins converging to segment X which is about half as wide as segment IX and with margins that converge more strongly to the apex. *Genitalia*. Poculum starting two thirds of the way through abdominal segment VIII, broad with rounded margins, and ending in an apex that slightly passes the anterior

margin of segment X and has a distinct cleft in the center (Fig. 6D). Cerci long and slender with at least half of their length protruding from under the terminal abdominal segment, margins slightly cupped, surface covered throughout in thin setae and a granular surface. Vomer not particularly broad, with nearly straight sides evenly converging to the single apical point that hooks upwards into the paraproct (Fig. 6D). *Legs*. Profemoral exterior lobe smoothly arcing evenly end to end and at its widest is only slightly thinner than the interior lobe. Profemoral exterior lobe margin lacking teeth but does have a slightly granular surface with minimal short setae throughout (Fig. 6B). Profemoral interior lobe rounded without a strong angle and marked with three to four prominent serrate teeth with wide looping gaps between each tooth, the gap in the center is only slightly wider than the gaps on each side (Fig. 6B). Mesofemoral exterior lobe arcs end to end with a distinct bend on the distal third which marks the widest portion of the lobe, no teeth present on the exterior lobe. Mesofemoral interior lobe thinner than the exterior lobe, smoothly arcing from end to end without a distinct bend and with six serrate teeth on the distal half only. Metafemoral exterior lobe without serrate teeth and not broad, straight along the metafemoral shaft. Metafemoral interior lobe wider than the exterior, gently arcing with ten to eleven small serrate teeth throughout the distal three quarters of the length. Protibiae lacking exterior lobe, interior lobe reaching end to end in a rounded scalene triangle, broadest on the distal end (Fig. 6B). Meso- and metatibiae simple, lacking lobes completely.

Phyllium (*Walaphyllium*) *monteithi* Brock & Hasenpusch, 2003

Figs 1, 3C, D, 8A–F, 9A–D, 10A–C, 11E–H, 12

Distribution. Australia, Queensland: Mt. Lewis, near Julatten (Holotype: QMBA); Garrandunga, Polly Creek (Coll RC); Windsor Tableland, NE Mt. Carbine (Paratype: QMBA); Mt. Windsor, Tableland (Paratype: UQIC); Kuranda (Paratype: ANIC; Coll JHT); Innisfail (Paratype: QMBA); Atherton, Tableland (Paratype: QDPC); Cairns District (Paratype: UQIC); Gadgarra State Forest, nr Lake Tinaroo (Paratype: QDPC).

Records taken from specimens examined and from Brock and Hasenpusch (2003).

Discussion. *Phyllium monteithi* is the most common phylliid species from Australia (the second and only other species being *Nanophyllium australianum* Cumming, Le Tirant, & Teemsma, 2018 which is exceedingly rare). For the *Phyllium* (*Walaphyllium*) new subgenus, this is the most commonly encountered species and has been in the phasmid breeding community for numerous years.

Female *Phyllium monteithi* can be differentiated from *Phyllium zomproi* by several morphological features. One is the number of teeth on the stridulatory file of the third antennal segment with 27 to 29 teeth on *P. monteithi* (Fig. 10C) and 48 to 50 teeth noted on *P. zomproi* (Hennemann et al. 2009). There is a notable difference in body size between the two species, with *P. monteithi* a medium sized species ranging from 75.0–76.0 mm and *P. zomproi* a large species ranging from 80.0–86.0 mm in length. Additionally, the tubercles on the thorax of *P. zomproi* are more prominent than those

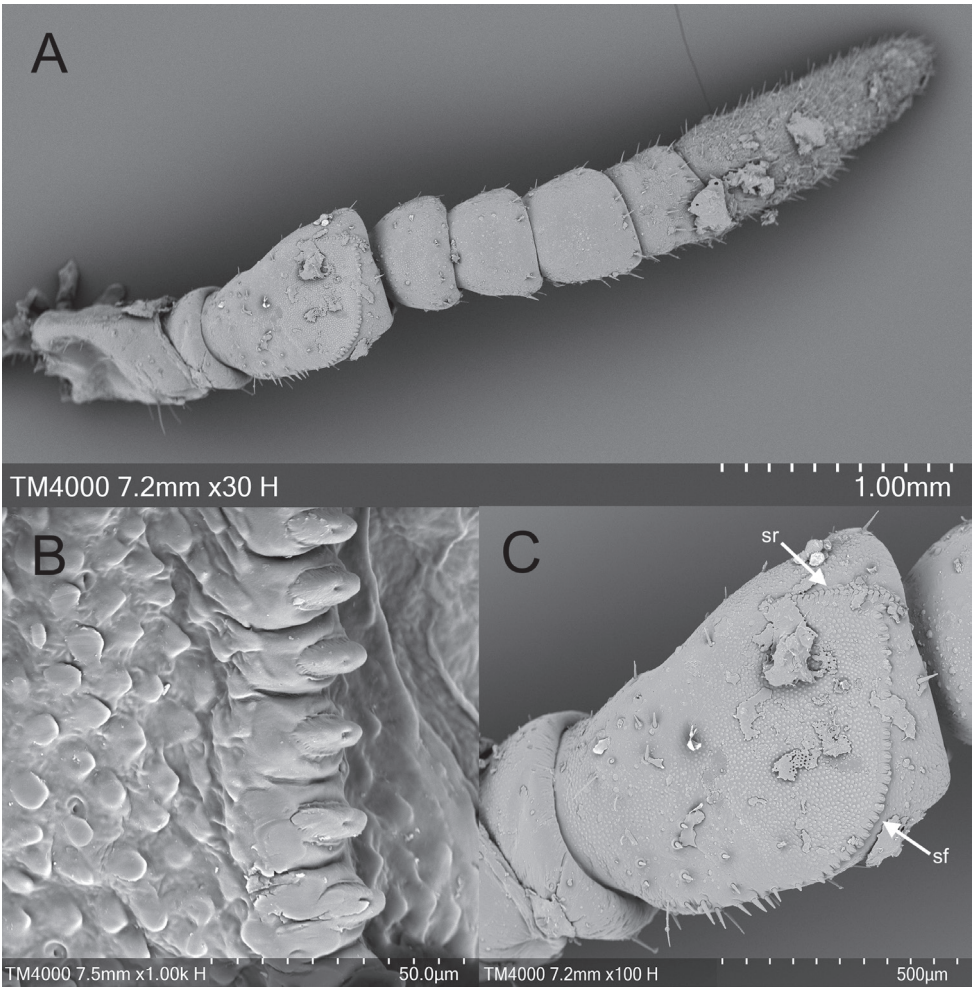

Figure 10. SEM image of female *Phyllium monteithi* antennae, Coll JHT. **A** full antenna **B** details of the stridulatory file of the third antennomere **C** antennomere III in full. Abbreviations: sf = stridulatory file; sr = stridulatory ridge.

found on *P. monteithi* and the point of the subgenital plate in *P. zomproi* is more pronounced than in *P. monteithi*.

Body size: males: 61.0–64.0 mm, females: 75.0–76.0 mm.

Newly hatched nymph coloration. General color throughout the antennae, head, and thorax is dark brown (Fig. 12). The abdomen is of a similar dark brown color but with pale green and brown muddled in. Margins of abdominal segments II through IV with pale mint green margins versus the other segments which have margins which are of a similar muddled brown color like the base color of the segment. Metanotum lateral margins with a distinct pale mint green patch of color. Base coloration of the legs goes from lightest on the anterior pair to darkest on the posterior pair, with the first pair having a burnt orange color, the middle pair a

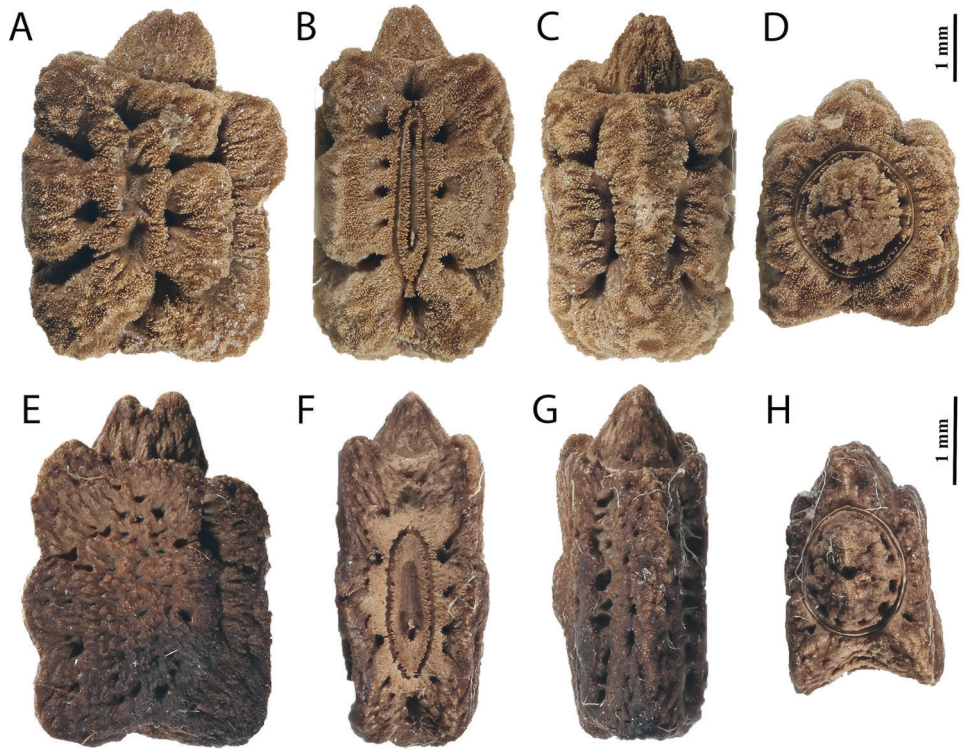

Figure 11. Known eggs for the *Phyllium* (*Walaphyllium*). **A–D** *P. zomproi*, (Coll RC 19-161) **A** lateral **B** dorsal **C** ventral **D** opercular (anterior) **E–H** *P. monteithi*, (Coll RC 17-289) **E** lateral **F** dorsal **G** ventral **H** opercular (anterior).

reddish brown color, and the final pair the darkest with a similar dark brown color found on the rest of the body. Meso- and metafemora with a small transverse white band on the proximal end and a broken white transverse line in the middle of the leg segment. Protibiae are the same burnt orange color as the profemora. Meso- and metatibiae are the same color as their adjoining femora, and both have a white patch of color on the proximal portion. Probasitarsi are a golden yellow and the other basitarsi are cream in color.

***Phyllium* (*Walaphyllium*) *lelantos* sp. nov.**
http://zoobank.org/23FAE495-5290-4671-BE92-9A61439B0BE8
Figs 3E, 13A, B, 14A–D

Type material. Holotype ♂: Papua New Guinea, Watut, Morobe Province, I.1992. NHMUK 012497024. Deposited in the Natural History Museum, United Kingdom (NHMUK), (Fig. 3E).

Figure 12. *Phyllium* (*Walaphyllium*) *monteithi* recently emerged first instar nymph showing the unique coloration which may be present in the other members of this new subgenus. Photographs courtesy of Bruno Kneubühler. **A** dorsolateral view **B** dorsal view.

Discussion and differentiation. The female and eggs are currently unknown; therefore, differentiation is only given for male morphology. This new species is the smallest within the newly erected subgenus, with the holotype only 53.3 mm long, versus males of *P. monteithi* 61.0–64.0 mm or *P. zomproi* at 79.0 mm (Figs 3B, 3D, versus 3E). An easy morphological feature to differentiate males of the three species is the radial venation of the tegmina. In *P. lelantos* sp. nov. the radial vein is split only once into the first radial and the radial sector; *P. zomproi* has the radial split twice, into the radial sector, the first radial, and the second radial; *P. monteithi* has the radial split more than the others with at least four prominent radials as well as the radial sector (and occasionally a weak but present fifth radial near the wing apex is also present in some specimens). The profemoral exterior lobe is also notably thinner in *P. lelantos* sp. nov. only one or one and a half times wider than the profemoral shaft width (Fig. 14B) versus *P. monteithi* and *P. zomproi* which can have a profemoral exterior lobe width as many as two or two and a half times wider than the profemoral shaft (Figs 6B, 8B).

Morphologically, *P. lelantos* sp. nov. appears to be most similar to *P. monteithi* based on the thorax spination, with the less pronounced mesopleurae tubercles and the anterior prescutum rim with a weakly formed sagittal tubercle (Fig. 14D) versus the prominently raised anterior prescutum rim in *P. zomproi* (Fig. 7E). Another similarity of *P. monteithi* and *P. lelantos* sp. nov. are the terminal abdominal segments with the lateral margins of abdominal segments VIII and IX having straight converging margins, versus *P. zomproi* which has rounded terminal abdominal segments.

Description. Female and egg. Unknown.

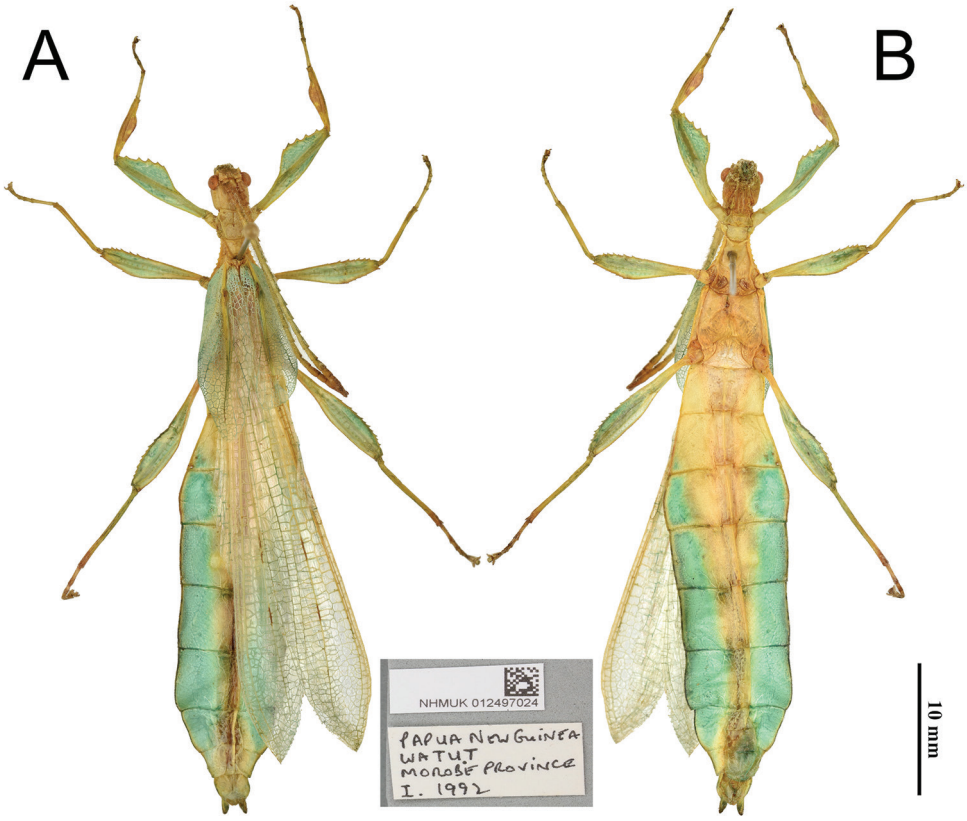

Figure 13. *Phyllium lelantos* sp. nov. holotype male, NHMUK. **A** dorsal **B** ventral. Insert Data labels, "Papua New Guinea, Watut, Morobe Province, I. 1992; NHMUK 012497024".

Male. ***Coloration.*** Coloration description is based on the single preserved holotype specimen. It is expected that live individuals are likely vibrant green in life. Overall coloration green throughout with yellow to tan discoloration in places due to the drying of the specimen. Compound eyes and the four terminal antennae segments are of a rusty brown color darker than the tan on the head or thorax. The rest of the antennae are of a tan to green color. The protibial interior lobe has brown marking throughout most of the surface, this is the only lobe that has brown colorations, the others are a normal green like the rest of the body. The head through to the thorax are more tan than green in the dried specimen but were likely a darker green in life. There are two faint circular eye spots on the fifth abdominal segment with all others lacking markings.

Morphology. *Head*. Head capsule slightly longer than wide, with a vertex marked by sparse, small evenly sized nodes. Frontal convexity stout with sides that converge to the point which is slightly recurved, not straight; the surface is sparsely covered in thin transparent setae (Fig. 14A). *Antennae*. Antennae consist of 22 segments (including the scapus and pedicellus). The scapus and pedicellus lack setae, the terminal five antennae segments are covered in dense setae that are short, and the remaining anten-

nae segments are covered in long, thin setae which are longer than each segment is wide. Compound eyes are large, notably protruding away from the head capsule and taking up about half of the length of the capsule lateral margins (Fig. 14A). Ocelli are present and well-developed (Fig. 14A). *Thorax*. Pronotum with anterior margin that is slightly concave and lateral margins that are straight and uniformly converging to a straight posterior margin that is about half the width of the anterior rim. Anterior and lateral margins of the pronotum have distinct rims, and the posterior margin lacks a rim (Fig. 14A). Face of the pronotum is marked by a distinct sagittal and transverse furrow meeting at a central pit with the remainder of the surface slightly lumpy in texture. Prosternum is moderately granulose throughout with nodes of even size and slightly uneven spacing as well as a slightly more prominent central node which is more prominent than the others (Fig. 14D). Mesosternum surface wrinkled and marked with nodes throughout. Prescutum anterior margin is wider than the prescutum is long, with lateral margins that converge to the posterior margin that is approximately three-quarters as wide as the anterior rim. Lateral rims with five nodes of slightly varying size but nearly even spacing. Prescutum crest along the sagittal plane nearly bare, with only a single small node present near the anterior rim and one more small one near the posterior, the rest of the sagittal crest lacks features and is just smooth (Fig. 14D). Prescutum anterior margin not particularly prominent, only marked with a single small tubercle (Fig. 14D). Mesopleurae narrow, with margins which are straight, only slightly diverging along their length. Lateral margin marked with six tubercles spread throughout the length almost evenly, with the smallest near the anterior rim and the rest slightly increasing in size as they span towards the posterior (Fig. 14A). Face of the mesopleurae smooth except for two faint divots, one on the anterior third and one on the posterior third. *Wings*. Tegmina short, only extending half way through abdominal segment III. Tegmina venation can only be noted to the best of our ability from the folded wings of the holotype specimen. For the tegmina, the subcosta (Sc) is the first vein and rather long, running smoothly along the wing and terminates just past the midline of the wing length. The radius (R) spans the entire length of the tegmina with the radial sector (Rs) terminating at the wing apex and a single first radius (R1) branching just before the midline and terminating at the margin three quarters of the way through the tegmina length. The media (M) also spans the entire length of the tegmina (as the media anterior MA, which terminates at the wing apex). There are two posterior media veins, the first posterior media (MP1) branches before the midline and meets the cubitus at the wing margin where the first posterior media terminates. The second posterior media (MP2) branches after the first posterior media near the midline and meets with the cubitus near the wing margin. The cubitus (Cu) vein runs along most of the tegmina margin and terminates about three quarters of the way through the tegmina length upon meeting the second media posterior. The first anal (1A) vein terminates upon reaching the cubitus about one-third of the way along the tegmina length. Alae long and well developed in an oval fan configuration, extending to the posterior margin of abdominal segment IX. Alae wing venation cannot be seen fully due to the folded wings, but what can be seen is that there is a fully developed

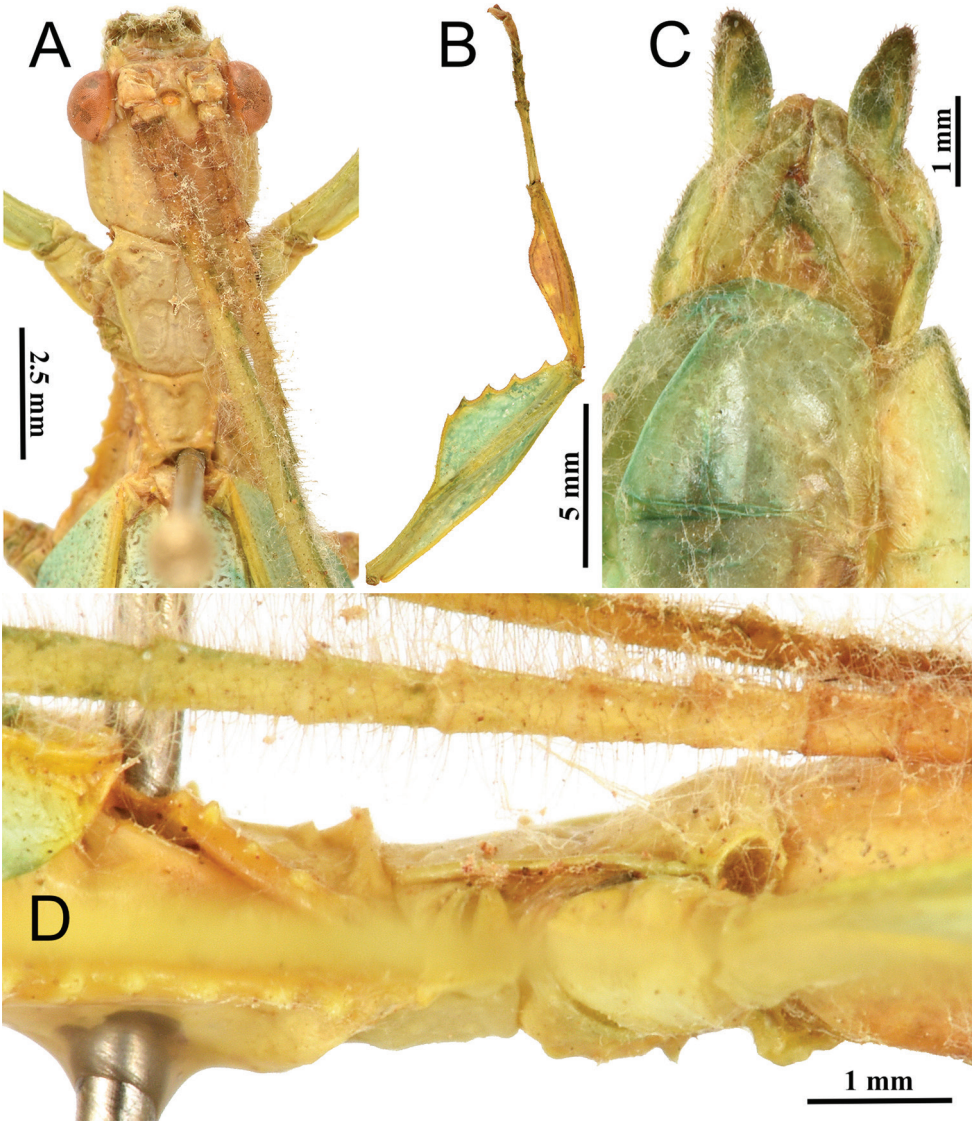

Figure 14. *Phyllium lelantos* sp. nov. holotype male. **A** head and thorax, dorsal **B** front leg, protibiae and profemora, dorsal **C** genitalia, ventral **D** thorax, lateral view.

costa (C), subcosta (Sc), and first radius (R1) present along the length of the alae running parallel with each other to the apex of the wing. *Abdomen*. Abdominal segments II through the anterior half of IV gradually and uniformly diverging, posterior half of IV through VII parallel, with each segment only about one and a half times wider than long giving the abdomen a thin boxy appearance. Segments VIII through X converging to the apex but with slightly rounded margins, not perfectly straight. Abdominal segment X has margins which are lined with stout setae, very similar to

those which line the cerci margins. *Genitalia*. Poculum starting at the anterior margin of abdominal segment VIII, uniformly broad throughout its length, and ends in a broad slightly rounded apex that slightly passes the anterior margin of segment X (Fig. 14C). Cerci about as long as the vomer, with about half of the length extending from under abdominal segment X. Cerci are slightly cupped and have a surface which is weakly granular. Cerci margins are lined with stout tan setae with those on the exterior margins more prominent than those on the interior margins. Vomer moderately long, extending about three-quarters of the way under segment X with sides that are evenly converging, the single apical point is broad and hooks upwards into the paraproct (Fig. 14C). *Legs*. Profemora exterior lobe slightly wider than half the width of the interior lobe, no small teeth are present but the entire length has short tan setae relatively evenly spaced, and the lobe arcs smoothly along the profemoral shaft without a distinct bend. Profemoral interior lobe roundly triangular without a strong angle and marked with five teeth. The proximal most tooth is smaller than the rest but clearly present, the remaining four teeth are of a similar size and with wide looping spacing except between the distal two which have slightly wider spacing than the others. Exterior mesofemoral lobe arcs end to end with a slight rounded angle in the center, and only on the distal half of that gentle bend are three to five small serrate teeth. The exterior mesofemoral lobe ends in a prominent spur near the mesotibial joint, this spur is larger than any of the preceding small serrate teeth. Interior mesofemoral lobe is slightly narrower than the exterior lobe and lacks a distinct bend, instead hugging the mesotibial shaft. On the distal half only of the interior mesofemoral lobe there are five to six serrate teeth which are larger than the exterior lobes teeth. Metafemoral exterior lobe lacks teeth, is nearly straight, and runs uniformly along the metafemoral shaft. Metafemoral interior lobe slightly wider than the exterior lobe and with nine to ten small serrate teeth throughout slightly more than half of the length. Protibiae lacking an exterior lobe, interior lobe reaching end to end in a smooth scalene triangle, with the broadest portion on the distal end (Fig. 14B). Uniformly throughout the protibial lobe margins are similar stout setae as those found on the profemoral lobes margins. Meso- and metatibiae simple, lacking lobes completely.

Etymology. Noun. Because leaf insects are such cryptic insects so rarely observed, or in this case only known from a single specimen, we felt that the homage of Lelantos the Greek minor Titan of "moving unseen" was fitting. Lelantos' name is derived from the Greek Ληλαντος (*lêthô*, *lanthanô*, and *lelathon*), meaning "to escape notice", "move unseen", or "go unobserved" (Rouse 1942).

Distribution. Only known from the holotype specimen from Papua New Guinea, Morobe Province, Watut (Fig. 4).

Measurements of holotype [mm]. Length of body (including cerci and head, excluding antennae) 53.3, length/width of head 3.8/2.8, antennae (but slightly bent so measurement is slightly off) 12.0, pronotum 2.5, mesonotum 1.5, length of tegmina 15.1 (left) and 11.8 (right, which appears to be slightly aberrant and dwarfed), length of alae 38.5, greatest width of abdomen 10.5, profemora 7.4, mesofemora 8.8, metafemora 11.0, protibiae 5.8, mesotibiae 5.7, metatibiae 7.5.

Biogeography

The Torres Strait is a narrow body of water which separates mainland points of northern Queensland, Australia from southern New Guinea by approximately 130 km (Sands and New 2008). While presently separated, these two regions lay on the Sahul shelf and were connected by a land bridge until roughly 19 to 22 KYA at the end of the last glacial maximum (Clark et al. 2009; Yokoyama et al. 2000). Maps considering potential sea level fluctuations from 17-250 KYA revealed the Torres Strait region remained as a relatively stable land bridge between Australia's Cape York Peninsula and southern New Guinea (Voris 2000). These past connections across the Torres Strait and the tectonic structure of the region have been used to explain the complex biogeography of modern species in northern Australia and southern New Guinea (Crisp et al. 1995; De Boer and Duffels 1996; Heads 2001; Heads 2014; Grehan and Mielke 2018) and may explain the restricted distribution of *Phyllium* (*Walaphyllium*) subgen. nov.

The present status of the Torres Strait as a barrier has been debated for different taxa (Taylor 1972; Sands and New 2008) as it consists of over 150 islands (Green et al. 2010) which could serve as potential habitats. However, these islands may still act as a barrier to the Phylliidae as they consist of dry, bare rock, sandy banks, coral cays, swamps or mangroves, none of which are suitable to the rainforest dwelling Phylliidae. Additionally, recent sea level rise has been accompanied by aridification, with the Cape York Peninsula's wet forests becoming reduced to mountainous scarps along the eastern coastline since the last glacial maximum (Hope et al. 2004). The most extensive block of present-day rainforests in Cape York are the Kutini-Payamu (Iron Range-McIlwraith Region) which is where the rare *Nanophyllium australianum* Cumming, Le Tirant, & Teemsma, 2018 occurs (Rentz 1988; Adam 1992). This species closely resembles *Nanophyllium pygmaeum* Redtenbacher, 1906, which is known from southern New Guinea near the tip of Cape York, supporting potential descent from New Guinea. *Phyllium* (*Walaphyllium*) subgen. nov. has a restricted distribution at each end of the Torres Strait with the northernmost species, *P. lelantos* sp. nov. in the Morobe Province and *P. zomproi* found in the Morobe and Gulf Provinces of Papua New Guinea. The most southern extension is found with *P. monteithi*, which occurs throughout the Wet Tropics of Northeast Queensland. The Wet Tropics consists of the largest continuous area of rainforest in Australia (Adam 1992) and remains as a patch of the rainforests which may have extended across the Sahul shelf, connecting Papua New Guinea and Australia. Future investigation into molecular phylogenies for this clade will help reveal the underlying higher taxonomy within Phylliidae and potential dispersal patterns or evolutionary centers.

Discussion

While reviewing specimens of this clade we propose herein as *Walaphyllium*, we found that they contained a combination of morphological features which made it unclear to which taxonomic level it should be placed (as a genus or a subgenus). Presently the

genus *Phyllium* has several morphologically distinct clades which are treated taxonomically as subgenera (*Phyllium* Illiger, 1798; *Pulchriphyllium* Griffini, 1898; and *Comptaphyllium* Cumming et al. 2019). However, there are other distinct clades within the Phylliidae which are currently classified as genera (*Chitoniscus* Stål, 1875; *Nanophyllium* Redtenbacher, 1906; *Microphyllium* Zompro, 2001; and *Pseudomicrophyllium* Cumming, 2017).

Ultimately, we decided to place this clade as a subgenus of *Phyllium*, but not as a genus of their own due to several morphological factors. First, the two previously described species we here transfer to *Walaphyllium* (*P. monteithi* and *P. zomproi*) have historically been placed within the morphologically diverse *siccifolium* species group of the *Phyllium* subgenus, which concealed their unique combination of features (Hennemann et al. 2009). It wasn't until we tabulated the morphological diversity of the *Phyllium* subgenera (see Table 1), that we realized that the *Walaphyllium* clade essentially contained a mixture of morphological features which are shared between the *Pulchriphyllium*, *Comptaphyllium*, and/or the *Phyllium* subgenera.

Features which are shared between the *Walaphyllium* and the subgenera *Comptaphyllium* and *Phyllium* are: females with the media and cubitus veins which have spacing between them several times wider than a single vein width (*Pulchriphyllium* has these two veins close together, with a distance less than one vein width apart). On the other hand, a shared feature between the *Pulchriphyllium* and the *Walaphyllium* that separates them from the other subgenera are the eggs, which lack pinnae, have a brittle pitted surface, and have an operculum which is conically raised. No other features were found that were worth noting as unique between clades, either due to variability within subgenera or simply the features were universal among them and not worth noting (see Table 1 for a summary).

The only autapomorphy we were able to identify for the *Walaphyllium* is that the female tegmina have the posterior cubitus branched into the first and second posterior cubitus veins (Fig. 5A), other phylliid females have an unbranched posterior cubitus. We felt that with so few features which are exclusively unique to the *Walaphyllium*, and with a combination of features which link this clade to the other *Phyllium* subgenera, that at this time it is most appropriate to place this clade as a subgenus within *Phyllium*, not as their own genus.

A possible autapomorphy for the *Walaphyllium* is the morphology of the individual teeth on the stridulatory file of the female third antennomere. Unfortunately, there are very few published SEM images of stridulatory files for the different phylliid clades so our observations lack sufficient support to be considered definitive. Friedemann et al. (2012) imaged what they call "*Phyllium siccifolium*" but due to the extreme rarity of that species and incongruous morphological features it is dubious that it is a true *Phyllium siccifolium*. The specimen was only partially imaged and did not note a collection location. Based on the whole antennae image in their figure 4A, which has a ten segmented antennae, the fourth antennal segment which is not short and disk-like, and the number of teeth visible on the stridulatory file, it is possible that the species they actually imaged was *Phyllium philippinicum* Hennemann et al., 2009. Either way,

Table 1. Morphological comparison of the four recognized *Phyllium* subgenera.

Feature	*Pulchriphyllium* Griffini, 1898	*Walaphyllium* subgen. nov.	*Phyllium* Illiger, 1798	*Comptaphyllium* Cumming et al., 2019
Egg Capsule	No pinnae (surface pitted and brittle)	No Pinnae (instead an irregular porous, sponge-like texture, brittle, not flexible)	Pinnae (rope, feather, or moss-like of various lengths, all flexible)	Pinnae (feather-like)
Egg Operculum	Conically raised	Conically raised	Flat, margin with rope, or feather-like pinnae or conically raised, with moss-like pinnae	Flat, with a prominent sagittal fan of feather-like pinnae through the center
Male Tegmina (Radial)	Variable: can be branched once into first radius and radial sector, or branched into the first radius, second radius, and radial sector	Variable: can be branched once into first radius and radial sector, or branched as many as four times	Variable: can be branched once into first radius and radial sector, or branched as many as three times	Branched once into first radius and radial sector
Male Tegmina (Media)	With an anterior media vein (MA) and two posterior media veins (MP1 and MP2)	With an anterior media vein (MA) and two posterior media veins (MP1 and MP2)	Variable: can simply be branched into the anterior media (MA) and posterior (MP) or with an anterior media vein (MA) and two posterior media veins (MP1 and MP2)	Branched into the anterior media (MA) and posterior (MP) only
Female Tegmina (Media and Cubitus)	Media and cubitus side by side (touching or or less than one vein width away) until the media posterior diverges to the wing margin	Media and cubitus with spacing between many times wider than the width of a vein for a majority of the length	Media and cubitus with spacing between many times wider than the width of a vein for a majority of the length	Media and cubitus with spacing between many times wider than the width of a vein for a majority of the length
Female Tegmina (Cubitus Branching)	With an anterior and posterior cubitus only	With an anterior cubitus and a branched posterior cubitus into the first and second posterior cubitus	With an anterior and posterior cubitus only	With an anterior and posterior cubitus only
Male Vomer	1 hook	1 hook	1 or 2 hooks	1 hook
Tibial Exterior Lobes (Male and Female)	Yes	No	Yes or No	No

this would represent a member of the *siccifolium* species group of the *Phyllium* (*Phyllium*) subgenus and can be used for comparative purposes. These stridulatory file teeth, although not individually imaged, appear in figure 4B of Friedemann et al. (2012) to be raised ovoids with a smooth surface.

Fortunately, members of the other *Phyllium* subgenera have had their stridulatory files imaged with a SEM. The *Phyllium* (*Pulchriphyllium*) based on an individual of *Phyllium bioculatum* Gray, 1832 was presented in figure 5 of Bradler (2009) and the *Phyllium* (*Comptaphyllium*) clade was imaged on *Phyllium riedeli* Kamp & Hennemann, 2014 in their figure 2E. Both of these subgenera appear to have individual teeth which are raised ovoids with a smooth surface, similar to the *Phyllium* (*Phyllium*) subgenus.

In contrast, *P. monteithi*, instead has teeth which are raised ovoids with a distinct central pit at the apex of each individual tooth (Fig. 10B). This feature could possibly be an autapomorphy for the *Walaphyllium* clade but these few examples leave much unknown and no significant conclusions can be drawn from these limited observations.

Our inclusion of SEM images of the *P. monteithi* antennae structure is largely an attempt to illustrate the stridulatory file morphology, to visualize this previously unpublished fine detail, and to demonstrate that there is variable morphology at this level

which should be included in future revisionary works. Future SEM visualization projects will image all phylliid clades and several representatives within each clade to allow better morphological comparison and possibly reveal underlying morphological relationships.

Despite the *Walaphyllium* being a small clade of only three species, there are morphological features which suggest the internal relatedness of these species. Based on the spination of the thorax it appears as though *P. monteithi* and *P. lelantos* sp. nov. are likely sister species as evident by their weakly formed prescutum anterior sagittal tubercle (Fig. 14D) and less pronounced mesopleurae tubercles (Fig. 8F), versus *P. zomproi* which has a prominently raised prescutum anterior sagittal tubercle (Fig. 7E) and prominent mesopleurae tubercles (Fig. 7B). Unfortunately the female and egg morphology for *P. lelantos* sp. nov. are unknown at present, and it is possible that these unknowns might hold additional features which illustrate the relationship of species within the *Walaphyllium* clade with more clarity. But with the females and eggs only known for the other two species we cannot at the present draw conclusions as to the internal *Walaphyllium* clade relationships beyond what is suggested by male morphology alone.

These morphologically based observations are currently the compelling evidence to differentiate the *Walaphyllium* from other clades. It is expected that upcoming molecular analyses will help to clarify the higher taxonomy within the Phylliidae, and will reveal if the *Walaphyllium* is a sublineage within the *Phyllium* or if this clade warrants treatment as a separate genus. But, at the present we do not have molecular evidence to suggest the proper placement of this clade, and therefore we place it under the taxonomic umbrella of *Phyllium*.

Identification key to known males of *Phyllium* (*Walaphyllium*) subgen. nov.

Females and eggs are only known for *Phyllium monteithi* and *Phyllium zomproi*, therefore only a key to males is included here. See Brock and Hasenpusch (2003) for a discussion on the morphological differences between *Phyllium monteithi* and *Phyllium zomproi* females and eggs.

1 Profemoral exterior lobe less than two times the greatest width of the profemoral shaft; tegmina with a radial sector vein (RS) and only one additional radial vein (R1); Papua New Guinea..... ***P. lelantos* sp. nov.**

– Profemoral exterior lobe wider than two times the greatest width of the profemoral shaft; tegmina with a radial sector vein (RS) and more than one additional radial vein (two to four additional radials) **2**

2 Large body size (~79.0 mm); margin of abdominal segments VIII and IX not uniformly converging to the terminal abdominal segment, instead segment VIII is subparallel, and segment IX is strongly rounded, not straight; tegmina with a radial sector vein (RS) and two additional radial veins only (R1 and R2); Papua New Guinea ..... ***P. zomproi***

– Medium body size (61.0–64.0 mm); margin of abdominal segments VIII and IX with straight margins uniformly converging to the terminal abdominal segment; tegmina with a radial sector vein (RS) and four additional radial veins (R1, R2, R3, and R4); Northeastern Australia..... ***P. monteithi***

Acknowledgments

The authors thank René Limoges, entomological technician at the Montreal Insectarium, Canada for taking many photos for this work, as well as for many professional courtesies. Jack Hasenpusch (Australia) for photographs of live *Phyllium monteithi* and habitat for this work. Judith Marshall and Benjamin Price at the Natural History Museum United Kingdom (NHMUK) for processing the loan of the holotype specimen despite the lack of an Orthopteroid collection curator and for measuring the holotype specimen for us. Doug Yanega (USA) for reviewing our etymology section and offering suggestions. Dave Rentz for his supply of live male *Phyllium monteithi* from light-traps and Minibeast Wildlife for providing female specimens of *P. monteithi*. Kathryn Green for her help in using SEM equipment at the Centre for Microscopy and Microanalysis (CMM). The authors are also indebted to the work of Robert Dixon on indigenous languages of northern Queensland, Australia. Thank you to Bruno Kneubühler (Switzerland) for allowing us to use his photos of freshly emerged nymphs for this work.

References

Adam P (1992) An Overview of Australian Rainforests. Australian Rainforests. Oxford. Biogeography Series. Oxford University Press, Oxford, 328 pp.

Bradler S (2009) Die Phylogenie der Stab- und Gespenstschrecken (Insecta: Phasmatodea) "Phylogeny of the stick and leaf insects (Insecta: Phasmatodea)". Species, Phylogeny and Evolution 2: 3–139. https://doi.org/10.17875/gup2009-710

Brock PD, Büscher TH, Baker E (2020) Phasmida SF: Phasmida Species File Version 5.0/5.0. In: Roskov Y., et al. (Eds) Species 2000 & ITIS Catalogue of Life. Species 2000: Naturalis, Leiden. https://www.catalogueoflife.org/col

Brock PD, Hasenpusch J (2003) Studies on the leaf insects (Phasmida: Phylliidae) of Australia. Journal of Orthoptera Research 11: 199–205. https://doi.org/10.1665/1082-6467(2002)011[0199:SOTLIP]2.0.CO;2

Burt DRR (1932) The venation of the wings of the leaf-insect *Pulchriphyllium crurifolium*. Ceylon Journal of Science, Spolia Zeylanica 17: 29–37.

Clark PU, Dyke AS, Shakun JD, Carlson AE, Clark J, Wohlfarth B, Mitrovica JX, Hostetler SW, McCabe AM (2009) The Last Glacial Maximum. Science 325: 710–714. https://doi.org/10.1126/science.1172873

Crisp MD, Linder HP, Weston PH (1995) Cladistic biogeography of plants in Australia and New Guinea: Congruent pattern reveals two endemic tropical tracks. Systematic Biology 44: 457–473. https://doi.org/10.2307/2413654

Cumming RT, Le Tirant S, Teemsma S (2018) Northeastern Australia record of *Nanophyllium pygmaeum* Redtenbacher, 1906, now recognized as a new species, *Nanophyllium australianum* n. sp. (Phasmida, Phylliidae). Faunitaxys 6: 1–5.

Cumming RT, Le Tirant S, Hennemann FH (2019) A new leaf insect from Obi Island (Wallacea, Indonesia) and description of a new subgenus within *Phyllium* Illiger, 1798 (Phasmatodea: Phylliidae: Phylliinae). Faunitaxys 7: 1–9.

Cumming RT, Bank S, Le Tirant S, Bradler S (2020) Notes on the leaf insects of the genus *Phyllium* of Sumatra and Java, Indonesia, including the description of two new species with purple coxae (Phasmatodea, Phylliidae). ZooKeys 913: 89–126. https://doi.org/10.3897/zookeys.913.49044

De Boer AJ, Duffels JP (1996) Historical biogeography of the cicadas of Wallacea, New Guinea and the West Pacific: A geotectonic explanation. Palaeogeography, Palaeoclimatology, Palaeoecology 124: 153–177. https://doi.org/10.1016/0031-0182(96)00007-7

Dixon RM (1972) The Dyirbal Language of North Queensland. Cambridge University Press, London, 420 pp. https://doi.org/10.1017/CBO9781139084987

Friedemann K, Wipfler B, Bradler S, Beutel RG (2012) On the head morphology of *Phyllium* and the phylogenetic relationships of Phasmatodea (Insecta). Acta Zoologica 93: 184–199. https://doi.org/10.1111/j.1463-6395.2010.00497.x

Green D, Alexander L, McInnes K, Church J, Nicholls N, White N (2010) An assessment of climate change impacts and adaptation for the Torres Strait Islands, Australia. Climatic Change 102: 405–433. https://doi.org/10.1007/s10584-009-9756-2

Grehan JR, Mielke CGC (2018) Evolutionary biogeography and tectonic history of the ghost moth families Hepialidae, Mnesarchaeidae, and Palaeosetidae in the Southwest Pacific (Lepidoptera: Exoporia). Zootaxa 4415: 243–275. https://doi.org/10.1007/s10584-009-9756-2

Griffini A (1898) Intorno al *Phyllium geryon* Gray. Bollettino dei Musei di Zoologia ed Anatomia comparata della Royal Università di Torino 8: 1–4. https://biodiversitylibrary.org/page/11257682 https://doi.org/10.5962/bhl.part.27225

Größer D (2001) Wandelnde Blätter. Ein Katalog aller bisher beschriebenen Phylliinae-Arten und deren Eier mit drei Neubeschreibungen. Frankfurt am Main, Germany (Edition Chimaira), 119 pp.

Heads M (2001) Birds of paradise, biogeography and ecology in New Guinea: A review. Journal of Biogeography 28: 893–925. https://doi.org/10.1046/j.1365-2699.2001.00600.x

Heads M (2014) Biogeography of Australasia: A Molecular Analysis. Systematic Biology 64: 163–166. https://doi.org/10.1093/sysbio/syu074

Hennemann FH, Conle OV, Gottardo M, Bresseel J (2009) On certain species of the genus *Phyllium* Illiger, 1798, with proposals for an intra-generic systematization and the descriptions of five new species from the Philippines and Palawan (Phasmatodea: Phylliidae: Phylliinae: Phylliini). Zootaxa 2322: 1–83. https://doi.org/10.11646/zootaxa.2322.1.1

Illiger JKW (1798) Verzeichnis der Käfer Preussens. Johann Jacob Gebauer, Halle, 510 pp. https://biodiversitylibrary.org/page/52579286

Kamp TVD, Hennemann FH (2014) A tiny new species of leaf insect (Phasmatodea, Phylliidae) from New Guinea. Zootaxa 3869: 397–408. https://doi.org/10.11646/zootaxa.3869.4.4

Key KHL (1970) Ch. 22, Phasmatodea (Stick-insects). In: CSIRO (Ed.) The Insects of Australia, A textbook for students and research workers, 348–359. Melbourne University Press, Melbourne.

Key KHL (1974) Phasmatodea (Stick-insects). In: CSIRO (Ed.) The Insects of Australia. Supplement 1974, 48–49. Melbourne University Press, Melbourne.

McKeown KC (1940) Australian Insects. VIII, Orthoptera: 3. Stick and leaf insects. The Australian Museum Magazine 7: 125–130.

Monteith GB (1978) The First Male Leaf Insect from Australia. The Entomological Society of Queensland 5: 138–139.

Monteith GB (1971) Leaf Insects from Australia. The Entomological Society of Queensland 78: 14–15.

Musgrave A (1942) An Interesting New Guinea Phasmid. The Australian Museum Magazine 7: 414.

Patz E (1991) 'Djabugay.' The Handbook of Australian languages, Vol. 4. Oxford University Press, Oxford, 314–331.

Poitout F (2007) Dictionnaire étymologique des noms scientifiques des Phasmes (Phasmatodea). L'Association PHYLLIE, Paris, France, 1–702.

Ragge DR (1955) The wing-venation of the Order Phasmida. The Transactions of the Royal Entomological Society of London 106: 375–392. https://doi.org/10.1111/j.1365-2311.1955.tb01272.x

Rentz DCF (1988) *Nanophyllium pygmaeum* Redtenbacher (Phasmatodea: Phylliidae: Phylliinae), A Leaf Insect Recently Recognized in Australia. Australian Entomological Magazine 15: 3–5.

Rouse WHD (1942) Nonnos Dionysiaca, with an English translation by W. H. D. Rouse. Harvard University Press, Cambridge, Massachusetts, United States, 517 pp.

Sands DPA, New TR (2008) Conservation status and needs of butterflies (Lepidoptera) on the Torres Strait Islands. Insect Conservation and Islands 12: 131–138. https://doi.org/10.1007/978-1-4020-8782-0_11

Schneeberg K, Bauernfeind R, Pohl H (2017) Comparison of cleaning methods for delicate insect specimens for scanning electron microscopy. Microscopy Research and Technique 80: 1199–1204. https://doi.org/10.1002/jemt.22917

Simon S, Letsch H, Bank S, Buckley TR, Donath A, Liu S, Machida R, Meusemann K, Misof B, Podsiadlowski L, Zhuo X, Wipfler B, Bradler S (2019) Old World and New World Phasmatodea: Phylogenomics Resolve the Evolutionary History of Stick and Leaf Insects. Frontiers in Ecology and Evolution 7: 1–14. https://doi.org/10.3389/fevo.2019.00345

Smith WA (1966) A record of *Phyllium* (Phasmida: Phyllidae) from Queensland. Journal of the Entomological Society of Queensland 5: 45.

Taylor RW (1972) Biogeography of insects of New Guinea and Cape York Peninsula. In: Walker D (Ed.) Bridge and barrier: the natural and cultural history of Torres Strait. Research School of Pacific Studies, Australian National University, Canberra, 213–230.

Yokoyama Y, Lambeck K, Deckker PDe (2000) Timing of the Last Glacial Maximum from observed sea-level minima. Nature 406: 1998–2001. https://doi.org/10.1038/35021035

ZooKeys 939: 29–43 (2020)
doi: 10.3897/zookeys.939.51272
https://zookeys.pensoft.net

RESEARCH ARTICLE

A peer-reviewed open-access journal
ZooKeys
Launched to accelerate biodiversity research

Notes on *Macroteleia* Westwood (Hymenoptera, Scelionidae) from China, with description of a new species

Chun-Dan Hong[1], Ovidiu Alin Popovici[2], Hua-Yan Chen[3]

1 *Bureau of Agriculture and Rural Affairs of Longhu, Shantou 515000, China* **2** *University "Al. I. Cuza" Iași, Faculty of Biology, CERNESIM, Boulevard Carol I 11, RO-700506, Iași, Romania* **3** *State Key Laboratory of Biocontrol, School of Life Sciences / School of Ecology, Sun Yat-sen University, Guangzhou 510275, China*

Corresponding author: Hua-yan Chen (chenhuayan@mail.sysu.edu.cn)

Academic editor: K. van Achterberg | Received 19 February 2020 | Accepted 19 April 2020 | Published 9 June 2020

http://zoobank.org/577E10AF-8E82-4B19-AEDD-0AA5B20E5878

Citation: Hong C-D, Popovici OA, Chen H-Y (2020) Notes on *Macroteleia* Westwood (Hymenoptera, Scelionidae) from China, with description of a new species. ZooKeys 939: 29–43. https://doi.org/10.3897/zookeys.939.51272

Abstract

The wasp genus *Macroteleia* Westwood from China has been previously revised, but some species are only known from males. Here the females of two known species are described: *M. carinigena* Chen, Johnson, Masner & Xu and *M. gracilis* Chen, Johnson, Masner & Xu. In addition, one species is redescribed: *M. variegata* Kozlov & Kononova; and one species is described as new: *Macroteleia xui* Hong & Chen, **sp. nov.** *Macroteleia ischtvani* Kononova, **syn. nov.** is proposed as new synonym of *M. variegata* Kozlov & Kononova.

Keywords

Egg parasitoid, new distribution record, Platygastroidea, redescription, taxonomy

Introduction

The species of the wasp genus *Macroteleia* Westwood are egg parasitoids of long-horned grasshoppers (Orthoptera, Tettigoniidae) (Muesebeck 1977). These wasps are spread worldwide, except Antarctica, but most species occur in tropical and subtropical regions (Masner 1976; Chen et al. 2013). Species of *Macroteleia* are easily recognized because of the unarmed propodeum, the marginal vein as long as, or longer,

than the stigmal vein, and the peculiar shape of T6 in female (strongly compressed laterally) (Chen et al. 2013). The Chinese fauna of *Macroteleia* have been revised by Chen et al. (2013), with several new species described from the tropical and subtropical regions of China. However, of the seven new species proposed by Chen et al. (2013), three species were described based only on males. Considering the sexual dimorphism (displayed especially in the structure of the antenna and in the shape and the structure of the metasoma) and the importance of the shape of metascutellum and the structure of propodeum (divided, or not, into two lobes) in females to separate species of *Macroteleia* (Muesebeck 1977; Chen et al. 2013), the discovery of females in species known only from the males should enhance our knowledge of the concept of these species.

In this study the females of two species, previously known only from males, are described. Furthermore, a newly recorded species (*Macroteleia variegata* Kozlov & Kononova, 1987) from China is redescribed and another, *Macroteleia xui* is described as new for science.

Materials and methods

This work is based upon specimens in the following collections, with abbreviations used in the text: **BMNH**, The Natural History Museum, London, UK; **IZCAS**, Institute of Zoology, Chinese Academy of Sciences, Beijing, China; **SCAU**, Hymenoptera Collection, South China Agricultural University, Guangzhou, China; **SYSBM**, Sun Yat-sen University, The Museum of Biology, Guangzhou, China; **UASK**, Schmalhausen Institute of Zoology of National Academy of Sciences of Ukraine, Kiev, Ukraine.

Abbreviations and morphological terms used in text: **A1, A2, ..., A12**: antennomere 1, 2, …, 12; **LOL**: lateral ocellar line, shortest distance between inner margins of median and lateral ocelli (Masner 1980); **OOL**: ocular ocellar line, shortest distance from inner orbit and outer margin of posterior ocellus (Masner 1980); **POL**: posterior ocellar line, shortest distance between inner margins of posterior ocelli (Masner 1980); **T1, T2, ..., T7**: metasomal tergite 1, 2, ..., 7; **S1, S2, …, S7**: metasomal sternite 1, 2, …, 7. Morphological terminology otherwise generally follows Masner (1980), Mikó et al. (2007) and Chen et al. (2013).

In the Material examined section the specimens studied are recorded in an abbreviated format, using unique identifiers (numbers prefixed with "SCAU") for the individual specimens. The label data for all specimens have been georeferenced and recorded in the Hymenoptera Online database; details on the data associated with these specimens can be accessed at mbd-s.asc.ohio-state.edu by entering the identifier in the search form (note the space between the acronym and the number).

Images and measurements were made using Nikon SMZ25 microscope with a Nikon DS-Ri 2 digital camera system. Images were post-processed with Abobe Photoshop CS6 Extended.

Taxonomy

***Macroteleia carinigena* Chen, Johnson, Masner & Xu, 2013**
http://zoobank.org/42427976-EE7B-4B81-8910-EF308AE8716E
Figures 1–6

Macroteleia carinigena Chen, Johnson, Masner & Xu, 2013: 13, 19 (original description, keyed).

Material examined. ***Holotype***, male: China: Hainan Prov., Mount Yinggeling, 28.V.2007, L.-Q. Weng, SCAU 000032 (deposited in SCAU). ***Paratypes*:** China: 1 male, Hainan, Mt Diaoluo, 18°39'N, 109°53'E, 29.V.2007, Bin Xiao, SCAU 000033 (SCAU); 1 male, China: Hainan, Mt Diaoluo, 18°39'N, 109°53'E, 29.V.2007, Jingxian Liu, SCAU 000034 (SCAU).

Other material. China: 2 females, Hainan, Mt Diaoluoshan, 18°39'N, 109°53'E, 16–17.VII.2006, Jingxian Liu, SCAU 3040365, 3040366, 3048585 (SYSBM).

Description. Female. Body length: 6.88–6.94 mm ($N = 3$).

***Color*.** Body black; mandible reddish brown; palpi yellow; legs yellow throughout; A1–A5 yellow, remainder of antenna dark brown to black; fore wing hyaline.

***Head*.** Transverse in dorsal view, 1.4–1.56 × as wide as long, slightly wider than mesosoma; lateral ocellus contiguous with inner orbit of compound eye; POL 1.5–1.67 × LOL; occipital carina continuous medially, irregularly crenulate throughout; central keel absent; medial frons punctate with irregularly shaped smooth area; ventrolateral frons punctate rugulose to densely punctate; frons below median ocellus punctate reticulate; vertex densely punctate with punctures in part contiguous; gena with a strong carina parallel to occipital carina, punctate rugose dorsally; length of A3 1.24–1.30 × length of A2.

***Mesosoma*.** Cervical pronotal area densely punctate; dorsal pronotal area areolate; lateral pronotal area smooth dorsally, irregularly depressed ventrally; netrion densely finely punctate; notaulus shallow, irregularly foveolate; middle lobe of mesoscutum densely punctate, becoming denser anteriorly and posteriorly; lateral lobes of mesoscutum densely punctate throughout; mesoscutellum densely punctate, becoming denser laterally; metascutellum transverse, posterior margin slightly pointed medially, longitudinally carinate; propodeum continuous medially, not divided into two separated lobes, posterior margin narrowly notched medially, each side with rugose sculpture covered by dense, recumbent, white setae; upper mesepisternum with a row of robust longitudinal carinae below subalar pit; lower mesepisternum densely punctate rugulose; mesopleural depression smooth; metapleuron longitudinally striate with coarse punctures in interstices, or longitudinally punctate rugose.

***Legs*.** Slender; hind femur weakly swollen, 4.00–4.55 × as long as its maximum width; hind tibia without spines over outer surface; hind basitarsus 7.67–9.00 × as long as its maximum width.

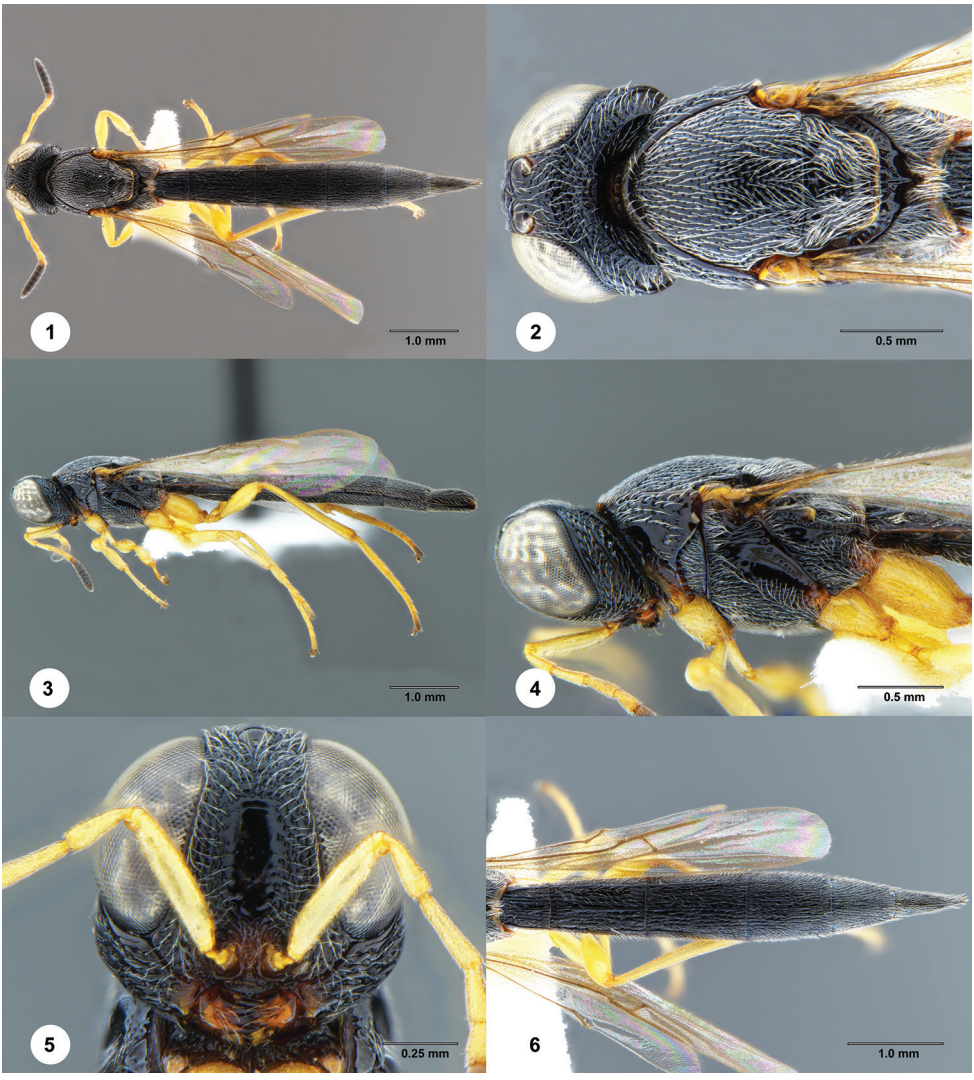

Figures 1–6. *Macroteleia carinigena* Chen, Johnson, Masner & Xu, female (SCAU 3048585) **1** dorsal habitus **2** head and mesosoma, dorsal view **3** lateral habitus **4** head and mesosoma, lateral view **5** head, anterior view **6** metasoma, dorsal view.

Wings. Apex of fore wing extending from as far as basal of T5; R 1.46–1.60 × as long as r-rs, R1 1.95–2.43 × length of R.

Metasoma. Posterior margin of transverse sulcus on T2 strongly convex; sublateral tergal carinae well developed on T1–T3, weakly developed on anterior half of T4; T1–T4 sparsely longitudinally striate medially, with delicate punctures in interstices, punctate rugulose laterally; T5–T6 densely longitudinally striate, with numerous delicate punctures in interstices; length of T3 1.28–1.4 × length of T6; T5 distinctly longer

than wide; S2–S6 densely longitudinally striate, with delicate punctures in interstices; prominent longitudinal median carina present on S2–S5.

Distribution. China (Hainan).

Macroteleia emarginata Dodd, 1920

http://zoobank.org/42427976-EE7B-4B81-8910-EF308AE8716E
Figures 7–12

Macroteleia emarginata Dodd, 1920: 326 (original description); Masner 1965: 82 (type information); Johnson 1992: 426 (cataloged, type information); Chen, Johnson, Masner and Xu 2013: 12, 14, 33 (description, keyed, distribution).

Material examined. ***Holotype***, female, Malaysia: Kuching [Quop, Oct. 1906], [P. Cameron Coll. 1914-110], [*Macroteleia flavipes* Cam. Type Borneo], [*Macroteleia emarginata* Dodd. ♀ Type], [Type 9.480] (deposited in BMNH).

Other material. China: 2 females, 1 male, Yunnan, Xishuangbanna, Menghai, Bulangshan Village, 21°44.746'N, 100°26'E, 1610 m, Area D, grass, MT (Malaise trap), 20.VI–20.VII.2018, Li Ma, SCAU 3048682–3048684 (SYSBM); 2 females, Yunnan, Xishuangbanna, Menghai, Bulangshan Village, 21°44.746'N, 100°26'E, 1610 m, Area D, grass, MT (Malaise trap), 17.V–20.VI.2018, Li Ma, SCAU 3048685, 3048686 (SYSBM).

Distribution. China (Fujian, Hunan, Guangdong, Hainan, Guizhou, Yunnan); Malaysia.

Comments. Chen et al. (2013) recorded this species from the Oriental Region of China based upon the careful description provided by Alan Dodd in the original publication. Here, we provide the images of the holotype and additional records of this species from China. The specimens examined by Chen et al. (2013) and the ones we record here match well with the holotype.

Macroteleia gracilis Chen, Johnson, Masner & Xu, 2013

http://zoobank.org/FC1AC5B9-9F13-4AC7-9057-7DD106F227AB
Figures 13–18

Macroteleia gracilis Chen, Johnson, Masner & Xu, 2013: 14, 40 (original description, keyed).

Material examined. China: 1 female, Guangdong, Nanling Nature Reserve, 24°54'N, 113°00'E, 9–18.VII.2004, Juanjuan Ma, SCAU 3040368 (SYSBM); 1 male, Hainan, Haikou, Hainan University, Haidian campus, orchard, 20°3'15"N, 110°19'21"E, MT (Malaise trap), 14–20.IX.2017, Youxing Zhou, SCAU 3040367 (SYSBM); 1 male, Hainan, Haikou, Hainan University, Haidian campus, orchard,

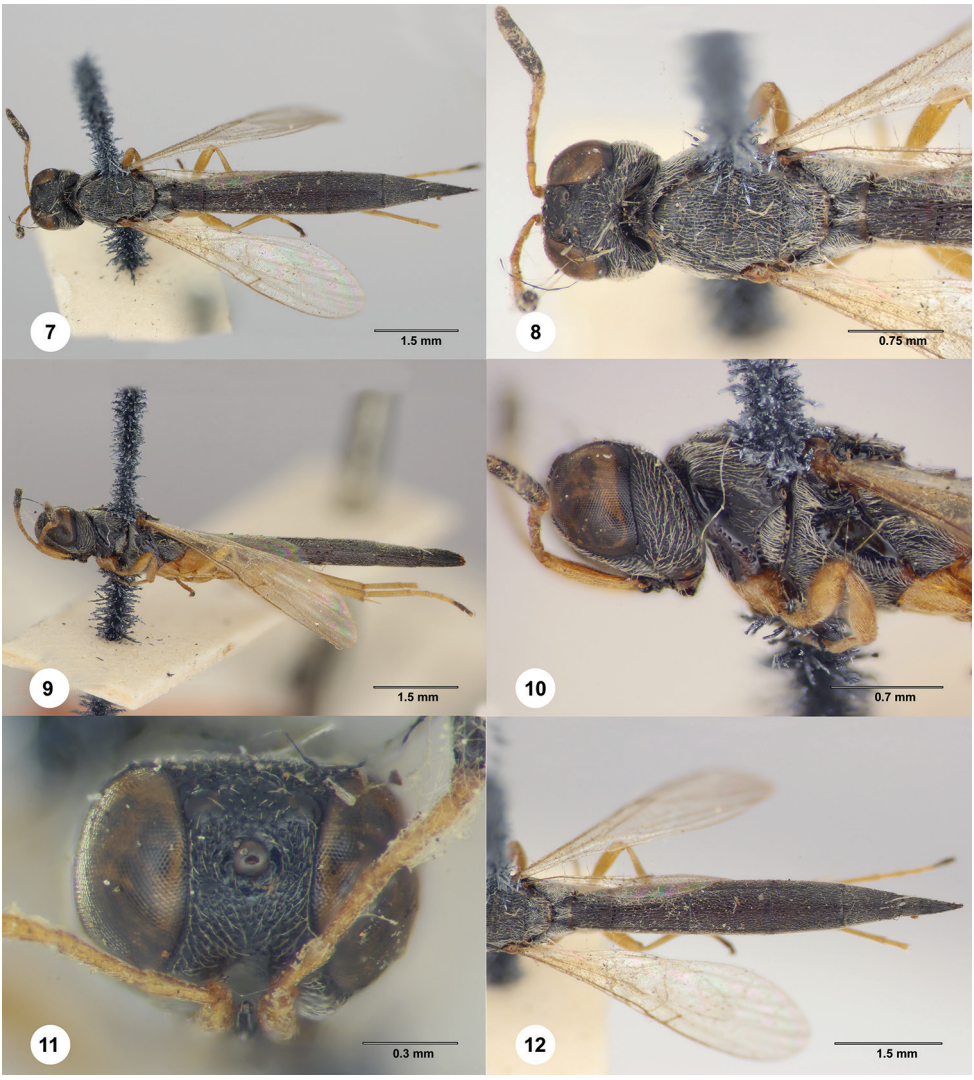

Figures 7–12. *Macroteleia emarginata* Dodd, holotype, female (B.M. TYPE HYM. 9.480) **7** dorsal habitus **8** head and mesosoma, dorsal view **9** lateral habitus **10** head and mesosoma, lateral view **11** head, anterior view **12** metasoma, dorsal view.

20°3'15"N, 110°19'21"E, MT (Malaise trap), 3–9.VIII.2017, Youxing Zhou, SCAU 3040368 (SYSBM).

Description. Female. Body length: 6.17 mm (N = 1).

Color. Body black; mandible reddish brown; palpi yellow; legs yellow throughout; A1–A6 yellow, remainder of antenna dark brown to black; fore wing hyaline.

Head. Transverse in dorsal view, 1.4–1.5 × as wide as long, slightly wider than mesosoma; lateral ocellus contiguous with inner orbit of compound eye; POL 1.5–1.54 ×

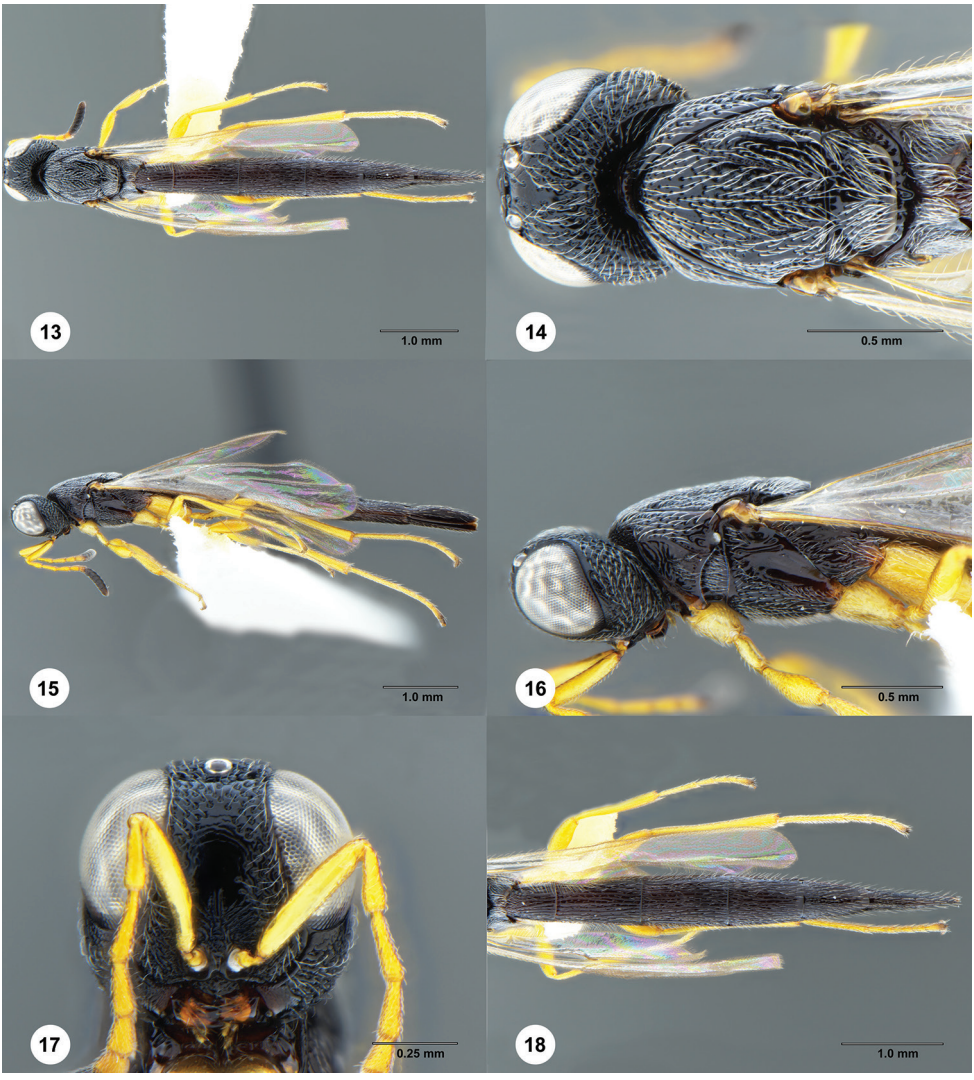

Figures 13–18. *Macroteleia gracilis* Chen, Johnson, Masner & Xu, female (SCAU 3048586) **13** dorsal habitus **14** head and mesosoma, dorsal view **15** lateral habitus **16** head and mesosoma, lateral view **17** head, anterior view **18** metasoma, dorsal view.

LOL; occipital carina continuous medially, irregularly punctate; central keel weakly developed, extending onto interantennal process; medial frons punctate rugose ventrally, with irregularly shaped smooth area dorsally; frons below median ocellus densely punctate; vertex sparsely punctate to smooth behind posterior ocelli, becoming densely punctate posteriorly; gena punctate rugose; length of A3 1.1–1.2 × length of A2.

Mesosoma. Cervical pronotal area densely punctate; dorsal pronotal area punctate rugulose; lateral pronotal area smooth dorsally, punctate rugulose ventrally; netrion

finely punctate rugulose; notaulus shallow, foveolate; middle lobe of mesoscutum densely punctate, sculpture becoming denser anteriorly; lateral lobes of mesoscutum densely finely punctate throughout; mesoscutellum densely finely punctate throughout; metascutellum transverse, posterior margin slightly pointed medially, longitudinally carinate; propodeum continuous medially, not divided into two separated lobes, posterior margin narrowly notched medially, each side with several irregular longitudinal carinae medially, otherwise punctate rugulose, covered by dense, recumbent, white setae; upper mesepisternum with a row of somewhat robust longitudinal carinae below subalar pit; lower mesepisternum variably smooth to punctate rugulose; mesopleural depression smooth; metapleuron longitudinally striate throughout.

***Legs*.** Slender; hind femur weakly swollen, 4.23–4.80 × as long as its maximum width; hind tibia without spines over outer surface; hind basitarsus 12.60–14.00 × as long as its maximum width.

***Wings*.** Apex of fore wing extending from as far as posterior margin of T4; R 2.06–2.46 × as long as r-rs, R1 1.63–1.90 × length of R.

***Metasoma*.** Posterior margin of transverse sulcus on T2 slightly convex; sublateral tergal carinae well developed on T1–T4, weakly developed on anterior half of T4; T1–T4 sparsely longitudinally striate medially, with delicate punctures in interstices, punctate rugulose laterally; T5–T6 densely longitudinally striate, with numerous delicate punctures in interstices; length of T3 0.90–0.95 × length of T6; T5 distinctly longer than wide; S2–S6 densely longitudinally striate, with delicate punctures in interstices; prominent longitudinal median carina present on S2–S4.

Distribution. China (Guangdong, Hainan).

Macroteleia xui Hong & Chen, sp. nov.

http://zoobank.org/9A0F15EC-FD9A-4BC2-BB64-8053834F46C9
Figures 19–24

Material examined. ***Holotype***, female: China: Hebei, Baoding, Hebei Agricultural Unv., West Campus, MT, 38°49'44"N, 115°27'1"E, 30.VIII–6.IX.2017, Fan Fan, SACU 3040364 (deposited in SYSBM). ***Paratypes*:** China: 1 female, Yunnan, Xishuangbanna, Menghai, Bulangshan Village, 1595 m, Area D, forest, 21°44.761'N, 100°25.959'E, 20.IV-20.VII.2018, MT (Malaise trap), Li Ma, SCAU 3040370 (SYSBM); 1 female, Shandong, Shanghe County, MT4, 37°16'4"N, 117°9'10"E, 18–24.VIII.2018, Jiahe Yan, SCAU 3048687 (SYSBM); 3 females, Shandong, Shanghe County, MT4, 37°16'4"N, 117°9'10"E, 7–14.IX.2018, Jiahe Yan, SCAU 3048593–3048595 (SYSBM).

Diagnosis. This species is most similar to *M. striativentris* Crawford in color and size but can be distinguished by the medially divided propodeum and triangular metascutellum.

Description. Female. Body length: 5.48–5.60 mm (N = 6).

***Color*.** Head and mesosoma black, metasoma dark brown to black; mandible brown with teeth dark brown; palpi yellow; legs pale brown throughout; A1–A6 yellow, remainder of antenna black; fore wing hyaline.

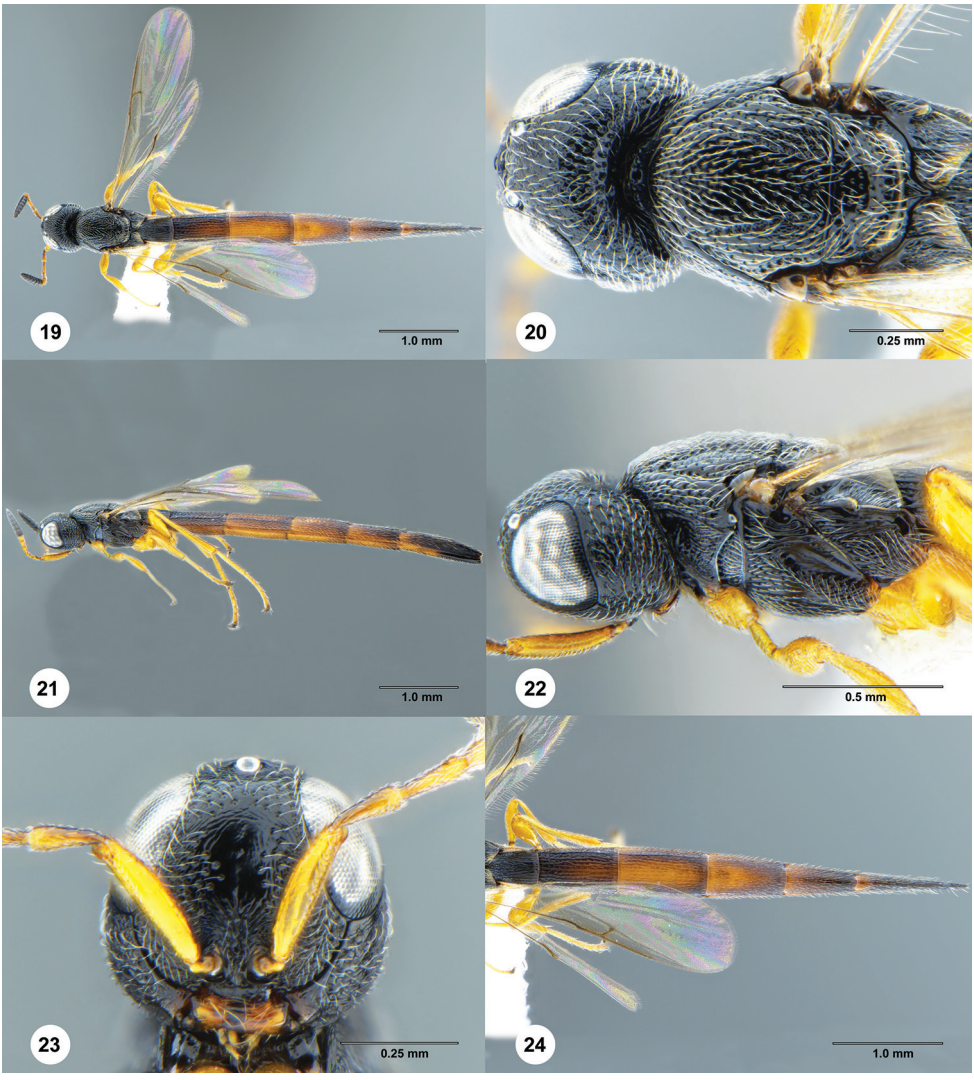

Figures 19–24. *Macroteleia xui* sp. nov., holotype, female (SACU 3040364) **19** dorsal habitus **20** head and mesosoma, dorsal view **21** lateral habitus **22** head and mesosoma, lateral view **23** head, anterior view **24** metasoma, dorsal view.

Head. Transverse in dorsal view, 1.4–1.5 × as wide as long, slightly wider than mesosoma; OOL short, 0.17–0.20 × times minimum diameter of lateral ocellus; POL 1.5–1.54 × LOL; occipital carina continuous medially, irregularly punctate; central keel weakly developed, extending onto interantennal process; medial frons punctate rugose ventrally, with irregularly shaped smooth area dorsally; frons below median ocellus punctate rugulose; posterior vertex sparsely punctate rugulose behind posterior ocelli, becoming densely punctate posteriorly; gena punctate rugose; length of A3 as long as A2.

***Mesosoma*.** Cervical pronotal area densely punctate; dorsal pronotal area punctate rugulose; lateral pronotal area smooth dorsally, punctate rugulose ventrally; netrion densely finely punctate; notaulus shallow, foveolate; mesoscutum densely punctate; mesoscutellum moderately finely punctate throughout; metascutellum triangular, strongly produced medially, extending into space between propodeal lobes; propodeum narrowly divided into two subtriangular lobes, each side with several irregular longitudinal carinae medially, otherwise punctate rugulose; upper mesepisternum with a row of robust longitudinal carinae below subalar pit; lower mesepisternum variably smooth to punctate rugulose; mesopleural depression smooth; metapleuron longitudinally striate dorsally, punctate rugose ventrally.

***Legs*.** Slender; hind femur weakly swollen, 3.4–4.0 × as long as its maximum width; hind tibia without spines over outer surface; hind basitarsus 10.60–11.20 × as long as its maximum width.

***Wings*.** Apex of fore wing extending from as far as middle of T4; R 1.97–2.06 × as long as r-rs, R1 1.83–1.90 × length of R.

***Metasoma*.** Posterior margin of transverse sulcus on T2 straight; sublateral tergal carinae well developed on T1–T3; T1–T3 densely longitudinally striate medially, with delicate punctures in interstices, punctate rugulose laterally; T4–T6 densely longitudinally striate, with numerous delicate punctures in interstices; length of T3 0.78–0.81 × length of T6; T5 distinctly longer than wide; S2–S6 densely longitudinally striate, with delicate punctures in interstices; prominent longitudinal median carina present on S2–S4.

Male. Unknown.

Etymology. This speices is named *xui* in honor of the late Professor Zaifu Xu for his great contribution to Chinese Hymenoptera taxonomy.

Distribution. China (Hebei, Shandong, Yunnan).

Macroteleia variegata Kozlov & Kononova, 1987

http://zoobank.org/720C6A99-4641-4BAE-9B1D-39D3B55FB607
Figures 25–36

Macroteleia variegata Kozlov & Kononova, 1987: 94, 95, 99 (original description, keyed); Kozlov and Kononova 1990: 190, 199 (description, keyed); Johnson 1992: 433 (cataloged, type information); Kononova 1995: 70 (keyed); Kononova and Petrov 2003: 606 (keyed); Kononova and Kozlov 2008: 234, 248 (description, keyed).
Macroteleia ischtvani Kononova, 2008: 234, 250 (original description, keyed), syn. nov.

Material examined. ***Holotype***, female, *M. variegata*: Russia: [Primorskiy kr., Shkotovskiy r-n, okr. Apisimovki, Kononova 3.8.1977] [Holotypus *Macroteleia variegata*, Kononova], UASK 0104 (deposited in UASK). ***Holotype***, female, *M. ischtvani*: Hungary: [Hungary, Tiszaizolátum TIAD, 1995.08.15, leg. JATE ökológia] [Holotypus, *M. ischtvani*, Kononova], UASK 0100 (deposited in UASK).

Other material. China: 1 male, Xinjiang, Gongliu County, Hetaogou, 43°25'38"N, 82°15'6"E, 1–2.VII.2016, Yicheng Li et al., yellow pan trap, SCAU 3048584 (SYSBM); 1 female, Hebei, Xiaowutai National Nature Reserve, 1364 m, 39°52.048'N, 114°56.446'E, 10–17.IX.2012, Malaise trap, Haiming Zhang, SCAU 3040369 (IZCAS); 1 female, Inner Mongolia, Xing'an Meng, 46°4'56"N, 122°2'15"E, 8.VIII.2011, Feng Yuan, SCAU 3041128 (IZCAS).

Redescription. Female. Body length: 5.20–5.37 mm (N = 2).

***Color*.** Head yellow with upper frons and vertex dark brown to black; mesosoma variably yellow to dark brown; mandible yellow with teeth dark brown; palpi yellow; legs yellow throughout; A1–A5 brown, remainder of antenna dark brown to black; fore wing hyaline.

***Head*.** Transverse in dorsal view, 1.5–1.65 × as wide as long, as wide as mesosoma; OOL short, 0.20–0.30 × times minimum diameter of lateral ocellus; POL 1.38–1.4 × LOL; occipital carina interrupted medially; central keel weakly developed, extending onto interantennal process; medial frons punctate rugose ventrally, with irregularly shaped smooth area dorsally; frons below median ocellus densely punctate; posterior vertex rugulose behind posterior ocelli, becoming punctate reticulate posteriorly; gena punctate rugose; length of A3 1.1–1.2 × length of A2.

***Mesosoma*.** Cervical pronotal area densely punctate; dorsal pronotal area punctate rugulose; lateral pronotal area smooth dorsally, punctate rugulose ventrally; netrion densely finely punctate; notaulus shallow, foveolate; middle lobe of mesoscutum densely punctate, sculpture becoming denser anteriorly and posteriorly; lateral lobes of mesoscutum densely finely punctate throughout; mesoscutellum densely finely punctate throughout; metascutellum transverse, posterior margin slightly pointed medially, longitudinally carinate; propodeum continuous medially, not divided into two separated lobes, posterior margin narrowly notched medially, each side with several irregular longitudinal carinae medially, otherwise punctate rugose, covered by dense, recumbent, white setae; upper mesepisternum with a row of somewhat robust longitudinal carinae below subalar pit; lower mesepisternum variably smooth to punctate rugulose; mesopleural depression smooth; metapleuron punctate rugose throughout.

***Legs*.** Slender; hind femur weakly swollen, 3.60–3.80 × as long as its maximum width; hind tibia without spines over outer surface; hind basitarsus 9.60–10.20 × as long as its maximum width.

***Wings*.** Apex of fore wing extending from as far as middle of T5; R 1.56–1.67 × as long as r-rs, R1 1.63–1.70 × length of R.

***Metasoma*.** Posterior margin of transverse sulcus on T2 strongly convex; sublateral tergal carinae well developed on T1–T2, weakly developed on anterior half of T3; T1 densely longitudinally striate, with punctate rugulose sculpture in interstices anteriorly, punctate rugulose laterally; T2–T4 densely longitudinally striate with numerous large delicate punctures in interstices; T5–T6 densely punctate; length of T3 1.35–1.40 × length of T6; T5 distinctly wider than long; S2–S4 densely longitudinally striate, with delicate punctures in interstices; S5–S6 densely finely punctate; prominent longitudinal median carina absent on sternites.

Figures 25–30. 25, 26 *Macroteleia ischtvani* Kononova, holotype, female (UASK 0100): **25** dorsal habitus **26** lateral habitus **27, 28** *Macroteleia variegata* Kozlov & Kononova, holotype, female (UASK 0104): **27** dorsal habitus **28** lateral habitus **29, 30** *Macroteleia variegata* Kozlov & Kononova, male, (SCAU 3048584) **29** dorsal habitus **30** apex of metasoma, dorsal view.

Male. Differing from female as follows: body length 3.76 mm (N = 1); A1 yellow, the remainder of antenna dark brown to black; mesosoma dark brown to black dorsally, yellow laterally; T1–T4 densely longitudinally striate, with numerous delicate punctures in interstices; T5–T6 densely and finely punctate; T7 largely smooth except finely rugulose posterolaterally; T6 wider than long; length of T6 2.50 × length of T7; T7 transverse, apex truncate; length of T7 as long as S7; S7 granulate.

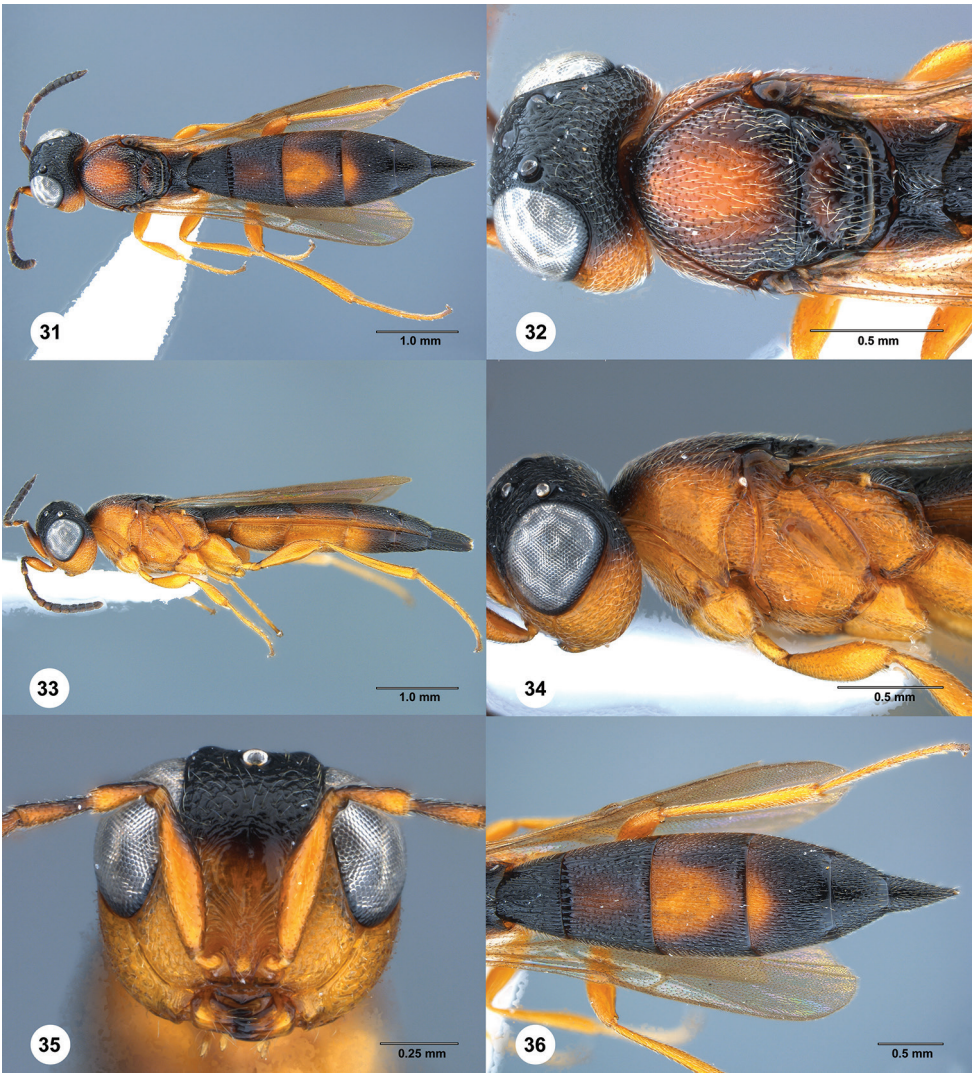

Figures 31–36. *Macroteleia variegata* Kozlov & Kononova, female, (SCAU 3041128) **31** dorsal habitus **32** head and mesosoma, dorsal view **33** lateral habitus **34** head and mesosoma, lateral view **35** head, anterior view **36** metasoma, dorsal view.

Distribution. China (Xinjiang, Hebei, Inner Mongolia); Russia, Hungary.

Comments. *Macroteleia variegata* is recorded here from China for the first time. We examined the holotypes of *M. variegata* and *M. ischtvani* and found no distinct differences between the two species except the trivial variations in colors and the relative length of metasomal tegites, which Kononova and Kozlov (2008) used heavily in the key to species of the Palearctic *Macroteleia*. Therefore, we here treat *M. ischtvani* as a synonym of *M. variegata*. We also examined a paratype of *M. elissa* Kozlov & Kon-

onova, 1987 deposited in UASK that we believe is conspecific with *M. variegata*, but we cannot confirm if *M. elissa* should be treated as a synonym of *M. variegata* until we can examine the holoype of *M. elissa*. Color and size variations could be due to temperature or host egg size during the developmental stage of the parasitoids, which are quite commonly seen in Scelionidae. DNA barcoding could be useful in species delimitation for the species in such situations.

Acknowledgments

Thanks to L. Musetti and S. Hemly (The Ohio State University) for critical assistance with specimen databasing. Thanks also to the journal reviewers, Norman F. Johnson (The Ohio State University) and Ali Asghar Talebi (Tarbiat Modares University) for their help in improving the manuscript. This material is based upon work supported in part by the National Natural Science Foundation of China (31900346).

References

Chen H-y, Johnson NF, Masner L, Xu Z-f (2013) The genus *Macroteleia* Westwood (Hymenoptera, Platygastridae s. l., Scelioninae) from China. ZooKeys 300: 1–98. https://doi.org/10.3897/zookeys.300.4934

Dodd AP (1920) Notes on the exotic Proctotrupoidea in the British and Oxford University Museums, with descriptions of new genera and species. Transactions of the Entomological Society of London 1919: 321–382. https://doi.org/10.1111/j.1365-2311.1920.tb00008.x

Johnson NF (1992) Catalog of world Proctotrupoidea excluding Platygastridae. Memoirs of the American Entomological Institute 51: 1–825.

Kononova SV (1995) [Fam. Scelionidae.] In: Lehr PA (Ed.) Key to insects of Russian Far East in six volume (Vol. 4). Neuropteroidea, Mecoptera, Hymenoptera. Part 2. Hymenoptera. Dal'nauka, Vladivostok, 600 pp.

Kononova SV, Kozlov MA (2008) Scelionids of the Palearctic (Hymenoptera, Scelionidae). Subfamily Scelioninae. Tovarishchestvo Nauchnykh Izdanii KMK, Saint Petersburg, 489 pp.

Kononova SV, Petrov S (2003) New species of egg parasites of the family Scelionidae (Hymenoptera, Proctotrupoidea) of the Palearctic fauna.] Zoologicheskii Zhurnal 82: 603–612.

Kozlov MA, Kononova SV (1987) New Palearctic species of the genus *Macroteleia* Westwood, 1835 (Hymenoptera, Scelionidae, Scelioninae).] In: Lehr PA, Storozheva NA (Eds) [New data on the systematics of insects of the Far East.] Acad. Sci. USSR, Far East Branch, Biology & Soil Institute, Vladivostok, 144 pp.

Kozlov MA, Kononova SV (1990) [Scelioninae of the Fauna of the USSR (Hymenoptera, Scelionidae, Scelioninae).] Nauka, Leningrad, 344 pp.

Masner L (1965) The types of Proctotrupoidea (Hymenoptera) in the British Museum (Natural History) and in the Hope Department of Entomology, Oxford. Bulletin of the British Museum (Natural History) Entomology Supplement 1: 1–154.

Masner L (1976) Revisionary notes and keys to world genera of Scelionidae (Hymenoptera: Proctotrupoidea). Memoirs of the Entomological Society of Canada 97: 1–87. https://doi.org/10.4039/entm10897fv

Masner L (1980) Key to genera of Scelionidae of the Holarctic region, with descriptions of new genera and species (Hymenoptera: Proctotrupoidea). Memoirs of the Entomological Society of Canada 113: 1–54. https://doi.org/10.4039/entm112113fv

Mikó I, Vilhelmsen L, Johnson NF, Masner L, Pénzes Z (2007) Skeletomusculature of Scelionidae (Hymenoptera: Platygastroidea): head and mesosoma. Zootaxa 1571: 1–78. https://doi.org/10.11646/zootaxa.1571.1.1

Muesebeck CFW (1977) The parasitic wasps of the genus *Macroteleia* Westwood of the New World (Hymenoptera, Proctotrupoidea, Scelionidae). U.S. Department of Agriculture Technical Bulletin 1565: 1–57.

ZooKeys 939: 45–64 (2020)
doi: 10.3897/zookeys.939.49309
https://zookeys.pensoft.net

RESEARCH ARTICLE

A peer-reviewed open-access journal
ZooKeys
Launched to accelerate biodiversity research

A revised taxonomy of Asian snail-eating snakes *Pareas* (Squamata, Pareidae): evidence from morphological comparison and molecular phylogeny

Ping Wang[1,2], Jing Che[3], Qin Liu[1], Ke Li[1], Jie Qiong Jin[3], Ke Jiang[3], Lei Shi[2], Peng Guo[1]

1 *College of Life Science and Food Engineering, Yibin University, Yibin 644007, China* **2** *College of Animal Science, Xinjiang Agricultural University, Urumqi 830052, China* **3** *State Key Laboratory of Genetic Resources and Evolution, Kunming Institute of Zoology, Chinese Academy of Sciences, Kunming 650223, China*

Corresponding author: Peng Guo (ybguop@163.com)

Academic editor: Robert Jadin | Received 13 December 2019 | Accepted 16 April 2020 | Published 9 June 2020

http://zoobank.org/312215D0-BED2-4996-AECE-6FD0A5DBF2D8

Citation: Wang P, Che J, Liu Q, Li K, Jin JQ, Jiang K, Shi L, Guo P (2020) A revised taxonomy of Asian snail-eating snakes *Pareas* (Squamata, Pareidae): evidence from morphological comparison and molecular phylogeny. ZooKeys 939: 45–64. https://doi.org/10.3897/zookeys.939.49309

Abstract

The Asian snail-eating snakes *Pareas* is the largest genus of the family Pareidae (formerly Pareatidae), and widely distributed in Southeast Asia. However, potential diversity remains poorly explored due to their highly conserved morphology and incomplete samples. Here, on basis of more extensive sampling, interspecific phylogenetic relationships of the genus *Pareas* were reconstructed using two mitochondrial fragments (cyt b and ND4) and two nuclear genes (c-mos and Rag1), and multivariate morphometrics conducted for external morphological data. Both Bayesian Inference and Maximum Likelihood analyses consistently showed that the genus *Pareas* was comprised of two distinct, monophyletic lineages with moderate to low support values. Based on evidences from molecular phylogeny and morphological data, cryptic diversity of this genus was uncovered and two new species were described. In additional, the validity of *P. macularius* is confirmed.

Keywords

Molecular, morphology, new species, snakes, southeast Asia, systematics

Introduction

Pareidae Romer, 1956 is a small family of snakes found largely in Southeast Asia, including the Malay Archipelago, Indo China Peninsula, Bhutan, Bangladesh, India,

and China (Zhao 2006; Das 2012; Uetz et al. 2019). It was once considered a subfamily (called Pareatinae) of Colubridae (Smith 1943; Zhao et al. 1998; Zug et al. 2001; Zhao 2006). However, an increasing number of molecular phylogenetic studies have revealed that it is not closely related to the colubrids, and thus has been elevated to family rank (called Pareatidae) (Slowinski and Lawson 2002; Kelly et al. 2003; Lawson et al. 2005; Vidal et al. 2007; Pyron et al. 2013). Recently, Savage (2015) corrected the spelling of Pareatidae to Pareidae. The family Pareidae encompasses 26 species in four genera (*Aplopeltura* Duméril, 1853; *Asthenodipsas* Peters, 1864; *Pareas* Wagler, 1830; and *Xylophis* Beddome, 1878) divided into two subfamilies (Pareinae and Xylophiinae) (Deepak et al. 2018; Uetz et al. 2019).

Pareas is the largest genus of Asian snail-eating snakes in Pareidae and contains 14 species (Uetz et al. 2019). Due to its specialized feeding (terrestrial snails and slugs) and foraging behavior, the systematics and evolutionary biology of this group have received much attention in recent years (Hoso and Hori 2008; Hoso et al. 2010; Guo et al. 2011; Vogel 2015; You et al. 2015; Hoso 2017), and considerable progress has been made for resolving *Pareas* systematics (Guo et al. 2011; Pyron et al. 2013; You et al. 2015). For example, based on integrated mitochondrial sequence phylogeny, nuclear haplotype network, and multivariate morphometrics You et al. (2015) explored the taxonomic status of *Pareas* species from Taiwan, including the Ryukyus and adjacent regions. Their results consistently recovered *P. formosensis* Denburgh, 1909 and *P. komaii* Maki,1931 as valid species and *P. compressus* Oshima, 1910 as a junior synonym of *P. formosensis*. In addition, the validity of *P. chinensis* Barbour, 1912 was supported and a new species *P. atayal* You, Poyarkov & Lin, 2015 was described from Taiwan, China (You et al. 2015).

Due to its wide distribution and morphological conservativeness, however, the taxonomy of *Pareas* remains controversial despite the increasing research (Guo et al. 2011; Loredo et al. 2013; Guo and Zhang 2015; Vogel 2015; You et al. 2015). Previous studies on DNA-based phylogeny have indicated that *Pareas* is not monophyletic, but contains two highly supported clades, consistent with scale characters (Guo et al. 2011). However, due to incomplete samples and insufficient morphological data, Guo et al. (2011) deferred making a decision on the division of *Pareas*.

Here, using an integrated taxonomic methods and more extensive sampling, we reconstruct phylogenetic relationships of *Pareas* based on mitochondrial and nuclear DNA, and conducted a morphological comparison between species and populations. Our main goal was to clarify interspecific relationships and explore whether cryptic diversity was present within this diverse Asian snail-eating snakes *Pareas*.

Materials and methods

Molecular phylogenetic sampling and sequencing

In total, 52 individuals of *Pareas* representing ten putative species and two unidentified taxa were collected from Southeast Asia through fieldwork or tissue loans from

colleagues and museums (Suppl. material 1: Appendix S1). Additional sequences representing 12 species were retrieved from previous studies (Kraus and Brown 1998; You et al. 2015; Figueroa et al. 2016; Deepak et al. 2018). Representatives of *Aplopeltura*, *Asthenodipsas*, and *Xylophis* were also included to investigate the monophyly of *Pareas*.

Total DNA was extracted from liver, muscle or skin preserved in 85% ethanol using an OMEGA DNA Kit (Omega Bio-Tek, Inc., Norcross, GA, USA). The sequences of two mitochondrial gene fragments: cytochrome b (cyt b) and NADH dehydrogenase subunit 4 (ND4), as well as two nuclear genes: oocyte maturation factor mos (c-mos) and recombination activating gene 1 (Rag1) were amplified by polymerase chain reaction (PCR) using primers L14910/H16064 (Burbrink et al. 2000), ND4/Leu (Arèvalo et al. 1994), S77/S78 (Lawson et al. 2005), and R13/R18 (Groth and Barrowclough 1999), respectively. The cycling parameters were identical to those described in the above studies. The double-stranded products were purified and sequenced at Genewiz Co. (Suzhou, China). Sequences were edited and managed manually using SEQMAN in LASERGENE.v7.1 (DNASTAR Inc., Madison, WI, USA), MEGA 7 (Kumar et al. 2016), and GENEIOUS BASIC 4.8.4 (Kearse et al. 2012). For individuals which were detected to be heterozygous in nuclear gene sequences, they were phased using the software program PHASE with default sets of iterations, burn-in, and threshold (Stephens et al. 2001), on the web-server interface SEQPHASE (Flot 2010). One of the phased copies was selected at random to represent each individual in subsequent analyses.

Phylogenetic analyses

Phylogenetic analyses were conducted using Bayesian inference (BI) and Maximum Likelihood (ML) methods with *Xenodermus javanicus* Reinhardt, 1836, *Gloydius brevicaudus* Stejneger, 1907, and *Lycodon rufozonatus* Cantor, 1842 selected as outgroups based on previous work (Guo et al. 2011; Deepak et al. 2018). Phylogenetic trees were estimated separately for mitochondrial DNA fragments (cyt b and ND4) and nuclear genes (c-mos and Rag1). The best-fit substitution model was selected in PARTITIONFINDER 2.1.1 (Lanfear et al. 2017) with Akaike Information Criterion (AIC).

The BI analyses were performed using MRBAYES 3.2 (Ronquist et al. 2012) with three independent runs of four Markov chains. Each run consisted of ten million generations, started from random trees and sampled every 1 000 generations, with the first 25% discarded as burn-in. Convergence was assessed by examining effective sample sizes and likelihood plots through time in TRACER v1.6 (Rambaut et al. 2014). The resultant trees were combined to calculate Bayesian posterior probabilities (PP) for each node, with nodes of PP ≥ 95% considered strongly supported (Felsenstein 2004). The ML analyses were completed in RAXMLGUI 1.5 (Silvestro and Michalak 2012) under the GTRGAMMA model with 1000 non-parametric bootstraps to replicate topology and assess branch support. Nodes with bootstrap support values (BS) ≥ 70% were considered strongly supported (Hillis and Bull 1993).

Average divergence estimates were calculated from cyt b or ND4 data among congeners under the K2P model with 1 000 bootstraps using MEGA 7 (Kumar et al. 2016).

Morphological examination

A suite of characters was examined and recorded from 42 voucher specimens (Appendix 1). Except for snout-vent length (SVL) and tail length (TL), which were measured using a measuring tape to the nearest 1 mm, all other characters were measured and recorded following Zhao (2006). For comparison, data for other species were taken from prior published work (Boulenger 1900, 1905; Zhao et al. 1998; Grossmann and Tillack 2003; Guo and Deng 2009; Guo et al. 2011; Loredo et al. 2013; Vogel 2015; You et al. 2015; Hauser 2017).

Results

Sequence data

A total of 1 767 (1 095 bp from cyt b, 672 bp from ND4) and 1 635 (612 bp from c-mos and 1 023 bp from Rag1) aligned base pairs were obtained from the two mtDNA fragments and two nuclear genes, respectively. Sequences were translated into amino acids to confirm that no pseudogenes had been amplified. Novel sequences generated were deposited in GenBank (Suppl. material 1: Appendix S1).

Phylogenetic relationships

The best-fit model selected by PARTITIONFINDER was three-partition (partitioned by codon positions) for both mtDNA and nDNA datasets (Table 1). BI and ML analyses based on two separate datasets depicted consistent topological trees, which are in general accordance with those of Guo et al. (2011) and You et al. (2015).

All analyses strongly supported monophyly of Pareidae as a whole and reciprocal monophyly of *Aplopeltura* (lineage C), *Asthenodipsas* (lineage D), and *Xylophis* (lineage E) (Figs 1, 2).

Monophyly of *Pareas* was supported by either analysis based on mtDNA or nDNA-based BI analysis with moderate support values, and ML analysis based on nDNA data with high support value. Here, *Pareas* consists of two highly supported lineages (A and B). Lineage B is composed of *P. carinatus* Boie, 1828, *P. nuchalis* Boulenger, 1900, and a clade containing four specimens from southern Yunnan, China (Figs 1, 2). Lineage A contains the remaining species, with each putative species and relationships between congeners being highly supported; the specimens from Mengzi, Yunnan, China, formed a well-supported clade, close to *P. hamptoni* Boulenger, 1905.

Divergence estimates

Table 2 provides the mean K2P divergences among the four lineages (A–D). Lineage A diverged from B by an average genetic distance of 21.3%, which is much higher than that between genera *Aplopeltura* and *Asthenodipsas* (15.1%).

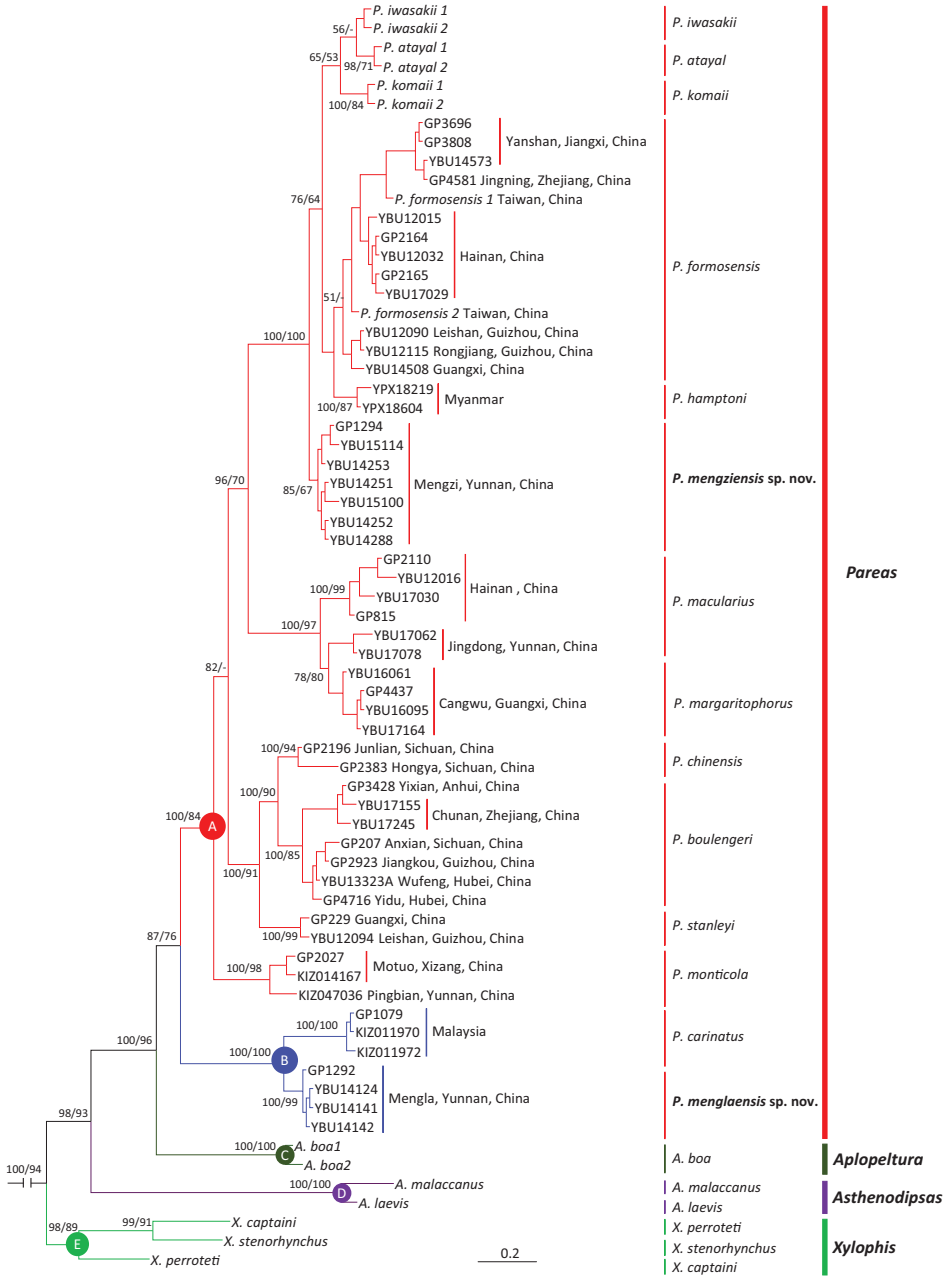

Figure 1. Bayesian inference tree of the Pareidae based on nDNA dataset. Branch support measures are Bayesian posterior probabilities/ML bootstrap support (only where >50%). Branch support indices are not given for most intrageneric nodes to preserve clarity.

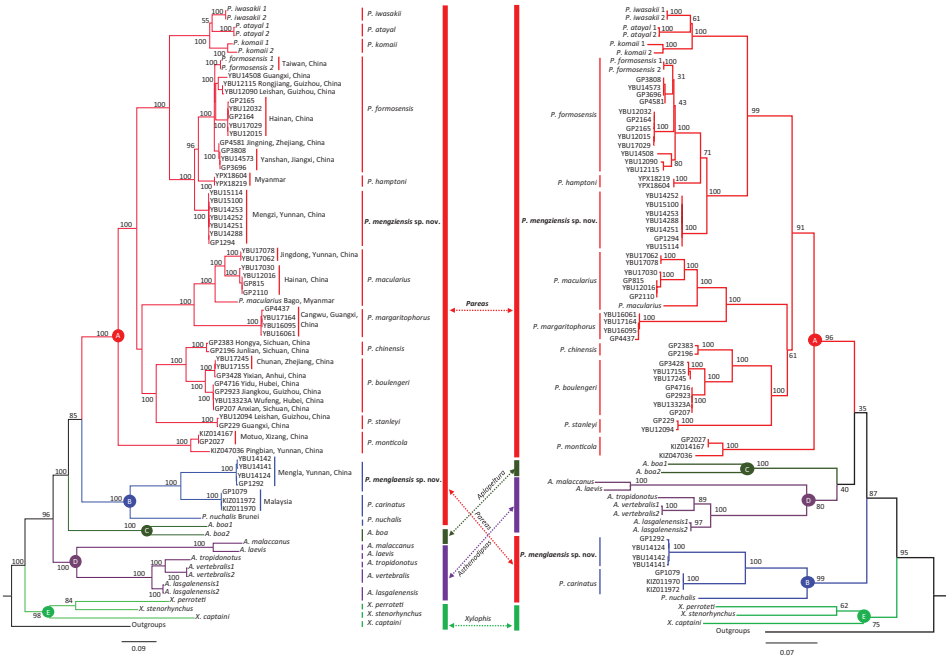

Figure 2. Bayesian inference(left) and Maximum Likelihood(right) trees of the Pareidae based on mtDNA dataset. Branch support measures are Bayesian posterior probabilities and ML bootstrap support respectively. Branch support indices are not given for most intrageneric nodes to preserve clarity.

Table 1. The best partition scheme suggested by PARTITIONFINDER 2.1.1 under AIC.

Partition	Model	Partition	Model
cyt b/ND4, position 1	TVM+I+G	c-mos/Rag1, position 1	K81UF+G
cyt b/ND4, position 2	GTR+I+G	c-mos/Rag1, position 2	TVM+I
cyt b/ND4, position 3	TIM+G	c-mos, position 3	TVM+G
		Rag1, position 3	K81UF+G

Table 2. The average genetic divergence estimates (%, Kimura 2-parameter model with gamma correction) among four lineages (A–D) based on Cyt b.

	lineage A	lineage B	lineage C
lineage A/*Pareas*			
lineage B/*Pareas*	21.3		
lineage C/*Aplopeltura*	18.4	23.0	
lineage D/*Asthenodipsas*	16.9	21.6	15.1

Within lineage A, genetic divergence between species varied from 6.5% (*P. hamptoni* and the population from Mengzi, Yunnan; *P. iwasakii* Maki, 1937 and *P. komaii*) to 29.5% (*P. hamptoni* and *P. margaritophorus* Jan, 1866) based on cyt b and from 8.5% (*P. formosensis* and the population from Mengzi, Yunnan, *P. formosensis* and

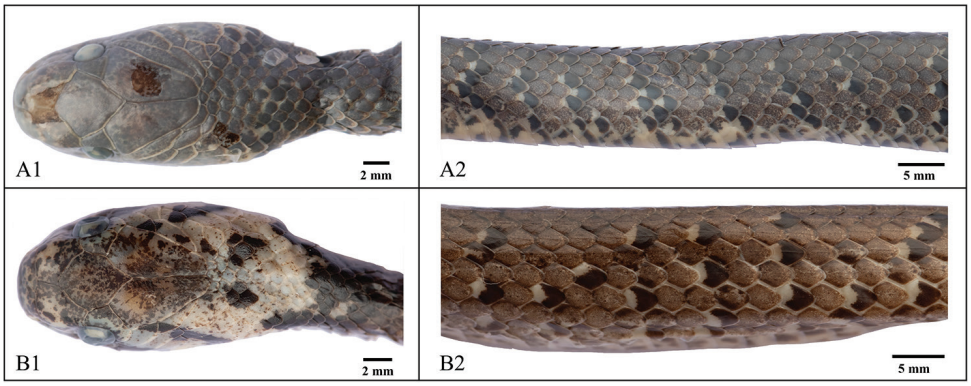

Figure 3. The comparisons of dorsal head (row 1) and median dorsal (row 2) between *Pareas macularius* and *P. margaritophorus*. **A** *P. margaritophorus* **B** *P. macularius*.

P. hamptoni) to 30% (*P. monticola* Cantor, 1839 and *P. komaii*) based on ND4 (Table 3). Furthermore, the population from Mengzi, Yunnan showed genetic divergences of between 6.5% to 28.8% from the other species.

Within lineage B, the sublineage containing the four individuals from southern Yunnan demonstrated genetic divergences of 18.5% and 26.5% from *P. nuchalis* and *P. carinatus*, respectively, based on the ND4 sequences (Table 3).

Morphological examination

A total of 30 characters were measured and recorded for 42 specimens representing seven species and two unidentified taxa of *Pareas* (Appendix 1). Some species or specimens showed markedly different external morphology from their congeners or close relatives. For example, *P. macularius* Theobald, 1868 could be distinguished from *P. margaritophorus* by its keeled dorsal scales (vs. smoothed dorsal scales) (Fig. 3). A detail comparison of morphological characters is listed in Suppl. material 2: Appendix S2 and shown in Suppl. material 4: Figure S1.

The four specimens collected from Mengla County, Yunnan Province, China, were close to those of *P. carinatus*, but could be distinguished from the latter by having 11 rows of strongly keeled dorsal scales at mid-body (vs. 3–5 rows feebly keeled) (Rooij 1917; Smith 1943). The specimens collected from Mengzi, Yunnan Province, China, possessed exclusive characters differed from their congeners, including solid black marking on top of head and dorsal body, three rows of enlarged mi-dorsal scales, and eight or nine infralabials (Suppl. material 4: Fig. S1).

Descriptions of two new taxa

Multiple studies on species identification and evolution have relied solely on external morphology, which is misguided in reptiles (Guo et al. 2012, 2013, 2014; Xie et al.

Table 3. The average divergence estimates (%, Kimura 2-parameter model with gamma correction) of *Pareas* based on cyt b/ND4.

	Taxa	1	2	3	4	5	6	7	8	9	10	11	12	13	14
1	*P. mengziensis* sp. nov.														
2	*P. hamptoni*	6.5/10.7													
3	*P. formosensis*	7.5/8.5	7.1/8.5												
4	*P. komaii*	16.8/22.4	17/25.2	14.6/20.4											
5	*P. iwasakii*	17.4/–	17.2/–	16/–	6.5/–										
6	*P. atayal*	18.5/21.8	18.1/22.3	17.8/20.8	7.8/8.7	8/–									
7	*P. macularius*	23.5/26.4	24.4/26	21.9/27	19.1/28.5	24.4/–	23.4/26.6								
8	*P. margaritophorus*	28.8/25.5	29.5/26.6	26.7/26	23.8/29.5	26.1/–	26.2/29.4	15.5/18.3							
9	*P. boulengeri*	23.3/23.2	23.2/24	19.9/24.6	22.7/26.8	23.3/–	24.9/25.2	21.6/22.5	25.4/23.7						
10	*P. chinensis*	23.4/23.6	24.7/22.2	20.7/22.9	21.5/27.3	24.3/–	25.1/29.1	20.9/24.7	24.6/26.6	8.6/10.6					
11	*P. stanleyi*	28.1/27.7	26.1/30.8	25.4/27.2	21.3/26.4	26.1/–	27/28.3	23.8/22.8	26.9/29	20.9/18.1	19.3/22.3				
12	*P. monticola*	24.4/25.6	24.9/23.1	22.8/24.1	19.6/30	22.7/–	21.7/26.4	19.3/24.5	26.3/26.2	23.7/22.2	23.5/22.9	24.7/28.3			
13	*P. carinatus*	35.8/32.5	37/31.3	36.5/28	34.5/37.9	38.4/–	34.8/37.1	32.4/31.5	36.9/35.2	34.2/33.3	34.5/33.9	39.2/36.7	33.7/29		
14	*P. menglaensis* sp. nov.	35.8/32.3	35.7/30.2	36.1/29.3	35.2/32	38.2/–	35.2/30.7	33.9/31.6	38.8/31.5	35/29.3	39.5/33.9	41.2/33.7	32.4/27.8	18.5/26.5	
15	*P. nuchalis*	–/33.2	–/31.5	–/27.7	–/33.8	–/–	–/32.7	–/32.2	–/34.2	–/34	–/34.8	–/37.9	–/28.7	–/24.8	–/18.5

2018). In particular, widely distributed species are often proven to be complexes of multiple species (Ukuwela et al. 2013; You et al. 2015; Krysko et al. 2016; Chen et al. 2017; Wang et al. 2019). The snakes of *Pareas* have wide distribution in Asia, its highly morphological conservation has contributed to its frequent misidentification and confusion (You et al. 2015). Morphological comparisons indicated that the specimens collected from Mengzi and Mengla, Yunnan, China were significantly different from their congeners respectively. In addition, the specimens from the two populations were also highly divergent from their closest relatives. Thus, we regarded these specimens as two undescribed taxa.

***Pareas menglaensis* sp. nov.**
http://zoobank.org/9AB5DAEE-19AA-4A63-8922-713BF1FBFD09
Figure 4

Holotype. YBU 14124, adult female, collected from Mengla County, Yunnan Province, China, at an elevation of 700 m above sea level in June 2014.

Paratypes. YBU 14141 and YBU 14142, two adult males from the same locality as the holotype but collected in July 2012.

Diagnosis. (1) prefrontal separating from orbit; (2) three chin-shield pairs, anterior pair smaller than other two; (3) 9–13 rows of mid dorsal scales keeled; (4) three rows of mid dorsal scales enlarged; (5) single loreal, not bordering orbit; (6) two preoculars, 2–3 suboculars, single postocular; (7) 9–11 temporals (3+3+3, 3+4+4, or 3+4+3); (8) seven supralabials, not bordering orbit; (9) 7–8 infralabials; (10) 3–5 maxillary teeth; (11) cloaca undivided; (12) dorsal scales in 15 rows throughout; (13) 176–177 ventral scales; (14) 65–79 subcaudals, paired.

Description of holotype. Male, SVL 472 mm, TL 111 mm, TL/total length 0.24; body elongated; snout distinctly blunt; head distinct from neck. Rostral invisible from above, much deeper than broad; nasals undivided. Internasals subtriangular, wider than long; prefrontals pentagonal, length equal to width, not touching eyes; frontal hexagonal, longer than wide; parietals irregular, longer than wide; one supraocular, longer than diameter of orbit; single loreal, separating from eyes; two preoculars; one postocular; two suboculars; nine or ten temporals, 3+4+3 on left and 3+3+3 on right; seven supralabials, not bordering orbit; seven or eight infralabials, first four in contact with anterior chin-shields; three chin-shield pairs, posterior pair larger than other two; ventral scales 177; cloaca undivided; subcaudals 65, paired; dorsal scales in 15 rows throughout, three median rows enlarged, all keeled except for outer two; five maxillary teeth on both sides.

Dorsal surface nearly uniformly light brown with slightly visible black crossbands. Head light brown with black dusted spots. Thin postorbital stripe extending from postocular to neck. Belly yellowish white, anterior portion without spots except for lateral edges mottled with almost striped dark brown spots, striped spots gradually becoming invisible backwards. Spots and specks on posterior portion of belly appear and become denser later.

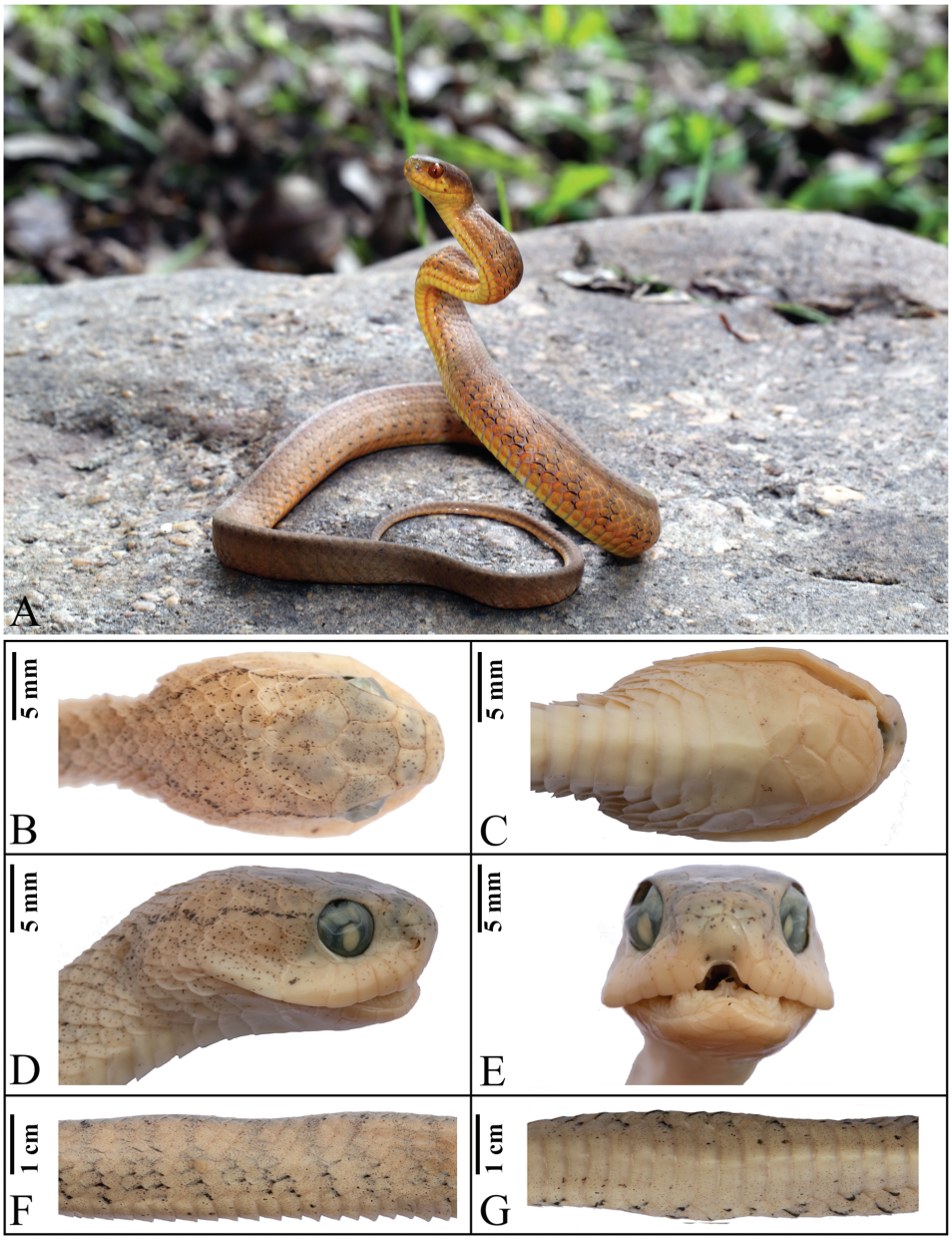

Figure 4. Holotype of *Pareas menglaensis* sp. nov. (YBU 14124). General view(**A**); dorsal (**B**), ventral (**C**), lateral **(D)** and frontal (**E**) views of the head; dorsal (**F**) and ventral (**G**) views of the median body.

Description of paratypes. The paratypes agree in most respects with the description of the holotype. A comparison of the most important morphological characters is summarized in Suppl. material 3: Appendix S3.

Etymology. The specific species is named after the type locality, Mengla County, Yunnan, China. We suggest the common name "Mengla Snail-eating Snake" in English and "Mengla Dun-tou-she" (勐腊钝头蛇) in Chinese.

Distribution. This species is currently known only from the type locality Mengla County, Yunnan, China, with low mountain evergreen broad-leaved forest and a tropical monsoon climate type. It is expected to be found in the surrounding low mountainous areas and in neighboring Laos and Myanmar.

Comparison. *Pareas menglaensis* sp. nov. can be distinguished from *P. carinatus* by 11 rows of dorsal scales strongly keeled at mid-body (vs. 3–5 rows feebly keeled), from *P. nuchalis* by prefrontal separated from orbit (vs. prefrontal bordering orbit), and from all other species of *Pareas* by two or three distinct narrow suboculars (vs. one thin elongated subocular).

***Pareas mengziensis* sp. nov.**

http://zoobank.org/EC677F21-D01B-4C53-998F-D77C7457081B

Figure 5

Holotype. YBU 14252, adult female, collected from Mengzi, Yunnan Province, China, at an elevation of 1 900 m above sea level in July 2014.

Paratypes. Two adult females (YBU 141251 and YBU 15100) and three adult males (YBU 14253, YBU 14288, and YBU 15114) from the same locality and adjacent regions collected in July 2014 and July 2015.

Diagnosis. (1) solid black marking on back of head extending along whole dorsal of body; (2) single preocular; (3) postocular fused with subocular; (4) loreal not bordering orbit; (5) temporals 2+3+3; (6) prefrontal bordering orbit; (7) three rows of mid dorsal scales slightly enlarged; (8) 3–7 rows of mid dorsal scales keeled; (9) 6–7 supralabials; (10) 8–9 infralabials; (11) 6–7 maxillary teeth; (12) cloaca undivided; (13) ventral scales 167–173; (14) subcaudals 54–61, paired.

Description of holotype. Female, SVL 426 mm, TL 98 mm, TL/total length 0.187; body elongated; head distinct from neck. Internasals sub-triangular, wider than long; prefrontals sub-rectangular, wider than long, bordering orbits; frontal shield-shaped; one relatively small supraocular; parietals irregular, longer than wide; rostral almost invisible from above, wider than deep; nasals undivided; single loreal, separating from eyes; single preocular; single thin elongated subocular; postocular fused with subocular, supraocular sub-triangular; temporals 2+3+3; seven supralabials, separating from eyes; 8–9 infralabials, anterior-most in contact with opposite between mental and anterior chin-shields, first four in contact with anterior chin-shields; three chin-shields pairs, anterior pairs larger than other two; ventral scales 170; cloaca undivided; subcaudals 54, paired; dorsal scales in 15 rows throughout, three median rows enlarged, 3–7 rows of mid dorsal scales keeled; 6–7 maxillary teeth.

Solid black marking on back of head extending along whole dorsal of body and tail; sides of head light brownish yellow, speckled with small, irregular, dark brown spots; two

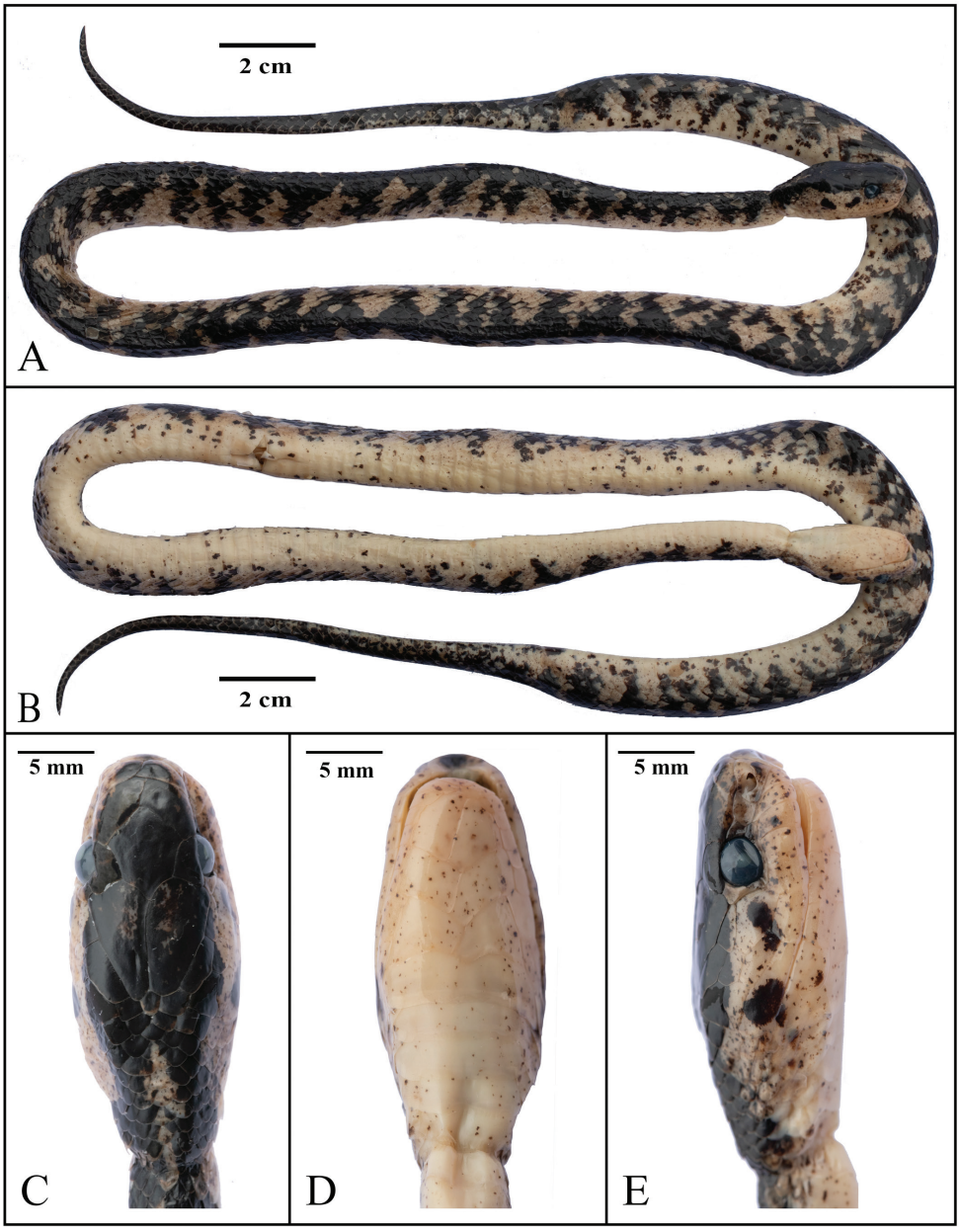

Figure 5. Holotype of *Pareas mengziensis* sp. nov. (YBU 14252). Dorsal (**A**) and ventral (**B**) of general views; dorsal (**C**), ventral (**D**), and lateral (**E**) views of the head.

black spots on each side of head, anterior one on intersection of anterior two temporals and 6th and 7th supralabials, posterior one on middle of 7th supralabial; vertical brownish yellow stripe on neck, eight scales long and 1–2 scales wide; body brownish yellow with

numerous irregular black cross-bands on lateral of body, contacting with solid black dorsal of body, some extending to edges of ventral scales; belly light brown with sparse dark brown spots; tail purely black except for first 20 pairs of subcaudals light brown.

Description of paratypes. The paratypes agree in most respects with the description of the holotype. A comparison of the most important morphological characters is summarized in Suppl. material 3: Appendix S3.

Etymology. The new species is named after the type locality Mengzi City, Yunnan Province, China. We suggest the common name "Mengzi Snail-eating Snake" in English and "Mengzi Dun-tou-she (蒙自钝头蛇)" in Chinese.

Distribution. This species is currently known only from the type locality Mengzi City, Yunnan, China, in deciduous broad-leaved forest with a subtropical monsoon climate. It is expected to be located in the surrounding plateau regions.

Comparison. *Pareas mengziensis* sp. nov. can be distinguished from *P. carinatus*, *P. nuchalis*, and *P. menglaensis* sp. nov. by having one thin elongated subocular (vs. two or three suboculars). It is most similar to *P. yunnanensis* Mell, 1931, *P. niger* Pope, 1928, and *P. nigriceps* in terms of color pattern, but differs from these species by eight or nine infralabials (vs. seven) and three rows of mid dorsal scales enlarged (vs. not enlarged or only one enlarged mid dorsal scale). It differs from the remaining species of *Pareas* by having a large solid black area on back of head and body.

Validity of *Pareas macularius* Theobald, 1868

Zhao et al. (1998) suggested *Pareas* to be composed of two types of color pattern: color pattern I (*P. macularius* and *P. margaritophorus*) and color pattern II (other species of *Pareas*). *Pareas macularius* was named based on specimens from Martaban, Myanmar. It is distinguished from *P. margaritophorus* by its slightly keeled dorsal scales. However, Huang (2004) held that dorsal scales, keeled or not, are undiagnosable, and thus synonymized *P. macularius* with *P. margaritophorus*. Hauser (2017) compared the morphological characters of more than 60 specimens of the two putative species from northern Thailand, and claimed *P. macularius* as a valid species, distinguishable from *P. margaritophorus* by the 7–13 rows of mid dorsal scales feebly keeled at midbody and the form and color of the nuchal collar. Our phylogenetic results showed that the species with color pattern I suggested by Zhao et al. (1998) were polyphyletic, with two distinct lineages including *P. margaritophorus* (dorsal scales smoothed) and *P. macularius* (dorsal scales keeled) (Figs 1–3). The average divergences of these two lineages were 15.5% (cyt b based) and 18.3% (ND4 based), indicating that separation occurred very early. Therefore, *P. macularius* should be considered a valid taxon.

It was noticed that both morphological comparisons and molecular analyses consistently showed that *Pareas* contained two distinct evolutionary lineages with distinguishable morphological differences and significant genetic divergences; however, the non-monophyly of *Pareas* was not well supported, and the loci used and specimens measured were limited. Whether *Pareas* should be split into two distinct genera needs more data to clarify.

Finally, a key to the species of *Pareas* is provide in Appendix 2.

Acknowledgements

This project was supported by grants from the Strategic Priority Research Program of the Chinese Academy of Sciences (CAS) (XDA 20050201) , the Second Tibetan Plateau Scientific Expedition and Research (STEP) program (No. 2019QZKK05010105), Southeast Asia Biodiversity Research Institute, the Chinese Academy of Sciences (CAS) (Y4ZK111B01: 2017CASSEABRIQG002), the Animal Branch of the Germplasm Bank of Wild Species, CAS (Large Research Infrastructure Funding), and the National Natural Science Foundation of China (NSFC 31372152). We are grateful to Guanghui Zhong, Ting Tang, Yulin Xie, Yimin Yang, Fei Zhu, Jichao Wang, Tongliang Wang, Yufan Wang, Liang Zhang, Hongman Chen, and Shuai Wang for their assistance in field work; Anita Malhotra, Li Ding, and Mian Hou are acknowledged for tissue loans. We thank Wuyi Mountain National Nature Reserve of Jiangxi Province, Jianfengling National Forest Park of Hainan Province, and Zhejiang Forest Resources Monitoring Center for support in our field work.

References

Arèvalo E, Davis SK, Sites JW (1994) Mitochondrial DNA sequence divergence and phylogenetic relationships among eight chromosome races of the *Sceloporus grammicus* complex (Phrynosomatidae) in central Mexico. Systematic Biology 43(3): 387–418. https://doi.org/10.1093/sysbio/43.3.387

Boulenger GA (1900) Descriptions of new reptiles and batrachians from Borneo. Proceedings of the Zoological Society of London, Blackwell Publishing Ltd, Oxford 69(2): 182–187. https://doi.org/10.1111/j.1096-3642.1890.tb01716.x

Boulenger GA (1905) Descriptions of two new snakes from Upper Burma. Bombay Natural History Society 16: 235–236. https://doi.org/10.1080/03745480509443665

Burbrink FT, Lawson R, Slowinski JB (2000) Mitochondrial DNA phylogeography of the polytypic North American rat snake (*Elaphe obsoleta*): a critique of the subspecies concept. Evolution 54(6): 2107–2118. https://doi.org/10.1111/j.0014-3820.2000.tb01253.x

Chen JM, Zhou WW, Poyarkov NA, Stuart BL, Brown RM, Lathrop A, Wang YY, Yuan ZY, Jiang K, Hou M (2017) A novel multilocus phylogenetic estimation reveals unrecognized diversity in Asian horned toads, genus *Megophrys sensu lato* (Anura: Megophryidae). Molecular Phylogenetics and Evolution 106: 28–43. https://doi.org/10.1016/j.ympev.2016.09.004

Das I (2012) A naturalist's guide to the snakes of South-east Asia (2nd ed). Bloomsbury Publishing Plc, London, 344–346.

Deepak V, Ruane S, Gower DJ (2018) A new subfamily of fossorial colubroid snakes from the Western Ghats of peninsular India. Journal of Natural History 52(45–46): 2919–2934. https://doi.org/10.1080/00222933.2018.1557756

Felsenstein J (2004) Inferring phylogenies, Vol. 2. Sinauer associates, Sunderland, MA, 664 pp.

Figueroa A, McKelvy AD, Grismer LL, Bell CD, Lailvaux SP (2016) A species-level phylogeny of extant snakes with description of a new colubrid subfamily and genus. PLoS ONE 11(9): e0161070. https://doi.org/10.1371/journal.pone.0161070

Flot J (2010) SEQPHASE: a web tool for interconverting PHASE input/output files and FASTA sequence alignments. Molecular Ecology Resources 10(1): 162–166. https://doi.org/10.1111/j.1755-0998.2009.02732.x

Grossmann W, Tillack F (2003) On the taxonomic status of *Asthenodipsas tropidonotus* (Van Lidth de Jeude, 1923) and *Pareas vertebralis* (Boulenger, 1900) (Serpentes: Colubridae: Pareatinae). Russian Journal of Herpetology 10(3): 175–190.

Groth JG, Barrowclough GF (1999) Basal divergences in birds and the phylogenetic utility of the nuclear RAG-1 gene. Molecular Phylogenetics and Evolution 12(2): 115–123. https://doi.org/10.1006/mpev.1998.0603

Guo KJ, Deng XJ (2009) A new species of *Pareas* (Serpentes: Colubridae: Pareatinae) from the Gaoligong Mountains, southwestern China. Zootaxa 2008: 53–60.

Guo P, Liu Q, Myers EA, Liu SY, Xu Y, Liu Y, Wang YZ (2012) Evaluation of the validity of the ratsnake subspecies *Elaphe carinata deqenensis* (Serpent: Colubridae). Asian Herpetological Research 3: 219–226. https://doi.org/10.3724/SP.J.1245.2012.00219

Guo P, Zhang L, Liu Q, Li C, Pyron RA, Jiang K, Burbrink FT (2013) *Lycodon* and *Dinodon*: one genus or two? evidence from molecular phylogenetics and morphological comparisons. Molecular Phylogenetics and Evolution 68(1): 144–149. https://doi.org/10.1016/j.ympev.2013.03.008

Guo P, Zhu F, Liu Q, Zhang L, Li JX, Huang YY, Pyron RA (2014) A taxonomic revision of the Asian keelback snakes, genus *Amphiesma* (Serpentes: Colubridae: Natricinae), with description of a new species. Zootaxa 3873(4): 425–440. https://doi.org/10.11646/zootaxa.3873.4.5

Guo YH, Wu YK, He SP, Shi HT, Zhao EM (2011) Systematics and molecular phylogenetics of Asian snail-eating snakes (Pareatidae). Zootaxa 3001(1): 57–64. https://doi.org/10.11646/zootaxa.3001.1.4

Guo YH, Zhang QL (2015) Review of systematics on the Asian Snail-eating snakes. Chinese Journal of Zoology 50(1): 153–158. [in Chinese]

Hauser S (2017) On the validity of *Pareas macularius* Theobald, 1868 (Squamata: Pareidae) as a species distinct from *Pareas margaritophorus* (Jan in Bocourt, 1866). Tropical Natural History 17(1): 25–52.

Hillis DM, Bull JJ (1993) An empirical-test of bootstrapping as a method for assessing confidence in phylogenetic analysis. Systematic Biology 42: 182–192. https://doi.org/10.1093/sysbio/42.2.182

Hoso M (2017) Asymmetry of mandibular dentition is associated with dietary specialization in snail-eating snakes. PeerJ 5: e3011. https://doi.org/10.7717/peerj.3011

Hoso M, Hori M (2008) Divergent shell shape as an antipredator adaptation in tropical land snails. American Naturalist 172(5): 726–732. https://doi.org/10.1086/591681

Hoso M, Kameda Y, Wu SP, Asami T, Kato M, Hor, M (2010) A speciation gene for left-right reversal in snails results in anti-predator adaptation. Nature Communications 1: 133. https://doi.org/10.1038/ncomms1133

Huang QY (2004) *Pareas macularius* Theobald, 1868 should be a junior synonym of *Pareas margaritophorus* (Jan, 1866). Sichuan Journal of Zoology 23(3): 207–208. [in Chinese]

Kearse M, Moir R, Wilson A, Stones-Havas S, Cheung M, Sturrock S, Buxton S, Cooper A, Markowitz S, Duran C (2012) Geneious Basic: an integrated and extendable desktop software platform for the organization and analysis of sequence data. Bioinformatics 28(12): 1647–1649. https://doi.org/10.1093/bioinformatics/bts199

Kelly CM, Barker NP, Villet MH (2003) Phylogenetics of advanced snakes (Caenophidia) based on four mitochondrial genes. Systematic Biology 52(4): 439–459. https://doi.org/10.1080/10635150390218132

Kraus F, Brown WM (1998) Phylogenetic relationships of colubroid snakes based on mitochondrial DNA sequences. Zoological Journal of the Linnean Society 122(3): 455–487. https://doi.org/10.1111/j.1096-3642.1998.tb02159.x

Krysko KL, Granatosky MC, Nunez LP, Smith DJ (2016) A cryptic new species of Indigo Snake (genus *Drymarchon*) from the Florida Platform of the United States. Zootaxa 4138(3): 549–569. https://doi.org/10.11646/zootaxa.4138.3.9

Kumar S, Stecher G, Tamura K (2016) MEGA7: Molecular Evolutionary Genetics Analysis version 7.0 for bigger datasets. Molecular Biology and Evolution 33(7): 1870–1874. https://doi.org/10.1093/molbev/msw054

Lanfear R, Frandsen PB, Wright AM, Senfeld T, Calcott B (2017) PartitionFinder 2: new methods for selecting partitioned models of evolution for molecular and morphological phylogenetic analyses. Molecular Biology and Evolution 34(3): 772–773. https://doi.org/10.1093/molbev/msw260

Lawson R, Slowinski JB, Crother BI, Burbrink FT (2005) Phylogeny of the Colubroidea (Serpentes): new evidence from mitochondrial and nuclear genes. Molecular Phylogenetics and Evolution 37(2): 581–601. https://doi.org/10.1016/j.ympev.2005.07.016

Loredo AI, Wood PL, Quah ES, Anuar S, Greer L, Norhayati A, Grismer LL (2013) Cryptic speciation within *Asthenodipsas vertebralis* (Boulenger, 1900) (Squamata: Pareatidae), the description of a new species from Peninsular Malaysia, and the resurrection of *A. tropidonotus* (Lidth de Jude, 1923) from Sumatra: an integrative taxonomic analysis. Zootaxa 3664(4): 505–524. https://doi.org/10.11646/zootaxa.3664.4.5

Pyron RA, Burbrink FT, Wiens JJ (2013) A phylogeny and revised classification of Squamata, including 4161 species of lizards and snakes. BMC Evolutionary Biology 13: 93. https://doi.org/10.1186/1471-2148-13-93

Rambaut A, Suchard M, Xie D, Drummond A (2014) Tracer, version 1.6, MCMC trace analysis package. http://beast.bio.ed.ac.uk/Tracer

Ronquist F, Teslenko M, Van Der Mark P, Ayres DL, Darling A, Höhna S, Larget B, Liu L, Suchard MA, Huelsenbeck JP (2012) MrBayes 3.2: efficient Bayesian phylogenetic inference and model choice across a large model space. Systematic Biology 61(3): 539–542. https://doi.org/10.1093/sysbio/sys029

Rooij ND (1917) The Reptiles of the Indo-Australian Archipelago: Ophidia, Vol. 2. Hardpress publishing, Leiden, 277 pp.

Savage JAYM (2015) What are the correct family names for the taxa that include the snake genera *Xenodermus*, *Pareas*, and *Calamaria*. Herpetological Review 46(4): 664–665.

Silvestro D, Michalak I (2012) raxmlGUI: a graphical front-end for RAxML. Organisms Diversity and Evolution 12(4): 335–337. https://doi.org/10.1007/s13127-011-0056-0

Slowinski JB, Lawson R (2002) Snake phylogeny: evidence from nuclear and mitochondrial genes. Molecular Phylogenetics and Evolution 24(2): 194–202. https://doi.org/10.1016/S1055-7903(02)00239-7

Smith MA (1943) The fauna of British India, Ceylon and Burma, including the whole of the Indo-Chinese sub-region, Vol. III Serpentes. Taylor and Francis, London, 121 pp.

Stephens M, Smith NJ, Donnelly P (2001) A new statistical method for haplotype reconstruction from population data. The American Journal of Human Genetics 68(4): 978–989. https://doi.org/10.1086/319501

Uetz P, Freed P, Hošek J (2019) The Reptile Database. http://www.reptile-database.org

Ukuwela KD, De SA, Fry BG, Lee MS, Sanders KL (2013) Molecular evidence that the deadliest sea snake *Enhydrina schistosa* (Elapidae: Hydrophiinae) consists of two convergent species. Molecular Phylogenetics and Evolution 66(1): 262–269. https://doi.org/10.1016/j.ympev.2012.09.031

Vidal N, Delmas AS, David P, Cruaud C, Couloux A, Hedges SB (2007) The phylogeny and classification of caenophidian snakes inferred from seven nuclear protein-coding genes. Comptes Rendus Biologies 330(2): 182–187. https://doi.org/10.1016/j.crvi.2006.10.001

Vogel G (2015) A new montane species of the genus *Pareas* Wagler, 1830 (Squamata: Pareatidae) from northern Myanmar. TAPROBANICA: The Journal of Asian Biodiversity 7(1): 1–7. https://doi.org/10.4038/tapro.v7i1.7501

Wang P, Shi L, Guo P (2019) Morphology-based intraspecific taxonomy of *Oreocryptophis porphyraceus* (Cantor, 1839) in mainland China (Serpentes: Colubridae). Zoological Research 40(4): 324–330. https://doi.org/10.24272/j.issn.2095-8137.2019.048

Xie YL, Wang P, Zhong GH, Zhu F, Liu Q, Che J, Shi L, Murphy RW, Guo P (2018) Molecular phylogeny found the distribution of *Bungarus candidus* in China (Squamata: Elapidae). Zoological Systematics 43(1): 109–117.

You CW, Poyarkov NA, Lin SM (2015) Diversity of the snail-eating snakes *Pareas* (Serpentes, Pareatidae) from Taiwan. Zoologica Scripta 44(4): 349–361. https://doi.org/10.1111/zsc.12111

Zhao EM (2006) Snakes of China, Vol. 1. Anhui Science Technology Publishing House, Hefei, 244–245. [in Chinese]

Zhao EM, Huang MH, Zong Y (1998) Fauna Sinica Reptilia, vol. 3: Squamata: Serpentes. Science Press, Beijing, 219–221. [in Chinese]

Zug GR, Vitt LJ, Caldwell JP (2001) Herpetology: an introductory biology of amphibians and reptiles (2nd ed.). Academic Press, San Diego, 523–528.

Appendix 1

Specimens morphologically examined in this study

***Pareas formosensis*:** Hainan, China (YBU 12015, YBU 12032, YBU 17029, R0263, R0542, R0543), Leishan, Guizhou, China (YBU 12090), Rongjiang, Guizhou, China (YBU 12115), Fangchenggang, Guangxi, China (YBU14508), Yanshan, Jiangxi, China (YBU 14573). ***P. mengziensis* sp. nov.:** Mengzi, Yunnan, China (YBU 14251, YBU 15252, YBU 14253, YBU 14288), Kaiyuan, Yunnan, China (YBU 15100, YBU 15114). ***P. boulengeri*:** Chunan, Zhejiang, China (YBU 17155, YBU 17245), Wufeng, Hubei, China (YBU 13323A). ***P. chinensis*:** Junlian, Sichuan, China (YBU 14126, YBU 16134, YBU 17043), Yingjing, Sichuan, China (YBU 16119, YBU 16122). ***P. stanleyi*:** Leishan, Guizhou, China (YBU 12094). ***P. macularius*:** Hainan, China (R0047, R0048, R0210, R0545, R0546, R0547, YBU 12016, YBU 17030), Jingdong, Yunnan, China (YBU 17062, YBU 17078). ***P. margaritophorus*:** Cangwu, Guangxi, China (YBU 16061, YBU 16077, YBU 16095, YBU 17164). ***P. menglaensis* sp. nov.:** Mengla, Yunnan, China (YBU 14124, YBU 14141, YBU 14142).

Appendix 2

Key to *Pareas* species

1	Two or three distinct narrow suboculars	**2**
–	One thin elongated subocular	**4**
2	Prefrontal bordering orbits, a large black blotch on the nape	***P. nuchalis***
–	Prefrontal separated from orbit, absence black blotch on the nape	**3**
3	3–5 rows of middle dorsal scales keeled	***P. carinatus***
–	9–13 rows of middle dorsal scales keeled	***P. menglaensis* sp. nov.**
4	Uniform purple brown or blue gray above with bicolored cross bars (color pattern I)	**5**
–	Light or dark brown above without bicolored dorsal scales (color pattern II)	**6**
5	All dorsal scales smooth	***P. macularius***
–	Dorsal scales keeled	***P. margaritophorus***
6	Loreal bordering orbit	7
–	Loreal separating from orbit	**10**
7	Vertebral scales enlarged	***P. monticola***
–	Vertebral scales not enlarged	**8**
8	Supralabials 6	***P. vindumi***
–	Supralabials 7 or 8	**9**

9	All dorsal scales smooth	***P. boulengeri***
–	Five rows of middle dorsal scales keeled	***P. stanleyi***
10	Dorsal scales not enlarged	***P. chinensis***
–	Dorsal scales enlarged	**11**
11	Three rows middle dorsal scales enlarged	**12**
–	Only vertebral scales enlarged	**14**
12	A large black area on the back of head and body	***P. mengziensis* sp. nov.**
–	Absence large black area on the back of head and body	**13**
13	Temporals 2+4, 5–9 rows middle dorsal scales keeled	***P. atayal***
–	Temporals 2+3 or 3+4, 9–13 rows middle dorsal scales keeled	***P. komaii***
14	Temporals 1+2	**15**
–	Temporals 2+3 or 3+4	**16**
15	The back of head purely black, postocular absent	***P. nigriceps***
–	The back of head pale brown with black spots, postocular 1	***P. hamptoni***
16	All dorsal scales smooth or 2 middle rows feebly keeled	***P. formosensis***
–	Middle dorsal scales keeled in rows 5–7	***P. iwasakii***

Supplementary material 1

Appendix S1

Authors: Ping Wang, Jing Che, Qin Liu, Ke Li, Jie Qiong Jin, Ke Jiang, Lei Shi, Peng Guo

Data type: occurrence

Explanation note: Samples and sequences used in this study (BHNS: Bombay Natural History Society, Mumbai, India; CAS: California Academy of Science, San Francisco, USA; CES: Centre for Ecological Sciences, IISc, Bengaluru, India; FK: voucher listed by Kraus and Brown (1998); FMNH: Field Museum of Natural History, Chicago, USA; GP: P. Guo own catalogue number; HC: Cryobanking project, Taiwan, China; KIZ: Kunming Institute of Zoology, Chinese Academy of Sciences, Kunming, China; LSUHC: La Sierra University Herpetological Collection, Riverside, California, USA; NMNS: National Museum of Natural Science, Taiwan, China; YBU: Yibin University, Sichuan, China; YPX: Field number of KIZ).

Link: https://doi.org/10.3897/zookeys.939.49309.suppl1

Supplementary material 2

Appendix S2

Authors: Ping Wang, Jing Che, Qin Liu, Ke Li, Jie Qiong Jin, Ke Jiang, Lei Shi, Peng Guo

Data type: measurement

Explanation note: Characters recorded of *Pareas*.

Link: https://doi.org/10.3897/zookeys.939.49309.suppl2

Supplementary material 3

Appendix S3

Authors: Ping Wang, Jing Che, Qin Liu, Ke Li, Jie Qiong Jin, Ke Jiang, Lei Shi, Peng Guo

Data type: measurement

Explanation note: A comparison between holotype and paratypes of two new described species.

Link: https://doi.org/10.3897/zookeys.939.49309.suppl3

Supplementary material 4

Figure S1

Authors: Ping Wang, Jing Che, Qin Liu, Ke Li, Jie Qiong Jin, Ke Jiang, Lei Shi, Peng Guo

Data type: multimedia

Explanation note: The comparisons of anterior dorsal and head (column 1), lateral middle body (column 2) and subcaudal coloration (column 3) among Mengzi specimens and relatives. **A** Mengzi specimens **B** *Pareas formosensis* **C** *P. chinensis* **D** *P. boulengeri* **E** *P. stanleyi*.

Link: https://doi.org/10.3897/zookeys.939.49309.suppl4

ZooKeys 939: 65–85 (2020)
doi: 10.3897/zookeys.939.31764
https://zookeys.pensoft.net

RESEARCH ARTICLE

A peer-reviewed open-access journal
ZooKeys
Launched to accelerate biodiversity research

Taxonomic revision and phylogenetic position of the flying squirrel genus *Biswamoyopterus* (Mammalia, Rodentia, Sciuridae, Pteromyini) on the northern Indo-China peninsula

Guogang Li[1], Ye Htet Lwin[1], Bin Yang[1], Tao Qin[1,2], Phouthong Phothisath[3], Kyaw-Win Maung[4], Rui-Chang Quan[1], Song Li[2]

1 *Southeast Asia Biodiversity Research Institute, Chinese Academy of Sciences & Center for Integrative Conservation, Xishuangbanna Tropical Botanical Garden, Chinese Academy of Sciences, Mengla, Yunnan, 666303, China* **2** *Kunming Natural History Museum of Zoology, Kunming Institute of Zoology, Chinese Academy of Sciences, 32 Jiaochang Donglu, Kunming, Yunnan 650223, China* **3** *Biotechnology and Ecology Institute, Ministry of Science and Technology of Laos, P. O. Box 2279, Vientiane Capital, Lao People's Democratic Republic* **4** *Forest Research Institute, Forest Department, Ministry of Environmental Conservation and Forestry, Yezin, Nay Pyi Taw, 05282, Myanmar*

Corresponding author: Rui-Chang Quan (quanrc@xtbg.ac.cn); Song Li (lis@mail.kiz.ac.cn)

Academic editor: R. López-Antoñanzas | Received 19 November 2018 | Accepted 3 August 2019 | Published 9 June 2020

http://zoobank.org/CDB10133-5AC4-40CF-91C7-EE9A81CDB77F

Citation: Li G, Lwin YH, Yang B, Qin T, Phothisath P, Maung K-W, Quan R-C, Li S (2020) Taxonomic revision and phylogenetic position of the flying squirrel genus *Biswamoyopterus* (Mammalia, Rodentia, Sciuridae, Pteromyini) on the northern Indo-China peninsula. ZooKeys 939: 65–85. https://doi.org/10.3897/zookeys.939.31764

Abstract

The flying squirrel genus *Biswamoyopterus* (Rodentia: Sciuridae: Pteromyini) was once considered to contain three species, *Biswamoyopterus biswasi* from northeastern India, *B. laoensis* from central Laos and *B. gaoligongensis* from southwest China, all identified from morphological characteristics of one or two specimens. However, based on similar morphological characteristics of two samples of the genus *Biswamoyopterus* collected recently from northern Laos and northern Myanmar, and the small genetic distances on mitochondrial DNA and nuclear DNA between them, the results strongly support these two samples as representatives of the same species. The phylogenetic analyses strongly support *Biswamoyopterus* as an independent genus of Pteromyini, as a sister group to *Aeromys*. *Biswamoyopterus biswasi* is distributed in the

northern Indo-China peninsula, where it is exposed to a series of threats, such as intense hunting activity, illegal trade, and rapid habitat loss; this should warrant its classification as critically endangered according to the International Union for Conservation of Nature (IUCN) Red List criteria. Here, the molecular data for genus *Biswamoyopterus* and two new specimen records from northern Laos and northern Myanmar are presented.

Keywords
Biswamoyopterus, flying squirrel, Indo-China peninsula, taxonomic revision.

Introduction

Flying squirrels (Mammalia: Rodentia: Sciuridae: Pteromyini), occurring in northern coniferous forests to the tropical lowlands of North America and Eurasia, are great masters of gliding locomotion using well-developed membrane structures (Thorington et al. 2002). Pteromyini comprises 15 monophyletic genera nested within Sciuridae (Mercer and Roth 2003; Wilson and Reader 2005), with high external morphological diversification between genera. It is useful to understand the taxonomic theories behind these genera, based on skull characteristics and external morphology (Ellerman 1940; Ellerman and Morrison-Scott 1950; Corbet and Hill 1992; Nowak 1999; Thorington et al. 2002; Wilson and Reader 2005) (Table 1).

Many studies on the molecular phylogeny of Pteromyini genera have been performed since 2000 (Oshida 2000a, b, 2001, 2004; Mercer and Roth 2003; Yu et al. 2004, 2006; Lu et al. 2012); however, most of them were carried out with one or a few genera, and even the analyses by Mercer and Roth (2003), which examined 14 of the 15 genera, excluded the genus *Biswamoyopterus* (Figure 1). The genus *Biswamoyopterus* was described by Saha in 1981. Identified on respective morphological characteristics of one or two specimens, it comprises three species, *Biswamoyopterus biswasi* Saha,

Table 1. Taxonomic hypotheses of various authors regarding Pteromyidae/Pteromyini.

Ellerman (1940)	Ellerman and Morrison-Scott (1950)	Corbet and Hill (1992)	Nowak (1999)	Thorington et al. (2002)
	Aeretes	*Aeretes*	*Aeretes*	*Aeretes*
Aeromys		*Aeromys*	*Aeromys*	*Aeromys*
Belomys	*Belomys*		*Belomys*	*Belomys*
		Biswamoyopterus	*Biswamoyopterus*	*Biswamoyopterus*
Eoglaucomys			*Eoglaucomys*	*Eoglaucomys*
Eupetaurus	*Eupetaurus*	*Eupetaurus*	*Eupetaurus*	*Eupetaurus*
Glaucomys			*Glaucomys*	*Glaucomys*
Hylopetes	*Hylopetes*	*Hylopetes*	*Hylopetes*	*Hylopetes*
Iomys		*Iomys*	*Iomys*	*Iomys*
Petaurillus		*Petaurillus*	*Petaurillus*	*Petaurillus*
Petaurista	*Petaurista*	*Petaurista*	*Petaurista*	*Petaurista*
Petinomys	*Petinomys*	*Petinomys*	*Petinomys*	*Petinomys*
Pteromys	*Pteromys*		*Pteromys*	*Pteromys*
Pteromyscus		*Pteromyscus*	*Pteromyscus*	*Pteromyscus*
Trogopterus	*Trogopterus*	*Trogopterus*	*Trogopterus*	*Trogopterus*

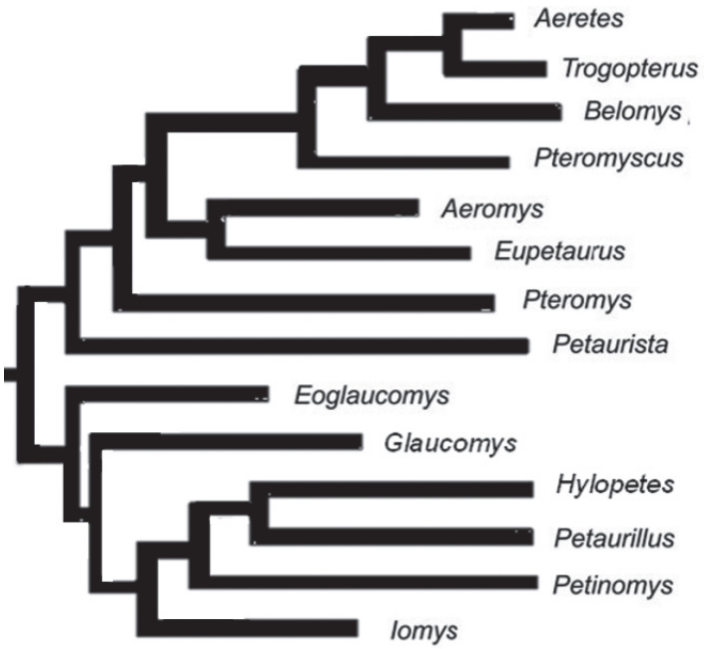

Figure 1. Phylogeny of Pteromyini genera. Cited from Mercer and Roth (2003).

1981 (specimen ZSI 20705) found in northeastern India, *B. laoensis* Sanamxay et al., 2013 (specimen NUoL FES. MM.12.163), found in central Laos, and *B. gaoligongensis* Li et al., 2019 (specimens ZSI 20705 & KIZ 034924), found in southwest China (Figure 2, see Saha 1981; Sanamxay et al. 2013; Li et al. 2019). No molecular data have been obtained about this genus so far.

Since 2014, the Southeast Asia Biodiversity Research Institute, Chinese Academy of Sciences (CAS-SEABRI), has conducted several biodiversity expeditions to the northern Indo-China peninsula (Li and Quan 2017; Li et al. 2017). This region is considered a globally important biodiversity hotspot for flora and fauna (Tordoff et al. 2005), from where many species of mammals have been discovered or rediscovered since the 1990s (Amato et al. 1999; Geissmann et al. 2011; Sanamxay et al. 2013; Fan et al. 2017). In this work, using combined mitochondrial DNA and nuclear DNA loci, and morphological examination, we aim to revise the taxonomic status of the genus *Biswamoyopterus* and assess its phylogenetic position among flying squirrels.

Materials and methods

Ethics statement

All samples used in this study were obtained by the CAS-SEABRI expeditions on the northern Indo-China peninsula, with export permits (no. L/2020-0001/MA-0004/

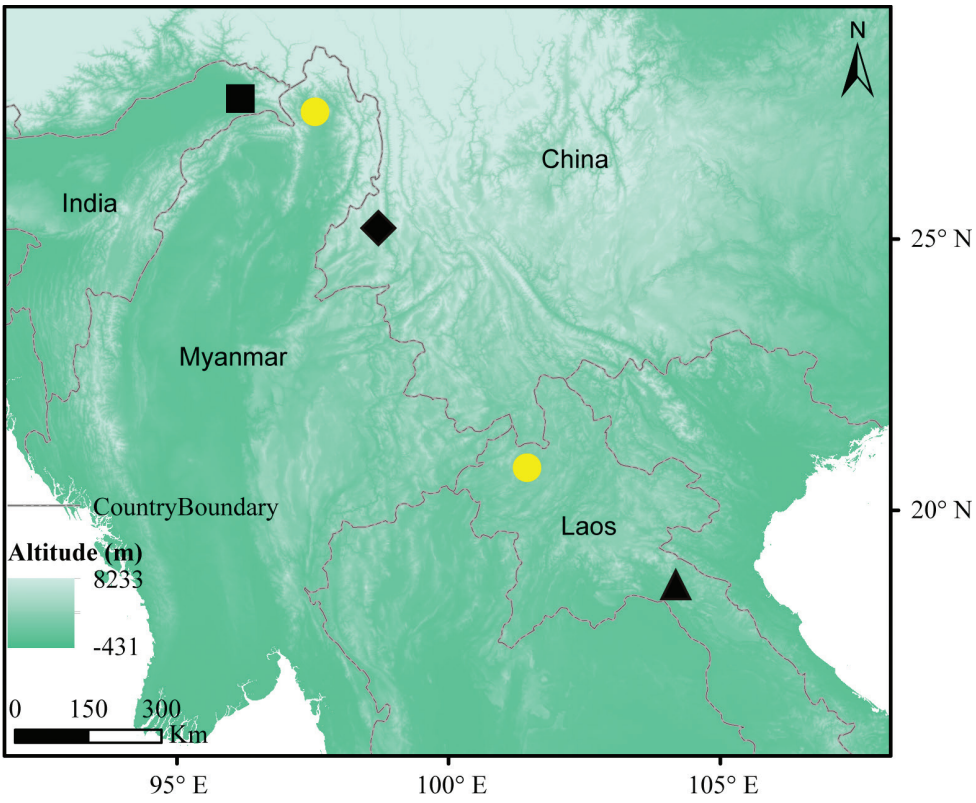

Figure 2. Localities of *Biswamoyopterus* specimens. The black square represents *B. biswasi*, ZSI 20705 (Saha, 1981); the black triangle represents *B. laoensis*, NUoL FES. MM.12.163 (Sanamxay et al. 2013); the black diamond represents *B. gaoligongensis*, KIZ 034924 and KIZ 035622 (Li et al. 2019); the yellow circles represent *Biswamoyopterus* sp., M644 and L35, collected in this study.

MA) issued by Biotechnology and Ecology Institute, Ministry of Science and Technology of Lao PDR, and permission (1567/XTBG/2017) issued by the Forest Research Institute, Forest Department, Ministry of Environmental Conservation and Forestry of Myanmar.

Materials

Twelve flying squirrel samples (two of *Biswamoyopterus* and ten of *Petaurista*) were collected from northern Myanmar and northern Laos during the expedition of 2014–2018 (see Suppl. material 1: Table S1). The samples M644 and L35 were recognized as belonging to the genus *Biswamoyopterus*. Specimen M644 (whole body) was collected from a local market in Putao county (27°20'31.20"N, 97°24'3.60"E; 446 m asl), Kachin State, Myanmar (Figure 2), on 24 November 2017, and has been deposited in CAS-SEABRI Myanmar Lab, Nay Pyi Taw, Myanmar. Specimen L35 was photographed (Suppl. material 2: Figure S1) in a local market in Louang Namtha,

northern Laos (Figure 2) on 27 March 2018, and only some tissue was collected for molecular data analysis. All sequences have been deposited in GenBank (accession numbers MK105519–MK105539); detailed sequence information has been listed in Suppl. material 1: Table S1.

Morphological methods

According to the taxonomic assignments of Wilson and Reader (2005), pelage and skull characteristics can be discriminated using traditional methods and compared with those of other genera using specimens (Appendix I) retained in the Kunming Natural History Museum of Zoology, Kunming Institute of Zoology, Chinese Academy of Sciences (**KIZ**) (Kunming, China); the Institute of Zoology, Chinese Academy of Sciences (**IOZ**) (Beijing, China); and the Guangdong Entomological Institute (**GDEI**) (Guangzhou, China); or using documented literature (Gunther 1873; Robinson and Kloss 1915; Ellerman 1940; Corbet and Hill 1992; Nowak 1999). Following the results of Li et al. (2019), 28 cranial variables were measured with a digital caliper to the nearest 0.01 mm and these are presented in Table 2 and Figure 3:

BB	Breadth of braincase,	**MYTL**	Maxillary tooth row length,
BH	Braincase height,	**NL**	Nasal length,
CBL	Condylobasal length,	**OB**	Orbit breadth,
DL	Diastema length,	**ONL**	Occipitonasal length,
FL	Frontal length,	**PL**	Palate length,
GPB	Greatest palatal breadth,	**POB**	Postorbital breadth,
IBG	Inter bullae gap,	**PPL**	Postpalatal length,
IOB	Interorbital breadth,	**RB**	Rostrum breadth,
LAB	Length of auditory bulla,	**WAAM**	Width of auditory bullae across the external auditory meati,
LBP	Length of bony palate,		
LIF	Length of the incisive foramina,	**WPFM**	Width of the bony palate at the first upper molar,
MB	Mastoid breadth,		
MH	Mandible height,	**ZB**	Zygomatic breadth,
ML	Mandible length,	**ZH**	Zygomatic height,
MRTL	Mandibular tooth row length,	**P**	Premolars,
MWN	Maximum width of nasals,	**M**	Molars.

Superscript (P^X, M^X) upper premolars and upper molars, and Subscript (P_X, M_X) lower premolars and lower molars.

In addition, measurements of the head and body length, tail length, hind foot length, and ear length were taken and compared with the original measurements labeled on the skins by the collectors. The skull measurements of M644 are listed in Table 2. Figures 4–7 display, respectively, the pelage and skull characteristics of M644 compared with all known *Biswamoyopterus* specimens, according to Saha (1981), Sanamxay et al. (2013), and Li et al. (2019).

Table 2. Comparison of five specimens of genus *Biswamoyopterus*. M644 was measured (millimeters) in this study, others were derived from Li et al. (2019).

Specimen	*B. biswasi*	*B. gaoligongensis*	*B. gaoligongensis*	*B. laoensis*	*Biswamoyopterus* sp. M644
Sex	male	male	unknown	female	unknown
Locality	Northeastern India	Southwestern China	Southwestern China	Central Laos	Northern Myanmar
Head and body length	405	440	–	455	540
Tail length	605	520	–	620	605
Hind feet length	78	75	–	74.5	71
Ear length	46	47	46	52	43
ONL	72.4	69.75	71.11	74.39	74.22
CBL	70.1	66.37	67.73	70.99	69.88
MB	–	30.72	33.5	30.79	27.15
ZB	47.5	48.41	48.3	47.72	47.09
ZH	–	4.61	4.58	4.86	5.03
BB	–	33.86	34.46	32.84	33.68
BH	–	22.9	24.15	22.55	22.37
RB	–	19.61	19.62	17.04	19.66
NL	20.9	19.35	20.7	22.57	21.83
MWN	–	13.15	12.51	13.37	13.23
IOB	19	15.75	16.38	14.06	14.29
POB	–	18.87	20.55	17.19	16.87
LIF	6.4	5.65	5.86	5.85	6.21
LBP	–	20.08	22.01	23.83	22.37
PPL	–	28.72	29.68	28.77	29.96
LAB	15.5	14.68	14.57	17.33	15.03
WAAM	–	35.88	36.76	35.96	36.96
IBG	–	6.52	6.76	5.01	6.41
MYTL	15.5	15.92	16.23	16.33	16.53
GPB	–	18.26	18.61	19.37	19.98
WPFM	–	8.58	8.03	8.05	8.34
MRTL	–	15.24	15.41	15.33	15.75
ML	–	44.44	46.53	45.36	44.67
MH	–	27.1	27.37	29.78	29.66
PL	34.7	32.6	32.87	–	35.08
DL	15.7	13.7	15.03	–	15.30
OB	24.6	26.17	26.5	–	28.42
FL	28.6	27.66	30.63	–	30.27

Molecular data and analyses

Total genomic DNA was extracted from tissue using a DNeasy Blood & Tissue kit (Qiagen, Shanghai, China). PCR mixtures contained approximately 100 ng of template DNA, 1 μL (10 pmol) of each primer, 5 μL of 10× reaction buffer, 2 μL of dNTPs (2.5 mM of each), and 2.0 U of Taq DNA polymerase, in a total volume of 50 μL. Reactions were carried out in a Veriti Thermal Cycler (Applied Biosystems, Carlsbad, CA, USA) and always included a negative control. Segments of the nuclear genes encoding the inter photoreceptor retinoid-binding protein (IRBP) and mitochondrial 12S and 16S ribosomal DNA of flying squirrels were amplified using PCR with universal primers described previously (Mercer and Roth 2003; Guha et al. 2007). Fragments were visualized using electrophoresis in 1% agarose gel, and PCR products were sequenced from both ends using an ABI PRISM 3700 sequencing system, using the same prim-

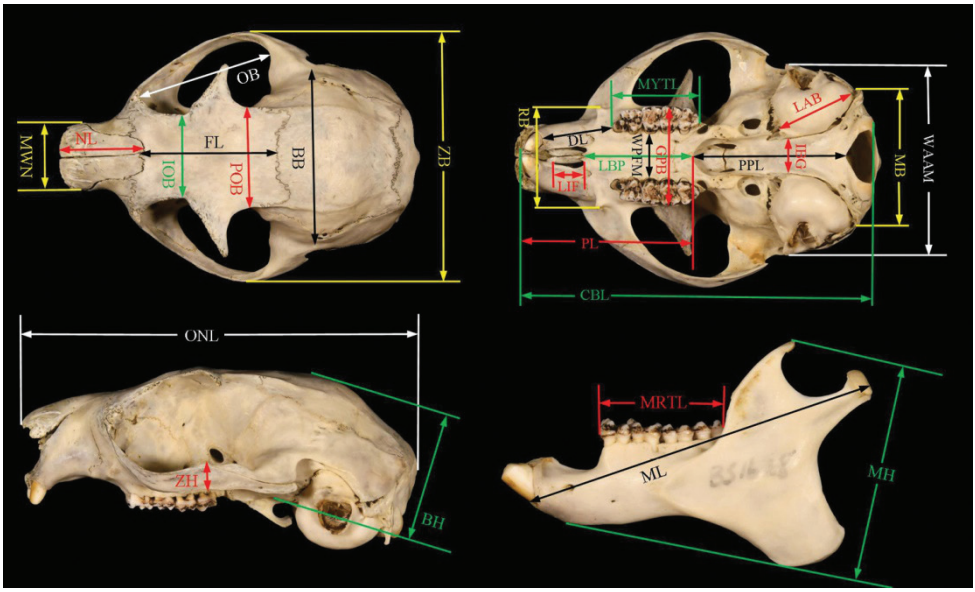

Figure 3. Illustration of the 28 cranial variables measured in this study was derived from Li et al. (2019).

ers as for PCR (Beijing Tianyi Huiyuan Bioscience and Technology Incorporation, Beijing, China).

DNA sequences were edited using the DNASTAR 5.0 (DNASTAR Inc.) program and aligned using the CLUSTALW algorithm in MEGA 6.06, with default parameters (Larkin et al. 2007; Tamura et al. 2013). Identical haplotypes were collapsed using DNASP 5.1 (Librado and Rozas 2009), and the base composition of mitogenomic sequences was analyzed using MEGA 6.06 (Tamura et al. 2013).

Phylogenies using the combined mitochondrial and nuclear DNA data from our collection and GenBank were reconstructed using maximum likelihood in RaxML version 8 (Stamatakis 2014) and Bayesian Inference (BI) in MRBAYES 3.2.6 (Ronquist et al. 2012), while the most appropriate nucleotide substitution models were selected using the Akaike Information Criterion in jMODELTEST 2.1.4 (Darriba et al. 2012). The significance of the hypothesized lineages from maximum-likelihood analyses was tested using Bootstrap analysis with 200 replicates with default settings. Markov Chain Monte Carlo (MCMC) analysis approximated posterior distributions with one cold and three heated chains, and samples of the trees and parameters were drawn every 100 steps from a total of one million MCMC generations; three additional runs were conducted beginning with random trees. The 50% majority rule consensus of the post-burn (using a burn-in of 25%) for all generations was computed for the four runs. Trees were visualized using FIGTREE 1.4 (Rambaut and Drummond 2012). Sequences representing *Tamiasciurus hudsonicus* and *Ratufa bicolor* were obtained from GenBank and used as outgroups to root the tree (Mercer and Roth 2003). Average genetic divergence was calculated between and within the studied flying squirrel species in MEGA 6.06 (Tamura et al. 2013).

Results

Morphological description of *Biswamoyopterus* sp. M644

Figures 4G, H, 5D, 6D, 7D

Remarks. Morphometrical data are presented in Table 2. As a whole, the dorsal pelage is reddish brown, with dense whitish hairs on the shoulders and hips, the ventral pelage is whitish, with yellowish brown on the edge of the membrane, the anus area is dull yellowish, but the base of the tail is brown-grey. The ears are black with few hairs, but with tufts of long, whitish hairs at the base. The feet backs are covered with black hairs, and the tail is cylindrical and reddish brown in its anterior part but gradually tending to blackish brown in its distal part. The skull is large with a GLS of 74.77 mm and a ZOB of 47.09 mm. The bullae are enlarged and each of them includes numerous septa (> 10) in a complex honeycomb pattern. The anterior edge of the nasals is slightly arc-shaped and extends slightly beyond the surface of the incisors. The surfaces of the upper and lower incisors are dull yellowish, without any orange. In the cheek teeth, P^3 is relatively enlarged and cone-shaped. The length of P^4 slightly exceeds each of the molars; P^4 has three well-developed cusps on the labial side and one large cusp on the lingual side. Both M^1 and M^2 have two well-developed cusps on the labial side and one large cusp and one smaller cusp on the lingual side, and there is a smaller cusp on the posterior transverse ridge of P^4, M^1, and M^2. M^3 is smaller than P^4, M^1, and M^2, and its later crown surface becomes a "U" shape, with a slight depression in its center.

The upper surface of the head is deep reddish brown, the muzzle is brown, the rim of the eyes is brown, the cheeks are reddish brown with occasional whitish hairs on their lower parts, the ears are black with few hairs but tufts with long, whitish hairs at the base, the back of the neck is reddish brown, and the throat and chin show whitish grey extending to both sides of the neck.

The back is mainly reddish brown, but is scattered with many white tips, especially on the shoulders and hips; individual hairs are variable in color but usually comprise the following components: whitish at the tip, reddish brown in the mid-part, and whitish grey at the base. The anterior margin of the forearms is black-brown. The chest is yellowish grey, the center of the abdomen is yellowish white, and the anus area is dull yellowish. The upper part of the membrane is reddish brown and the underpart whitish, extending to yellowish brown on the edge. The tail is cylindrical, reddish brown anteriorly, but gradually darkening towards the tip, so its posterior part is blackish brown, and the underpart area of the tail base is brown-grey. The fore and hind feet are covered with black hairs; however, the hind feet have denser hair than the fore feet, and both have dark hairless pads.

The skull is large, the frontal part is significantly depressed, the rostrum is short and wide, the anterior edge of the nasals is slightly beyond the surface of the incisors with a slight arc-shape, the incisive foramen is developed, the palatine posterior edge has an arc-shaped depressed deformation, the pterygoid is strong and the pterygoid

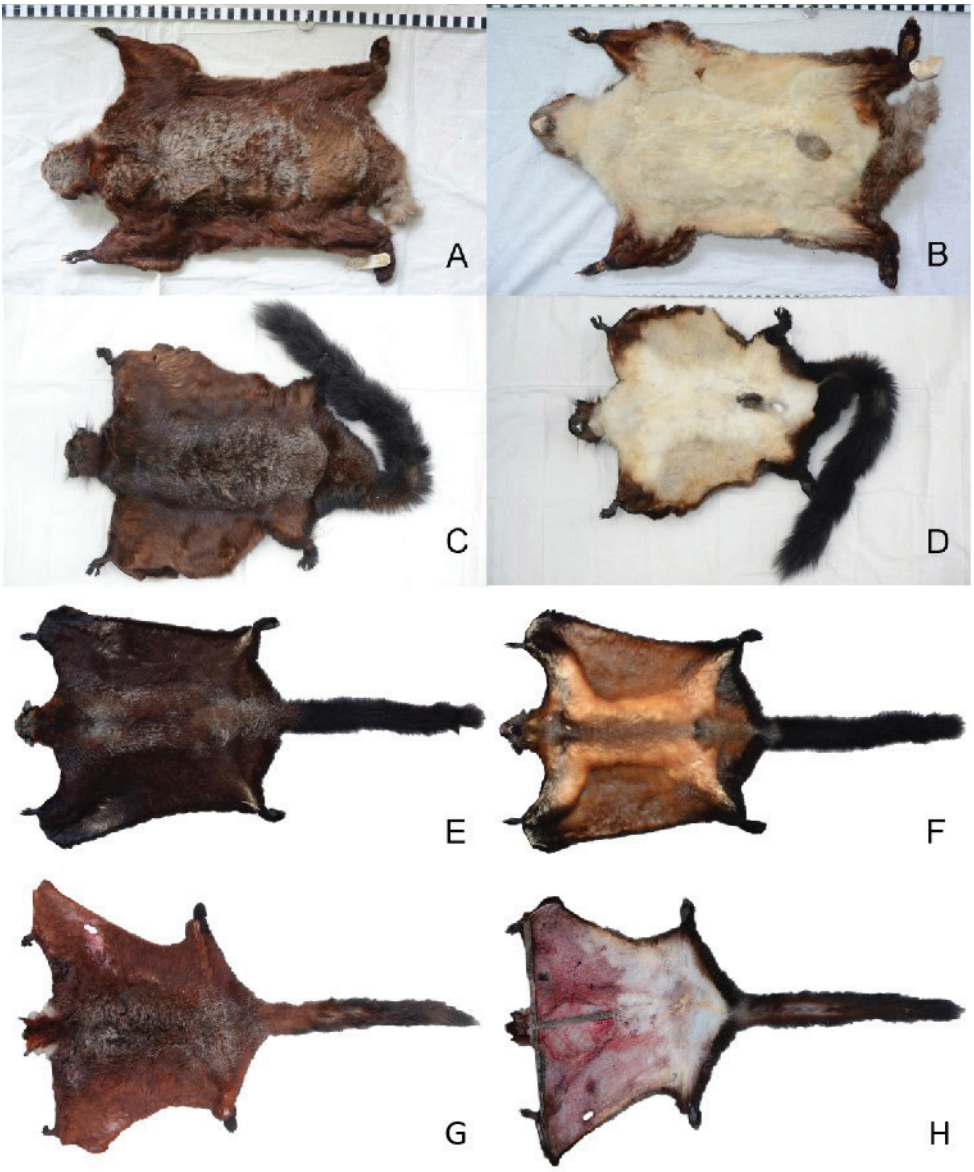

Figure 4. Comparison of skins of all known *Biswamoyopterus* specimens **A, B** *B. biswasi*, ZSI 20705 **C, D** *B. gaoligongensis*, KIZ 034924 **A–D** were derived from Li et al. (2019) **E, F** *B. laoensis*, NUoLFES. MM.12.163, from Sanamxay et al. (2013) **G, H** *Biswamoyopterus* sp. M644 from this study.

fossa wider, the bulla is developed with numerous septa (> 10) in a complex honeycomb pattern, the orbital regions are large and there is an incision on the edge of each orbit, the postorbital process is strong and curves down a little, the zygomatic plate is slant, the zygomatic arch is stronger with lower connection to the squamosal, the mastoid process is comparatively smaller, but the occipital condyle is strong.

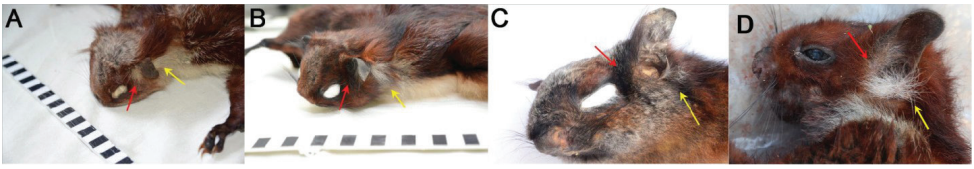

Figure 5. Comparison of ear tufts of all known *Biswamoyopterus* specimens. The red arrow indicates the anterior tufts, and the yellow arrow indicates the posterior tufts **A** *B. biswasi*, ZSI 20705 **B** *B. gaoligongensis*, KIZ 034924 **A, B** were derived from Li et al. (2019) **C** *B. laoensis* NUoL FES.MM.12.163 from Sanamxay et al. (2013) **D** *Biswamoyopterus* sp. M644 from this study.

Figure 6. The skulls (first three rows), left maxillary (the fourth rows) and left mandibular teeth (the last rows) of all known *Biswamoyopterus* specimens **A** *B. biswasi*, ZSI 20705 **B** *B. gaoligongensis*, KIZ 034924 **A, B** were derived from Li et al. (2019) **C** *B. laoensis*, NUoL FES.MM.12.163, from Sanamxay et al. (2013) **D** *Biswamoyopterus* sp. M644 from this study.

The mandible is strong, with the coronoid process developed, and the condylar process has a developed articular surface; the angular process is developed and curved towards the inside at its bottom. The upper incisors are strong and positioned vertically downwards; their outer surfaces are yellowish, without any orange. P^3 is cone-shaped

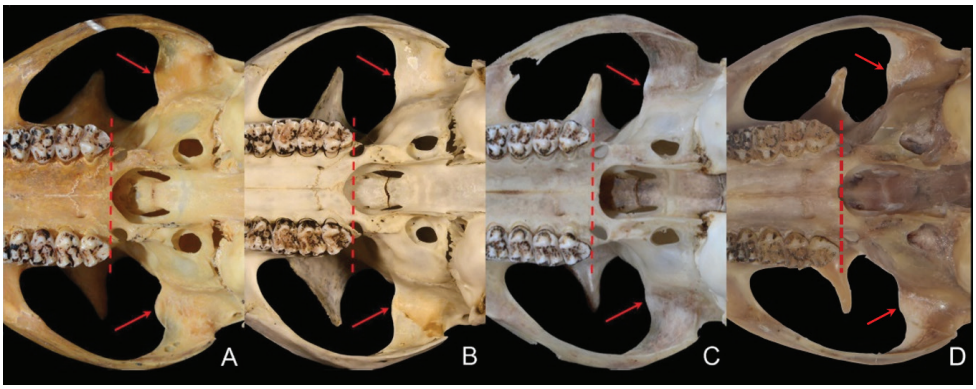

Figure 7. The posterior margin of the palatal bones relative to the posterior margin of M3 (dotted line) and shape of the preglenoid process (arrow) of all known *Biswamoyopterus* specimens **A** *B. biswasi*, ZSI 20705 **B** *B. gaoligongensis*, KIZ 034924) **A, B** were derived from Li et al. (2019) **C** *B. laoensis*, NUoL FES.MM.12.163, from Sanamxay et al. (2013) **D** *Biswamoyopterus* sp. M644 from this study.

and on the inside of the front of P^4; overall, the crown surface of P^4 appears as a triangle with three well-developed cusps on the labial side and one large cusp on the lingual side, and its labial side length is slightly longer than those of M^1, M^2, and M^3. M^1 and M^2 are approximately equal in size; both have two well-developed cusps on the labial side, and one large cusp and one smaller cusp on the lingual side. There is a smaller cusp on the posterior transverse ridge of P^4, M^1, and M^2. Compared with P^4, M^1, and M^2, M^3 is the smallest; its lingual side cusp is larger than the cusp on the labial side, and its later crown surface becomes a U-shape, with a small depression in its center.

The outer surface of the lower incisors is yellowish, the same as for the upper incisors; however, the inside part of the inner surface sinks deeply, making the outside margin sharp. From P_4 to M_3, the teeth enlarge gradually, and there are two labial and lingual cusps on each of them (the later lingual cusp of M_3 becomes a ridge); there is also a smaller cusp between, and slightly internal to, the two labial cusps on each of them. Different levels of depression occur in the centers of the crown surfaces of P_4, M_1, M_2, and M_3, with the largest in M_3.

Morphological description of *Biswamoyopterus* sp. L35

Table 3, Suppl. material 2: Figure S1

Remarks. The sample L35 from northern Laos shares the same pelage color of the tuft hair at the base of the ear and side of the neck (Figure 5, Suppl. material 2: Figure S1) with the *Biswamoyopterus laoensis* specimen (NUoL FES. MM.12.163) from central Laos. However, specimen M644 from northern Myanmar shares some key characters that have been used to distinguish the three known species from each other (Figures 4–7, Table 3): its large body size and long muzzle are similar to *B. laoensis* (NUoL FES. MM.12.163) from central Laos; the coloration of venter, tail, and ear tufts could

Table 3. Comparison of five specimens of genus *Biswamoyopterus*. M644 and L35 were described in this study, others were derived from Li et al. (2019).

Specimen	*B. biswasi*, ZSI 20705, ♂	*B. gaoligongensis*, KIZ 034924, ♂	*B. laoensis*, NUoL FES. MM.12.163, ♀	*Biswamoyopterus* sp. M644	*Biswamoyopterus* sp. L35
Locality	Northeastern India	Southwestern China	Central Laos	Northern Myanmar	Northern Laos
Size	Relatively small	Relatively small	Large	Large	Large
Dorsal coloration	Morocco-red speckled with white	Reddish brown speckled with white	Dark reddish brown speckled with whitish grey	Reddish brown speckled with whitish	Dark reddish brown speckled with whitish grey
Ventral Coloration	Light colored		Pale orange and marked with numerous, black, discontinuous lines	White	
	White	Yellowish-white			
Coloration of tail beyond the uropatagium	Partly colored tail with a dark tip		Black	Reddish brown with a brown-grey tip	
	Pale smoky grey with a dark tip	Black			
Ear tufts	Bicolored or white		Black	White	White
	White	The anterior tufts are black, and the posterior tufts are basally white and terminal black			
NL	Short		Long	Long	–
	Short	Shorter			
Outer margin of the nasal bone, orbital margin of the frontal bone, and post-orbital margin of the frontal bone vs. midline of the skull	Inclined	Almost	More	Inclined	–
Postorbital processes	Large	Large	Relatively small	Large	–
Preglenoid process	Forward protruding	Almost flat	Almost flat	Almost flat	–
Sutures of frontal and squamosal bone	Almost flat	Bulge	Almost flat	Almost flat	–
Auditory bulla	Smaller		Large	Relatively small	–
	Relatively small	Relatively small			
Posterior margin of the palatal bones	Concave forward		Flat	Concave forward	–
	The central point just meets the posterior margin of M^3	The central point lies in front of the posterior margin of M^3	The central point lies behind the posterior margin of M^3	The central point lies just a little in front of the posterior margin of M^3	
M^1 and M^2	Feeble metacone and hypocone, outline of M^1 and M^2 is sub-triangular	Most developed metacone and hypocone, outline of M^1 and M^2 is sub-square	Second developed metacone and hypocone, outline of M^1 and M^2 is sub-rectangle	Second developed metacone and hypocone, outline of M^1 and M^2 is sub-rectangle	–
M_1 and M_2	Second developed hypoconid	Most developed hypoconid	Feeble hypoconid	Feeble hypoconid	–

pertain to either *B. biswasi* (specimen ZSI 20705) from northeastern India or *B. gaoligongensis* (specimen KIZ 034924) from southwestern China, which are very similar.

Phylogeny and genetic divergence. Maximum Likelihood and Bayesian Inference analyses of the combined sequences of nuclear gene IRBP (1070 bp), mitochondrial 12S (823 bp), and 16S (535 bp) ribosomal DNA recovered similar tree topologies. The results showed that *Eupetaurus*, *Aeromys*, and *Biswamoyopterus* (sample M644 from Putao, northern Myanmar, and L35 from Louang Namtha, northern Laos) as a reciprocally monophyletic clade (Figure 8). Within this clade, *Aeromys* and *Biswamoyopterus* form sister groups with strong support (Figure 8).

For the nuclear gene IRBP, the range of original intergeneric (14 genera excluding the genus *Biswamoyopterus*) variation was 0.51–5.47% (Table 4). The genetic distances between *Biswamoyopterus* and other genera ranged from 1.57 to 5.27% (Table 4), which is greater than many intergeneric variations, such as 0.51% for *Aeretes* and *Trogopterus*,

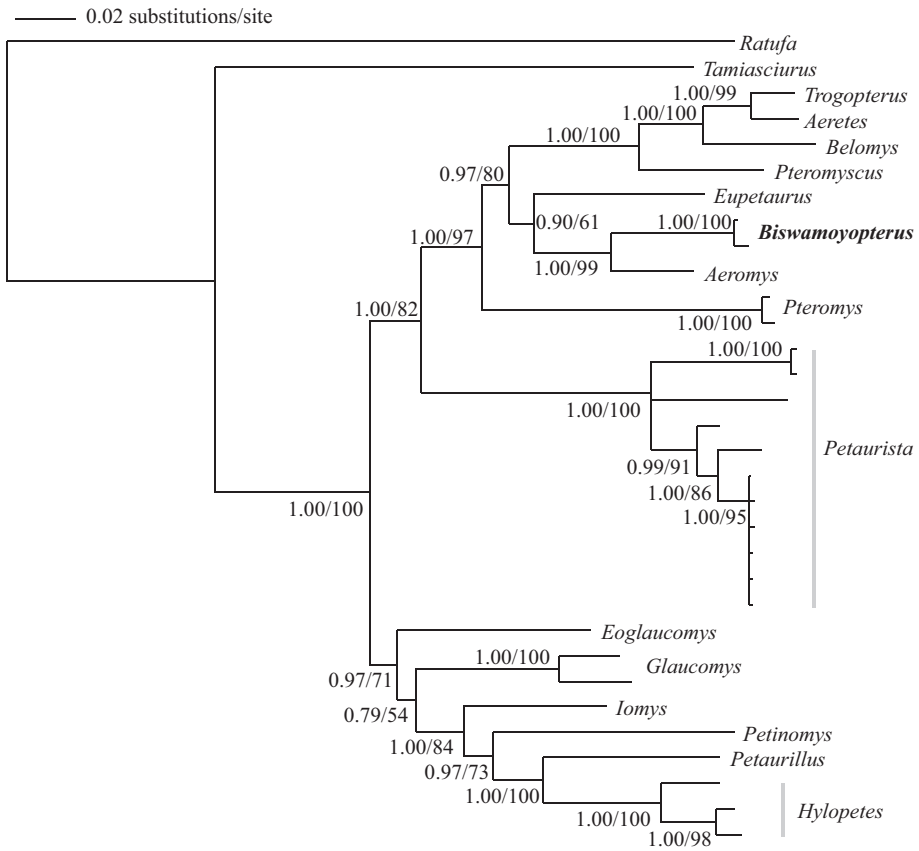

Figure 8. Bayesian Inference and Maximum Likelihood inference tree (GTR+G+I model) of flying squirrels based on combined mitochondrial and nuclear DNA data. Numbers on branches indicate posterior probability in BI and bootstrap support from ML.

Table 4. Average genetic distances (%) for nuclear IRBP-encoding sequences between the groups of studied flying squirrel species; intraspecific variations of genetic distances are also provided for each species.

	mel	tep	pea	cin	fim	vol	pha	hor	fus	phi	kin	ele	pul	set	ans	xan	Bis
Aeretes melanopterus (mel)																	
Aeromy tephromelas (tep)	2.86																
Belomys pearsonii (pea)	1.37	2.86															
Eupetaurus cinereus (cin)	2.68	2.16	3.03														
Eoglaucomys fimbriatus (fim)	4.09	4.01	4.19	3.74													
Glaucomys volans (vol)	5.18	4.90	5.00	4.64	3.47												
Hylopetes phayrei (pha)	3.94	4.20	3.76	4.20	3.13	3.66											
Iomys horsfieldi (hor)	3.92	4.01	3.76	3.84	2.69	2.95	2.60										
Petaurista alborufus (fus)	4.36	4.27	4.82	4.27	4.27	4.73	4.19	4.28									
Petaurista philippensis (phi)	3.77	4.08	4.39	3.77	3.67	4.49	4.09	3.67	1.06								
Petaurillus kinlochii (kin)	4.18	4.19	4.19	3.91	1.89	3.38	2.42	2.16	4.46	3.97							
Petaurista elegans (ele)	4.75	4.95	5.38	4.75	4.44	4.44	4.76	4.24	2.18	1.46	4.54						
Pteromyscus pulverulentus (pul)	1.28	2.77	1.46	2.59	3.92	4.91	3.85	3.66	4.74	3.88	3.91	4.85					
Petinomys setosus (set)	4.28	4.65	4.38	4.10	3.03	3.92	2.87	2.69	4.82	4.08	2.77	4.86	4.10				
Pteromys volans (ans)	4.00	3.91	3.83	3.91	4.18	5.08	4.29	4.47	4.99	4.90	4.55	5.47	3.75	4.56			
Trogopterus xanthipes (xan)	0.51	3.21	1.54	3.03	4.38	5.37	4.11	4.11	4.65	3.98	4.37	4.86	1.46	4.56	4.01		
Biswamoyopterus sp. (bis)	3.06	1.57	3.26	2.52	4.14	5.04	4.35	3.69	4.74	4.29	4.18	5.27	2.77	4.64	4.14	3.36	
Intraspecific variations	n/c	n/c	n/c	n/c	n/c	n/c	n/c	n/c	n/c	0.13	n/c	n/c	n/c	n/c	n/c	n/c	0.09

1.46% for *Belomys* and *Pteromyscus*, and 1.46% for *Pteromyscus* and *Trogopterus*. In the genus *Biswamoyopterus*, the genetic distance between M644 and L35 was 0.09%, which is smaller than the range of other interspecific variations (0.51–5.45%), close to 0.13% for intraspecific variations of *Pteromyscus pulverulentus*.

For the mitochondrial 16S ribosomal DNA sequences, the range of original intergeneric variation was 2.9–14.6% (Table 5). The genetic distances between *Biswamoyopterus* and other genera ranged from 5.2 to 12.8% (Table 5), which is greater than some intergeneric variations, such as 2.9% for *Aeretes* and *Trogopterus*. In the genus *Biswamoyopterus*, the genetic distance between M644 and L35 was 0.6%, which is really much smaller than the range of other interspecific variations (2.9–14.6%), close to 0.4% for intraspecific variations of *Petaurista philippensis*, and the same as 0.6% of *Pteromys volans*.

Discussion

According to morphological comparisons of our samples and those from previous studies (Saha 1981; Sanamxay et al. 2013; Li et al. 2019), *Biswamoyopterus* specimens L35 from northern Laos and M644 from northern Myanmar are confirmed as representing the genus *Biswamoyopterus*. However, *Biswamoyopterus* sp. M644 shares many key characters with all three known *Biswamoyopterus* species. Since each *Biswamoyopterus* species has been described on the basis of only one or two samples, it is possible that the observed morphological differences are the result of intraspecific variation. If so, it is plausible that all known *Biswamoyopterus* specimens might in fact be conspecific.

It was further implied by the molecular evidence that samples L35 and M644 belonged to the same species, with the smallest nuclear and mitochondrial DNA genetic distance among interspecific variations for any of the studied flying squirrel species (Tables 4, 5). Sanamxay et al. (2013) distinguished *B. laoensis* from *B. biswasi* mainly by 1) the large distance of 1250 km between the localities of the two species and 2) the different pelage colors present mostly on the ventral side: "white but washed with a faint orange-rufous" in *B. biswasi* versus "essentially orange" in *B. laoensis*. These factors were also true for samples L35 and M644, being separated by a long distance of more than 1000 km and different ventral pelage colors. Eliécer and Guilherme (2018) performed a study on species delimitation based on diagnosis and monophyly. The current molecular results and the morphological variability observed between *Biswamoyopterus* specimens M644 and L35 indicate that further studies should be performed to shed light on the relationships among *B. biswasi*, *B. laoensis*, and *B. gaoligongensis*.

The molecular phylogenetic analysis strongly supported *Biswamoyopterus* as an independent genus within Pteromyini, acting as a sister group to *Aeromys* (Figure 8). For nuclear and mitochondrial DNA sequences, the genetic distances between *Biswamoyopterus* and other genera are greater than many of the intergeneric variations (Tables 4, 5). Both nuclear and mitochondrial analyses suggested that *Biswamoyopterus* is a separate flying squirrel genus distinct from every validly described genus. We note that

Table 5. Average genetic distances (%) for 16S ribosomal DNA sequences between the groups of studied flying squirrel species; intraspecific variations of genetic distances are also provided for each species.

	mel	tep	pea	cin	fim	vol	pha	alb	hor	fus	hai	yun	phi	kin	ele	pul	set	ans	xan	Bis
Aeretes melanopterus (mel)																				
Aeromy tephromelas (tep)	9.5																			
Belomys pearsonii (pea)	6.5	11.6																		
Eupetaurus cinereus (cin)	10.4	8.2	11.5																	
Eoglaucomys fimbriatus (fim)	11.5	11.6	12.4	11.8																
Glaucomys volans (vol)	9.7	9.8	12.2	11.3	8.7															
Hylopetes phayrei (pha)	11.1	11.7	12.5	12.5	10.8	8.5														
Hylopetes alboniger (alb)	10.9	11.4	12.2	12.3	10.5	8.4	2.9													
Iomys horsfieldi (hor)	9.8	9.7	10.3	11.0	9.2	7.6	7.3	7.5												
Petaurista alborufus (fus)	11.3	10.9	12.4	12.1	13.2	11.6	10.6	11.1	10.5											
Petaurista hainana (hai)	12.2	11.8	12.4	11.3	13.4	11.3	11.7	11.3	10.1	7.6										
Petaurista yunanensis (yun)	11.7	11.6	12.9	11.1	12.7	11.0	10.3	10.2	9.8	6.1	2.3									
Petaurista philippensis (phi)	12.4	11.8	13.9	12.4	12.5	11.2	11.0	11.1	10.3	7.6	2.7	1.9								
Petaurillus kinlochii (kin)	9.4	10.6	11.0	11.5	9.0	7.4	7.1	8.0	5.6	11.2	9.7	8.8	9.9							
Petaurista elegans (ele)	11.9	13.0	12.6	12.5	13.4	13.0	10.4	10.0	10.9	7.9	6.5	6.6	6.8	10.5						
Pteromyscus pulverulentus (pul)	8.0	11.1	7.8	11.5	13.6	12.3	13.8	13.6	11.4	12.4	13.3	12.6	13.6	10.8	12.7					
Petinomys setosus (set)	11.7	11.2	12.9	12.7	8.4	10.6	8.9	8.6	10.1	12.9	13.3	12.1	12.6	9.0	11.7	14.6				
Pteromys volans (ans)	10.2	10.5	10.9	10.6	10.5	10.9	12.2	11.7	10.1	12.4	10.9	10.7	11.2	8.3	12.2	11.6	11.4			
Trogopterus xanthipes (xan)	2.9	10.4	6.1	10.4	12.2	10.7	10.9	10.9	9.6	11.3	12.2	11.7	12.4	9.2	11.4	8.0	12.1	10.6		
Biswamoyopterus sp. (bis)	8.9	5.2	8.9	8.0	8.9	9.3	9.9	9.6	8.8	11.0	12.3	11.1	11.1	9.5	12.8	10.9	11.2	10.3	8.5	
Intraspecific variations	n/c	n/c	n/c	n/c	n/c	3.3	5.1	n/c	n/c	n/c	n/c	n/c	0.4	n/c	0.4	n/c	n/c	0.6	n/c	0.6

DNA sequences for genus *Aeretes* cited in the literature may be based on mistaken institutional identifications, as reported recently by Roth and Mercer (2015). Therefore, additional molecular evidence is needed to determine the phylogenetic relationships among these flying squirrels more clearly in the future.

During the expedition of 2014–2018, only two samples of *Biswamoyopterus* were found. We therefore propose that *Biswamoyopterus* should be classified as critically endangered on the IUCN Red List, due to a series of threats on the Indo-China peninsula that include intense hunting, illegal trade, and rapid habitat loss (Rao et al. 2010; Geissmann et al. 2011). In order to understand the population status, range, and other biological features of *Biswamoyopterus*, further studies including biodiversity expeditions covering the whole Indo-China peninsula should be performed. With respect to biogeography, members of the genus *Biswamoyopterus* inhabit the northern Indo-China peninsula, which belongs to one of the global biodiversity hotspot regions (Myers et al. 2000). The mechanisms responsible for their differentiation and how they have adapted to the environment are still unknown; therefore, more studies should be carried out to explore the differentiation, adaptation, and evolution of genus *Biswamoyopterus* and to make every effort to conserve them.

Acknowledgements

This work was conducted at the Southeast Asia Biodiversity Research Institute, Chinese Academy of Sciences (CAS-SEABRI), and the Kunming Institute of Zoology, Chinese Academy of Sciences (KIZ, CAS). We sincerely thank the subject editor Raquel López-Antoñanzas, the editor Yasen Mutafchiev, and the reviewer John Mercer for their very helpful comments. Special thanks go to Dr. Chen Jun of the Institute of Zoology, CAS; Ms. Yang Ping for assistance with specimen examination; and Mr. Shu-Sen Shu for taking photographs of specimen M644. Laboratory work was completed in the Central Laboratory, Public Technology Service Center, Xishuangbanna Tropical Botanical Garden (XTBG), CAS. This study was supported by Lancang-Mekong Cooperation Special Fund (Biodiversity Monitoring and Network Construction along Lancang-Mekong River Basin project), CAS-SEABRI (Y4ZK111B01), CAS 135 program (no. 2017 XTBG-F03), Ministry of Science and Technology of the People's Republic of China (Grant No. 2005DKA21402), National Special Fund on Basic Research of Science and Technology of China (2014FY110100) and Postdoctoral Fellowship of XTBG, CAS.

References

Amato G, Egan MG, Rabinowitz A (1999) A new species of muntjac, *Muntiacus putaoensis* (Artiodactyla: Cervidae) from northern Myanmar. Animal Conservation 2: 1–7. https://doi.org/10.1017/S1367943099000293

Corbet GB, Hill JE (1992) The mammals of the Indomalayan region: a systematic review. Oxford University Press, New York, 307 pp.

Darriba D, Taboada GL, Doallo R, Posada D (2012) jModelTest 2: more models, new heuristics and parallel computing. Nature Methods 9: 1–772. https://doi.org/10.1038/nmeth.2109

Eliécer EG, Guilherme STG (2018) Species delimitation based on diagnosis and monophyly, and its importance for advancing mammalian taxonomy. Zoological Research 39: 301–308. https://doi.org/10.24272/j.issn.2095-8137.2018.037

Ellerman JR (1940) The Families and Genera of Living Rodents (Vol. I). British Museum, London, 281–290.

Ellerman JR, Morrison-Scott TCS (1950) Checklist of Palaearctic and Indian mammals, 1758 to 1946. British Museum (Natural History), London, 460–465.

Fan PF, He K, Chen X, Ortiz A, Zhang B, Zhao C, Li YQ, Zhang HB, Kimock C, Wang WZ, Groves C, Turvey ST, Roos C, Helgen KM, Jiang XL (2017) Description of a new species of *Hoolock gibbon* (Primates: Hylobatidae) based on integrative taxonomy. American Journal of Primatology 79: 1–15. https://doi.org/10.1002/ajp.22631

Geissmann T, Lwin N, Aung SS, Aung TN, Aung ZM, Hla TH, Grindley M, Momberg F (2011) A new species of snub-nosed monkey, genus *Rhinopithecus* Milne-Edwards, 1872 (Primates, Colobinae), from northern Kachin state, northeastern Myanmar. American Journal of Primatology 73: 96–107. https://doi.org/10.1002/ajp.20894

Guha S, Goyal SP, Kashyap VK (2007) Molecular phylogeny of musk deer: a genomic view with mitochondrial 16S rRNA and cytochrome *b* gene. Molecular Phylogenetics and Evolution 42: 585–597. https://doi.org/10.1016/j.ympev.2006.06.020

Gunther A (1873) Description of three new species of flying squirrels in the collection of the British Museum. Proceedings of the Zoological Society of London 1873: 413–414.

Larkin MA, Blackshields G, Brown NP, Chenna R, McGettigan PA, McWilliam H, Valentin F, Wallace IM, Wilm A, Lopez R, Thompson JD, Gibson TJ, Higgins DG (2007) Clustal W and Clustal X version 2.0. Bioinformatics 23: 2947–2948. https://doi.org/10.1093/bioinformatics/btm404

Librado P, Rozas J (2009) DnaSP v5: a software for comprehensive analysis of DNA polymorphism data. Bioinformatics 25: 1451–1452. https://doi.org/10.1093/bioinformatics/btp187

Li G-G, Zhang M-X, Kyaw S, Maung K-W, Quan R-C (2017) Complete mitochondrial genome of the leaf muntjac (*Muntiacus putaoensis*) and phylogenetics of the genus *Muntiacus*. Zoological Research 38(5): 310–316. https://doi.org/10.24272/j.issn.2095-8137.2017.058

Li Q, Li X-Y, Jackson SM, Li F, Jiang M, Zhao W, Song W-Y, Jiang X-L (2019) Discovery and description of a mysterious Asian flying squirrel (Rodentia, Sciuridae, *Biswamoyopterus*) from Mount Gaoligong, southwest China. ZooKeys 864: 147–160. https://doi.org/10.3897/zookeys.864.33678

Li S-Q, Quan R-C (2017) Taxonomy is the cornerstone of biodiversity conservation-SEABRI reports on biological surveys in Southeast Asia. Zoological Research 38(5): 213–214. https://doi.org/10.24272/j.issn.2095-8137.2017.061

Lu XF, Ge DY, Xia L, Zhang ZQ, Li S, Yang QS (2012) The evolution and paleobiogeography of flying squirrels (Sciuridae, Pteromyini) in response to global environmental change. Evolutionary Biology 40: 117–132. https://doi.org/10.1007/s11692-012-9191-6

Mercer JM, Roth VL (2003) The effects of Cenozoic global change on squirrel phylogeny. Science 299: 1568–1572. https://doi.org/10.1126/science.1079705

Myers N, Mittermeier RA, Mittermeier CG, da Fonseca GAB, Kent J (2000) Biodiversity hotspots for conservation priorities. Nature 403: 853–858. https://doi.org/10.1038/35002501

Nowak RM (1999) Walker's Mammals of the World (Vol. II, 6th Edn.). Johns Hopkins University Press, Baltimore, 1246–1306.

Oshida T, Lin LK, Masuda R, Yoshida MC (2000a) Phylogenetic relationships among Asian species of *Petaurista* (Rodentia, Sciuridae), inferred from mitochondrial cytochrome *b* gene sequences. Zoological Science 17: 123–128. https://doi.org/10.2108/zsj.17.123

Oshida T, Lin LK, Yanagawa J, Endo H, Masuda R (2000b) Phylogenetic relationships among six flying squirrel genera, inferred from mitochondrial cytochrome *b* gene sequences. Zoological Science 17: 485–489. https://doi.org/10.2108/zsj.17.485

Oshida T, Ikeda K, Yamada K, Masuda R (2001) Phylogenetics of the Japanese giant flying squirrel, *Petaurista leucogenys*, based on mitochondrial DNA control region sequences. Zoological Science 18: 107–114. https://doi.org/10.2108/zsj.18.107

Oshida T, Ikeda K, Yamada K, Masuda R (2004) A preliminary study on molecular phylogeny of giant flying squirrels, genus *Petaurista* (Rodentia, Sciuridae) based on mitochondrial cytochrome *b* gene sequences. Russian Journal of Theriology 3: 15–24. https://doi.org/10.15298/rusjtheriol.03.1.04

Rambaut A, Drummond A (2012) FigTree v1.4.3. http://tree.bio.ed.ac.uk/software/figtree/

Rao M, Htun S, Zaw T, Myint T (2010) Hunting, livelihoods and declining wildlife in the Hponkanrazi Wildlife Sanctuary, North Myanmar. Environmental Management 46: 143–153. https://doi.org/10.1007/s00267-010-9519-x

Robinson HC, Kloss CB (1915) *Aeromys*, a new genus of flying squirrel. Journal of the Federated Malay Museums 6: 1–23.

Ronquist F, Teslenko M, van der Mark P, Ayres DL, Darling A, Hohna S, Larget B, Liu L, Suchard MA, Huelsenbeck JP (2012) MrBayes 3.2: efficient Bayesian phylogenetic inference and model choice across a large model space. Systematic Biology 61: 539–542. https://doi.org/10.1093/sysbio/sys029

Roth VL, Mercer JM (2015) Themes and variation in sciurid evolution. In: Cox PG, Hautier L (Eds) Evolution of the Rodents: Advances in Phylogeny, Functional Morphology and Development, Cambridge University Press, Cambridge, 221–245. https://doi.org/10.1017/CBO9781107360150.009

Saha SS (1981) A new genus and a new species of flying squirrel (Mammalia: Rodentia: Sciuridae) from Northeastern India. Bulletin Zoological Survey of India 4: 331–336.

Sanamxay D, Douangboubpha B, Bumrungsri S, Xayavong S, Xayaphet V, Satasook C, Bates PJ (2013) Rediscovery of *Biswamoyopterus* (Mammalia: Rodentia: Sciuridae: Pteromyini) in Asia, with the description of a new species from Lao PDR. Zootaxa 3686: 471–481. https://doi.org/10.11646/zootaxa.3686.4.5

Stamatakis A (2014) RAxML version 8: a tool for phylogenetic analysis and post-analysis of large phylogenies. Bioinformatics 30: 1312–1313. https://doi.org/10.1093/bioinformatics/btu033

Tamura K, Stecher G, Peterson D, Filipski A, Kumar S (2013) MEGA6: Molecular Evolutionary Genetics Analysis version 6.0. Molecular Biology and Evolution 30: 2725–2729. https://doi.org/10.1093/molbev/mst197

Thorington RW, Pitassy D, Jansa SA (2002) Phylogenies of flying squirrels (Pteromyinae). Journal of Mammalian Evolution 9: 99–135. https://doi.org/10.1023/A:1021335912016

Tordoff AW, Eames JC, Eberhardt K, Baltzer MC, Davidson P, Leimgruber P, Than UA (2005) Myanmar: Investment Opportunities in Biodiversity Conservation. Birdlife International, Yangon, 23 pp.

Wilson DE, Reeder D (2005) Mammal Species of the World: A Taxonomic and Geographic Reference (3rd edn). Johns Hopkins University Press, Baltimore, 754–818.

Yu FH, Yu FR, McGuire PM, Kilpatrick CW, Pang JF, Wang YX, Lu SQ, Woods CA (2004) Molecular phylogeny and biogeography of woolly flying squirrel (Rodentia: Sciuridae), inferred from mitochondrial cytochrome *b* gene sequences. Molecular Phylogenetics and Evolution 33: 735–744. https://doi.org/10.1016/j.ympev.2004.05.008

Yu FR, Yu FH, Pang JF, Kilpatrick CW, McGuire PM, Wang YX, Lu SQ, Woods CA (2006) Phylogeny and biogeography of the *Petaurista philippensis* complex (Rodentia: Sciuridae), inter- and intraspecific relationships inferred from molecular and morphometric analysis. Molecular Phylogenetics and Evolution 38: 755–766. https://doi.org/10.1016/j.ympev.2005.12.002

Appendix I

Specimens examined (IOZ, Institute of Zoology, Chinese Academy of Sciences; GDEI, Guangdong Entomological Institute; KIZ, Kunming Institute of Zoology, Chinese Academy of Sciences).

Belomys: KIZ 61004, 630743, 630799, 72226, 200362, 200363. *Petaurista*: IOZ 10457, 10458, 10460, 15041, 15042, 15043, 15044, 24009, 25849, 61-003. KIZ 73442, 73445, 73744, 73745, 73823, 830207, 90039, 90043, 90051, 90407. GDEI 0403, 0404, 0499, 0524, 0611, 0618, 0621, 0622, 0623, 0624, 0625, 0626. *Trogopterus*: KIZ 57048, 630784, 640575, 73377, 88637. *Aeretes*: KIZ 57052. *Eupetaurus*: KIZ 73372, 73373. *Pteromys*: KIZ 57053. *Hylopetes*: KIZ 73281, 74543, 74544, 74546, 76332, 76658.

Supplementary material I

Table S1. GenBank numbers of sequences that were analyzed in this study

Authors: Guogang Li, Ye Htet Lwin, Bin Yang, Tao Qin, Phouthong Phothisath, Kyaw-Win Maung, Rui-Chang Quan, Song Li

Data type: molecular data

Link: https://doi.org/10.3897/zookeys.939.31764.suppl1

Supplementary material 2

Figure S1. Photograph of specimen L35 from northern Laos

Authors: Guogang Li, Ye Htet Lwin, Bin Yang, Tao Qin, Phouthong Phothisath, Kyaw-Win Maung, Rui-Chang Quan, Song Li

Data type: multimedia

Link: https://doi.org/10.3897/zookeys.939.31764.suppl2

ZooKeys 939: 87–165 (2020)
doi: 10.3897/zookeys.939.50612
https://zookeys.pensoft.net

RESEARCH ARTICLE

A peer-reviewed open-access journal
ZooKeys
Launched to accelerate biodiversity research

Immature stages of Palearctic *Mecinus* species (Coleoptera, Curculionidae, Curculioninae): morphological characters diagnostic at genus and species levels

Rafał Gosik[1], Jiří Skuhrovec[2], Roberto Caldara[3], Ivo Toševski[4,5]

1 *Department of Zoology and Nature Protection, Maria Curie-Skłodowska University, Akademicka 19, 20-033 Lublin, Poland* **2** *Group Function of Invertebrate and Plant Biodiversity in Agro-Ecosystems, Crop Research Institute, Prague 6–Ruzyně, Czech Republic* **3** *Center of Alpine Entomology, University of Milan, Via Celoria 2, 20133 Milan, Italy* **4** *CABI, Rue des Grillons 1, 2800 Delémont, Switzerland* **5** *Institute for Plant Protection and Environment, Banatska 33, 11080, Zemun, Serbia*

Corresponding author: Jiří Skuhrovec (jirislavskuhrovec@gmail.com)

Academic editor: M. Alonso-Zarazaga | Received 29 January 2020 | Accepted 15 April 2020 | Published 9 June 2020

http://zoobank.org/B2397011-4888-4712-880E-1069C943AD33

Citation: Gosik R, Skuhrovec J, Caldara R, Toševski I (2020) Immature stages of Palearctic *Mecinus* species (Coleoptera, Curculionidae, Curculioninae): morphological characters diagnostic at genus and species levels. ZooKeys 939: 87–165. https://doi.org/10.3897/zookeys.939.50612

Abstract

The immature stages of ten *Mecinus* species are described for the first time and those of two other species are redescribed, adding important chaetotaxy characters that were missing from previous descriptions. These species belong to six of the nine assemblages of *Mecinus* species previously established according to a phylogenetic analysis. All these groupings are confirmed on the basis of several characters of mature larvae and pupae. Moreover, all the species show several characters that are useful for distinguishing them from each other, including cryptic species that previously had few differential characters. Some characters that may be useful for separating *Mecinus* from other genera in the tribe are suggested. To confirm the taxonomic identification of some larvae, the mtCOII gene was obtained and compared with sequences from identified adult specimens. The most important characters for separating the immature stages of the genera and species groups in *Mecinus* are the number of palpomeres of the labial palpi (1 or 2), the number of air tubes of the thoracic and abdominal spiracles (unicameral or bicameral), and the number of

epipharyngeal setae. The species studied herein were compared with those known from other genera in the tribe Mecinini. Two keys, one to the described larvae and the other to the pupae, are provided. Detailed biological data, several of which are new, on some species are reported.

Keywords
biology, mature larva, Mecinini, *Mecinus*, morphology, pupa, taxonomy

Introduction

The genus *Mecinus* Germar, 1821 belongs to the tribe Mecinini (Curculionidae, Curculioninae) and includes approximately 50 Palearctic species (Alonso-Zarazaga et al. 2017). Adults of this tribe were recently subjected to morphological revision (Caldara and Fogato 2013) and phylogenetic analysis (Caldara et al. 2013). Based on this analysis, seven species groups and two "complexes" of species were recognised. Moreover, a phylogenetic study on the tribe Mecinini, based on morphological characters, suggests that *Mecinus* is the sister group of the remaining Mecinini like *Gymnetron* Schoenherr, 1825 and *Rhinusa* Stephens, 1829 (Caldara 2001). Preliminary molecular studies seem to confirm the systematic separation of these genera (I. Toševski, unpublished data).

All known *Mecinus* species live on angiosperms belonging to the tribes Plantagineae and Antirrhineae of the family Plantaginaceae as recently defined (Olmstead et al. 2001; Albach et al. 2005; APG 2016). The larvae develop inside the ovaries, stems, or roots of the host plants and are sometimes able to induce the formation of galls (Hoffmann 1958; Caldara 2001; Toševski et al. 2011). Several species of the genus have been the subject of detailed ecological studies (De Clerck-Floate and Harris 2002; De Clerck-Floate and Miller 2002; McClay and De Clerck-Floate 2002; Sing et al. 2005; Toševski et al. 2011) as potential biological control agents for some species of toadflax (*Linaria* spp.) that were introduced into North America and have since become invasive (Vujnovic and Wein 1997).

To date, larvae of only approximately 30 Mecinini species have been described, while descriptions of pupae have been made for 15 Mecinini species (see Skuhrovec et al. 2018 for complete references). However, there are only a few detailed descriptions of larvae and pupae that can be used for an adequate taxonomic comparison; these include immatures of three species of *Gymnetron* (Jiang and Zhang 2015), two species of *Rhinusa* (Gosik 2010; Ścibior and Łętowski 2018), five species of *Cleopomiarus* (Skuhrovec et al. 2018; Szwaj et al. 2018) and three species of *Miarus* (Skuhrovec et al. 2018). In fact, the comparison of approximately ten previously described immatures of mecinines, including two *Mecinus* species, *M. heydenii* Wencker, 1866 (Emden 1938) and *M. janthinus* Germar, 1821 (Scherf 1964), is somewhat problematic due to the absence of important details of the chaetotaxy and/or the absence of quality drawings.

Therefore, the aims of this study were to describe several larvae and pupae of *Mecinus* for the first time, to find characters that are diagnostic at genus and species levels, and finally to compare the characters on immature stages of this genus with other genera of the same tribe that might be phylogenetically informative.

Materials and methods

Insect collection

The material for this study was collected mainly from June to August 2017, in localities of Serbia, Macedonia, Bulgaria and France. The immature stages, i.e., L3 larvae and pupae from every studied species, were collected from their host plants and subsequently preserved in 2 ml screw-cap micro tubes (Sarstad, Germany) filled with 96% ethanol at 4–6 °C.

Molecular analysis

In specific cases, when two species inhabit the same host plant and larval development occurs in the same host niche, the taxonomic identity of collected larvae and pupae was confirmed by molecular methods. Since it is known that the immature specimens are unavoidably damaged by these procedures, before their sequencing the specimens were compared with the others used for the morphological study in order to be sure on their conspecificity. Total DNA was extracted using the QIAGEN Dneasy Blood & Tissue Kit (Qiagen, Hilden, Germany) according to the manufacturer's instructions. The mitochondrial cytochrome oxidase subunit II gene (mtCOII gene) was amplified using the primers TL2-J-3038 (5'-TAATATGGCAGATTAGTGCATTGGA-3') (Emerson et al. 2000) and TK-N 3782 (5'-GAGACCATTACTTGCTTTCAGTCATCT-3') (EVA-Harrison Laboratory, Cornell University, Ithaca, NY, USA). The polymerase chain reactions (PCRs) contained NH4 buffer (19), 5 mM MgCl2, 0.8 mM of each dNTP, 0.75 μM of each primer and 0.75 U of Taq polymerase (Fermentas) in a 20 μL final volume. PCR cycles were carried out in a Mastercycler EP Gradient S (Eppendorf, Germany) with the following thermal steps: 95 °C for 5 min (initial denaturation), 40 cycles at 95 °C for 1 min, 1 min at 45 °C (annealing), 72 °C for 2 min and a final extension at 72 °C for 10 min. The amplified products of the COII gene were sequenced with the forward primer only. The sequencing was performed on an ABI Prism 3700 automated sequencer using the commercial services of Macrogen Inc. (Seoul, South Korea). In addition, adult specimens of all species, whose larvae and pupae were described in this study, were identified by two of the authors (RC and IT), based on morphology. Subsequently, specimens were sequenced for the mitochondrial COII gene. The taxonomic identity of the larvae and pupae was done by comparing their sequences with the adult ones. Pairwise distances using the p-distance model were analysed using MEGA5 software (Tamura et al. 2011). The obtained sequences were deposited in the GenBank database under accession numbers MN991999–MN992012.

Confirmation of taxonomic status using molecular tools

Molecular analysis confirmed the taxonomic identity of the larval and pupal stages of *M. labilis* and *M. pascuorum* which occur together developing in pyxidia of

Plantago lanceolata L., and also helped to discriminate between the immature stages of *M. pirazzolii* and *M. ictericus* (Gyllenhal, 1838), which sometimes co-occur associated with *P. arenaria* Waldst. & Kit. All *Mecinus* taxa whose immature stages are described in this study were sequenced for the mtCOII gene. Sequences were edited with FinchTV v.1.4.0 (http://www.geospiza.com) and aligned with Clustal*W* integrated in the Mega5 software (Tamura et al. 2011). Aligned sequences were truncated to 655 bp from the 3' end prior to calculating the pairwise distances among the taxa. The recorded divergences among the analysed taxa ranged from 1.5 and 23.4% between *M. janthinus-M. janthiniformis* and *M. collaris-M. heydenii*, respectively (Table 1). The complete mtCOII gene showed different lengths across *Mecinus* species, ranging from a 678 bp (*M. janthinus*) group to 696 bp. in *M. pyraster*.

Morphological descriptions

Part of the larval and pupal material was preserved in Pampel fixation liquid (see Skuhrovec and Bogusch 2016) and used for the morphological descriptions. To prepare the slides, we followed May (1994): a larva was decapitated, and the head was cleared in a 10% potassium hydroxide (KOH) solution and then rinsed in distilled water. After clearing, the mouthparts were separated from the head capsule, and the head capsule and all mouthparts were mounted on permanent microscope slides in Euparal. All other body parts were mounted on temporary microscope slides in 10% glycerine.

The observations and measurements were conducted using a light microscope with calibrated ocular lenses (Olympus BX 40 and Nikon Eclipse 80i). The following characters were measured for each larva: head width, body length (larvae fixed in a C-shape were measured in segments), and body width in the widest place (i.e., metathorax or abdominal segments I–IV). For the pupae, the length and width at the widest place were measured. All results of the measurements are given in Table 2 (mature larva) and in Table 3 (pupa). The lengths of all setae are visible in the figures.

Table 1. Mitochondrial DNA cytochrome oxidase subunit II (COII) divergence based on pairwise analysis (p-distance method) among *Mecinus* species elaborated in this study. Numbers in brackets represent complete length of the COII gene.

Species	1	2	3	4	5	6	7	8	9	10	11	12
1. *M. circulatus* (696 bp)	–											
2. *M. pyraster* (696 bp)	0.145	–										
3. *M. collaris* (693 bp)	0.177	0.186	–									
4. *M. heydenii* (684 bp)	0.221	0.218	0.227	–								
5. *M. laeviceps* (684 bp)	0.218	0.223	0.214	0.114	–							
6. *M. peterharrisi* (684 bp)	0.214	0.217	0.227	0.114	0.066	–						
7. *M. janthinus* (678 bp)	0.184	0.180	0.184	0.236	0.226	0.236	–					
8. *M. janthiniformis* (678 bp)	0.178	0.178	0.180	0.236	0.233	0.233	0.018	–				
9. *M. sicardi* (678 bp)	0.181	0.168	0.181	0.211	0.208	0.212	0.103	0.100	–			
10. *M. labilis* (693 bp)	0.149	0.156	0.186	0.220	0.211	0.215	0.190	0.187	0.180	–		
11. *M. pascuorum* (693 bp)	0.184	0.187	0.173	0.208	0.204	0.205	0.201	0.193	0.180	0.183	–	
12. *M. pirazzolii* (693 bp)	0.192	0.181	0.190	0.217	0.214	0.215	0.198	0.193	0.193	0.176	0.189	–

Table 2. Measurements (in mm) of body parts (mature larva) in studied *Mecinus* species. [n] = number of specimens.

***Mecinus* species**	**Body length**	**Body width**	**Head width**
M. pascuorum	1.60[1], 1.70[2], 1.80[2], 1.90[1], 1.96[1]	1.00[2], 1.10[3], 1.20[2]	0.36[1], 0.38[2], 0.40[4]
M. labilis	1.40[1], 1.90[1], 2.00[1]	0.84[1], 0.90[1], 1.00[1]	0.36[1], 0.38[1], 0.40[1]
M. pirazzolii	1.40[2], 1.50[4], 1.60[2], 1.66[4], 1.83[2], 2.00[2]	0.73[8], 0.86[7], 1.00[1]	0.36[10], 0.40[6]
M. circulatus	2.33[1], 2.50[2], 2.66[1], 2.73[1]	0.83[1], 1.00[2], 1.06[2]	0.50[1], 0.53[4]
M. pyraster	2.00[1], 2.16[1], 2.66[1], 2.83[1]	0.83[2], 1.00[2]	0.50[1], 0.53[2], 0.56[1]
M. collaris	2.00[1], 2.33[1], 2.66[7], 2.83[2], 3.00[3], 3.16[4], 3.33[5], 3.66[2]	0.80[3], 0.83[8], 1.00[10], 1.16[4]	0.56[12], 0.60[8], 0.63[4], 0.66[1]
M. janthinus	4.00[2], 4.10[1], 4.50[2], 4.75[1]	1.00[1], 1.10[1], 1.25[4]	0.50[1], 0.52[1], 0.55[3], 0.57[1]
M. janthiniformis	1.66[1], 1.83[1], 2.00[1], 2.16[2], 2.50[1], 2.73[2], 2.90[2]	0.66[2], 0.73[2], 0.83[2], 1.00[2], 1.10[2]	0.53[4], 0.60[2], 0.63[1], 0.66[3]
M. sicardi	2.71[1], 3.40[1], 3.75[2]	1.10[2], 115[1], 1.25[1]	0.60[2], 0.62[1], 0.65[1]
M. heydenii	2.16[2], 2.20[1], 2.36[1], 2.53[1], 2.66[1]	0.83[1], 0.90[2], 0.96[1], 1.00[2]	0.30[4], 0.33[2]
M. laeviceps	1.67[1], 1.77[1], 1.90[1], 2.00[1], 2.27[2], 2.33[1], 2.67[1]	0.37[1], 0.40[1], 0.46[2], 0.57[3], 0.83[1]	0.30[4], 0.33[3], 0.40[1]
M. peterharrisi	2.00[3], 2.50[4], 2.75[5], 3.00[4], 3.50[6], 3.75[2]	0.65[5], 0.75[9], 1.00[10]	0.35[2], 0.36[8], 0.38[3], 0.40[5], 0.42[3], 0.43[3]

Table 3. Measurements (in mm) of body parts (pupa) in studied *Mecinus* species. [n] = number of specimens; BL = body length; BW = body width; HW = head width.

	Male			**Female**		
***Mecinus* species**	**BL**	**BW**	**HW**	**BL**	**BW**	**HW**
M. pascuorum	1.52[1], 1.70[2], 1.72[1], 1.74[1], 1.90[1], 1.96[1]	0.90[1], 0.94[1], 0.98[1], 1.00[3], 1.20[1]	0.32[3], 0.34[2], 0.36[1], 0.40[1]	1.70[1], 1.76[1], 1.88[3], 1.94[1], 2.00[1], 2.10[1]	0.94[1], 1.00[2], 1.06[1], 1.10[1], 1.12[1], 1.16[1], 1.20[1]	0.34[2], 0.36[1], 0.38[1], 0.40[4]
M. labilis	1.40[2], 1.80[1], 2.00[1]	1.00[2], 1.04[1], 1.40[1]	0.36[1], 0.38[3]	1.90[3], 2.20[1],	1.00[2], 1.10[2]	0.38[3], 0.40[1]
M. pirazzolii	1.63[2], 1.70[1], 1.73[1], 1.80[1]	0.93[4], 0.96[1]	0.33[4], 0.36[1]	1.80[1], 1.96[2], 2.03[1], 2.10[2]	0.96[3], 1.03[2], 1.16[1]	0.36[5], 0.40[1]
M. circulatus	2.56[1], 2.67[1]	1.20[1], 1.40[1]	0.46[1], 0.50[1]	2.50[1], 2.53[2], 2.60[1], 2.66[2], 2.73[1], 3.00[1]	1.16[1], 1.20[1], 1.23[2], 1.33[3], 1.40[1]	0.46[6], 0.50[2]
M. pyraster	3.33[1], 340[1]	1.40[1], 1.46[1]	0.53[2]	3.66[1], 3.83[1], 4.26[1]	1.66[2], 1.73[1]	0.60[2], 0.63[1]
M. collaris	1.66[1],1.83[1], 2.03[1], 2.16[2], 2.20[1], 2.23[1], 2.33[2], 2.26[1]	0.76[1], 0.96[1], 1.00[1], 1.03[1], 1.06[2], 1.13[3], 1.20[1]	0.30[3], 0.33[4], 0.36[3]	1.83[2], 2.00[4], 2.16[3], 2.33[2]	0.76[2], 0.90[1], 0.93[2], 1.00[4], 1.13[2]	0.33[6], 0.36[5]
M. janthinus	3.25[1], 3.60[1], 4.00[1]	1.16[2], 1.23[1]	0.46[1], 0.50[2]	3.70[1], 3.75[1], 3.95[1], 4.05[1], 4.25[1]	1.16[1], 1.20[1], 1.36[1], 1.40[1], 1.50[1]	0.46[1], 0.50[3], 0.53[1]
M. janthiniformis	3.23[1], 3.33[1], 3.66[1], 3.93[1], 4.00[1], 4.33[1]	1.20[1], 1.33[1], 1.42[1],1.43[1], 1.50[2]	0.46[1], 0.50[1], 0.53[1], 0.60[3]	3.83[1], 4.00[2], 4.06[1], 4.16[1], 4.26[1]	1.26[1], 1.43[1], 1.50[2], 1.66[1], 1.80[1]	0.53[1], 0.60[3],0.63[1], 0.66[1]
M. sicardi	3.75[1], 4.25[2]	1.75[2], 1.80[1]	0.60[2], 0.65[1]	4.25[1]	2.00[1]	0.70[1]
M. heydenii	2.10[1], 2.20[1],2.33[1], 2.60[1] 2.66[1]	0.63[1], 0.66[1], 0.73[1], 1.06[1], 1.13[1]	0.30[2], 0.34[1], 0.30[1], 0.36[1]	2.36[1], 2.60[1],2.66[1], 2.73[1], 2.93[1]	0.70[2],0.83[1], 1.00[1], 1.16[1]	0.30[2], 0.34[2], 0.36[1]
M. laeviceps	2.12[1], 2.37[1]	0.87[1], 1.02[1]	0.35[2]	2.50[2]	1.07[2]	0.40[2]
M. peterharrisi	2.46[1], 2.83[5], 3.10[3]	0.83[2], 1.20[6], 1.33[1]	0.36[3], 0.40[6]	3.00[3], 3.23[5], 3.66[2]	1.20[2], 1.33[5], 1.50[3]	0.36[4], 0.40[3], 0.43[3]

Drawings were created with a drawing tube on a light microscope and processed by a computer (Adobe Photoshop, Corel Photo-Paint 11, GIMP 2). The numbers of setae in bilateral structures are given for one side.

We used the terms and abbreviations for the setae of the mature larvae and pupae found in Scherf (1964), May (1977, 1994), and Marvaldi (1998, 1999).

The sequence of the species followed that proposed by Caldara and Fogato (2013) and Caldara et al. (2013).

Botanical taxonomy

For families and subfamilies, we complied with APG (2016) whereas for the complex situation concerning the nomenclature of some common species of *Plantago*, we followed the proposals by Applequist (2006) and Dowel and Shipunov (2017).

Results

Morphology of immature stages

Genus *Mecinus* Germar, 1821

Description of the mature larva (L3). ***Measurements*** (in mm). Body length: 1.66–4.75. Body width (metathorax or abdominal segments I–II) 0.37–1.25. Head width: 0.30–0.66.

Body distinctly white to yellow. Body curved, slender, rounded in cross section. Setae on body thin, in different colouration, distinctly different in length; piliform, integument often with some asperities. Prothorax slightly smaller than meso- and metathorax. Spiracle placed between the pro- and mesothorax (see e.g., Gosik et al. 2016). Abdominal segments I–III(VI) of almost equal length, next abdominal segments decreasing gradually to the terminal parts of the body. Abdominal segment X reduced to three or four anal lobes of unequal size. Anus located terminally. Thoracic spiracles uni- or bicameral, eight abdominal spiracles unicameral, all spiracles functional, close to anterior margin of segment. Prothorax with eight to eleven *prns*; two *ps*; and one *eus*. Mesothorax with one *prs*, two or three *pds*; one or two *as*; three *ss*; one *eps*; one *ps*; and one *eus*. Chaetotaxy of metathorax almost identical to that of mesothorax. Each pedal area of thoracic segments well separated, with three to six *pda*. Abdominal segments I–VIII with one *prs*; three or four *pds*; two or three *ss*; two long *eps*; one *ps*; one *lsts*; and two *eus*. Abdominal segment IX with two to four *ds*; one or two *ps*; and two *sts*. Abdominal segment X without or with up to two minute *ts*.

Head capsule yellow to pale brown, rounded or flattened laterally, endocarinal line distinct, half or more than half the length of frons. Frontal sutures extended to antennae. One or two stemmata (st), anterior stemma in the form of a pigmented spot with convex cornea. Dorsum of the epicranium with five setae; des_1 located in the central part of epicranium, des_2 lateral, des_3 located anteriorly on epicranium close to frontal suture, des_4 often medially, des_5 located anterolaterally. Frons with three to five *fs*, fs_1 sometimes absent, fs_2 absent except one exception; fs_4 and fs_5 subequal. Head with two *les*, one or two *ves*, and one to five *pes*. *Antennae* located at the end of the frontal suture on each side, membranous and distinctly convex basal article bearing three or four sensilla and a conical sensorium, the later elongated, narrow. ***Clypeus*** trapezium-

shaped, with one or two *cls*, and one sensillum (clss); all very close to margin with frons. Labrum with three *lms*; anterior margin bisinuated; lrs_1 placed posteromedially, lrs_2 anteromedially, lrs_3 posterolaterally. Epipharynx with three finger-like *als*; with two or three *ams*; and one or two *mes*; labral rods (lr) distinct, kidney-shaped. Mandibles distinctly broad, bifid, teeth of unequal height; slightly truncate; both setae piliform. Maxilla stipes with one *stps*, two *pfs* and one short to minute *mbs*; mala with six or seven finger-like *dms*; four or five *vms*; all *vms* distinctly shorter than *dms*. Maxillary palpi with two palpomeres; basal palpomere with one short *mxps* and two sensilla; distal palpomere with one sensillum and a group of microcuticular apical processes. Prelabium various in shape, with one *prms*; ligula with sinuate margin and two or three *ligs*; premental sclerite well sclerotised but without anterior and posterior extensions, U-shaped or cup-like. Labial palpi with one or two palpomeres; each of the palpomeres with one sensillum, distal palpomere with cuticular apical processes. Postlabium with three *pms*: pms_1 usually the shortest, placed anteromedially or anterolaterally, pms_2 the longest, placed laterally, and pms_3 short or medium, placed posterolaterally.

Description of pupa. ***Measurements*** (in mm). Head width: 0.28–0.75. Body width: 0.90–2.15. Body length: 1.20–5.00.

Body stout or elongate; normally white, but sometimes yellowish; cuticle smooth. Rostrum various in length, from two to five times as long as wide. Antennae short or elongate. Pronotum 1.1–2.2 times as wide as long. Meso- and metanotum often equal in length. Abdominal segments I–(IV)VII of equal length; segment VIII almost semi-circle, segment IX distinctly reduced. Spiracles on abdominal segments placed dorso-laterally; on segments I–V functional, on segment VI atrophied on next ones invisible. Urogomphi (ur) short or elongate.

Chaetotaxy often well developed, but sometimes almost invisible. Head capsule without or with one *vs*, without or with up to two *sos*, without or with up to two *os*. Rostrum without or with up to two *rs*, and without or with one *pas*. Pronotum without or with up to two *as*, without or with one *ds*, one or two *sls*, without or with up to two *ls*, and two to four *pls*. Dorsal parts of meso- and metathorax with two or three setae. Apex of femora normally with one short *fes*. Abdominal segments I–VIII without or with up to two setae laterally and without or with up to three setae ventrally. Dorsal parts of abdominal segments I–VII with three to seven setae; abdominal segment VIII with three to six setae dorsally. Abdominal segment IX without or with up to four micro-setae ventrally.

Descriptions of immature stages of the species

Mecinus pascuorum group

Differential diagnosis. Larva. (1) cuticle of the body tuberculate; (2) pedal lobes prominent, clearly distinct; (3) abdominal segment X reduced to three anal lobes; (4) thoracic spiracle unicameral; (5) abdominal setae various in length, progressively longer from abdominal segment I to VIII; (6) abdominal segments I–VIII with four

pds and two *ss*; (7) head white, rounded; (8) frontal suture weakly visible; (9) endocarina 4/5 length of frons; (10) des_4 short; (11) presence of fs_1; (12) absence of fs_2; (13) fs_3 very short; (14) head with one stemma; (15) absence of cls_1; (16) labial palpi one-segmented; (17) premental sclerite cup-like, posterior extension with short, dull apex; (18) surface of postlabium smooth.

Pupa. (1) body stout, rather short; (2) urogomphi short; (3) rostrum moderately slender; (4) setae various in length; (5) head with one *os*; (6) rostrum with one or two *rs*; (7) pronotum with two *as*, without or with one *ds*, two *ls*, three *pls*; (8) meso- and metanotum with two setae; (9) abdominal segments I–VII with two or three setae dorsally and three minute setae ventrally.

Remarks and comparative notes. The adults of this assemblage of several taxa are mostly very similar to each other, but, lacking synapomorphies, they were treated by Caldara et al. (2013) as a "complex" of species. Overall, they are characterised by small size (length shorter than 2.5 mm), usually with short, oval elytra, and with integument, at least in part, reddish. The larvae also have a combination of characters that distinguish them from those of the other groups, although with no clear autapomorphies. In contrast, the pupae are unique in having abdominal segments I–VII with 2–3 setae dorsally and three minute setae ventrally. Therefore, we can consider these species as an informal group like the other species groups.

Mecinus pascuorum (Gyllenhal, 1813)

Material examined. 7 L3 larvae and 13 pupae, Serbia, Staničenje, 6.07.2017, 43°12.915'N, 22°30.495'E, 364 m., ex *Plantago lanceolata*, lgt. I. Toševski. Accession numbers of sequenced specimens MN992009 (larva), MN992010 (pupa).

Description of mature larva (Figures 1A–D, 2A–F). ***Measurements*** (in mm). Body length: 1.60–1.96. Body width (metathorax): 1.00–1.20. Head width: 0.36–0.40.

Body (Figure 1A–D) white, slender, curved. Chaetotaxy of thoracic segments relatively well developed, setae capilliform, different in length, light yellow, on thoracic segments elongated or medium, on abdominal segments very short. Prothorax (Figure 1B) with eight *prns* of almost equal length, two *ps* and one *eus*. Meso- and metathorax (Figure 1B) with one medium *prs*, three medium *pds*, equal in length; one medium *as*, three medium *ss*, equal in length; one long *eps*, one long *ps* and one long *eus*. Pedal area with five long, equal in length *pda*. Abdominal segments I–VIII (Figure 1C, D) with one very short *prs*, four short *pds* (arranged along the posterior margin), two minute *ss*, two short *eps*, one short *ps*, one short *lsts* and two short *eus*. Abdominal segment IX (Figure 1D) with three medium *ds*, all located close to the posterior margin, one short *ps* and two short *sts*. Each of anal lobes with two minute *ts*.

Head capsule (Figures 1A, 2A–F) white, almost rounded. $Des_{1–3,\ 5}$ long, des_4 two times shorter than des_1. Fs_1 as long as des_1, $fs_{4,\ 5}$ elongated, equal in length. Les_1 medium, les_2 long; both *ves* very short, and two very short *pes* (Figure 2A). Antennae (Figure 2B) with conical, elongated sensorium (Se), four times as long as wide, and three sensilla basiconica. Clypeus (Figure 2C) trapezium-shaped, anterior

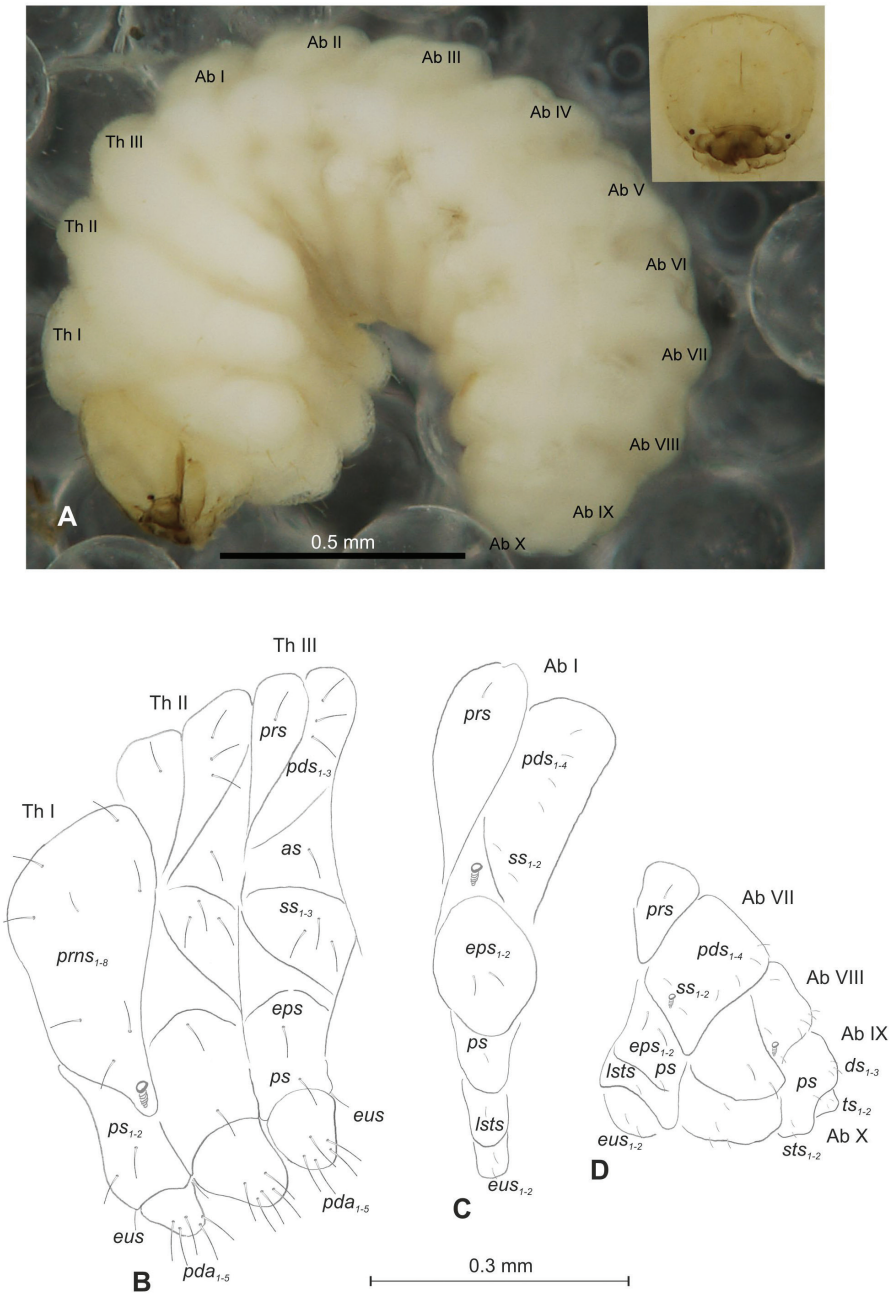

Figure 1. *Mecinus pascuorum* mature larva, habitus and chaetotaxy **A** habitus of the body and frontal view of the head **B** lateral view of thoracic segments **C** lateral view of abdominal segment I **D** lateral view of abdominal segments VII–X. Abbreviations: Th. I–III – number of thoracic segments, Abd. I–X – number of abominal segments, setae: *as* – alar, *ds* – dorsal, *eps* – epipleural, *eus* – eusternal, *lsts* – laterosternal, *pda* – pedal, *pds* – postdorsal, *prns* – pronotal, *prs* – prodorsal, *ps* – pleural, *ss* – spiracular, *sts* – sternal, *ts* – terminal.

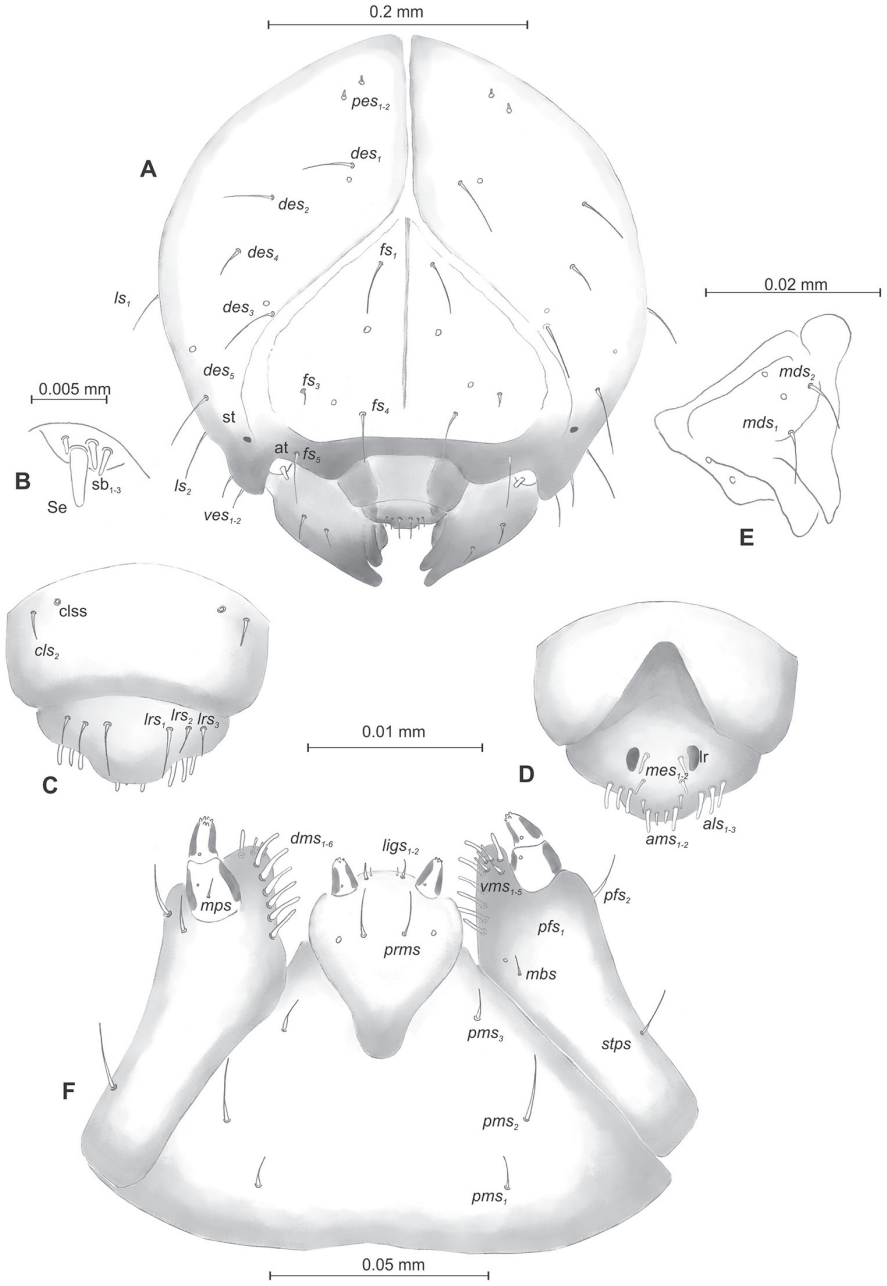

Figure 2. *Mecinus pascuorum* mature larva, head and mouth parts **A** head, frontal view **B** antenna **C** clypeus and labrum, dorsal view **D** epipharynx **E** left mandible **F** maxillolabial complex, ventral aspect. Abbreviations: at – antenna, clss – clypeal sensorium, *des* – dorsal epicranial, lr – labral rods, sb – sensillum basiconicum, Se – sensorium, st – stemmata, setae: *als* – anterolateral, *ams* – anteromedial, *cls* – clypeal, *dms* – dorsal malar, *fs* – frontal, *ligs* – ligular, *lrs* – labral, *ls* – lateral epicranial, *mbs* – malar basiventral, *mds* – mandibular, *mes* – median, *mxps* – maxillary palp, *pes* – postepicranial, *ves* – ventral, *pfs* – palpiferal, *pms* – postlabial, *prms* – prelabial, *stps* – stipal, *vms* – ventral malar.

margin slightly concave; cls_2 short; clss close to cls_2. Labrum (Figure 2C) narrow, trapezium-shaped, anterior margin distinctly sinuate; lrs_1 long, lrs_2 and lrs_3 medium. Epipharynx (Figure 2D) with three finger-like *als* of almost equal length; two finger-like *ams*, different in length; two short finger-like *mes*; surface smooth; labral rods very short, rounded. Mandibles (Figure 2E) conical, rather wide, with divided apex (teeth of different lengths, curved); small protuberance in the middle of the cutting edge; with two medium *mds* capilliform, equal in length, placed transversely. Maxilla (Figure 2F) with one medium *stps* and two medium *pfs*; *mbs* short; mala with six long rod-like *dms* of almost equal size, five *vms* different in length. Maxillary palpi: basal palpomere distinctly wider and longer than distal. Prelabium (Figure 2F) cup-like with one long *prms*; ligula with two short *ligs* of different length; premental sclerite weakly developed, cup-like. Postlabium (Figure 2F) with short pms_1, long pms_2, and short pms_3.

Description of pupa (Figure 3A–C). ***Measurements*** (in mm). Head width: 0.32–0.40. Body width: 0.90–1.20. Body length: 1.52–2.10.

Body moderately stout, slightly curved, white. Rostrum moderately slender, medium long, about 2.5 times as long as wide, reaching mesocoxae. Antennae rather short. Pronotum 1.7 times as wide as long, with two, conical, protuberances apically (p–pr). Urogomorpi (ur) short, conical, with sclerotised apex (Figure 3A–C).

Chaetotaxy well visible, all setae (except those on rostrum and ventral part of abdomen) almost equal in length, medium. Head with one *os*. Rostrum with one minute *rs* (Figure 3A). Pronotum with two *as* placed beside protuberances, two *ls*, one *ds* and three *pls*. Dorsal parts of meso- and metathorax with two setae placed laterally. Abdominal segments I–VIII with three setae situated posteriorly, two elongated setae laterally and three short setae ventrally (median setae distinctly bigger than others). Abdominal segment IX with two micro-setae ventrally.

Biological notes. This species lives on *Plantago lanceolata* L. In spring, the female lays one egg per developing pyxidium, and each larva consumes the contents of a pyxidium, usually two seeds, without causing externally visible modification. Pupation takes place within the same pyxidium. Adults emerge from the beginning of summer until September. They overwinter in the soil (Hoffmann 1958; Scherf 1964; Dickason 1968; Nieminen and Vikberg 2015).

Remarks and comparative notes. This species is one of the most common species in the genus, with a very large range of distribution: Europe, the Caucasian states, the Middle East, central Asia, and Algeria (Caldara and Fogato 2013). It has been imported to North America, Australia and New Zealand (O'Brien and Wibmer 1982; Debinski and Holt 2000) and recently collected in South Africa (Caldara et al. 2009). Morphologically, this species is more closely related to other species of the group, i.e., *M. latiusculus* (Jacquelin du Val, 1855) and *M. ictericus* than to *M. labilis* studied herein, and this seems also to be corroborated by the preliminary molecular data (I. Toševski, unpublished data). However, the relationships among the immatures of these species are closer than their relationships with all the other species currently known.

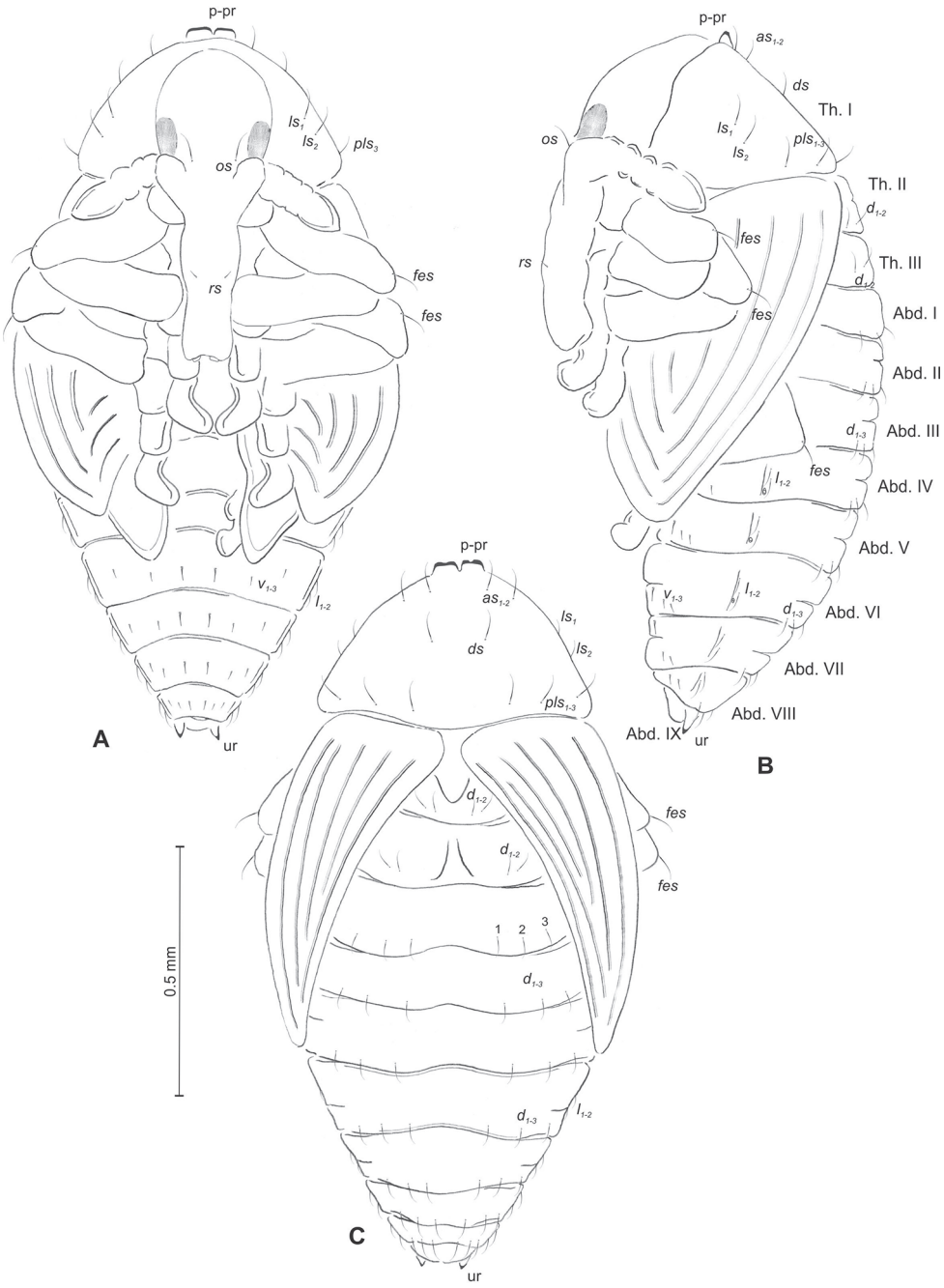

Figure 3. *Mecinus pascuorum* pupa habitus and chaetotaxy **A** ventral view **B** lateral view **C** dorsal view. Abbreviations: Th. I–III – number of thoracic segments, Abd. I–IX – number of abdominal segments, p–pr – pronotal protuberances, ur – urogomphi, setae: *as* – apical, *d* – dorsal, *ds* – discal, *fes* – femoral, *l*, *ls* – lateral, *os* – orbital, *pls* – posterolateral, *rs* – rostral.

***Mecinus labilis* (Herbst, 1795)**

Material examined. 3 L3 larvae and 9 pupae, Serbia, Staničenje, 6.07.2017, 43°12.915'N 22°30.495'E, 364 m., ex *Plantago lanceolata*, lgt. I. Toševski. Accession numbers of sequenced specimen MN992008.

Description of mature larva (Figures 4A–D, 5A–F). ***Measurements*** (in mm). Body length: 1.40–2.00. Body width (metathorax): 0.84–1.00. Head width: 0.36–0.40.

Body (Figure 4A–D) white, moderately slender, slightly curved. Chaetotaxy of thoracic segments relatively well developed, setae capilliform, different in length, light yellow, on abdominal segments I–VII very short, on segments VIII and IX of medium length. Prothorax (Figure 4B) with eleven long *prns* of almost equal length, two long *ps* and one long *eus*. Meso- and metathorax (Figure 4B) with one short *prs*, three *pds* (pds_1 short, $pds_{2–3}$ long), one long *as*, three *ss* different in length (one minute and two medium), one long *eps*, one long *ps* and one long *eus*. Pedal area with four *pda* (two long and two medium). Abdominal segments I–VIII (Figure 4C, D) with one short *prs*, four short *pds* arranged along posterior margin, two minute *ss*, two short *eps*, one short *ps*, one short *lsts* and two short *eus*. Abdominal segment IX (Figure 4D) with three medium *ds*, all located close to posterior margin, one medium *ps* and two rather short *sts*. Each of anal lobes with one minute seta.

Head capsule (Figures 4A, 5A–F) white, almost rounded. $Des_{1–3,5}$ long, des_4 very short. Fs_1 slightly shorter than des_1, fs_4 and fs_5 equal in length, almost as long as des_1. Les_1 and les_2 long; one *ves* very short (Figure 5A). Antennae (Figure 5B) with elongated sensorium (Se), four times as long as wide, and two sensilla basiconica and one sensillum ampullaceum. Clypeus (Figure 5C) trapezium-shaped, anterior margin almost straight; cls_2 short, clss placed close to cls_2. Labrum (Figure 5C) narrow, trapezium-shaped, anterior margin distinctly sinuate; lrs_1 long, lrs_2 and lrs_3 medium. Epipharynx (Figure 5D) with three elongated, finger-like *als* of equal length; two relatively elongated, finger-like *ams*; two short finger-like *mes*; surface smooth; labral rods very short, rounded. Mandibles (Figure 5E) conical, rather wide, with divided apex; both *mds* capilliform, short, equal in length, placed transversely. Maxilla (Figure 5F) with one medium *stps* and two medium *pfs*; *mbs* short; mala with six long rod-like *dms* of almost equal size, five *vms* different in length. Maxillary palpi: basal palpomere distinctly wider than distal. Prelabium (Figure 5F) cup-like with one short *prms*; ligula with one minute *lig*; premental sclerite weakly developed, cup-like. Postlabium (Figure 5F) with very short pms_1, long pms_2, and very short pms_3.

Description of pupa (Figure 6A–C). ***Measurements*** (in mm). Head width: 0.36–0.40. Body width: 1.00–1.40. Body length: 1.40–2.20.

Body rather stout, slightly curved, white. Rostrum slender, moderately short, about 2.0 times as long as wide, reaching procoxae. Antennae short. Pronotum 2.2 times as wide as long. Urogomorpi (ur) very short, conical, only slightly reaching outline of the body (Figure 6A–C).

Chaetotaxy almost invisible, all setae minute, possible to observation only under higher magnification. Head with one *os*. Rostrum with two *rs* placed medially (Fig-

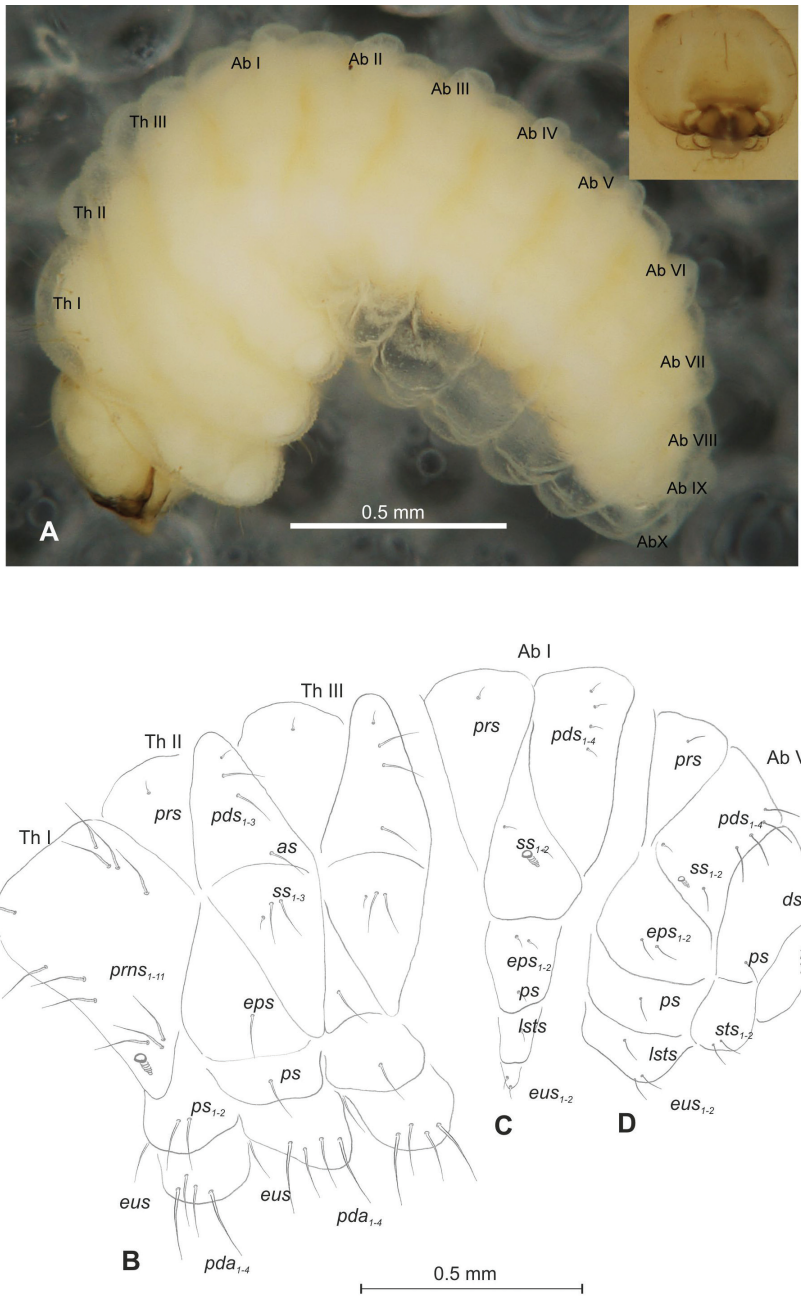

Figure 4. *Mecinus labilis* mature larva, habitus and chaetotaxy **A** habitus of the body and frontal view of the head **B** lateral view of thoracic segments **C** lateral view of abdominal segment I **D** lateral view of abdominal segments VII–X. Abbreviations: Th. I–III – number of thoracic segments, Abd. I–X – number of abominal segments, setae: *as* – alar, *ds* – dorsal, *eps* – epipleural, *eus* – eusternal, *lsts* – laterosternal, *pda* – pedal, *pds* – postdorsal, *prns* – pronotal, *prs* – prodorsal, *ps* – pleural, *ss* – spiracular, *sts* – sternal, *ts* – terminal.

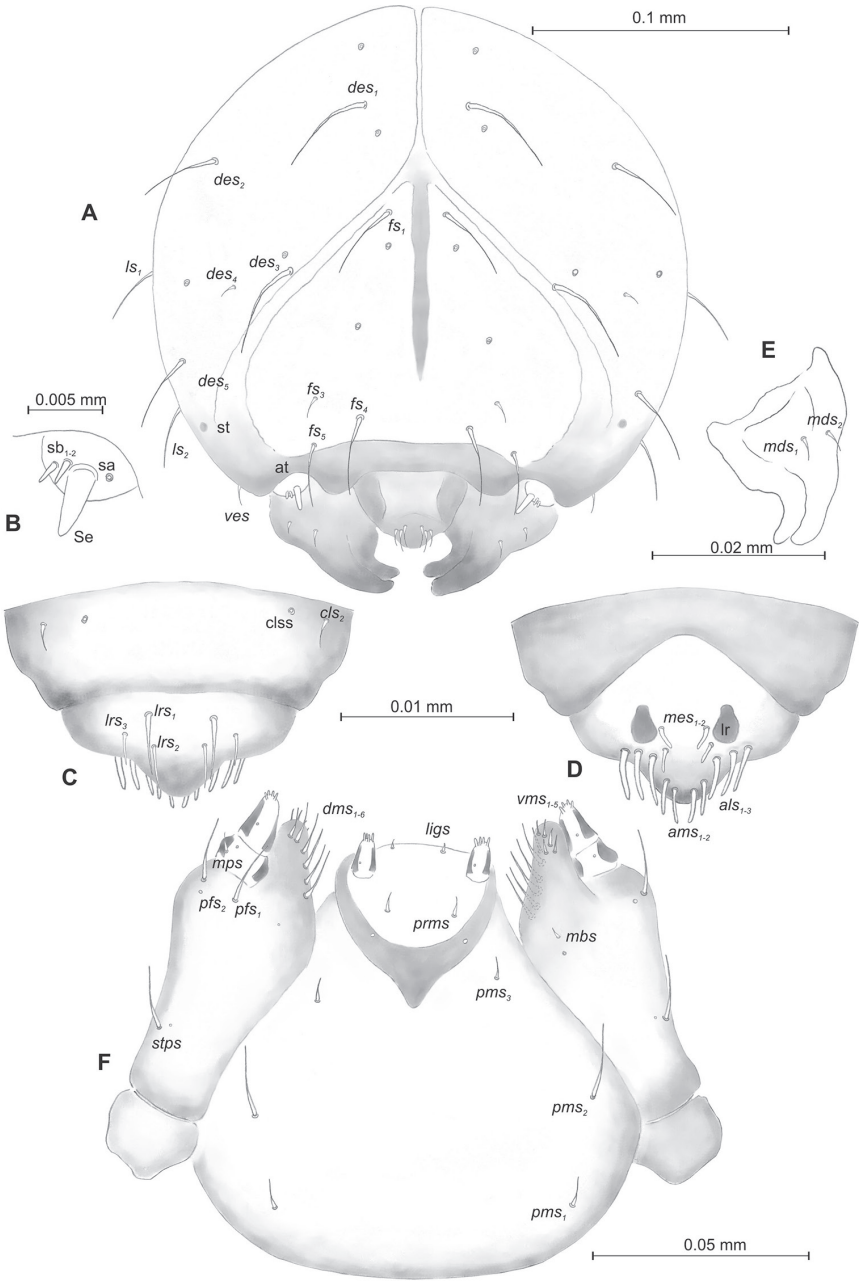

Figure 5. *Mecinus labilis* mature larva, head and mouth parts **A** head, frontal view **B** antenna **C** clypeus and labrum, dorsal view **D** epipharynx **E** left mandible **F** maxillolabial complex, ventral aspect. Abbreviations: at – antenna, clss – clypeal sensorium, *des* – dorsal epicranial, lr – labral rods, sa – sensillum ampullaceum, sb – sensillum basiconicum, Se – sensorium, st – stemmata, setae: *als* – anterolateral, *ams* – anteromedial, *cls* – clypeal, *dms* – dorsal malar, *fs* – frontal, *ligs* – ligular, *lrs* – labral, *ls* – lateral epicranial, *mbs* – malar basiventral, *mds* – mandibular, *mes* – median, *mxps* – maxillary palp, *pes* – postepicranial, *ves* – ventral, *pfs* – palpiferal, *pms* – postlabial, *prms* – prelabial, *stps* – stipal, *vms* – ventral malar.

ure 6A). Pronotum with two *as*, two *ls*, one *ds* and three *pls*. Dorsal parts of meso- and metathorax with two setae placed laterally. Abdominal segments I–VIII with three setae situated posterolaterally, two setae laterally and three setae ventrally. Abdominal segment IX with two micro-setae ventrally.

Biological notes. Larvae feed on *Plantago lanceolata* L. in galled pyxidia, where they pupate in the collar without causing externally visible modifications (Hoffmann 1958).

Remarks and comparative notes. This species is widely distributed in Europe, the Caucasian states, and Turkey. Concerning the adults, the pattern of the elytral integument (reddish with two black oblique bands from interstria 1 to 7) and the shape of the rostrum (in lateral view moderately curved in basal half then straight to apex) allow us to separate these two species from all the others. With regard to the immatures, the differences from the other studied species of the group, *M. pascuorum*, are several and are reported in the key. Molecular data also do not show a close relationship between these two species (I. Toševski, unpublished data).

Mecinus simus group

Differential diagnosis. Larva. (1) cuticle of the body smooth; (2) pedal lobes prominent; (3) abdominal segment X reduced to three anal lobes of equal size; (4) thoracic spiracle unicameral; (5) all abdominal setae short or very short, without trend to become progressively longer from abd. segment I to VIII; (6) abdominal segments I–VIII with three *pds* and two *ss*; (7) head white, rounded; (8) frontal suture poorly developed; (9) endocarina 3/4 of the frons; (10) des_4 three times shorter than des_1; (11) absence of fs_1; (12) absence of fs_2; (13) fs_3 three times shorter than fs_4; (14) head with one stemma; (15) absence of cls_1; (16) labial palpi one-segmented; (17) premental sclerite cup-like, posterior extension with elongated, acute apex; (18) surface of postlabium smooth.

Pupa. (1) body stout and short; (2) urogomphi extremely short, not reaching outline of the body; (3) rostrum short, tapering to the top; (4) setae minute, almost invisible; (5) head with one *os*; (6) rostrum with one *rs*; (7) pronotum with two *as*, one *ds*, one *ls*, three *pls*; (8) meso- and metanotum with two setae; (9) abdominal segments I–VII with three setae dorsally and without setae ventrally.

Remarks and comparative notes. The very short, conical and in lateral view straight rostrum, and the protibiae with apical third distinctly enlarged, sometimes with outer margin and apex bearing stout denticles, are truly noteworthy and unique in Mecinini. Both characters are oddly similar to those of a mole, and the tibiae are similar to those of Scarabaeidae. Since nothing was known about their biology except for their host plants, Caldara and Fogato (2013) speculated on the possibility that the species of this group deposit eggs in plant roots. The new biological data on *M. pirazzolii* below reported exclude this hypothesis and suggest that most likely the female

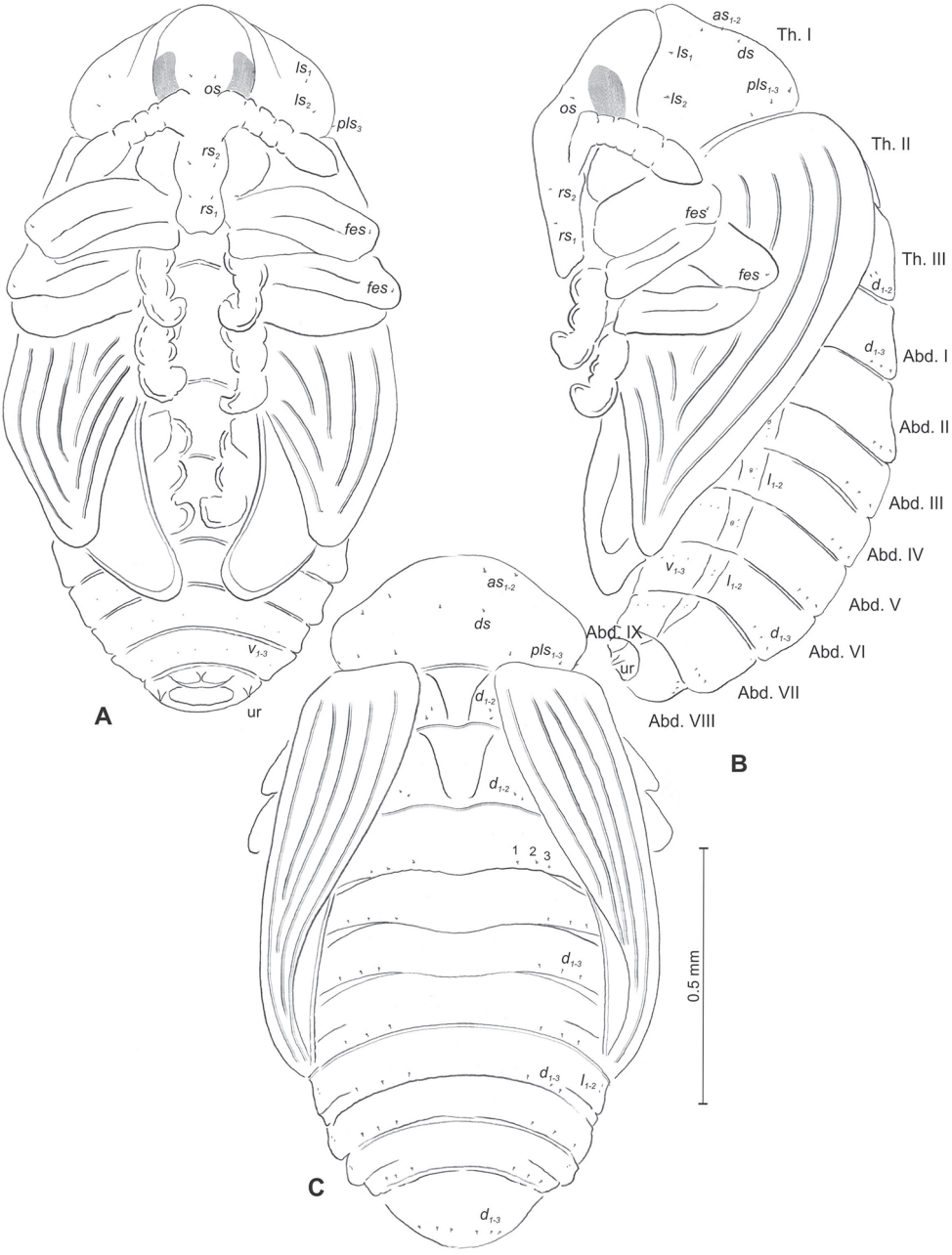

Figure 6. *Mecinus labilis* pupa habitus and chaetotaxy **A** ventral view **B** lateral view **C** dorsal view. Abbreviations: Th. I–III – number of thoracic segments, Abd. I–IX – number of abdominal segments, ur – urogomphi, setae: *as* – apical, *d* – dorsal, *ds* – discal, *fes* – femoral, *l*, *ls* – lateral, *os* – orbital, *pls* – posterolateral, *rs* – rostral, *sls* – superlateral.

is able to approach as close as possible to the pistil of the flower and deposit the egg thanks to the shape of its protibiae, since it is regularly found deeply stuck between *Plantago* inflorescences. This group might be related to the *M. collaris* group on the basis of the morphological characters of the adults (Caldara et al. 2013), whereas it seems more related to the *M. circulatus* group according to the preliminary molecular data (I. Toševski, unpublished data). Unfortunately, the study of immatures did not clarify this situation. In fact, the presence of one palpomere on the labial palpi and of all spiracles unicameral contradicts this hypothesis, and the same combination of these two characters is found only in *M. pascuorum* and *M. heydenii* groups, with the former of which the *M. simus* group might have major similarities. However, the immatures of the *M. simus* group have some autapomorphies, such as a smooth body cuticle and prominent pedal lobes in larvae and abdominal segments I–VII with three setae dorsally and without setae ventrally, apart from an obvious extraordinarily short rostrum tapering to the apex in pupae.

Mecinus pirazzolii (Stierlin, 1867)

Material examined. 20 L3 larvae and 10 pupae, Serbia, Veliko Gradište, 14.07.2017, 44°45.039'N, 21°31.426'E, 86 m., *ex Plantago arenaria*, lgt. I. Toševski. Accession numbers of sequenced specimens MN992011 (larva), MN992012 (pupa).

Description of mature larva (Figures 7A–D, 8A–F). ***Measurements*** (in mm). Body length: 1.40–2.00. Body width (metathorax): 0.73–1.00. Head width: 0.36–0.40.

Body (Figure 7A–D) white, slender, curved. Chaetotaxy of thoracic segments relatively well developed, setae capilliform, different in length, light yellow; on abdominal segments almost invisible (except dorsal parts of abdominal segments IX and X). Prothorax (Figure 7B) with eight *prns* of unequal length (seven relatively long and one medium), two relatively long *ps* and one short *eus*. Meso- and metathorax (Figure 7B) with one medium *prs*, two long *pds*, equal in length, one long *as*, three *ss* different in length (two relatively long, one short), one long *eps*, one long *ps* and one short *eus*. Pedal area with five long *pda*, equal in length. Abdominal segments I–VIII (Figure 7C, D) with one very short *prs*, three short *pds* (on segment VIII medium, equal in length), arranged along posterior margin, two minute*ss*, one short *eps*, one short *ps*, one short *lsts* and two short *eus*. Abdominal segment IX (Figure 7D) with three medium *ds*, all located close to posterior margin, one short *ps* and two short *sts*. Each of anal lobes with one minute seta.

Head capsule (Figures 7A, 8A–C) light white, almost rounded. $Des_{1,3,5}$ long; des_2 two times shorter than des_1; des_4 three times shorter than des_1. $Fs_{4,5}$ equal in length, almost as long as des_1. Les_1 medium, les_2 long; one very short *ves*, and one *pes* (Figure 8A). Antennae (Figure 8B) with conical, elongated sensorium (Se), four times as long as wide, and three sensilla basiconica. Clypeus (Figure 8C) trapezium-shaped, anterior margin slightly concave; cls_2 short; clss situated close to cls_2. Labrum (Figure 8C) narrow, trapezium-shaped, anterior margin slightly sinuate; lrs_1 long, lrs_2 medium lrs_3

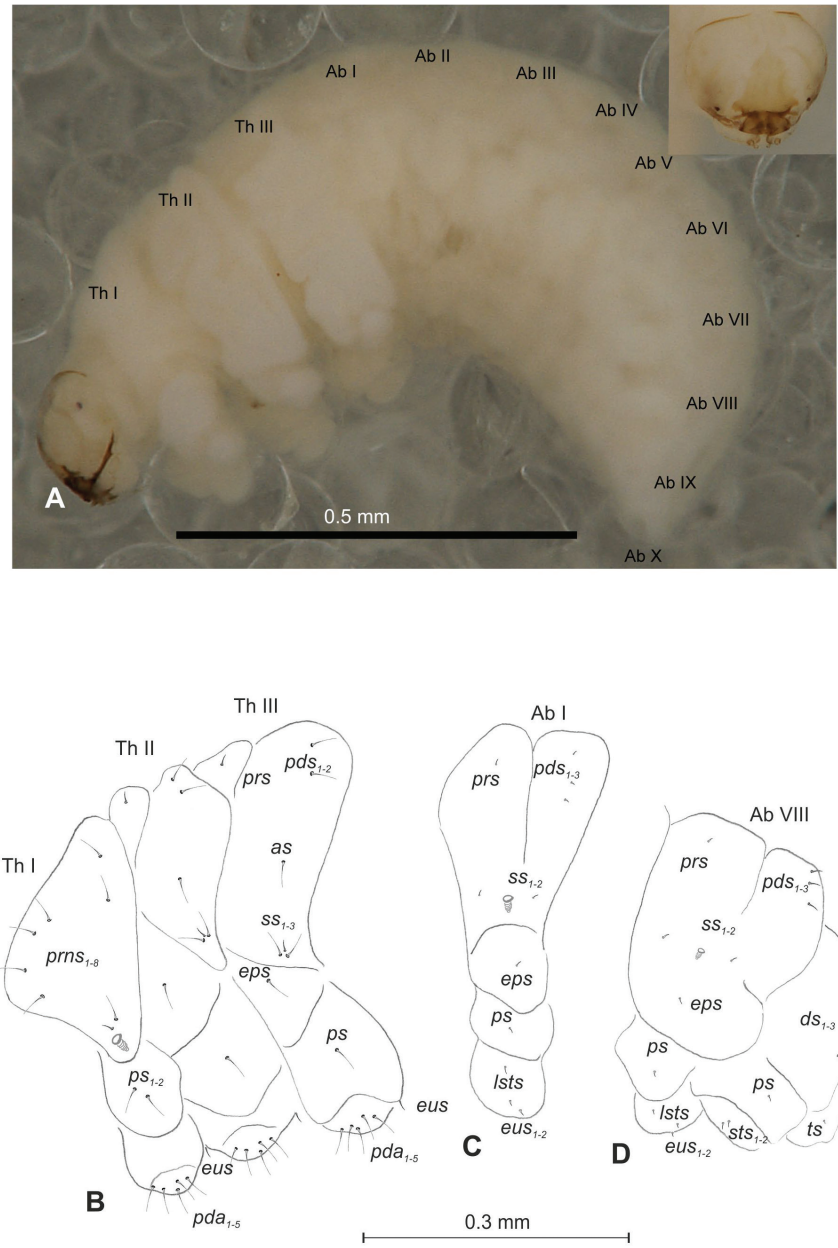

Figure 7. *Mecinus pirazzolii* mature larva, habitus and chaetotaxy **A** habitus of the body and frontal view of the head **B** lateral view of thoracic segments **C** lateral view of abdominal segment I **D** lateral view of abdominal segments VII–X. Abbreviations: Th. I–III – number of thoracic segments, Abd. I–X – number of abominal segments, setae: *as* – alar, *ds* – dorsal, *eps* – epipleural, *eus* – eusternal, *lsts* – laterosternal, *pda* – pedal, *pds* – postdorsal, *prns* – pronotal, *prs* – prodorsal, *ps* – pleural, *ss* – spiracular, *sts* – sternal, *ts* – terminal.

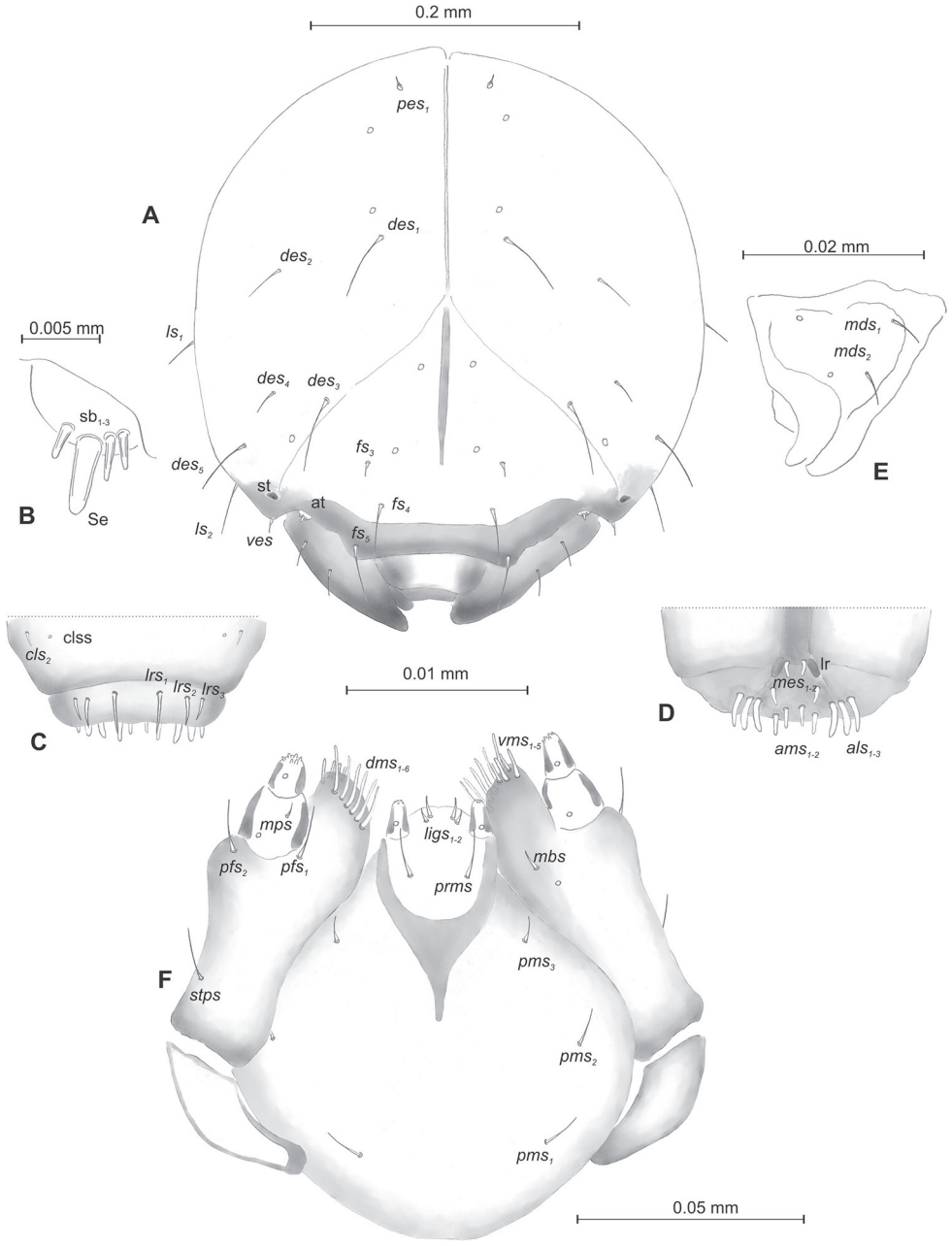

Figure 8. *Mecinus pirazzolii* mature larva, head and mouth parts **A** head, frontal view **B** antenna **C** clypeus and labrum, dorsal view **D** epipharynx **E** left mandible **F** maxillolabial complex, ventral aspect. Abbreviations: at – antenna, *des* – dorsal epicranial, lr – labral rods, sb – sensillum basiconicum, Se – sensorium, st – stemmata, setae: *als* – anterolateral, *ams* – anteromedial, *cls* – clypeal, *dms* – dorsal malar, *fs* – frontal, *ligs* – ligular, *lrs* – labral, *ls* – lateral epicranial, *mbs* – malar basiventral, *mds* – mandibular, *mes* – median, *mxps* – maxillary palp, *pes* – postepicranial, *ves* – ventral, *pfs* – palpiferal, *pms* – postlabial, *prms* – prelabial, *stps* – stipal, *vms* – ventral malar.

short. Epipharynx (Figure 8D) with three finger-like *als* of almost equal length; two medium finger-like *ams*; two short finger-like *mes*; surface smooth; labral rods very short, rounded. Mandibles (Figure 8E) conical, rather wide, with a small protuberance in the middle of the cutting edge; both *mds* capilliform, medium, equal in length, placed transversely. Maxilla (Figure 8F) with one *stps* and two *pfs* of equal length; *mbs* short; mala with six long rod-like *dms* of almost equal size, five *vms* different in length. Maxillary palpi: basal palpomere distinctly wider and longer than distal. Prelabium (Figure 8F) cup-like with one long *prms*; ligula with two short *ligs*; premental sclerite clearly visible, cup-shaped, posterior extension with acute apex. Postlabium (Figure 8F) with medium pms_1, medium pms_2, and short pms_3.

Description of pupa (Figure 9A–C). ***Measurements*** (in mm). Head width: 0.33–0.40. Body width: 0.93–1.16. Body length: 1.63–2.10.

Body stout, slightly curved, white. Rostrum slender, very short, tapering to its top. Antennae moderately elongated. Pronotum 2.0 times as wide as long. Urogomorpi (ur) very short, conical, not reaching outline of the body (Figure 9A–C).

Chaetotaxy almost invisible, all setae minute, possible to observation only under higher magnification. Head with one *os*. Rostrum with one *rs* placed medially (Figure 9B). Pronotum with two *as*, one *ls*, one *ds* and three *pls*. Dorsal parts of meso- and metathorax with two setae placed laterally. Dorsal parts of abdominal segments I–VIII with three setae situated posterolaterally and one seta laterally. Abdominal segment IX without setae.

Biological notes. This species is associated with the annual plant *Plantago arenaria* Waldst. & Kit. The adult aggregation on plants is followed by the appearance of flowering stems with spikes in late spring. The females lay one egg onto the base of the pistil or the initialised seed. The act of oviposition is followed by proliferative growth of the ovarian tissue in the form of gall but without changes in the external morphology of the pyxidium. During development, the larvae consume all the tissue inside the pyxidium, leaving only the fruit shell intact. The larvae pupate inside the fruit shell, from which adults emerge after being completely sclerotised. Overwintering takes place in the soil litter near the host plant (I. Toševski, pers. obs.). Sympatric occurrence with *M. ictericus* is common (Caldara and Fogato 2013).

Remarks and comparative notes. This species is distributed in eastern Central Europe, southeastern Europe and Turkey. In our keys, this species is closer to the species of the *M. pascuorum* group than to others, as already discussed in the Remarks for the group.

Mecinus circulatus group

Differential diagnosis. Larva. (1) body covered with asperities; (2) pedal lobes prominent well isolated; (3) abdominal segment X reduced to three anal lobes of unequal size; (4) thoracic spiracle bicameral; (5) abdominal setae very short, slightly growing from abdominal segment I to VIII; (6) abdominal segments I–VIII with three *pds* and

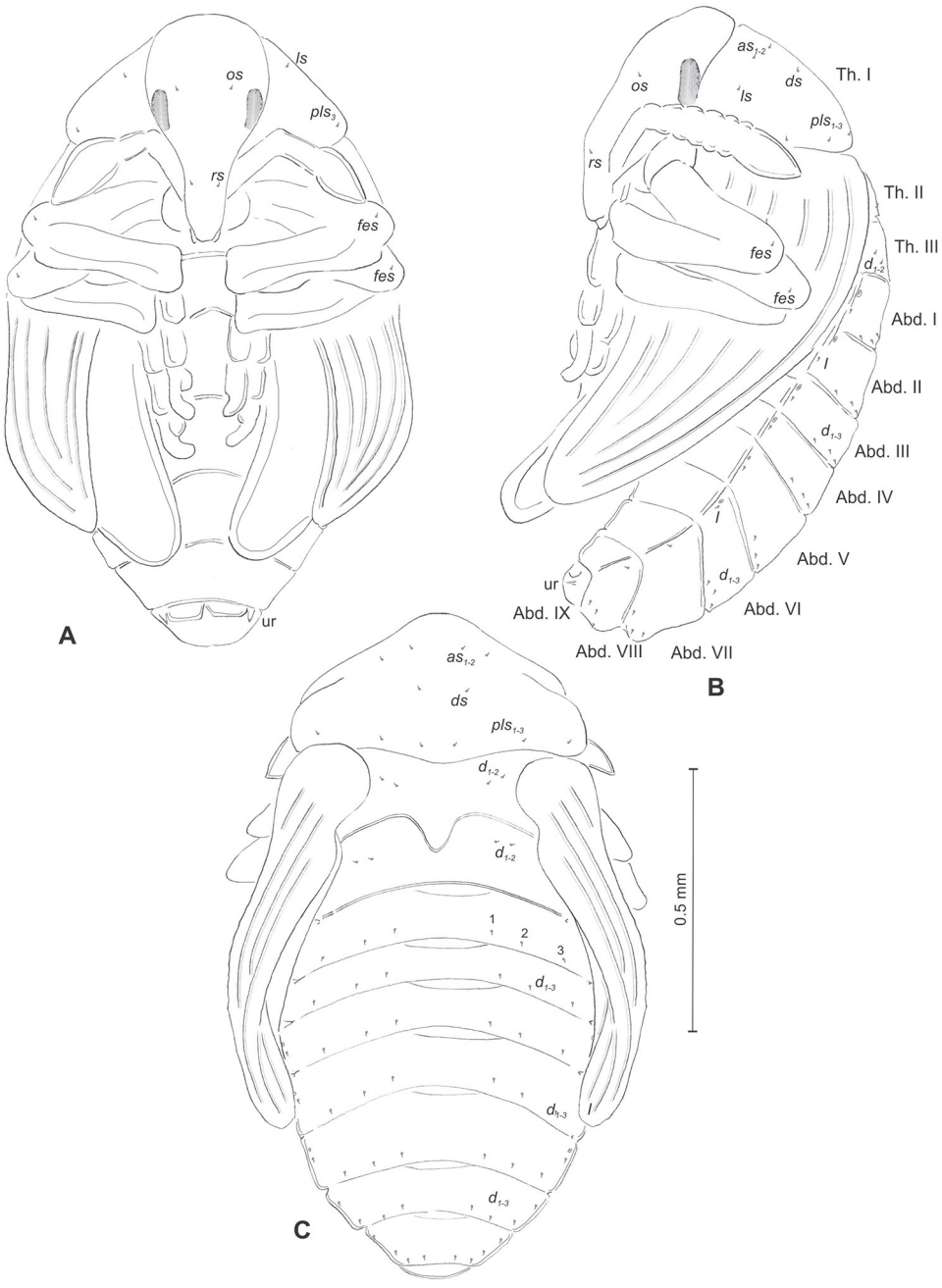

Figure 9. *Mecinus pirazzolii* pupa habitus and chaetotaxy **A** ventral view **B** lateral view **C** dorsal view. Abbreviations: Th. I–III – number of thoracic segments, Abd. I–IX – number of abdominal segments, ur – urogomphi, setae: *as* – apical, *d* – dorsal, *ds* – discal, *fes* – femoral, *l*, *ls* – lateral, *os* – orbital, *pls* – posterolateral, *rs* – rostral.

two *ss*; (7) head brown, distinctly flattened laterally; (8) frontal suture poorly or well visible; (9) endocarina 1/2 of the frons; (10) des_4 very short or short; (11) presence of fs_1; (12) absence of fs_2; (13) fs_3 very short; (14) head with two stemmata; (15) presence of cls_1; (16) labial palpi one-segmented; (17) premental sclerite cup-like; (18) surface of postlabium smooth.

Pupa. (1) body elongated or very elongated; (2) urogomphi slender, short or medium, reaching outline of the body, directed downward; (3) rostrum moderately elongated; (4) setae minute or medium; (5) head with one *vs*, one or two *sos*, one or two *os*; (6) rostrum with one *pas* and one *rs*; (7) pronotum with one or two *as*, without or with one *ds*, two *sls*, without or up to two *ls*, two or three *pls*; (8) meso- and metanotum with two setae; (9) abdominal segments I–VII with three or five setae dorsally.

Remarks and comparative notes. The adults of this group are characterised by body elongate, subcylindrical, elytral integument reddish and black to completely black, protibiae with apical part of ventral surface distinctly directed outward. On the basis of these characters, this group might be related to *M. collaris* and especially to the *M. simus* group (Caldara et al. 2013). The study of the immatures does not support this latter relationship. The immatures of this group lack autapomorphies. However, the larvae possess the unique combination of one palpomere + thoracic spiracle bicameral and abdominal spiracles unicameral, which do not share with the species of the *M. simus* group, *M. pirazzolii*, that we have studied.

Mecinus circulatus (Marsham, 1802)

Material examined. 5 L3 larvae and 10 pupae, 1.07.2017, Zemun, Serbia, GPS 44°39.030'N, 21°28.355'E, 162 m., lgt. I. Toševski. Accession number of sequenced specimen MN991999.

Description of mature larva (Figures 10A–D, 11A–F). ***Measurements*** (in mm). Body length: 2.33–2.73. Body width (metathorax): 0.83–1.06. Head width: 0.50–0.53.

Body (Figure 10A–D), light yellow, slender, curved (Figure 10B). Thoracic segments larger than abdominal segment I. Abdominal segments I–VI of almost equal length; segments VII–IX decreasing gradually to the terminal body part; segment X reduced to three anal lobes of those lateral are the largest, and dorsal the smallest (sometimes absent). Chaetotaxy weakly developed, setae short, transparent, difficult to observe (Figure 10B). Prothorax (Figure 10B) with eight *prns* (six medium and two very short); two medium *ps* and one very short *eus*. Meso- and metathorax (Figure 10B) with one very short *prs*, two *pds* (one very short, one medium), one medium *as*, three *ss* (two medium and one very short), one medium *eps*, one medium *ps* and one very short *eus*. Pedal area with three *pda* (one medium and two very short). Abdominal segments I–VIII (Figure 10C, D) with one very short *prs*, three *pds* arranged along the posterior margin (order: very short, medium and very short), two *ss* different in length,

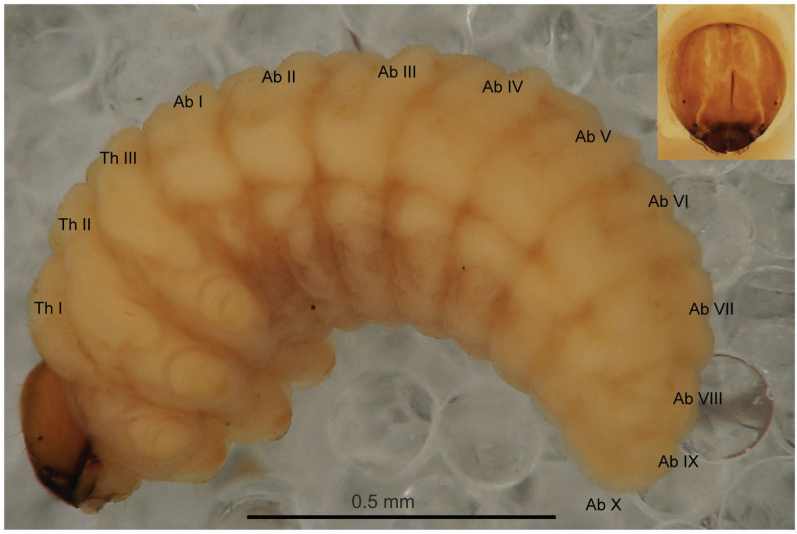

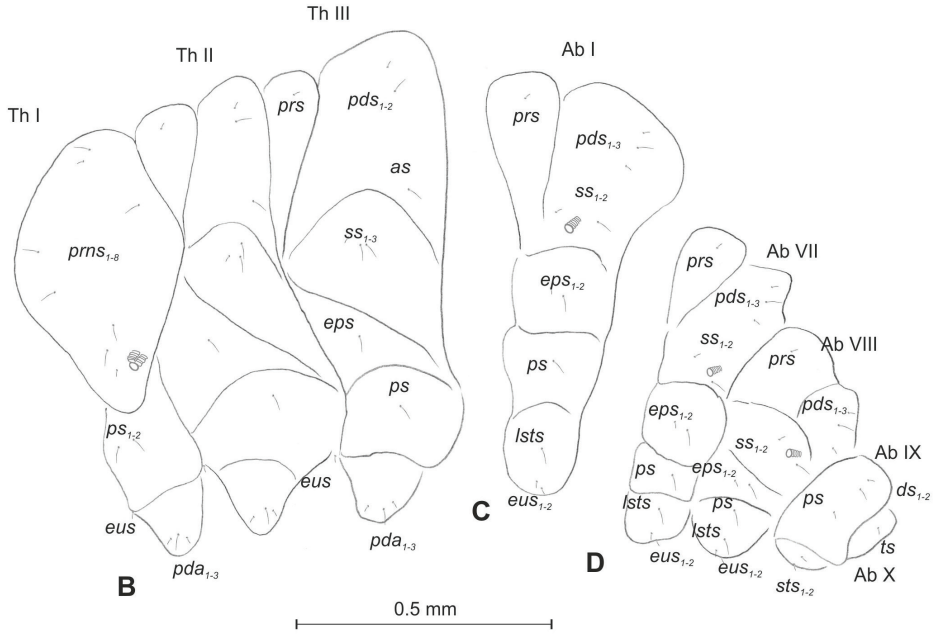

Figure 10. *Mecinus circulatus* mature larva, habitus and chaetotaxy **A** habitus of the body and frontal view of the head **B** lateral view of thoracic segments **C** lateral view of abdominal segment I **D** lateral view of abdominal segments VII–X. Abbreviations: Th. I–III – number of thoracic segments, Abd. I–X – number of abominal segments, setae: *as* – alar, *ds* – dorsal, *eps* – epipleural, *eus* – eusternal, *lsts* – laterosternal, *pda* – pedal, *pds* – postdorsal, *prns* – pronotal, *prs* – prodorsal, *ps* – pleural, *ss* – spiracular, *sts* – sternal, *ts* – terminal.

two *eps* different in length, one medium *ps*, one medium *lsts* and two very short *eus*. Abdominal segment IX (Figure 10D) with two *ds* (one medium and one very short), all located close to the posterior margin, one very short *ps* and two very short *sts*. Each lateral anal lobe (abd. seg. X) with one minute seta.

Head capsule (Figures 10A, 11A–F) pale brown, narrowed bilaterally. Frontal suture poorly visible. Des_{1-3} very long, equal in length, des_4 four times shorter than des_1, des_5 slightly shorter than des_1. Fs_1 short; fs_3 short, $fs_{4,5}$ long. Les_1 and les_2 equal in length, slightly shorter than des_1; both *ves* short, and five short *pes* (Figure 11A). Antennae (Figure 11B) with conical sensorium (Se) four times as long as wide, and three sensilla basiconica. Clypeus (Figure 11C) trapezium-shaped, anterior margin concave; cls_{1-2} relatively short; clss placed close to cls_2. Labrum (Figure 11C) with distinctly sinuate anterior margin; lrs_1 very long, lrs_2 slightly shorter than lrs_1, lrs_3 two times shorter than lrs_1. Epipharynx (Figure 11D) with three medium, finger-shaped *als* of almost equal length; two rod-like *ams*, equal in length; one finger-like *mes* of medium length; surface smooth; labral rods close to kidney-shaped. Mandibles (Figure 11E) conical, wide, with a small protuberance in the middle of the cutting edge; both *mds* capilliform, medium, equal in length, placed mediolaterally. Maxilla (Figure 11F) with one *stps* and two *pfs* equal length; *mbs* very short; mala with six finger-like *dms* of almost equal size; four *vms* different in length. Maxillary palpi: basal palpomere distinctly wider and slightly longer than distal. Prelabium (Figure 11F) cup-like with one relatively short *prms*; ligula with two *ligs* different in length; premental sclerite well visible, cup-shaped. Postlabium (Figure 11F) with medium pms_1, long pms_2, and medium pms_3.

Description of pupa. (Figure 12A–C). ***Measurements*** (in mm). Head width: 0.46–0.50. Body width: 1.16–1.40. Body length: 2.46–3.00.

Body moderately elongated, white. Rostrum rather short, about 3.2 times as long as wide, reaching up to mesocoxae. Antennae slender and elongated. Pronotum 1.25 times as wide as long. Mesonotum slightly shorter than metanotum. Urogomphi (ur) short, slender, conical, with sclerotised, sharp apex, slightly reaching outline of the body, directed downward (Figure 12A–C).

Chaetotaxy very sparse, setae short or minute. Head with one *vs*, one *os* and one *sos*. Rostrum with one *rs* and one *pas*. Setae on head and rostrum straight, as long as those on prothorax (Figure 12A). Pronotum with one *as*, one *ls*, two *sls*, and two *pls*. Dorsal parts of meso- and metathorax with two setae placed medially. Apex of femora with one minute *fes* (Figure 12A–C). Dorsal parts of each abdominal segments I–VIII with three setae placed posteromedially along margins of each segments. Abdominal segment IX with two micro-setae ventrally.

Biological notes. This species is very common on *Plantago lanceolata* L., while in southeastern Europe, it is also common on some other closely related species, such as *P. arenaria* (sub *P. psyllium* L.), *P. afra* L. (sub *P. cynops* L.) and *P. subulata* L. (Hoffmann 1958; Sprick 2001). The females oviposit in early spring on young growing vegetative shoot buds. Newly hatched larvae bore through the central part of the shoot bud, forming a 1–2 cm long larval channel that rarely rises above the root crown. The larvae

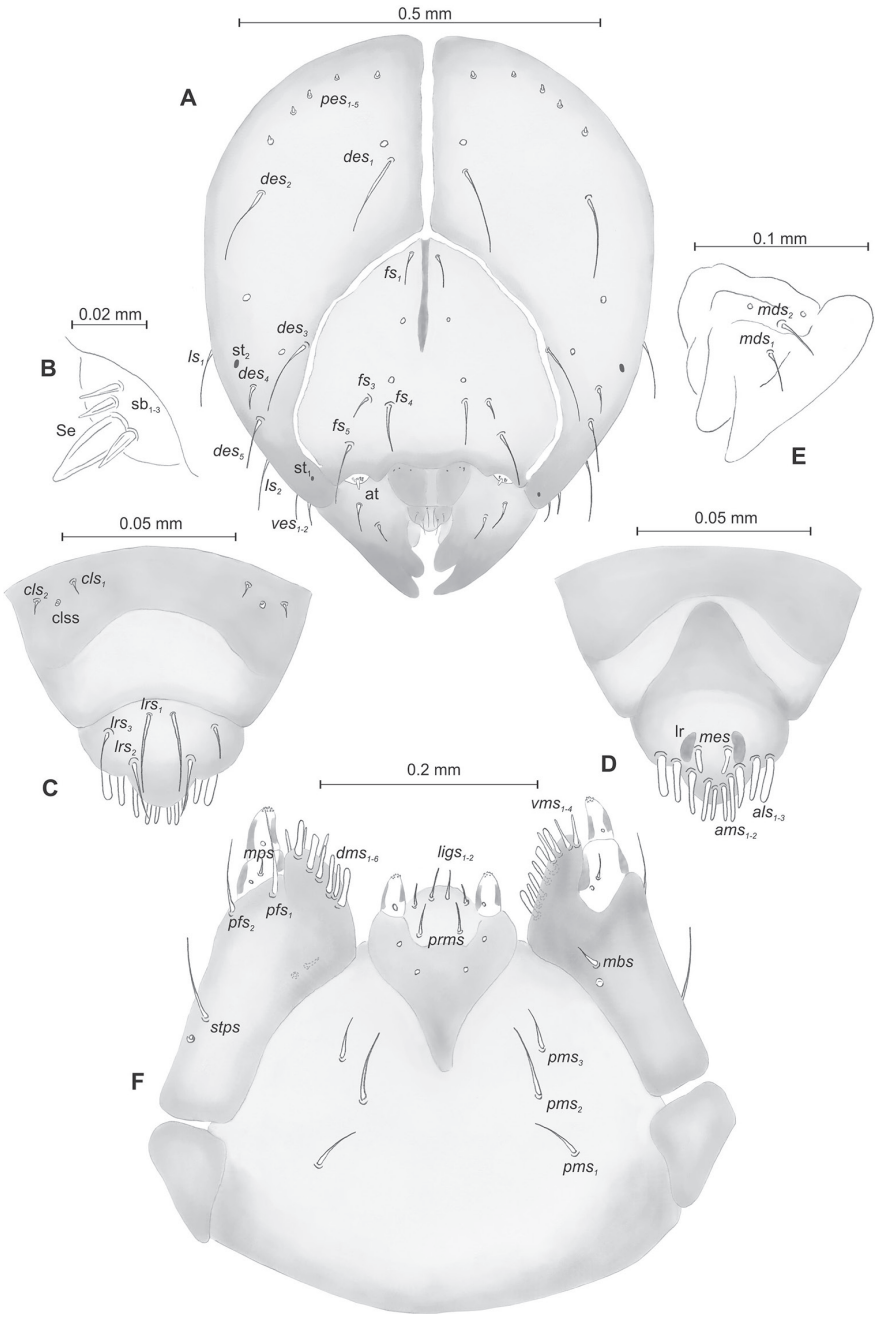

Figure 11. *Mecinus circulatus* mature larva, head and mouth parts **A** head, frontal view **B** antenna **C** clypeus and labrum, dorsal view **D** epipharynx **E** left mandible **F** maxillolabial complex, ventral aspect. Abbreviations: at – antenna, clss – clypeal sensorium, lr – labral rods, sb – sensillum basiconicum, Se – sensorium, st – stemmata, setae: *als* – anterolateral, *ams* – anteromedial, *cls* – clypeal, *des* – dorsal epicranial, *dms* – dorsal malar, *fs* – frontal, *ligs* – ligular, *lrs* – labral, *ls* – lateral epicranial, *mbs* – malar basiventral, *mds* – mandibular, *mes* – median, *mxps* – maxillary palp, *pes* – postepicranial, *ves* – ventral, *pfs* – palpiferal, *pms* – postlabial, *prms* – prelabial, *stps* – stipal, *vms* – ventral malar.

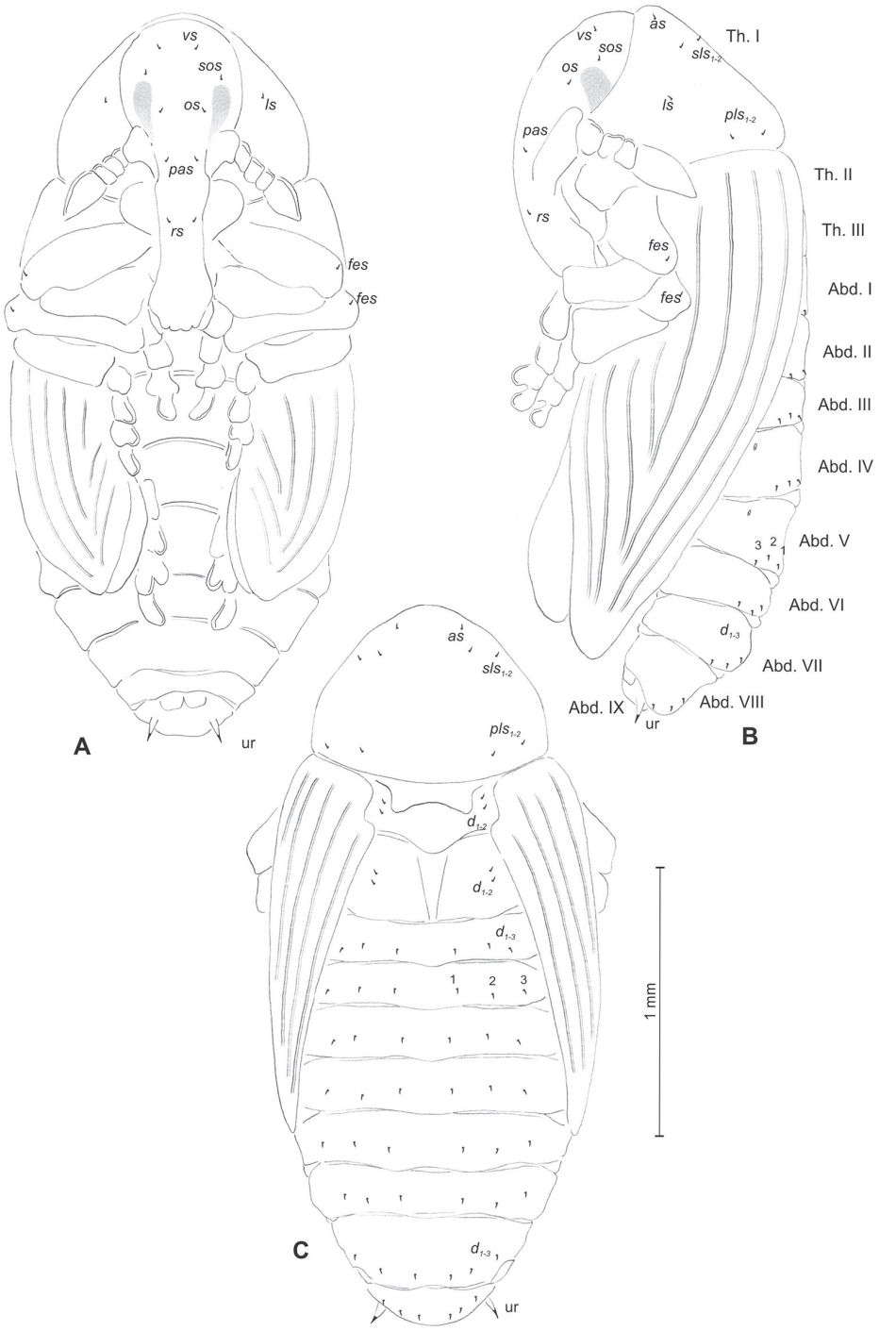

Figure 12. *Mecinus circulatus* pupa habitus and chaetotaxy **A** ventral view **B** lateral view **C** dorsal view. Abbreviations: Th. I–III – number of thoracic segments, Abd. I–IX – number of abdominal segments, ur – urogomphi, setae: *as* – apical, *d* – dorsal, *fes* – femoral, *l*, *ls* – lateral, *os* – orbital, *pas* – postantennal, *pls* – posterolateral, *rs* – rostral, *sls* – superlateral, *sos* – superorbital, *vs* – vertical.

pupate inside the larval channel, and the emerged adult leaves the pupa chamber after a short time. The adult overwinters in the soil litter near the host plant.

Remarks and comparative notes. This is a common species in western, central and southern Europe, northern Africa and the Middle East. By the colour of the elytral integument, with black and reddish vittae, the adults differ from *M. pyraster*, whose integument is completely black. However, both the study of the morphological characters in adults and immatures and the preliminary molecular study (I. Toševski, unpublished data) agree with the hypothesis of close relationships between these two species.

Larvae are easily separable from those of *M. pyraster*: the pronotum has eight *prns* instead of 11, the pedal lobes has three *pda* instead of five, the anal lobes with one *ts* instead of two, the head with five *pes* instead of four, the mandible with two *mds* instead of one, the mala with four *vms* instead of five, and the *prms* are shorter.

Pupae differ from those of *M. pyraster* by the head with one *sos* and one *os* instead of two, the pronotum with a different number of setae in all positions, and the abdominal segments I–VII with three setae dorsally instead of five.

Mecinus pyraster (Herbst, 1795)

Material examined. 4 L3 larvae and 5 pupae, Serbia, Zemun, 1.07.2017, GPS 44°39.030'N, 21°28.355'E, 162 m., ex l., ex *Plantago lanceolata*, lgt. I. Toševski. Accession number of sequenced specimen MN992000.

Description of mature larva (Figures 13A–D, 14A–F). ***Measurements*** (in mm). Body length: 2.00–2.83. Body width (metathorax or abdominal segments I–II): 0.83–1.00. Head width: 0.53–0.56.

Body (Figure 13A–D) yellowish, slender, curved, densely covered with asperities. Metathorax as large as abdominal segment I. Abdominal segments I–VI of almost equal length, abdominal segments VII–IX decreasing gradually to the terminal body part, segment X reduced to three anal lobes of those lateral are the largest, and dorsal the smallest (sometimes absent). Chaetotaxy weakly developed, setae short or medium. Prothorax (Figure 13B) with eleven *prns* (eight medium and three very short); two medium *ps* and one very short *eus*. Meso- and metathorax (Figure 13B) with one very short *prs*, two very short *pds*, one very short *as*, three *ss* (two medium and one very short), one medium *eps*, one medium *ps* and one very short *eus*. Pedal area with five *pda* (three medium and two very short). Abdominal segments I–VIII (Figure 13C, D) with one very short *prs*, three very short *pds* arranged along the posterior margin, two very short *ss*, two *eps* different in length, one medium *ps*, one medium *lsts* and two very short *eus*. Abdominal segment IX (Figure 13D) with three *ds* (one medium and two very short), all located close to the posterior margin, one medium *ps* and two very short *sts*. Each lateral anal lobe with two minute setae.

Head capsule (Figures 13A, 14A–F) dark brown, narrowed bilaterally. Frontal suture visible. $Des_{1–3,5}$ very long, equal in length; des_4 three times shorter than des_1. $Fs_{1,4,5}$ long; fs_3 very short. Les_1 and les_2 equal in length, slightly shorter than des_1; $ves_{1–2}$ short; $pes_{1–2}$ short (Figure 14A). Antennae (Figure 14B) with sensorium (Se) slender,

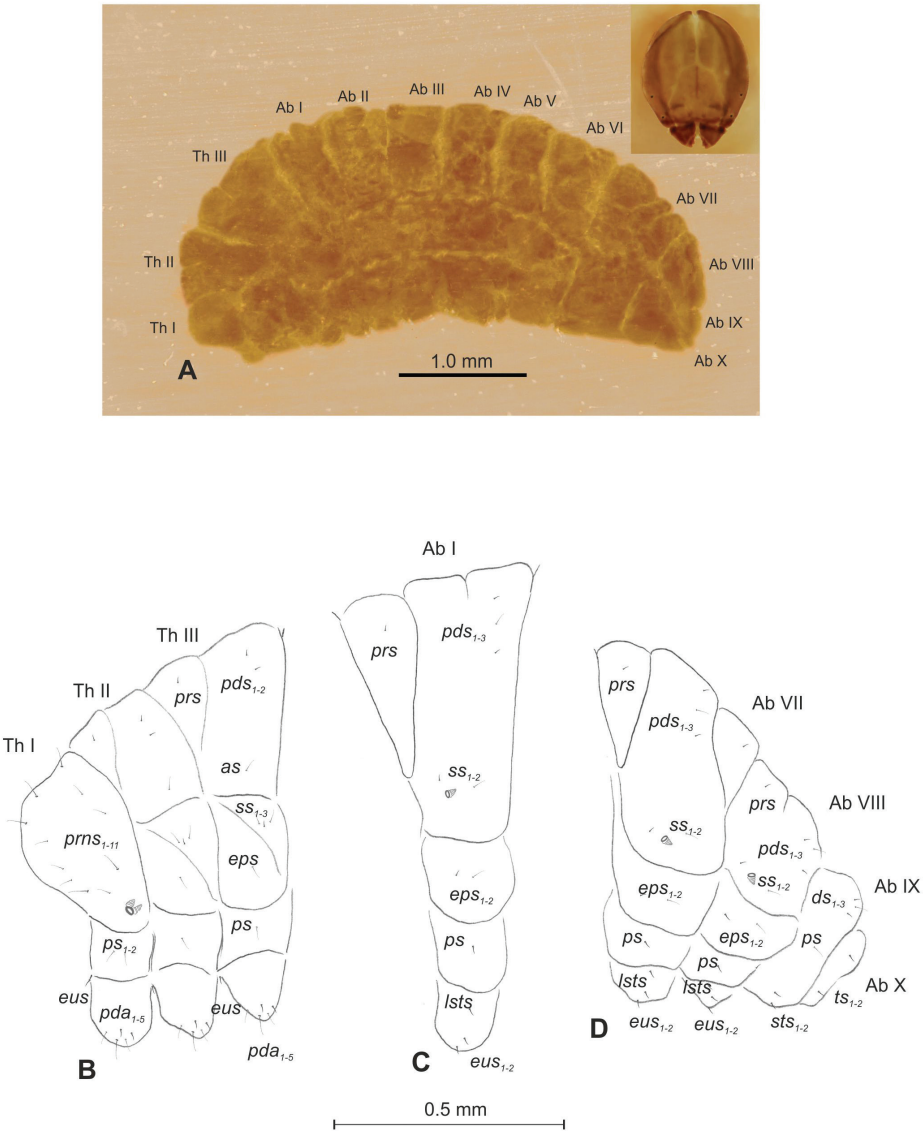

Figure 13. *Mecinus pyraster* mature larva, habitus and chaetotaxy **A** habitus of the body and frontal view of the head **B** lateral view of thoracic segments **C** lateral view of abdominal segment I **D** lateral view of abdominal segments VII–X. Abbreviations: Th. I–III – number of thoracic segments, Abd. I–X – number of abominal segments, setae: *as* – alar, *ds* – dorsal, *eps* – epipleural, *eus* – eusternal, *lsts* – laterosternal, *pda* – pedal, *pds* – postdorsal, *prns* – pronotal, *prs* – prodorsal, *ps* – pleural, *ss* – spiracular, *sts* – sternal, *ts* – terminal.

four times as long as wide, and three sensilla basiconica. Clypeus (Figure 14C) trapezium-shaped, anterior margin distinctly sinuated; both *cls* relatively long, clss absent. Labrum (Figure 14C) with slightly sinuate anterior margin; lrs_1 long, lrs_2 and lrs_3 medium. Epipharynx (Figure 14D) with three medium, finger-shaped *als* of almost equal

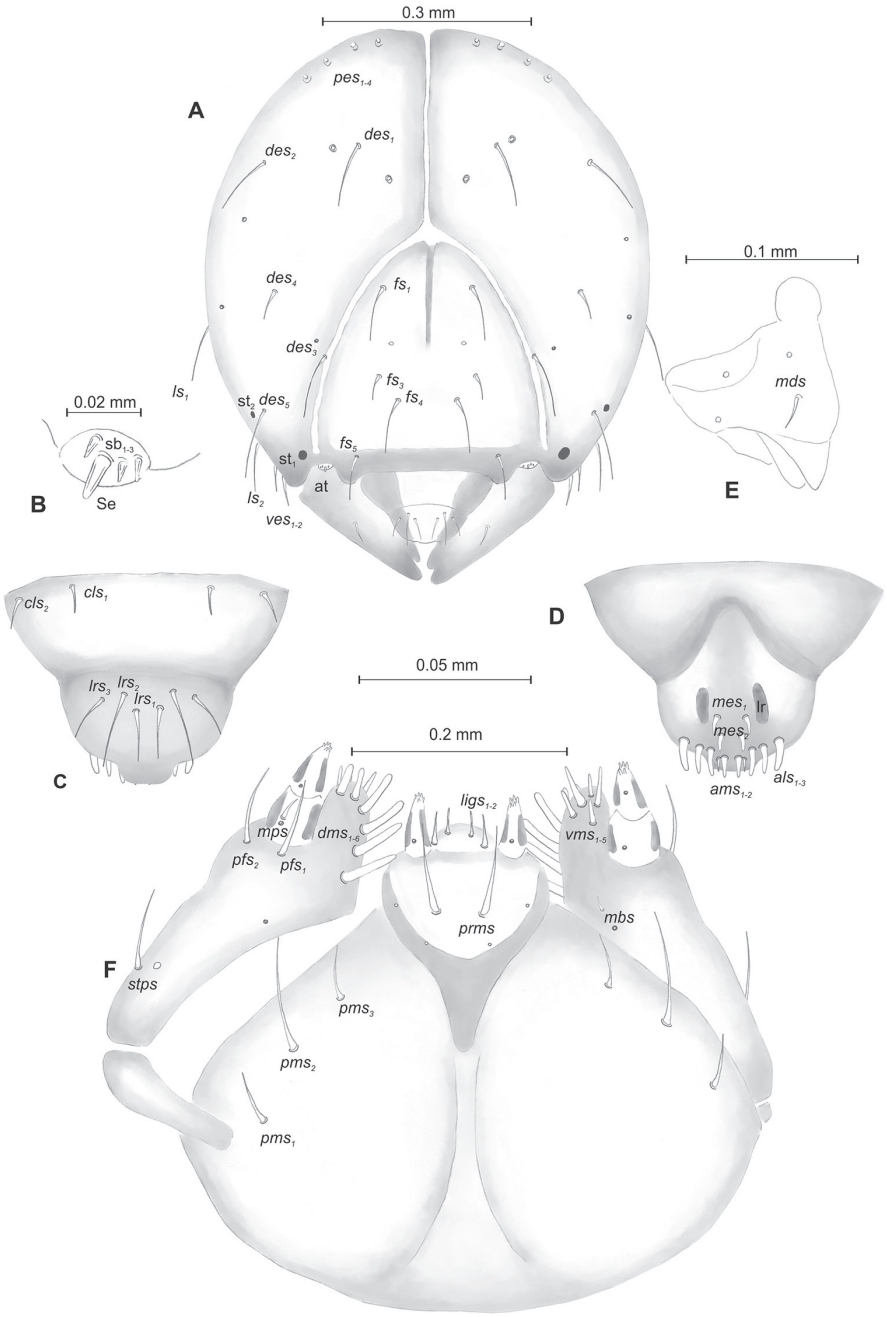

Figure 14. *Mecinus pyraster* mature larva, head and mouth parts **A** head, frontal view **B** antenna **C** clypeus and labrum, dorsal view **D** epipharynx **E** left mandible **F** maxillolabial complex, ventral aspect. Abbreviations: at – antenna, lr – labral rods, sb – sensillum basiconicum, Se – sensorium, st – stemmata, setae: *als* – anterolateral, *ams* – anteromedial, *cls*– clypeal, *des* – dorsal epicranial, *dms* – dorsal malar, *fs* – frontal, *ligs* – ligular, *lrs* – labral, *ls* – lateral epicranial, *mbs* – malar basiventral, *mds* – mandibular, *mes* – median, *mxps* – maxillary palp, *pes* – postepicranial, *ves* – ventral, *pfs* – palpiferal, *pms* – postlabial, *prms* – prelabial, *stps* – stipal, *vms* – ventral malar.

length; two rod-like *ams* different in length; two finger-like *mes* of medium length; surface smooth; labral rods close to kidney-shaped. Mandibles (Figure 14E) conical, wide, with small protuberance in the middle of the cutting edge; one capilliform *mds*, medium, placed mediolaterally. Maxilla (Figure 14F) with one *stps* and two *pfs* equal in length; *mbs* very short; mala with six finger-like *dms* of different size ($dms_{1–2}$ medium, $dms_{3–6}$ long to very long), five *vms* different in length. Maxillary palpi: basal palpomere slightly wider than distal, both palpomeres almost equal in length. Prelabium (Figure 14F) cup-like with one relatively long *prms*; ligula with two *ligs* different in length; premental sclerite well visible, cup-shaped. Labial palpi elongated, one-segmented. Postlabium (Figure 14F) with medium pms_1, long pms_2, and medium pms_3.

Description of pupa (Figure 15A–C). ***Measurements*** (in mm). Head width: 0.53–0.63. Body width: 1.40–1.73. Body length: 3.33–4.26.

Body elongated, white. Rostrum rather slender, about three times as long as wide, reaching almost up to mesocoxae. Antennae slender and elongated. Pronotum 1.8 times as wide as long. Urogomphi (ur) slender and rather elongated, conical, with sclerotised apex, reaching outline of the body, directed downward (Figure 14A–C).

Chaetotaxy well developed, setae rather short. Head capsule with one *vs*, two *sos* equal in length, two *os* equal in length. Rostrum with one *rs* and one *pas* (Figure 14A). Pronotum with two *as*, one *ds*, two *sls*, two *ls*, and three *pls* (Figure 14A–C); equal in length (Figure 14B). Setae on head and rostrum as long as those on prothorax. Dorsal parts of meso- and metathorax with two setae different in length placed medially. Abdominal segments I–VIII with two medium setae laterally and three medium setae ventrally, distributed in regular lines. Dorsal parts of abdominal segments I–VII with five setae (d_1 placed anteromedially, $d_{2–4}$ posteromedially and d_5 located posterolaterally); abdominal segment VIII with only four very long setae dorsally. Abdominal segment IX with two micro-setae ventrally.

Biological notes. This species is associated with some *Plantago* species (*P. lanceolata* L., *P. lagopus* L., *P. media* L.) (Hoffmann 1958; Sprick 2001). In west Palearctic larvae are most frequently found in the roots of *P. lanceolata*, boring channels in upper part of the root crown. Larger roots may inhabit several larvae. Pupation takes place during early summer in the pupal chamber situated in the upper part of larval channel. After emergence, adults overwinter in the soil litter nearby host plant.

Remarks and comparative notes. This species is very common and widespread in the Palearctic region. It was also reported in North America (O'Brien and Wibmer 1982). The adult is distinctly variable in the size and shape of the body and vestiture within the same population. It differs from *M. circulatus* by the black integument and ventrite 5 in the male bearing a median tuft of hair. In larvae, the pronotum has eleven *prns* instead of eight, the pedal lobes have five *pda* instead of three, the anal lobes with two *ts* instead of one, the head with four *pes* instead of five, the mandible with one *mds* instead of two, the mala with five *vms* instead of four, and the *prms* are longer. The pupae also differ from those of *M. circulatus* by a different number of setae on head, pronotum and abdominal segments I–VII (see key to the pupae). However, morphological and molecular studies (I. Toševski, unpublished data) demonstrate a clear relationship between *M. pyraster* and *M. circulatus*.

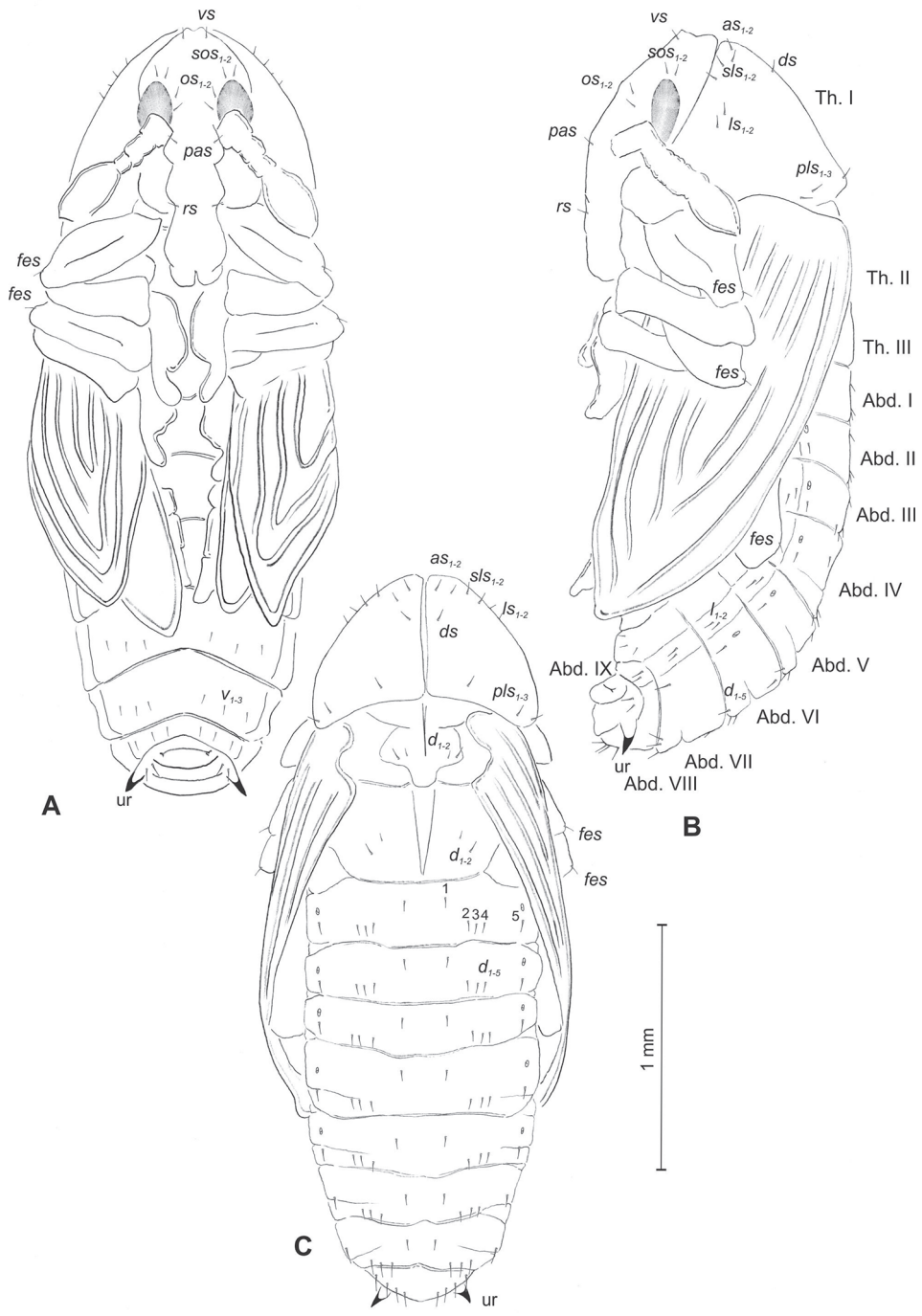

Figure 15. *Mecinus pyraster* pupa habitus and chaetotaxy **A** ventral view **B** lateral view **C** dorsal view. Abbreviations: Th. I–III – number of thoracic segments, Abd. I–IX – number of abdominal segments, ur – urogomphi, setae: *as* – apical, *d* – dorsal, *ds* – discal, *fes* – femoral, *l*, *ls* – lateral, *os* – orbital, *pas* – postantennal, *pls* – posterolateral, *rs* – rostral, *sls* – superlateral, *sos* – superorbital, *vs* – vertical.

Mecinus collaris group

Differential diagnosis. Larva. (1) slightly pressed dorso-ventrally, cuticle densely tuberculate, premental sclerite, pedal lobes and spiracular area of meso- and metathorax dark pigmented; (2) pedal lobes prominent well isolated; (3) abdominal segment X reduced to three anal lobes of equal size; (4) thoracic spiracle bicameral; (5) abdominal setae short; (6) abdominal segments I–VII with four *pds* and two *ss* (abd. segment VIII with one *ss*); (7) head brown, flattened laterally; (8) frontal suture visible; (9) endocarina 1/2 of the frons; (10) des_4 minute or short; (11) presence of fs_1; (12) absence of fs_2; (13) fs_3 minute; (14) head with one stemma; (15) presence of cls_1; (16) labial palpi two-segmented; (17) premental sclerite cup-like; (18) surface of postlabium smooth.

Pupa. (1) body elongated; (2) urogomphi slender, rather short, reaching outline of the body, directed downward; (3) rostrum moderately elongated; (4) setae different in length; (5) head with one *sos*; (6) rostrum with one *rs*; (7) pronotum with two *as*, one *ds*, one *sls*, one *ls*, four *pls*; (8) meso- and metanotum with two setae; (9) abdominal segments I–IV without setae dorsally; segments V–VII dorsally with five growing setae.

Remarks and comparative notes. The adults of this monobasic group are easily distinguishable from all other species of *Mecinus* by several autapomorphies, such as rostrum short and wide, straight in lateral view, scrobe not reaching anterior margin of eye, elytra elongate, broad scales densely covering base of pronotum, epimera and episterna. In contrast, immatures have few autapomorphies, i.e., larvae are slightly pressed dorsoventrally, with a densely tuberculate cuticle, whereas premental sclerite, pedal lobes and spiracular area of meso- and metathorax are dark pigmented; the pupae have abdominal segments I–IV lacking setae dorsally, whereas segments V–VII dorsally possess five growing setae.

Presently, it is unclear to which species *M. collaris* is more closely related. The other species with short and straight rostrum, such as those of the *M. simus* group, do not apparently share other synapomorphies with *M. collaris*. In contrast, the larvae of the latter share the number of palpomeres of the labial palpi (two) and the shape of the thoracic spiracle (bicameral) and abdominal spiracles (unicameral) with the *M. janthinus* group. The pupae of *M. collaris* differ from all the others studied here by the dorsal setae of the abdominal segments because segments I–IV are without setae and segments V–VII have setae growing gradually.

Mecinus collaris Germar, 1821

Material examined. 26 L3 larvae and 21 pupae, Serbia, Zavojskojezero, Pirot, 15.07.2017, GPS 43°12.508'N, 22°35.590'E, 675 m., ex *Plantago media*, lgt. I. Toševski. Accession numbers of sequenced specimen MN992001.

Description of mature larva (Figures 16A–D, 17A–F). ***Measurements*** (in mm). Body length: 2.00–3.66. Body width (metathorax): 0.80–1.16. Head width: 0.56–0.66.

Body (Figure 16A–D) light yellow, slender, curved, slightly pressed dorso-ventrally. Premental sclerite, pedal lobes and spiracular area of meso- and metathorax dark pigmented. Chaetotaxy of thoracic segments relatively well developed, setae capilliform, variable in length, light yellow, on thoracic segments medium or relatively long, on abdominal segments I–IX short or medium. Prothorax (Figure 16B) with eleven *prns* (six long and one short placed on premental sclerite), next three close to spiracle; two medium *ps* and one short *eus*. Meso- and metathorax (Figure 16B) with one medium *prs*, three medium *pds* of equal length, one medium *as*, three medium *ss*, equal in length, one long *eps*, one long *ps* and one short *eus*. Pedal area with three *pda*, long or medium. Abdominal segments I–VIII (Figure 16C, D) with one short *prs*, four short *pds* arranged along the posterior margin, two minute*ss*, one short *eps*, one short *ps*, one short *lsts* and two short *eus*. Abdominal segment IX (Figure 16D) with three short *ds*, all located close to posterior margin, one short *ps* and two rather short *sts*. Anal lobes without setae.

Head capsule (Figures 16A, 17A–C) dark brown, slightly narrowed bilaterally. $Des_{1–3,5}$ long, des_4 short; des_4 located in the central part of epicranium. Fs_1 long, fs_3 very short, $fs_{4,5}$ equal in length, almost as long as des_1. Les_1 and les_2 slightly shorter than des_1; two *ves*, and four *pes* very short (Figure 17A). Antennae (Figure 17B) with conical, elongated sensorium (Se), three times as long as wide, and two sensilla basiconica and two sensilla ampullacea. Clypeus (Figure 17C) trapezium-shaped, anterior margin almost straight; cls_{1-2} medium, equal in length; clss well visible. Labrum (Figure 17C) narrow, trapezium-shaped, anterior margin distinctly sinuate; lrs_1 long, lrs_2 and lrs_3 medium. Epipharynx (Figure 17D) with three elongated, finger-like *als* of equal length; two medium, straight *ams*; two short finger-like *mes*; surface smooth; labral rods very short, close to kidney-shaped. Mandibles (Figure 17E) conical, rather wide; both *mds* capilliform, medium, equal in length, placed transversely. Maxilla (Figure 17F) with one *stps* and two *pfs* of equal length; *mbs* short; mala with six long rod-like *dms* of almost equal size, five *vms* various in length. Maxillary palpi: basal palpomere distinctly wider and slightly shorter than distal. Prelabium (Figure 17F) cup-like with one long *prms*; ligula with two minute *ligs*, premental sclerite well developed, with elongated median part. Labial palpi two-segmented; basal palpomere wider and shorter than distal. Postlabium (Figure 17F) with short pms_1, long pms_2, and short pms_3.

Description of pupa (Figure 18A–C). ***Measurements*** (in mm). Head width: 0.30–0.36. Body width: 0.76–1.20. Body length: 1.66–2.33.

Body moderately elongated, light yellowish. Rostrum moderately stout, about 2.1 times as long as wide, reaching up to mesocoxae. Antennae relatively short. Pronotum 1.6 times as wide as long. Mesonotum distinctly shorter than metanotum. Urogomphi (ur) short, conical, with sclerotised, sharp apex, slightly reaching outline of the body, directed downward (Figure 18A–C).

Chaetotaxy sparse, setae short, unequal length. Head with only one *sos*. Rostrum with one *rs*. Setae on head and rostrum straight, much shorter than those on prothorax (Figure 18A). Pronotum with two *as*, one *sls*, one *ls*, one *ds* and four *pls*. Dorsal parts of meso- and metathorax with two setae placed medially. Dorsal parts of abdominal

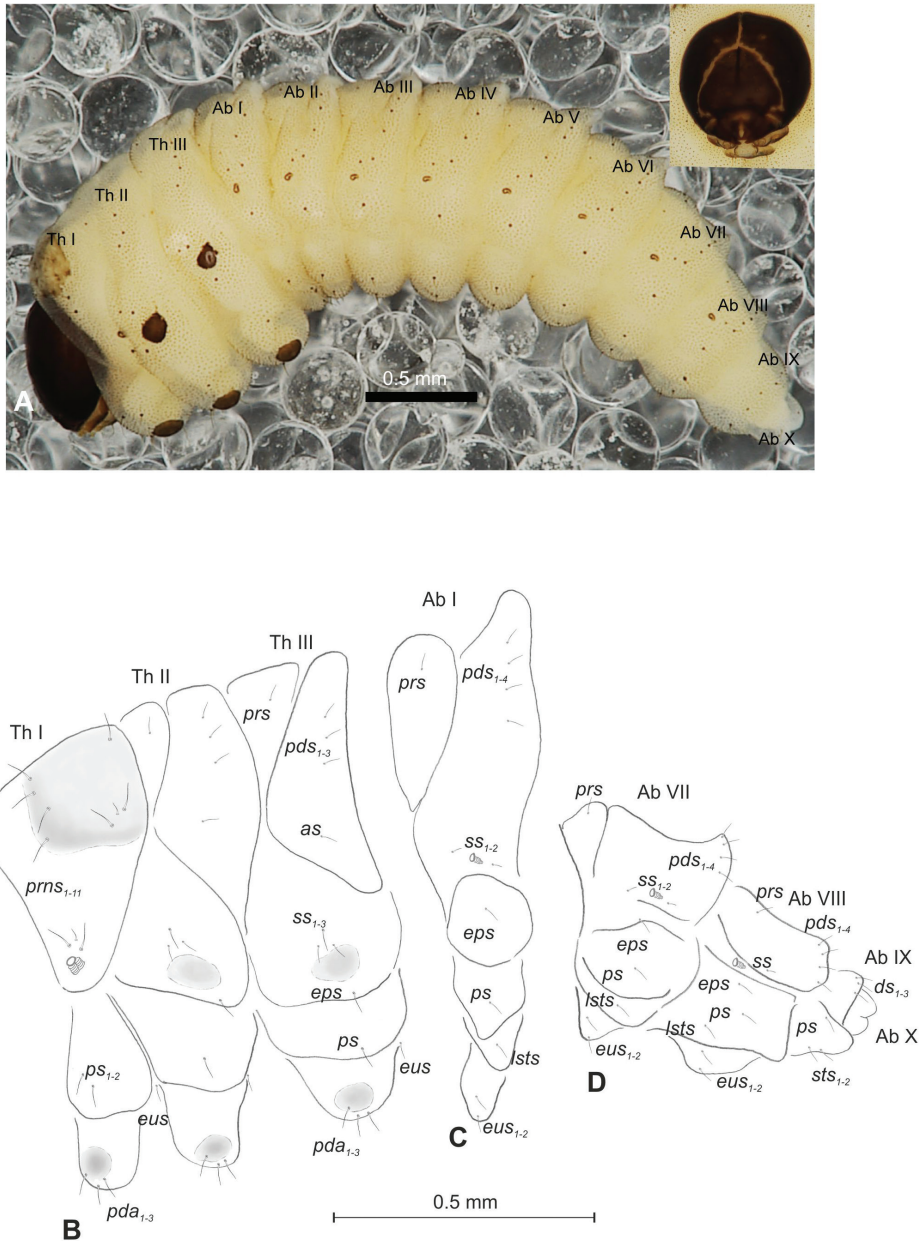

Figure 16. *Mecinus collaris* mature larva, habitus and chaetotaxy **A** habitus of the body and frontal view of the head **B** lateral view of thoracic segments **C** lateral view of abdominal segment I **D** lateral view of abdominal segments VII–X. Abbreviations: Th. I–III – number of thoracic segments, Abd. I–X – number of abominal segments, setae: *as* – alar, *ds* – dorsal, *eps* – epipleural, *eus* – eusternal, *lsts* – laterosternal, *pda* – pedal, *pds* – postdorsal, *prns* – pronotal, *prs* – prodorsal, *ps* – pleural, *ss* – spiracular, *sts* – sternal, *ts* – terminal.

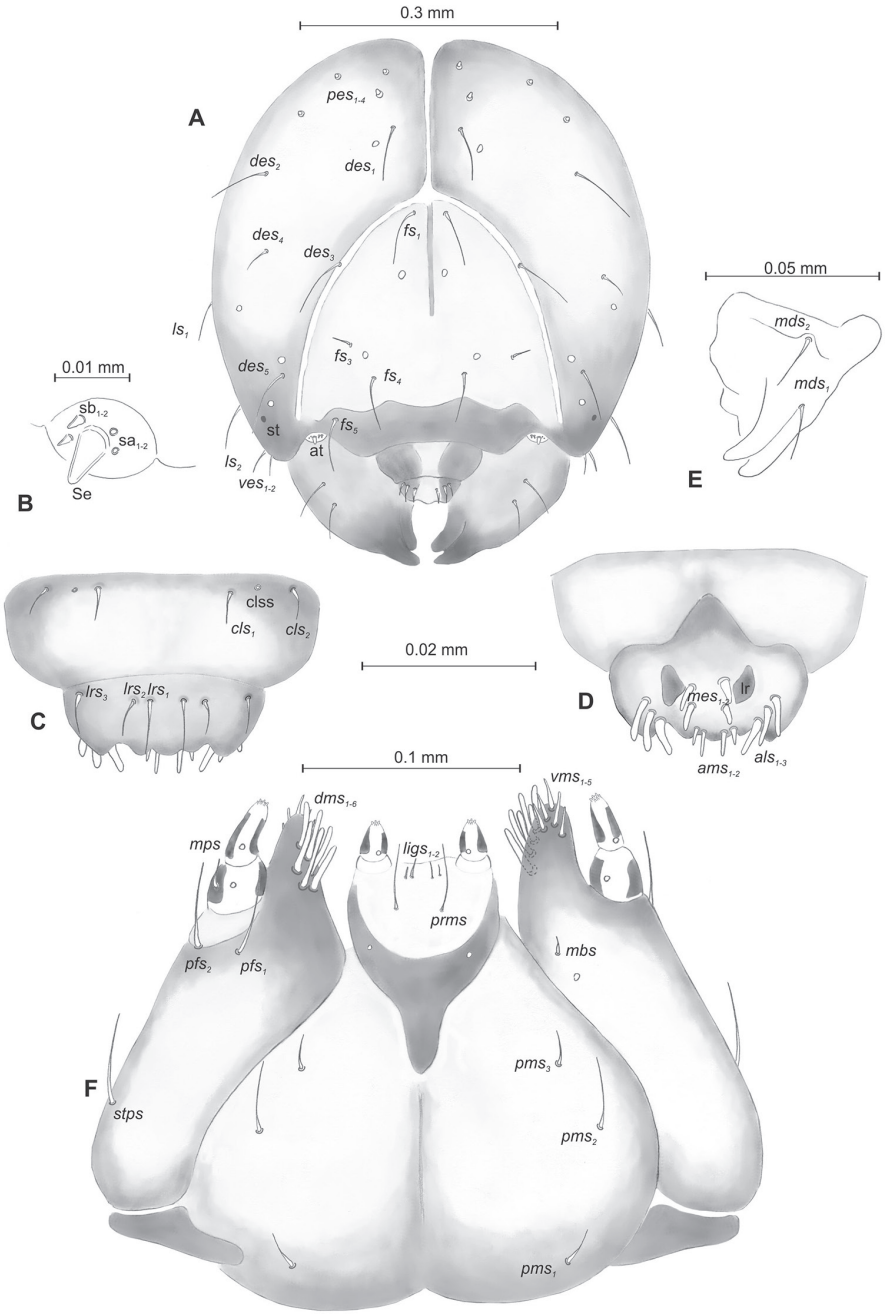

Figure 17. *Mecinus collaris* mature larva, head and mouth parts **A** head, frontal view **B** antenna **C** clypeus and labrum, dorsal view **D** epipharynx **E** left mandible **F** maxillolabial complex, ventral aspect. Abbreviations: at – antenna, clss – clypeal sensorium, *des* – dorsal epicranial, lr – labral rods, sa – sensillum ampullaceum, sb – sensillum basiconicum, Se – sensorium, st – stemmata, setae: *als* – anterolateral, *ams* – anteromedial, *cls* – clypeal, *dms* – dorsal malar, *fs* – frontal, *ligs* – ligular, *lrs* – labral, *ls* – lateral epicranial, *mbs* – malar basiventral, *mds* – mandibular, *mes* – median, *mxps* – maxillary palp, *pes* – postepicranial, *ves* – ventral, *pfs* – palpiferal, *pms* – postlabial, *prms* – prelabial, *stps* – stipal, *vms* – ventral malar.

segments I–IV without setae; segments V–VII with five setae (d_1 placed anteromedially, d_{2-4} posteromedially, d_5 posterolaterally, under spiracle); segment VIII with four setae dorsally. Abdominal segments I–VIII with four long setae ventrally, distributed in regular lines. Abdominal segment IX with two micro-setae ventrally, and next two on urogomphi.

Biological notes. Larvae feed on various species of *Plantago*, but mainly on *P. media* L. and *P. maritima* L. *Plantago lanceolata*, *P. coronopus* L., and *P. major* L. are also known as host plants. The adults are active from mid-spring following the growth of the flowering stems of the host plant. The female oviposits inside the upper parts of the flowering stem that are covered with floral spikes, which induces clearly visible oblong galls. Very often, several larvae develop in a single flowering shoot. The larvae pupate inside the galls and the adults emerge during summer. Overwintering takes place in the soil litter near the host plant.

Remarks. This species, which is widely distributed in the Palearctic region except in North Africa (Alonso-Zarazaga et al. 2017), is unique in *Mecinus*, being characterised by long elytra and whitish to orange, wide scales covering the base of the pronotum, the epimera and the episterna. For the differences from the immatures of the other species, see the remarks for the group.

Mecinus janthinus group

Differential diagnosis. Larva. (1) body densely covered with asperities; (2) pedal lobes weakly isolated; (3) abdominal segment X reduced to three anal lobes of unequal size; (4) thoracic spiracle bicameral; (5) abdominal setae medium to very long, distinclty growing from abdominal segment I to VIII; (6) abdominal segments I–VIII with four *pds* and usually three *ss*; (7) head brown, flattened laterally; (8) frontal suture distinct; (9) endocarina 4/5 of the frons; (10) des_4 usually shorter than des_1; (11) presence of fs_1; (12) absence of fs_2; (13) fs_3 as long as half of fs_4; (14) head with two stemmata; (15) presence of cls_1; (16) labial palpi two-segmented; (17) premental sclerite cup-like; (18) surface of postlabium densely covered with asperities.

Pupa. (1) body very slender and elongated; (2) urogomphi rather elongated, distinctly reaching outline of the body, directed outside; (3) rostrum elongated and slender; (4) setae more or less elongated; (5) head with one *vs*, two *sos*, two *os*; (6) rostrum with one or two *pas* and without or with one *rs*; (7) pronotum with two *as*, one *ds*, two *sls*, two *ls*, three or four *pls*; (8) meso- and metanotum with two or three setae; (9) abdominal segments I–VII dorsally with six or seven elongated, growing setae.

Remarks and comparative notes. The adult of this species is characterised by elytra distinctly elongate, dorsal integument black or blue, sometimes with metallic reflections.

The shape of the body together with the colour of the dorsal integument are characters that this group shares only with *M. heydenii*. These two groups include the species of *Mecinus* not living on *Plantago*. Nevertheless, they seem to be not closely related on the basis of both a phylogenetic study of the adults and of molecular data as well as the examination of the immatures. The adults of the species

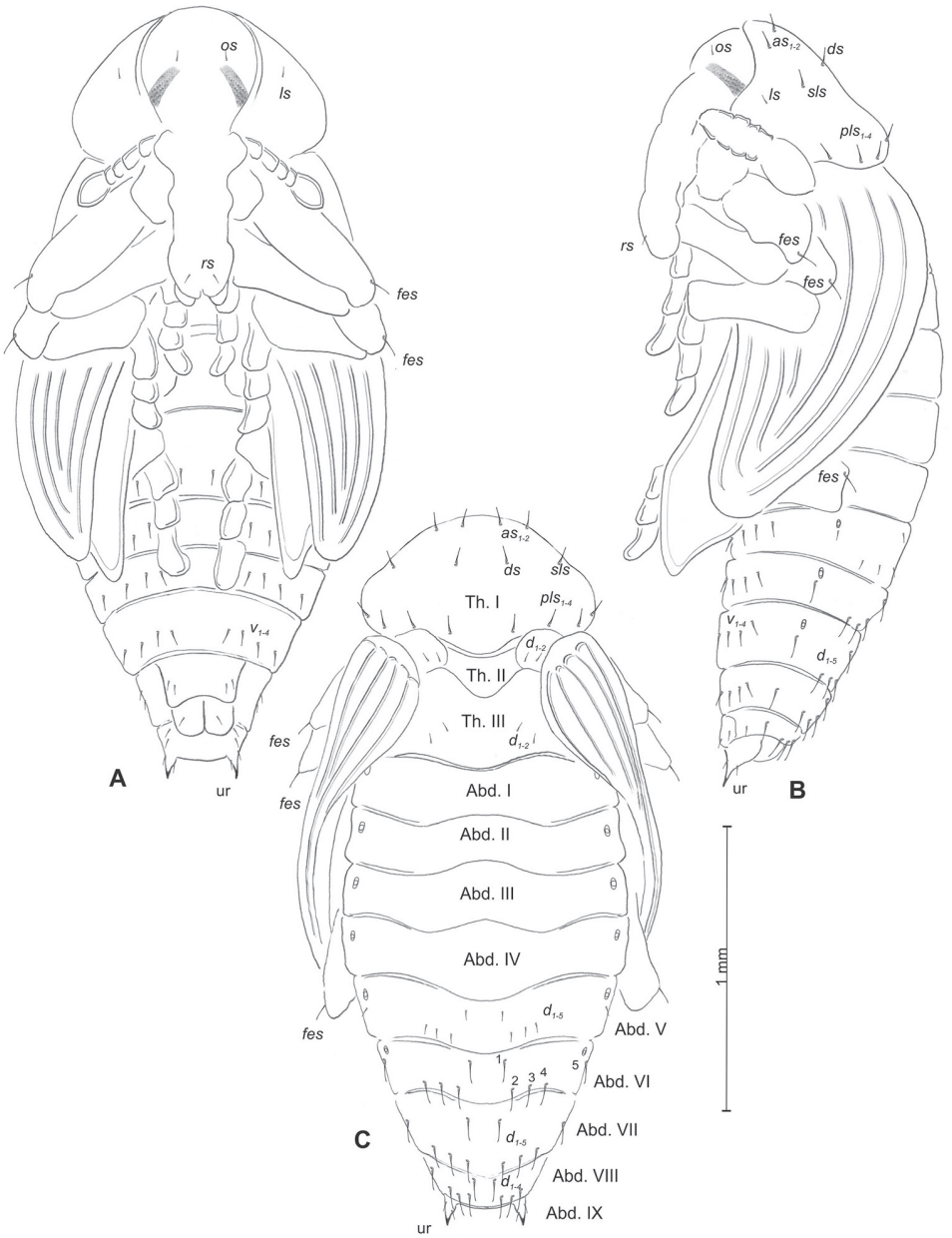

Figure 18. *Mecinus collaris* pupa habitus and chaetotaxy **A** ventral view **B** lateral view **C** dorsal view. Abbreviations: Th. I–III – number of thoracic segments, Abd. I–IX – number of abdominal segments, ur – urogomphi, setae: *as* – apical, *d* – dorsal, *ds* – discal, *fes* – femoral, *l*, *ls* – lateral, *pls* – posterolateral, *rs* – rostral, *sls* – superlateral, *sos* – superorbital.

related to *M. janthinus* are distinguishable from those related to *M. heydenii* by the less curved rostrum in lateral view, the shape of the penis, the distinctly longer flagellum and the completely unusual shape of the spermatheca that is reminiscent of

the Cionini. The larvae and pupae differ in a series of characters in the chaetotaxy. Moreover, the immatures of this group possess some autapomorphies, i.e., in larvae four *pds* and usually three *ss* on the abdominal segments I–VIII and the surface of postlabium densely covered with asperities, and in pupae, the more or less elongated setae on the body and the abdominal segments I–VII dorsally with six or seven elongated, growing setae.

Mecinus janthinus Germar, 1821

Material examined. 9 L3 larvae and 8 pupae, Serbia, Mihajlovac, 5.07.2009, 44°21.541'N, 22°28.650'E, 130 m., ex *L. vulgaris*; Serbia, Negotin, Tamnič, 2.08. 2007, 44°06.033'N, 22°30.105'E, 126 m., ex *L. vulgaris*; 8 pupae, Serbia, Mihajlovac, 5.07.2009, 44°21.683'N, 22°28.697'E, 125 m., ex *L. vulgaris*; 1 pupa, Serbia, DonjaKamenica, Kalna, 22.08.2011, 43°29.450'N, 22°19.712'E, 278 m., ex *L. vulgaris*. All collected by I. Toševski. Accession numbers of sequenced specimen MN992005.

Description of mature larva (Figures 19A–D, 20A–F). ***Measurements*** (in mm). Body length: 4.00–4.75. Body width (metathorax and abdominal segments I–II): 1.10–1.25. Head width: 0.50–0.57.

Body (Figure 19A–D) yellowish, very slender, densely covered with asperities. Prothorax smaller than meso- and metathorax. Abdominal segments I–V of almost equal length; segments VI–IX decreasing gradually to the terminal body part; segment X reduced to three anal lobes of those lateral are the largest, and dorsal the smallest (sometimes absent). Chaetotaxy well developed, setae capilliform, variable in length, greyish or yellow. Prothorax (Figure 19B) with eight long *prns* of equal length; two long *ps* and one short *eus*. Meso- and metathorax (Figure 19B) with one very short *prs*, three *pds*, variable in length (pds_1 short, $pds_{2–3}$ medium), one short *as*, three short *ss*, one long *eps*, one long *ps* and one long *eus*. Pedal area with five long *pda*. Abdominal segments I–VIII (Figure 19C, D) with one very short *prs*, four *pds* of different length (on segments I–V: $pds_{1–2}$ short, $pds_{3–4}$ long; on segments VI–VIII all *pds* very long, almost equal in length) and arranged along posterior margin; one minute and two medium *ss*, one short and one long *eps*, one long *ps*, one long *lsts* and two medium *eus*. Abdominal segment IX (Figure 19D) with four very long *ds*, all located close to the posterior margin, two long *ps* and two short *sts*. Each of lateral anal lobe with two minute setae.

Head capsule (Figures 19A, 20A–F) yellow, distinctly narrowed bilaterally. $Des_{1–3,5}$ very long, equal in length; des_4 half the length of other *des*; des_4 medially. $Fs_{1,4,5}$ long, fs_3 medium. Les_1 and les_2 long, equal in length; one *ves*, and four *pes* short (Figure 20A). Two stemmata of different size. Antennae (Figure 20B) with sensorium (Se) conical, twice as long as wide, and three sensilla of different types: one sa and two sb. Clypeus (Figure 20C) trapezium-shaped, anterior margin distinctly concave; two *cls* relatively long, located on protuberances; clss placed medially between *cls*. Labrum (Figure 20C) with sinuate anterior margin; lrs_{1-3} almost equal in length, all placed on protuberances.

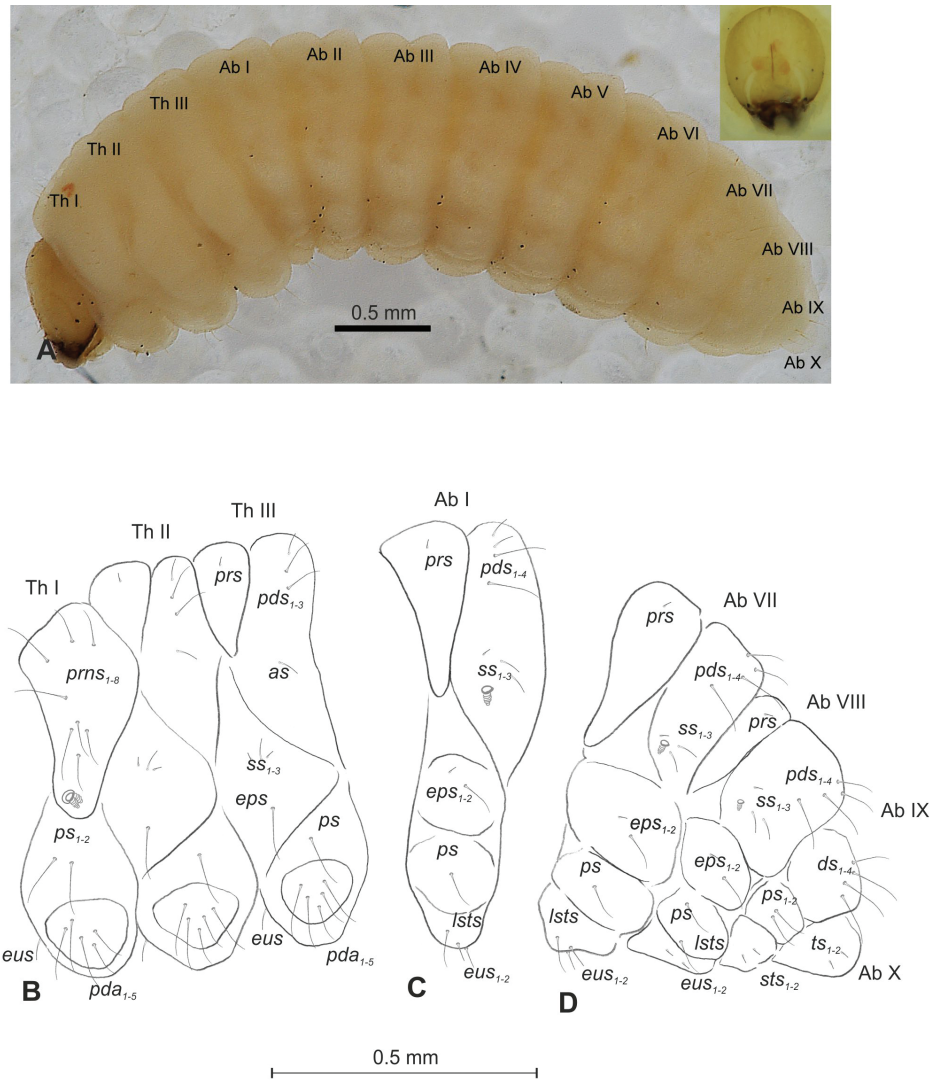

Figure 19. *Mecinus janthinus* mature larva, habitus and chaetotaxy **A** habitus of the body and frontal view of the head **B** lateral view of thoracic segments **C** lateral view of abdominal segment I **D** lateral view of abdominal segments VII–X. Abbreviations: Th. I–III – number of thoracic segments, Abd. I–X – number of abominal segments, setae: *as* – alar, *ds* – dorsal, *eps* – epipleural, *eus* – eusternal, *lsts* – laterosternal, *pda* – pedal, *pds* – postdorsal, *prns* – pronotal, *prs* – prodorsal, *ps* – pleural, *ss* – spiracular, *sts* – sternal, *ts* – terminal.

Epipharynx (Figure 20D) with three medium, finger-shaped *als* of almost equal length; two finger-like, different in length *ams*; two medium finger-like *mes*; surface smooth; labral rods close to kidney-shaped. Mandibles (Figure 20E) conical, wide, an elongated protuberance in the middle of the cutting edge; both *mds* capilliform, medium, equal in length, placed mediolaterally. Maxilla (Figure 20F) with one *stps* and two *pfs* of equal

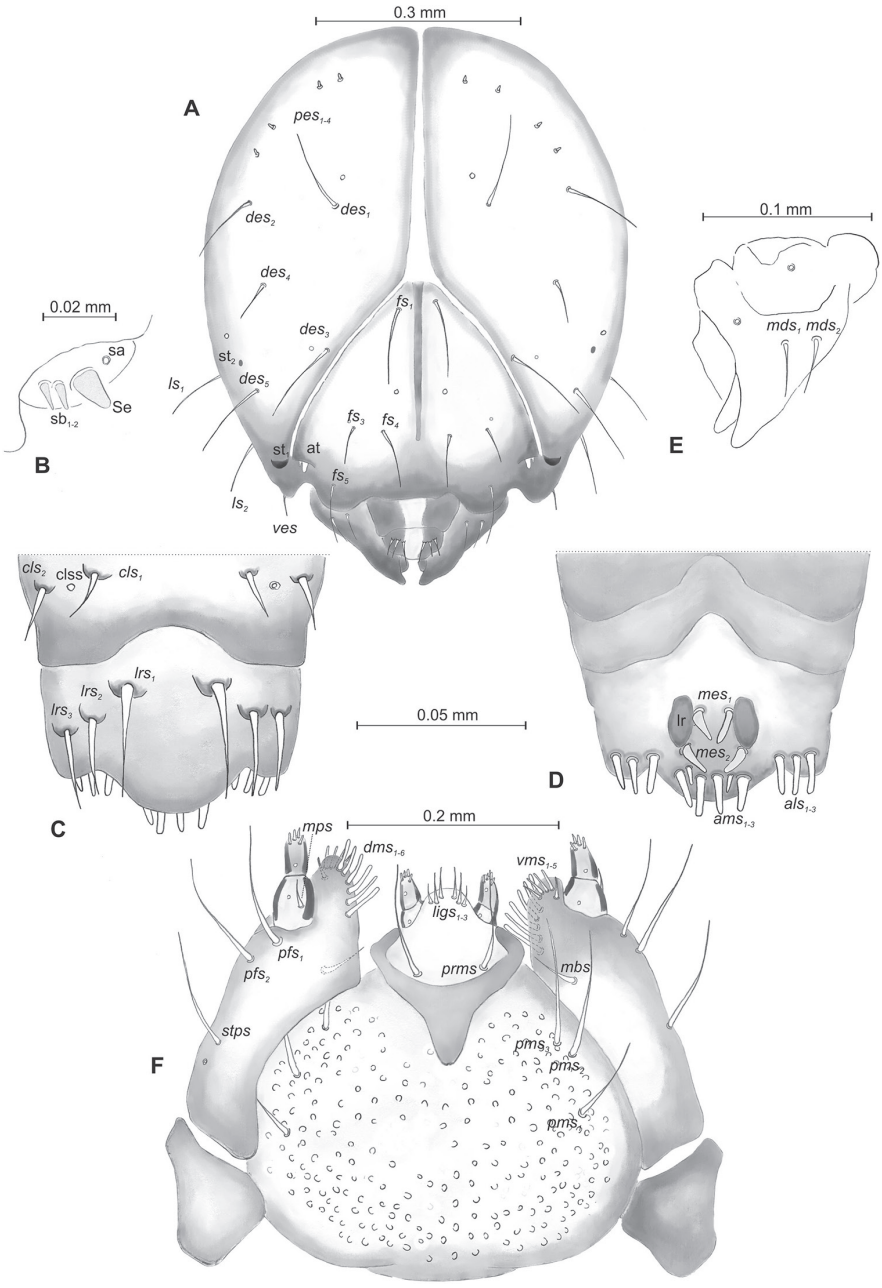

Figure 20. *Mecinus janthinus* mature larva, head and mouth parts **A** head, frontal view **B** antenna **C** clypeus and labrum, dorsal view **D** epipharynx **E** left mandible **F** maxillolabial complex, ventral aspect. Abbreviations: at – antenna, clss – clypeal sensorium, *des* – dorsal epicranial, lr – labral rods, sa – sensillum ampullaceum, sb – sensillum basiconicum, Se – sensorium, st – stemmata, setae: *als* – anterolateral, *ams* – anteromedial, *cls* – clypeal, *dms* – dorsal malar, *fs* – frontal, *ligs* – ligular, *lrs* – labral, *ls* – lateral epicranial, *mbs* – malar basiventral, *mds* – mandibular, *mes* – median, *mxps* – maxillary palp, *pes* – postepicranial, *ves* – ventral, *pfs* – palpiferal, *pms* – postlabial, *prms* – prelabial, *stps* – stipal, *vms* – ventral malar.

length; *mbs* medium; mala with six rod-like *dms* of almost equal size, five *vms* equal in length. Maxillary palpi: basal palpomere distinctly wider than distal, both of almost equal length. Prelabium (Figure 20F) cup-like with one very long *prms*; ligula with three medium *ligs*; premental sclerite clearly visible, cup-shaped. Labial palpi two-segmented; basal palpomere slightly wider and distinctly shorter than distal. Postlabium (Figure 20F) with three capilliform medium to long *pms*.

Description of pupa (Figure 21A–C). ***Measurements*** (in mm). Head width: 0.46–0.56. Body width: 1.16–1.50. Body length: 3.70–4.05.

Body elongated, white. Rostrum slender, about 3.4 times as long as wide, reaching almost up to mesocoxae. Antennae slender and elongated. Pronotum 1.1 times as wide as long. Mesonotum slightly shorter than metanotum. Urogomphi (ur) slender and elongated, conical, with sclerotised apex, distinctly reaching outline of the body, directed outside (Figure 21A–C).

Chaetotaxy well developed, setae short or medium long. Head with one *vs*, two *sos*, two *os* and two *pas*. Rostrum with one *rs* placed medially. All setae of head equal in length (Figure 21A, B). Pronotum with two *as*, one *ds*, two *sls*, two *ls*, and three *pls* (Figure 21B, C). All setae on pronotum elongated, equal in length (Figure 21C). Dorsal parts of meso- and metathorax with two setae placed medially. Abdominal segments I–VIII with two setae laterally and three medium long setae ventrally. Dorsal parts of abdominal segments I–VII with six setae (d_1 placed anteromedially, $d_{2–4}$ placed posteromedially, $d_{5–6}$ posterolaterally); segment VIII with five very long setae dorsally. Abdominal segment IX with two micro-setae ventrally.

Biological notes. The host plant of *M. janthinus* is the yellow toadflax, *Linaria vulgaris* Mill. This species is distributed in temperate regions of the eastern Palearctic region, inhabiting lowlands and hilly slopes up to 500 m altitude. From beginning of the 1990s, *M. janthinus* was introduced as biological control agent for the control of invasive toadflaxes in North America (Toševski et al. 2018). The adults emerge in early March and feed intensively on the newly growing shoots of the host plant. Oviposition occurs on actively growing shoots, and the preferred oviposition site is the widest part of the stem. Females lay one or, rarely, two eggs per shoot. This species is a true stem borer with larval feeding and mining in the central part of the stem. The adults overwinter in the stems of the host plant inside an elongated pupal chamber built by the last instar larva prior to pupation.

Remarks and comparative notes. *Mecinus janthinus* is largely distributed in northern, central and southeastern Europe, Russia from the western borders to southern central Siberia, the Caucasian states, and Turkey. This species was introduced in North America for the biological control of toadflaxes in 1991–1999 (Wilson et al. 2005). The adults can be easily confused with *M. janthiniformis*, both sympatric in part of their range of distribution, since the differences between them are few and subtle. In contrast, the larvae of these two species show numerous differences in the number of setae in many parts of the body, such as the head, antenna, pronotum and thoracic segments (see key).

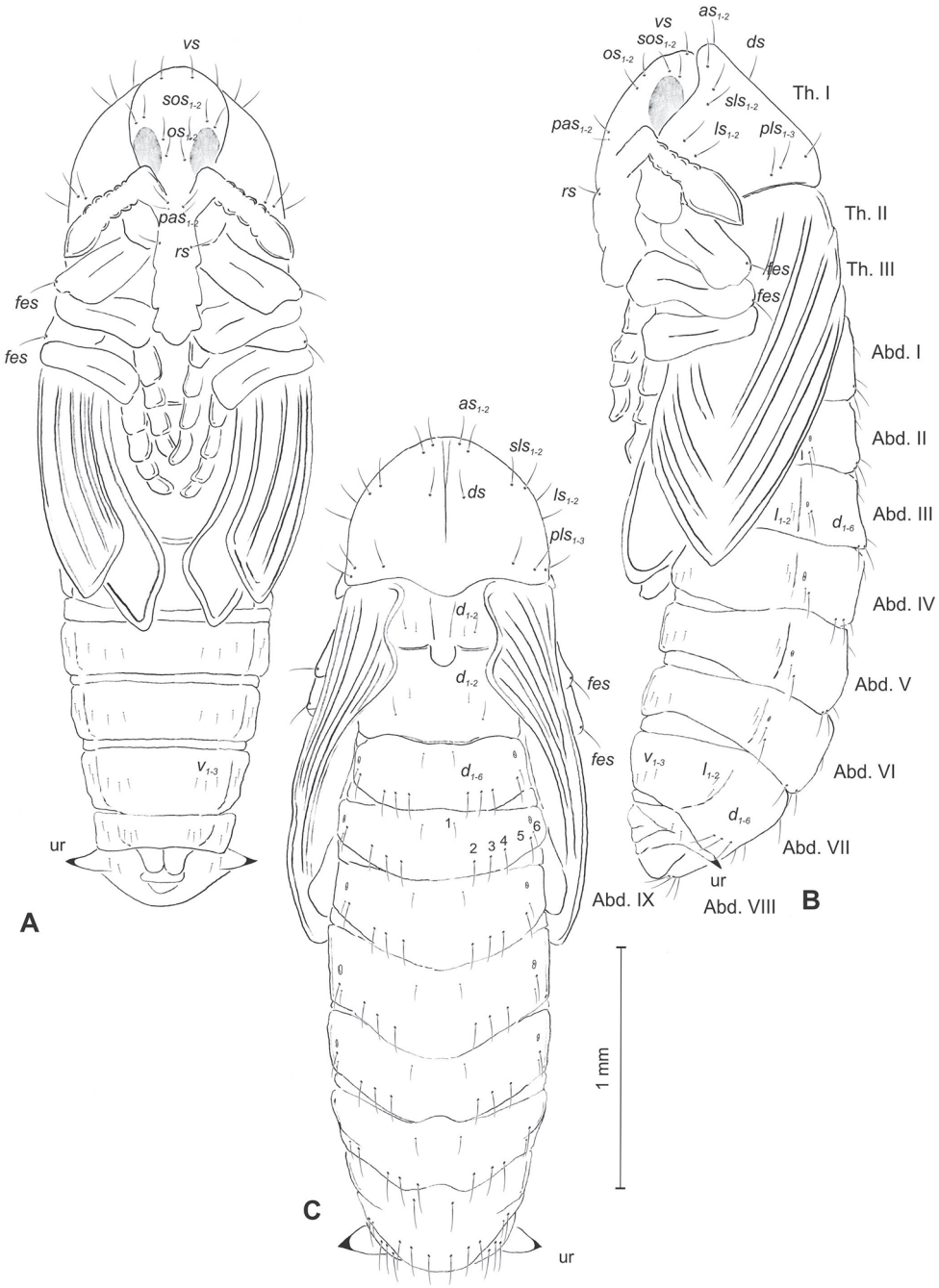

Figure 21. *Mecinus janthinus* pupa habitus and chaetotaxy **A** ventral view **B** lateral view **C** dorsal view. Abbreviations: Th. I–III – number of thoracic segments, Abd. I–IX – number of abdominal segments, ur – urogomphi, setae: *as* – apical, *d* – dorsal, *ds* – discal, *fes* – femoral, *l*, *ls* – lateral, *os* – orbital, *pas* – postantennal, *pls* – posterolateral, *rs* – rostral, *sls* – superlateral, *sos* – superorbital, *vs* – vertical.

Mecinus janthiniformis Toševski & Caldara, 2011

Material examined. 2 L3 larvae, Mecedonia, Prilep, 25.07.2017, (41°17.354'N, 21°29.983'E, 618 m.) ex *Linaria dalmatica macedonica* 1 L3 larva, 4 pupae, Bulgaria, Harmanli, 17.08.2008, 41°53.117'N, 25°52.373'E, 310 m., ex *Linaria genistifolia* 12 L3 larva, Bulgaria, Harmanli, 17.07.2011, 41°53.117'N, 25°52.373'E, 310 m., ex *L. genistifolia*; 2 L3 larvae, 1 pupa, Bulgaria, Slatino, 7.08.2011, 42°09.981'N, 23°02.371'E, 390 m., ex *L. genistifolia*; 1 pupa, Serbia, Kalna, 1.09.2010., 43°29.450'N, 22°19.712'E, 278 m., ex *L. genistifolia*; 3 pupae, Serbia, Bovansko Jezero, Aleksinac, 12.08.2010, 43°37.735'N, 21°42.917'E, 231 m., ex *L. genistifolia*; North Macedonia, Veles, 10.09.2009, 41°44.332'N, 21°46.893'E, 201 m., ex *L. genistifolia*; 1 pupa, Serbia, Vranje, Golemo Selo, 20.08.2009, 42°44.203'N, 21°50.696'E, 523 m., ex *L. genistifolia*; 3 pupae, Bulgaria, Slatino, 7.08.2007, 42°09.981'N, 23°02.371'E, 390 m., ex *L. genistifolia*. All collected by I. Toševski. Accession numbers of sequenced specimen MN992006.

Description of mature larva (Figures 22A–D, 23A–F). ***Measurements*** (in mm). Body length: 1.66–2.90. Body width (abdominal segments I–II): 0.66–1.10. Head width: 0.53–0.67.

Body (Figure 22A–D) yellowish. Prothorax smaller than meso- and metathorax. Abdominal segments I–VII of almost equal length; segments VIII and IX decreasing gradually to the terminal body part; segment X reduced to three anal lobes of those lateral are the largest, and dorsal the smallest (sometimes absent). Dorsum of abdominal segments I–VI divided into three lobes; on seventh into two lobes. Chaetotaxy well developed, setae various in length. Prothorax (Figure 22B) with eleven long *prns*; two medium *ps* and one medium *eus*. Meso- and metathorax (Figure 22B) with one short *prs*, three *pds* (pds_1 short, $pds_{2–3}$ medium), one medium *as*, three medium *ss*, one medium *eps*, one medium *ps* and one medium *eus*. Pedal area with six *pda* of different length (four of them placed on well isolated pedal sclerite). Abdominal segments I–VIII (Figure 22C, D) with one short *prs*, four *pds* (on segments I–V: $pds_{1,3}$ medium, $pds_{2,4}$ short; on segments VI–VIII all *pds* very long, equal in length), always arranged along the posterior margin, one minute and two long *ss*, one short and one medium e*ps*, one medium *ps*, one medium *lsts* and two medium *eus*. Abdominal segment IX (Figure 22D) with four long *ds* located close to posterior margin, two *ps* different in length, and two short *sts*. Each of anal lobe (abd. segment X) with two minute setae.

Head capsule (Figures 22A, 23A–F) dark yellow, narrowed bilaterally. $Des_{1–3,5}$ very long, equal in length, des_4 twice shorter than other *des*; des_4 medially. Fs_1 as long as des_1, fs_3 short, $fs_{4,5}$ long. Les_1 and les_2 equal in length, slightly shorter than des_1; two *ves* and three *pes* very short (Figure 23A). Two stemmata of different size. Antennae (Figure 23B) with sensorium (Se) conical, twice as long as wide, and four sensilla basiconica (sb). Clypeus (Figure 23C) trapezium-shaped, anterior margin concave; two medium *cls*, clss clearly visible. Labrum (Figure 23C) with sinuate anterior margin; lrs_1 long, lrs_2 and lrs_3 medium. Epipharynx (Figure 23D) with three relatively long, finger-shaped *als* of almost equal length; two finger-shaped *ams*, equal in length; two rod-like *mes* of medium length; surface smooth; labral rods short, kidney shaped. Mandibles (Figure 23E)

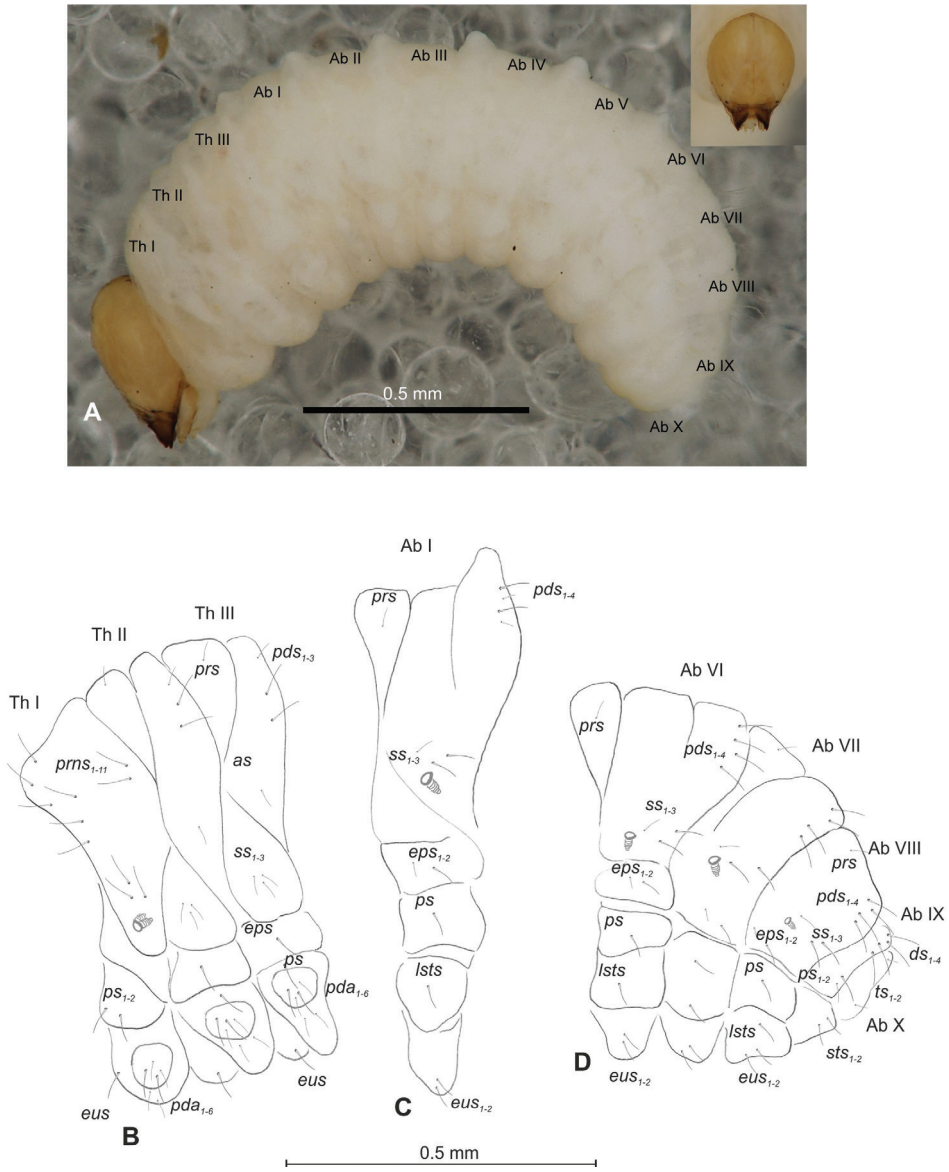

Figure 22. *Mecinus janthiniformis* mature larva, habitus and chaetotaxy **A** habitus of the body and frontal view of the head **B** lateral view of thoracic segments **C** lateral view of abdominal segment I **D** lateral view of abdominal segments VII–X. Abbreviations: Th. I–III– number of thoracic segments, Abd. I–X – number of abominal segments, setae: *as* – alar, *ds* – dorsal, *eps* – epipleural, *eus* – eusternal, *lsts* – laterosternal, *pda* – pedal, *pds* – postdorsal, *prns* – pronotal, *prs* – prodorsal, *ps* – pleural, *ss* – spiracular, *sts* – sternal, *ts* – terminal.

conical, wide, with a small protuberance in the middle of the cutting edge; both *mds* capilliform, relatively short, equal in length, placed mediolaterally. Maxilla (Figure 23F) with one *stps* and two *pfs* of equal length; *mbs* very short; mala with seven long finger-like

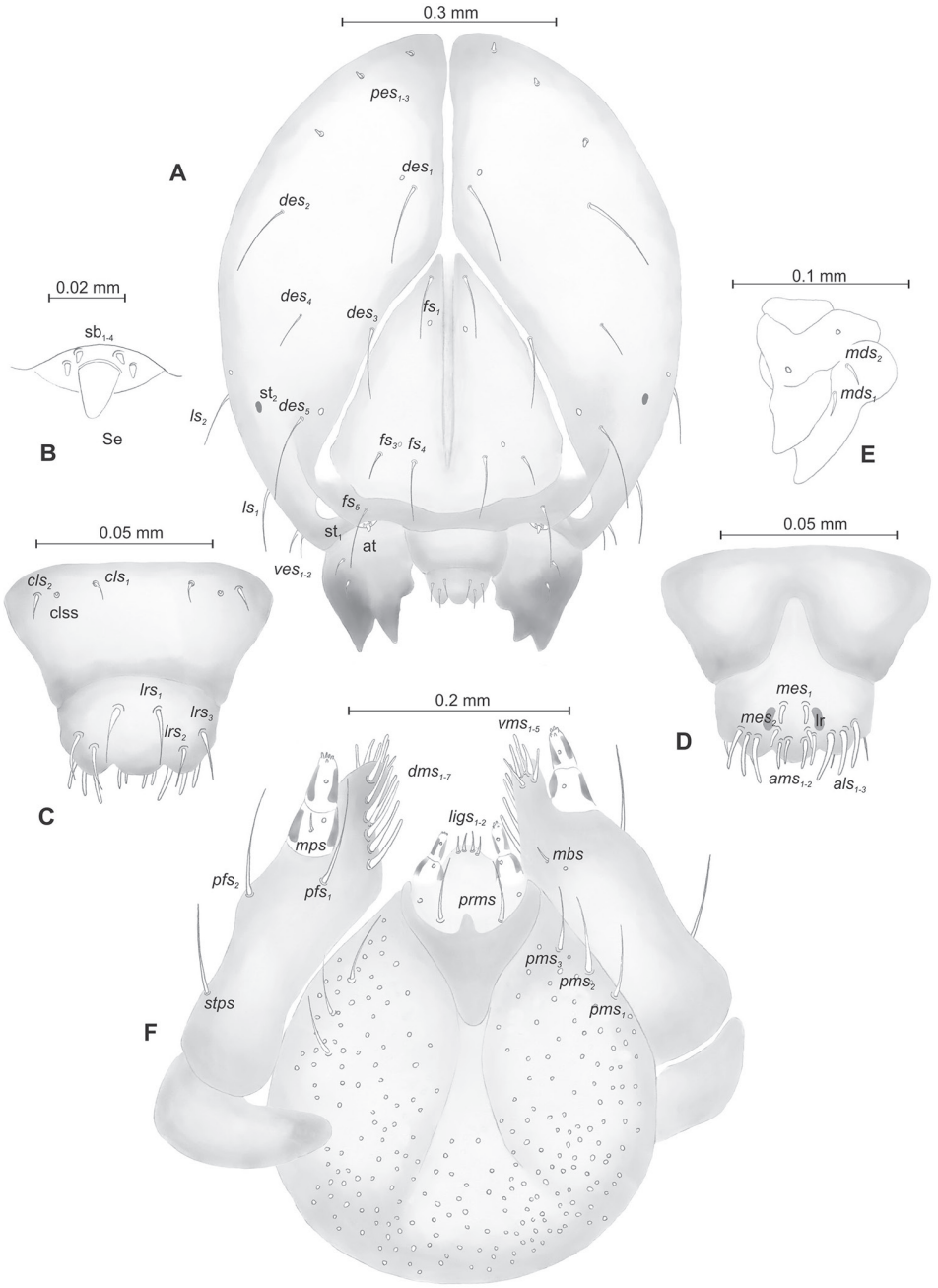

Figure 23. *Mecinus janthiniformis* mature larva, head and mouth parts **A** head, frontal view **B** antenna **C** clypeus and labrum, dorsal view **D** epipharynx **E** left mandible **F** maxillolabial complex, ventral aspect. Abbreviations: at – antenna, clss – clypeal sensorium, *des* – dorsal epicranial, lr – labral rods, sb – sensillum basiconicum, Se – sensorium, st – stemmata, setae: *als* – anterolateral, *ams* – anteromedial, *cls* – clypeal, *dms* – dorsal malar, *fs* – frontal, *ligs* – ligular, *lrs* – labral, *ls* – lateral epicranial, *mbs* – malar basiventral, *mds* – mandibular, *mes* – median, *mxps* – maxillary palp, *pes* – postepicranial, *ves* – ventral, *pfs* – palpiferal, *pms* – postlabial, *prms* – prelabial, *stps* – stipal, *vms* – ventral malar.

dms of almost equal size, five *vms* different in length. Maxillary palpi: basal palpomere wider than distal, both of almost equal length. Prelabium (Figure 23F) cup-shaped with one very long *prms*; ligula with two relatively long *ligs*; premental sclerite clearly visible, cup-like. Labial palpi two-segmented; basal palpomere distinctly wider than distal, both almost equal in length. Postlabium (Figure 23F) with three medium *pms*.

Description of pupa (Figure 24A–C). ***Measurements*** (in mm). Head width: 0.46–0.66. Body width: 1.20–1.66. Body length: 3.22–4.16.

Body elongated, white. Rostrum slender, about four times as long as wide, reaching almost up to mesocoxae. Antennae slender and elongated. Pronotum 1.3 times as wide as long. Urogomphi (ur) slender and elongated, conical, with sclerotised apex, distinctly reaching outline of the body, directed outside (Figure 24A, C).

Chaetotaxy well developed, setae medium long or elongated, unequal length. Head with one long *vs*, two *sos* different in length, two *os* different in length and two *pas* different in length. Rostrum with one *rs* (Figure 24A). Pronotum with two *as*, one *ds*, two *sls*, two *ls*, and three *pls* (Figure 24B, C). All setae on prothorax elongated, equal in length (Figure 24C). Setae on head and rostrum shorter than those on prothorax. Dorsal parts of meso- and metathorax with three setae placed medially. Abdominal segments I–VIII with two setae placed laterally and three medium long setae ventrally. Dorsal parts of abdominal segments I–VII with six setae (d_{1-4} placed posteromedially, d_{5-6} posterolaterally); segment VIII with five very long setae dorsally. Abdominal segment IX with two micro-setae ventrally.

Biological notes. The host plants of *M. janthiniformis* are *Linaria genistifolia* (L.) Mill. and *L. dalmatica* (L.) Mill., as well as all variable forms and hypothetical hybrids between these two plant species. *Mecinus janthiniformis* inhabits stands from lowlands to mountain pastures and meadows up to 1500 m. At the beginning of the 1990s, this species was introduced as a biological control agent for the control of invasive toadflaxes in North America (Toševski et al. 2018). Adults emerge in early spring and feed on the apical part of newly growing shoots. The females lay eggs over the next three months on the upper part of the main stem, including the lateral branches of the plant. Oviposition and larval development induce a slightly elongate gall in which the larvae pupate. The adults of this species overwinter inside the main stem of the host plant or inside induced galls on lateral branches (Toševski et al. 2011).

Remarks and comparative notes. The distribution of *M. janthiniformis* follows that of the two host plants, *L. genistifolia* (L.) Mill. and *L. dalmatica* (eastern part of central and southeastern Europe to southern central Siberia, the northern Caucasian states and Turkey). Its separation from *M. janthinus* at the species level was clearly shown based on very careful biological and genetic studies (Toševski et al. 2011), but unfortunately, easy identification is only possible by collecting the specimens together with their host plants. Usually, in *M. janthiniformis*, the body is larger (length 3.2–6.0 mm), the apical part of the rostrum in females in lateral view is more curved, the punctures of the pronotum are slightly smaller and more densely adpressed, and the scales of the elytral interstriae are denser, arranged in two rows on part of several interstriae. The larvae of these two species show numerous differences in the number of setae in many parts of the body, whereas the differences are few in the pupae (see keys).

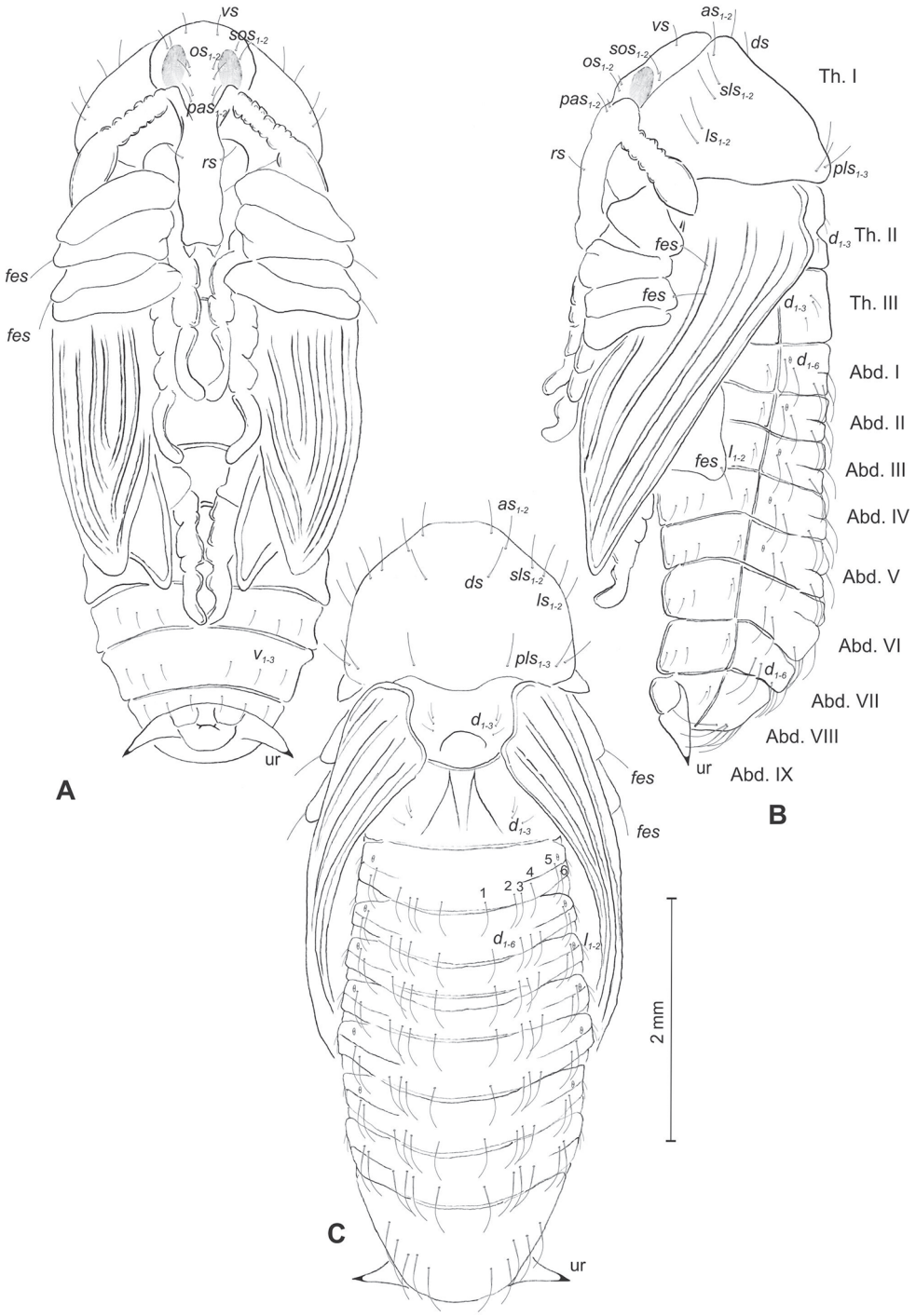

Figure 24. *Mecinus janthiniformis* pupa habitus and chaetotaxy **A** ventral view **B** lateral view **C** dorsal view. Abbreviations: Th. I–III – number of thoracic segments, Abd. I–IX – number of abdominal segments, ur – urogomphi, setae: *as* – apical, *d* – dorsal, *ds* – discal, *fes* – femoral, *l*, *ls* – lateral, *os* – orbital, *pas* – postantennal, *pls* – posterolateral, *rs* – rostral, *sls* – superlateral, *sos* – superorbital, *vs* – vertical.

Mecinus sicardi Hustache, 1920

Material examined. 6 L3 larvae and 1 pupa, France, Provence-Alpes-Côte d'Azur, Alpes Maritimes, road Èze-La Turbie, 20.07.2014, on *Antirrhinum latifolium* Mill. stems, lgt. and det. R. Caldara. Accession numbers of sequenced specimen MN992007.

Description of mature larva (Figures 25A–D, 26A–F). ***Measurements*** (in mm). Body length: 2.71–3.75. Body width (abdominal segments I–II): 1.10–1.25. Head width: 0.60–0.65.

Body (Figure 25A–D) yellowish, slender. All thoracic segments almost equal in length. Abdominal segments I–V of almost equal length; segments VI–IX decreasing gradually to the terminal body part; segment X reduced to three anal lobes of those lateral are the largest, and dorsal the smallest (sometimes absent). Chaetotaxy weakly developed, setae capilliform, variable in length, yellow. Prothorax (Figure 25B) with ten *prns* of unequal length (seven medium length, three short); two medium *ps* and one medium *eus*. Meso- and metathorax (Figure 25B) with one very short *prs*, three *pds*, different in length ($pds_{1,3}$ very short, pds_2 medium); one short *as*, three short *ss*, one medium long *eps*, one medium long *ps* and one medium *eus*. Pedal area with five *pda*, different in length. Abdominal segments I–VIII (Figure 25C, D) with one short *prs*, four *pds* of different length ($pds_{1,2,4}$ short, pds_3 medium; all *pds* on segments VI–VIII very long, equal in length) arranged along the posterior margin, one short and one medium *ss*, two medium *eps*, one medium *ps*, one medium *lsts* and two relatively long *eus*. Abdominal segment IX (Figure 25D) with three very long *ds*, all located close to the posterior margin, one medium *ps* and two medium *sts*. Each of lateral anal lobe with two minute setae.

Head capsule (Figures 25A, 26A–F) yellow, distinctly narrowed bilaterally. $Des_{1–3,5}$ equal in length, des_4 twice shorter than other *des*. $Fs_{1,4,5}$ long, equal in length, fs_3 medium. Les_1 and les_2 medium, equal in length; two *ves* short; four *pes* spine-like (Figure 26A). Two stemmata of different size. Antennae (Figure 26B) with sensorium (Se) conical, twice as long as wide, located medially, and three sensilla of different types: one sa and two sb. Clypeus (Figure 26C) trapezium-shaped, anterior margin slightly concave; two medium *cls*, located posteromedially; clss clearly visible. Labrum (Figure 26C) close to semi-circular, anterior margin sinuate; lrs_{1-3} almost equal in length. Epipharynx (Figure 26D) with three rod-shaped *als* of almost equal length; two medium, finger-like *ams*; one medium, finger-like *mes*; surface smooth; labral rods short and relatively wide. Mandibles (Figure 26E) conical, wide, with small protuberance in the middle of the cutting edge; both *mds* capilliform, medium, equal in length, placed transversely. Maxilla (Figure 26F) with one *stps* and two *pfs* of equal length; *mbs* short; mala with six rod-like *dms* of almost equal size, five *vms* different in size. Maxillary palpi: basal palpomere slightly wider than distal, both of almost equal length. Prelabium (Figure 26F) cup-like with one long *prms*; ligula with three minute *ligs*; premental sclerite clearly visible, cup-shaped, posterior extension with acute apex. Labial palpi two-segmented; basal palpomere distinctly wider than distal, both of almost equal length. Postlabium (Figure 26F) with three *pms*; pms_1 and pms_3 short, pms_2 three times as long as pms_1.

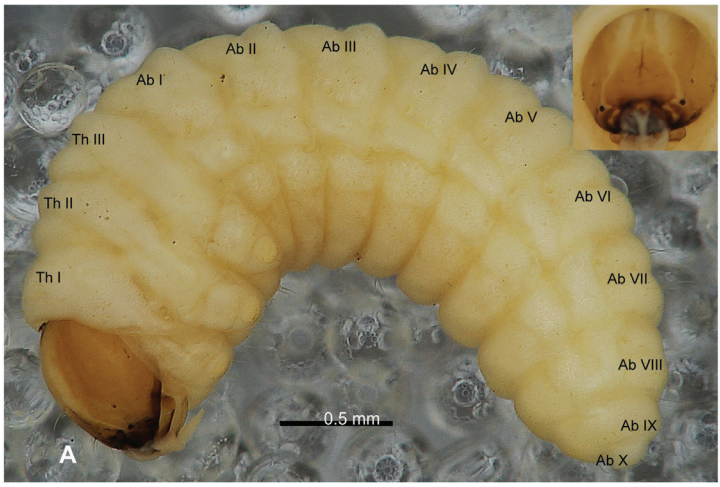

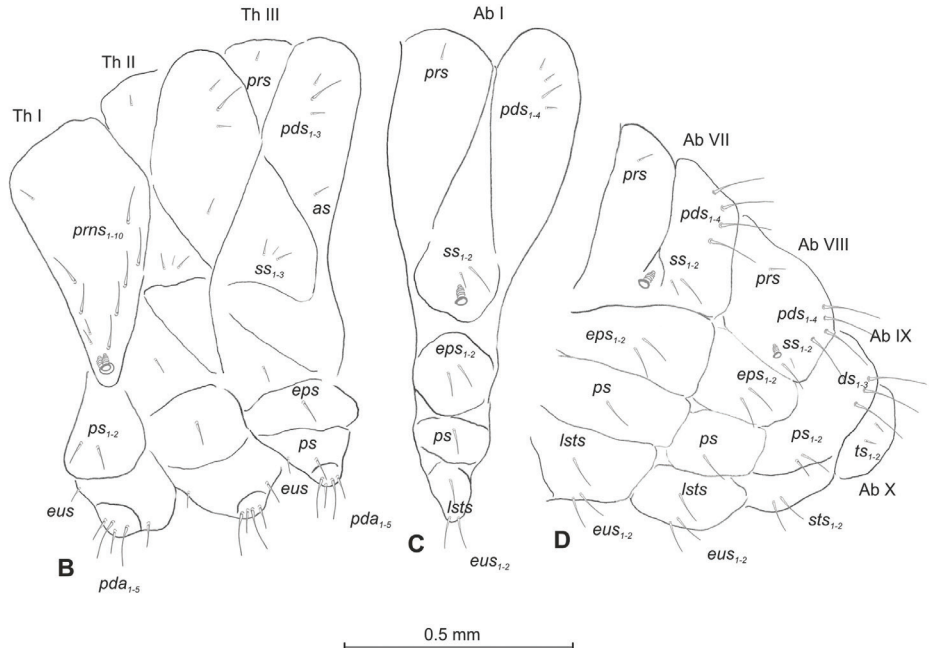

Figure 25. *Mecinus sicardi* mature larva, habitus and chaetotaxy **A** habitus of the body and frontal view of the head **B** lateral view of thoracic segments **C** lateral view of abdominal segment I **D** lateral view of abdominal segments VII–X. Abbreviations: Th. I–III – number of thoracic segments, Abd. I–X – number of abominal segments, setae: *as* – alar, *ds* – dorsal, *eps* – epipleural, *eus* – eusternal, *lsts* – laterosternal, *pda* – pedal, *pds* – postdorsal, *prns* – pronotal, *prs* – prodorsal, *ps* – pleural, *ss* – spiracular, *sts* – sternal, *ts* – terminal.

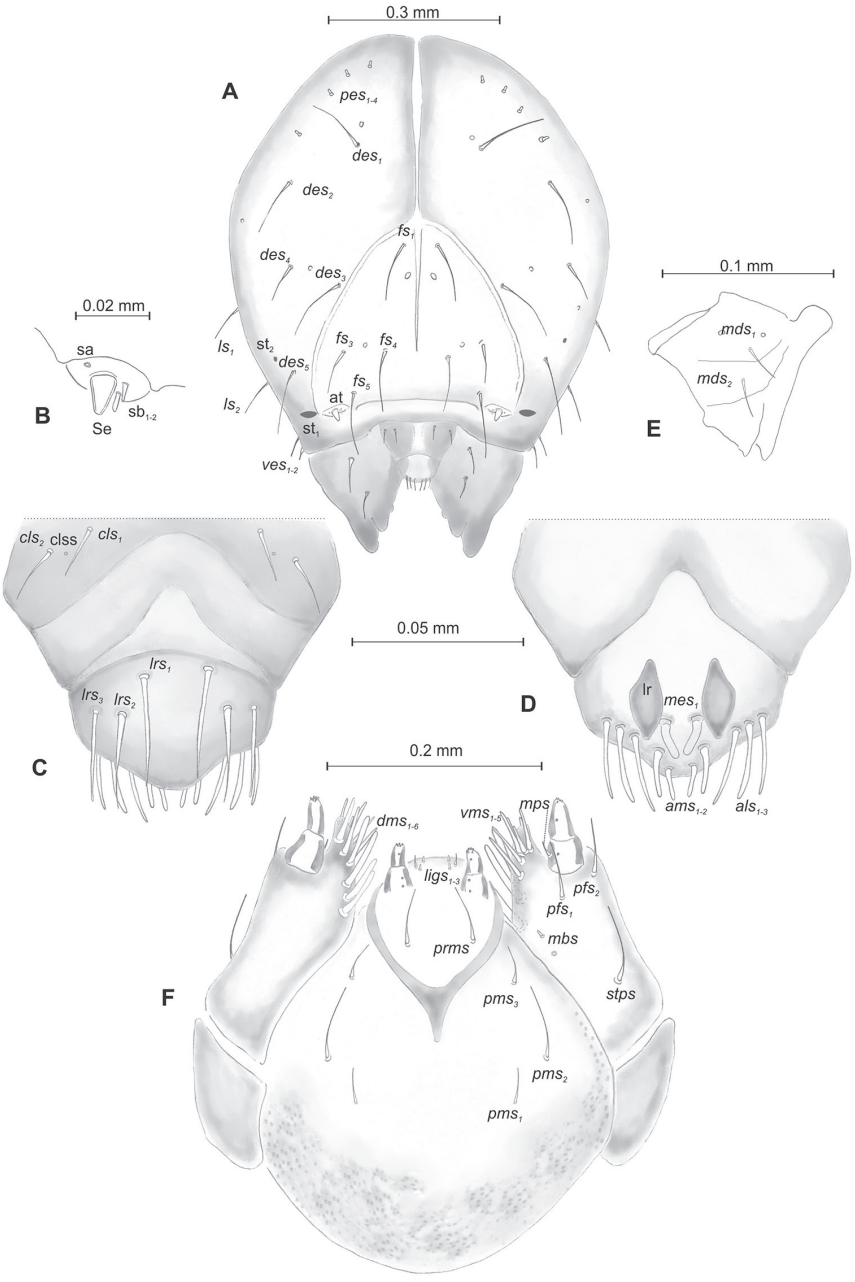

Figure 26. *Mecinus sicardi* mature larva, head and mouth parts **A** head, frontal view **B** antenna **C** clypeus and labrum, dorsal view **D** epipharynx **E** left mandible **F** maxillolabial complex, ventral aspect. Abbreviations: at – antenna, clss – clypeal sensorium, *des* – dorsal epicranial, lr – labral rods, sa – sensillum ampullaceum, sb – sensillum basiconicum, Se – sensorium, st – stemmata, setae: *als* – anterolateral, *ams* – anteromedial, *cls* – clypeal, *dms* – dorsal malar, *fs* – frontal, *ligs* – ligular, *lrs* – labral, *ls* – lateral epicranial, *mbs* – malar basiventral, *mds* – mandibular, *mes* – median, *mxps* – maxillary palp, *pes* – postepicranial, *ves* – ventral, *pfs* – palpiferal, *pms* – postlabial, *prms* – prelabial, *stps* – stipal, *vms* – ventral malar.

Description of pupa (Figure 27A–C). ***Measurements*** (in mm). Head width: 0.60–0.70. Body width: 1.75–2.00. Body length: 3.75–4.50.

Body elongated, white. Rostrum moderately slender, about 3.5 times as long as wide, reaching up to mesocoxae. Antennae elongated. Pronotum 1.8 times as wide as long. Urogomphi (ur) slender, conical, with sclerotised apex, both directed outside, distinctly reaching outline of the body (Figure 27A–C).

Chaetotaxy setae medium or elongated. Head with one *vs*, two *sos* and two *os*. Rostrum with one *pas*. Setae on head and rostrum straight, as long as those on prothorax (Figure 27A). Pronotum with two *as*, two *sls*, two *ls*, one *ds* and four *pls*. Dorsal parts of meso- and metathorax with three setae equal in length setae placed medially. Abdominal segments I–VIII with three very short setae ventrally and two setae laterally. Dorsal parts of abdominal segments I–VII with six setae growing gradually from segment I to VII (d_1 placed anteromedially, $d_{2–5}$ placed posteromedially, d_6 posterolaterally); segment VIII with five elongated setae dorsally. Abdominal segment IX with two micro-setae ventrally.

Biological notes. The host plant of this species, at least in Côte d'Azur, is *Antirrhinum latifolium* Mill. As reported by Caldara and Fogato (2013), larvae feed on the larger stems of the plant and dig tunnels, causing at most very small lateral deformations. They pupate in summer, and adults stay inside the plant until the spring of the following year. Before pupation, however, the mature larvae leave the main tunnel, which runs longitudinally, and produce a small oblique tunnel that ends just in proximity of the external cuticle of the stem. Therefore, when leaving their cells, adults have only to bore a thin layer, although in the meantime, the plant has become dry and hard.

Remarks and comparative notes. The adults of this rare species, with a narrow range of distribution – in fact, it is known in a few localities of southeastern Spain, eastern and southern France, and north-western Italy – differ from the other species studied here by the black elytra instead of blue. Due to this character, this species may be superficially confused with *M. pyraster*, from which it is easily distinguishable by the elytral vestiture composed of scales that are uniformly arranged and are all recumbent. The rostrum (in dorsal view) is distinctly wider, and the pronotum has sides slightly more rounded and is usually widest towards the middle. Finally, ventrite 5 of the male lacks a tuft of hairs, and the shape of the penis is different.

The larvae of this species differ from the others of the group by the abdominal segments I–VIII with two *ss* (instead of three) and asperities covering only the posterior part of postlabium, whereas pupae differ in having the rostrum with only one *pas* (instead of two) and without *rs* and the pronotum with four *pls* (instead of three).

Mecinus heydenii group

Differential diagnosis. Larva. (1) cuticle of the body tuberculate; (2) pedal lobes weakly isolated; (3) abdominal segment X reduced to three anal lobes of those lateral are the largest, and dorsal the smallest (sometimes absent); (4) thoracic spiracle unicameral; (5) abdominal setae very short to medium, become progressively longer from

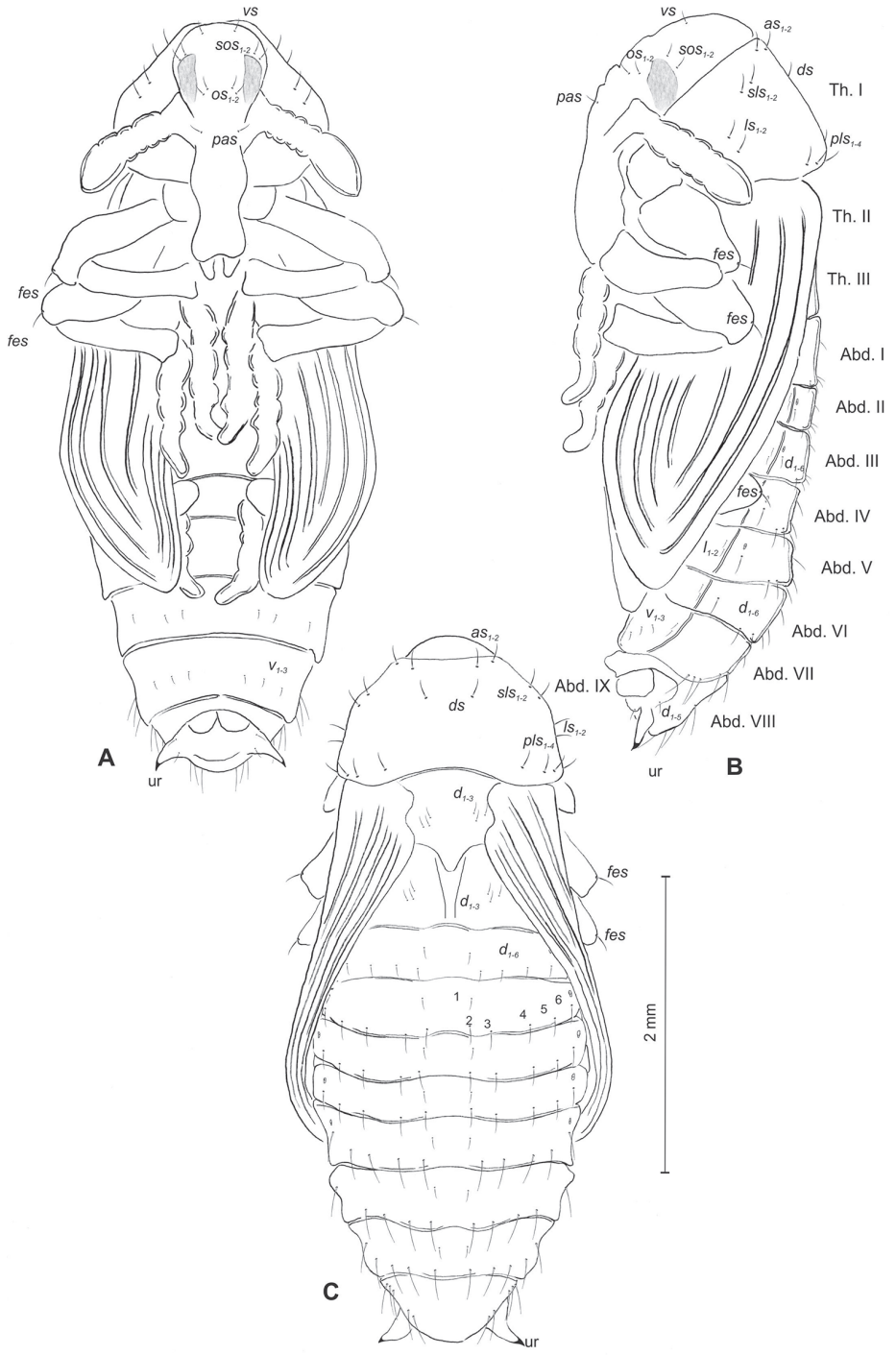

Figure 27. *Mecinus sicardi* pupa habitus and chaetotaxy **A** ventral view **B** lateral view **C** dorsal view. Abbreviations: Th. I–III – number of thoracic segments, Abd. I–IX – number of abdominal segments, ur – urogomphi, setae: *as* – apical, *d* – dorsal, *ds* – discal, *fes* – femoral, *l*, *ls* – lateral, *os* – orbital, *pas* – postantennal, *pls* – posterolateral, *rs* – rostral, *sls* – superlateral, *sos* – superorbital, *vs* – vertical.

abdominal segment I to VIII; (6) abdominal segments I–VIII with three *pds* and two *ss*; (7) head brown, flattened laterally; (8) frontal suture poorly or well visible; (9) endocarina 4/5 of the frons; (10) des_4 three times shorter than des_1; (11) fs_1 usually absent; (12) absence of fs_2 except one species; (13) fs_3 very short; (14) head with two stemmata; (15) absence of cls_1; (16) labial palpi one-segmented; (17) premental sclerite U-shaped; (18) surface of postlabium smooth.

Pupa. (1) body very slender and elongated; (2) urogomphi short, only slightly reaching outline of the body, directed downward; (3) rostrum slender and elongated; (4) setae minute; (5) head with one *os*; (6) rostrum with without or with one *pas* and one *rs*; (7) pronotum with without or with up to two *as*, one *ds*, without or with one *sls*, without or with one *ls*, three *pls*; (8) meso- and metanotum with three setae; (9) abdominal segments I–VII with three or five setae dorsally.

Remarks and comparative notes. The adults of this group are characterised by the rostrum in the basal half strongly and abruptly curved, the elytra distinctly elongate, and the dorsal integument black or blue, usually with metallic reflections apart from several characters of the male and female genitalia. In immatures, the autapomorphies seem limited to a U-shaped premental sclerite in larvae.

This group seems more closely related to the *M. janthinus* group than to other groups of *Mecinus* in both morphological characters (shape of body and colour of dorsal integument) and biology (hosts in Plantaginaceae other than *Plantago*). However, the species of the *M. heydenii* group clearly differ from those of the *M. janthinus* group by the rostrum being strongly curved in the basal half and by the shape of the penis and spermatheca. The study of immatures also did not show close relationships between these two unique groups living on Antirrhineae, since the species of the *M. heydenii* group have one palpomere on the labial palpi instead of two, and all spiracles are unicameral. The pupae also differ somewhat in the shape of the urogomphi, which are shorter, only slightly reaching the outline of the body, and directed downward. The setae of the head and pronotum are also shorter, and the dorsal setae of abdominal segments I–VII are less numerous.

Mecinus heydenii Wencker, 1866

Material examined. 4 L3 larvae and 6 pupae, Serbia, Negotin, 1.07.2017, 44°16.610'N, 22°30.480'E, 71 m., ex *L. vulgaris*, lgt. I. Toševski. Accession numbers of sequenced specimen MN992002.

Description of mature larva (Figures 28A–D, 29A–F). ***Measurements*** (in mm). Body length: 2.16–2.66. Body width (metathorax or abdominal segments I–II): 0.83–1.00. Head width: 0.30–0.33.

Body (Figure 28A–D) white-yellowish, very slender. Chaetotaxy weakly developed, setae (except pronotum and dorsal part of abdominal segment IX) extremely short, difficult to observe. Prothorax (Figure 28B) with four medium and four very short *prns*, two very short *ps* and one very short *eus*. Meso- and metathorax (Figure

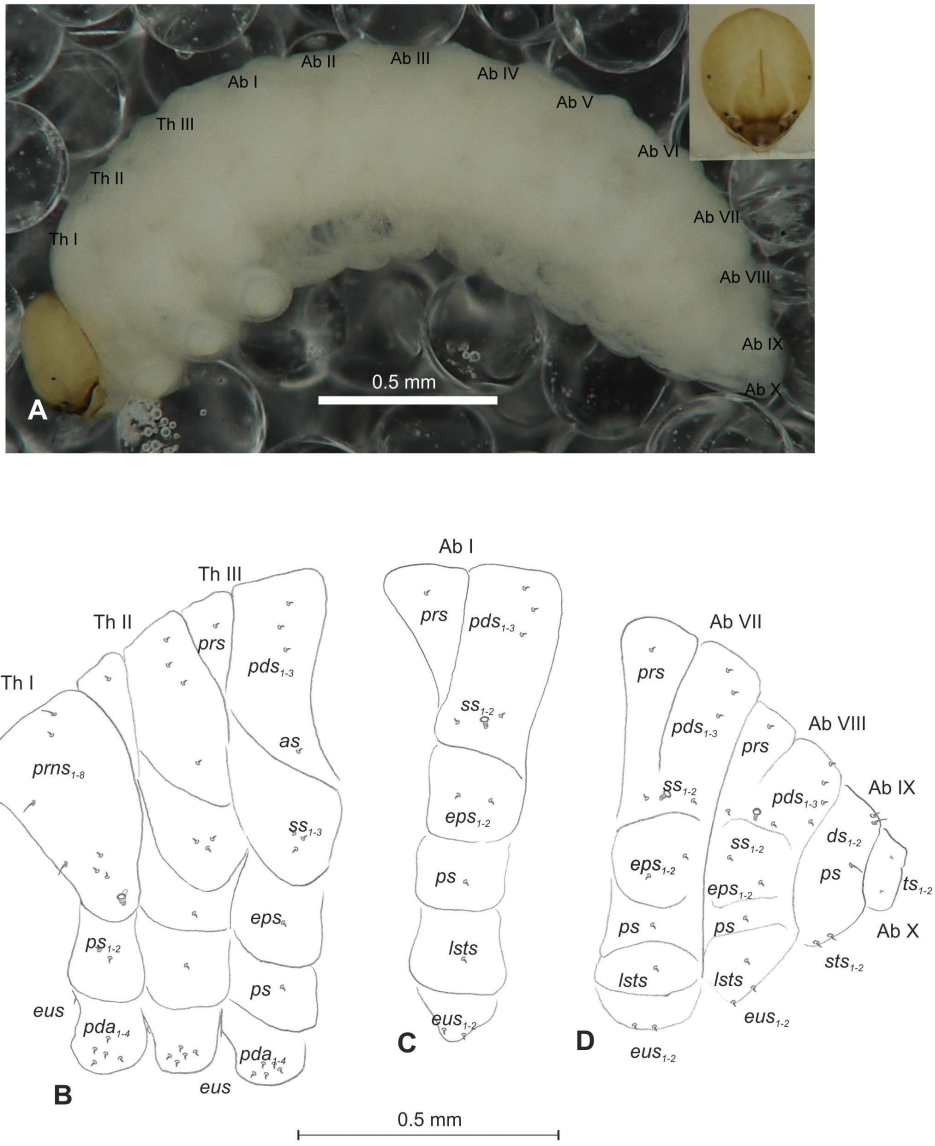

Figure 28. *Mecinus heydenii* mature larva, habitus and chaetotaxy **A** habitus of the body and frontal view of the head **B** lateral view of thoracic segments **C** lateral view of abdominal segment I **D** lateral view of abdominal segments VII–X. Abbreviations: Th. I–III – number of thoracic segments, Abd. I–X – number of abominal segments, setae: *as* – alar, *ds* – dorsal, *eps* – epipleural, *eus* – eusternal, *lsts* – laterosternal, *pda* – pedal, *pds* – postdorsal, *prns* – pronotal, *prs* – prodorsal, *ps* – pleural, *ss* – spiracular, *sts* – sternal, *ts* – terminal.

28B) with one short *prs*, three short *pds*, one very short *as*, three minute *ss*, one very short *eps*, one very short *ps* and one very short *eus*. Pedal area with four very short *pda*. Abdominal segments I–VIII (Figure 28C, D) with one very short *prs*, three very

short *pds* arranged along the posterior margin, two minute *ss*, two very short *eps*, one very short *ps*, one very short *lsts* and two very short *eus*. Abdominal segment IX (Figure 28D) with two *ds* (one medium and one very short), all located close to the posterior margin, one medium *ps* and two very short *sts*. Each lateral anal lobe with two minute setae.

Head capsule (Figures 28A, 29A–F) pale yellow, distinctly narrowed bilaterally. Frontal suture poorly visible. $Des_{1–3,5}$ very long, equal in length; des_4 four times shorter than other des_1. Fs_1 and fs_2 absent, fs_3 very short, fs_4 and fs_5 long. Les_1 shorter than les_2; two *ves* and four *pes* short (Figure 29A). Antennae (Figure 29B) with sensorium (Se) conical, thrice as long as wide, and three sensilla of different types: one sa and two sb. Clypeus (Figure 29C) trapezium-shaped, anterior margin slightly concave; cls_2 relatively long; clss clearly visible. Labrum (Figure 29C) with sinuate anterior margin; lrs_1 long, lrs_2 slightly shorter than lrs_1, lrs_3 two times shorter than lrs_1. Epipharynx (Figure 29D) with three medium, finger-shaped *als* of almost equal length; two rod-like, different in length *ams*; two finger-like *mes* of medium length; surface smooth; labral rods close to kidney-shaped. Mandibles (Figure 29E) conical, wide, with a small protuberance in the middle of the cutting edge; both *mds* capilliform, medium, equal in length, placed mediolaterally. Maxilla (Figure 29F) with one *stps* and two *pfs* long, of equal length; *mbs* very short; mala with six finger-like *dms* different in length ($dms_{1,2}$ medium, $dms_{3–6}$ long to very long), five *vms* different in length. Maxillary palpi: basal palpomere distinctly wider than distal, both of almost equal length. Prelabium (Figure 29F) almost rounded with one very long *prms*; ligula with two *ligs* different in length; premental sclerite clearly visible, U-shaped. Postlabium (Figure 29F) with short pms_1, long pms_2, and short pms_3.

Description of pupa (Figure 30A–C). ***Measurements*** (in mm). Head width: 0.30–0.60. Body width: 0.73–1.13. Body length: 2.33–2.93.

Body elongated, white. Rostrum slender, about five times as long as wide, but reaching up only to procoxae. Antennae slender and elongated. Pronotum 1.4 times as wide as long. Urogomphi (ur) very short, conical, with sclerotised apex, reaching outline of the body, directed downward (Figure 30A–C).

Chaetotaxy sparse, setae short, unequal length. Head with one *os*. Rostrum with one *rs* placed medially. Setae on head and rostrum straight, as long as those on prothorax (Figure 30A). Pronotum with two *as*, one *ds* and three *pls*. Dorsal parts of meso- and metathorax with three setae placed medially. Abdominal segments I–VIII with one seta laterally and three very short setae ventrally. Dorsal parts of abdominal segments I–VII with five setae (d_1 placed anteromedially, $d_{2–4}$ posteromedially, d_5 posterolaterally); segment VIII with four setae dorsally. Abdominal segment IX with two micro-setae ventrally.

Biological notes. This monophagous species is associated with yellow toadflax, *Linaria vulgaris* Mill. The adults are active from early spring, following the appearance of the first growing shoots of its host plant. The adults exhibit extreme cryptic behavior, which makes them difficult to collect. Oviposition occurs on actively growing young shoots, usually in the top or middle part of the stem. Females often lay several eggs distributed along the host plant shoot. Oviposition provokes primi-

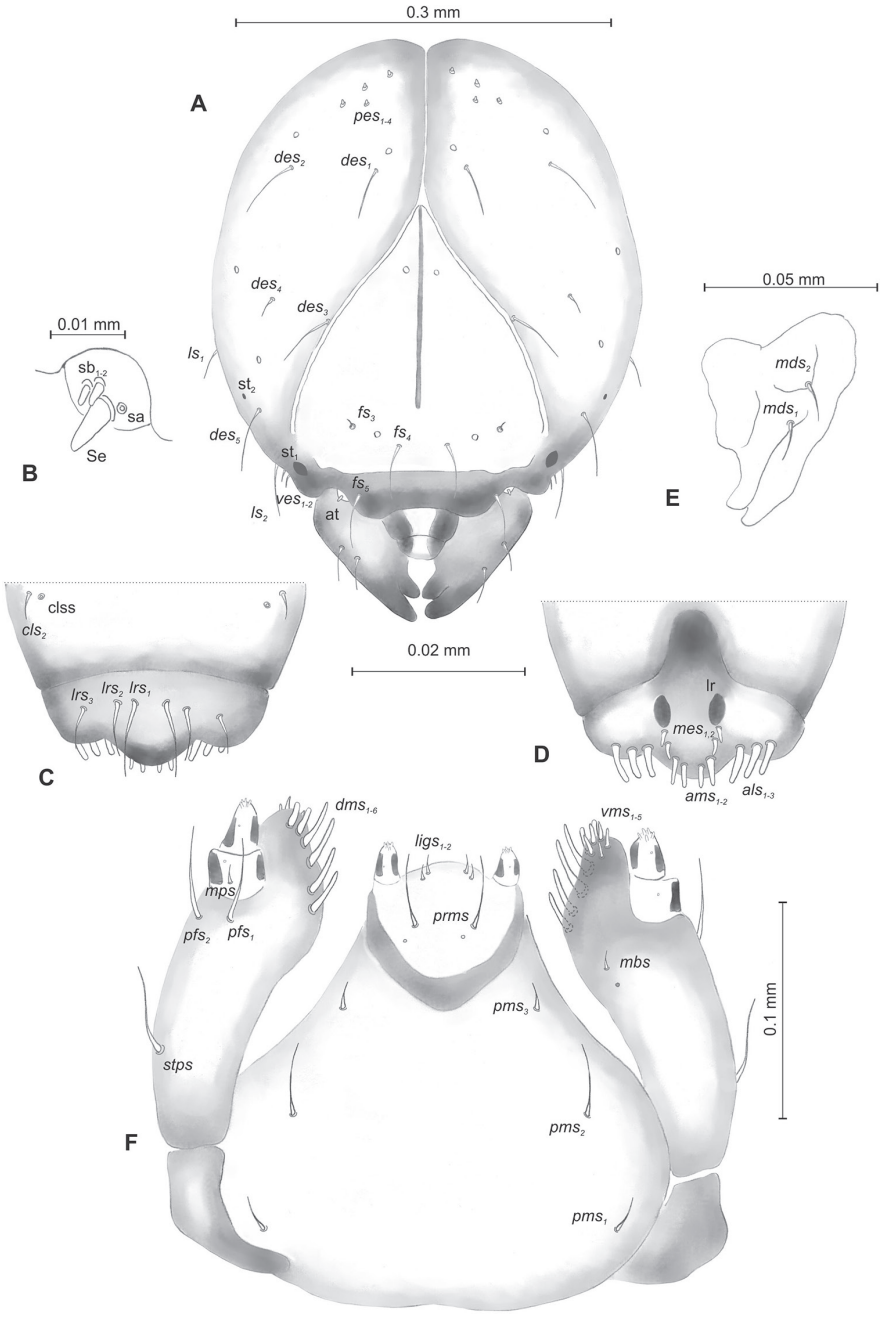

Figure 29. *Mecinus heydenii* mature larva, head and mouth parts **A** head, frontal view **B** antenna **C** clypeus and labrum, dorsal view **D** epipharynx **E** left mandible **F** maxillolabial complex, ventral aspect. Abbreviations: at – antenna, clss – clypeal sensorium, *des* – dorsal epicranial, lr – labral rods, sa – sensillum ampullaceum, sb – sensillum basiconicum, Se – sensorium, st – stemmata, setae: *als* – anterolateral, *ams* – anteromedial, *cls* – clypeal, *dms* – dorsal malar, *fs* – frontal, *ligs* – ligular, *lrs* – labral, *ls* – lateral epicranial, *mbs* – malar basiventral, *mds* – mandibular, *mes* – median, *mxps* – maxillary palp, *pes* – postepicranial, *ves* – ventral, *pfs* – palpiferal, *pms* – postlabial, *prms* – prelabial, *stps* – stipal, *vms* – ventral malar.

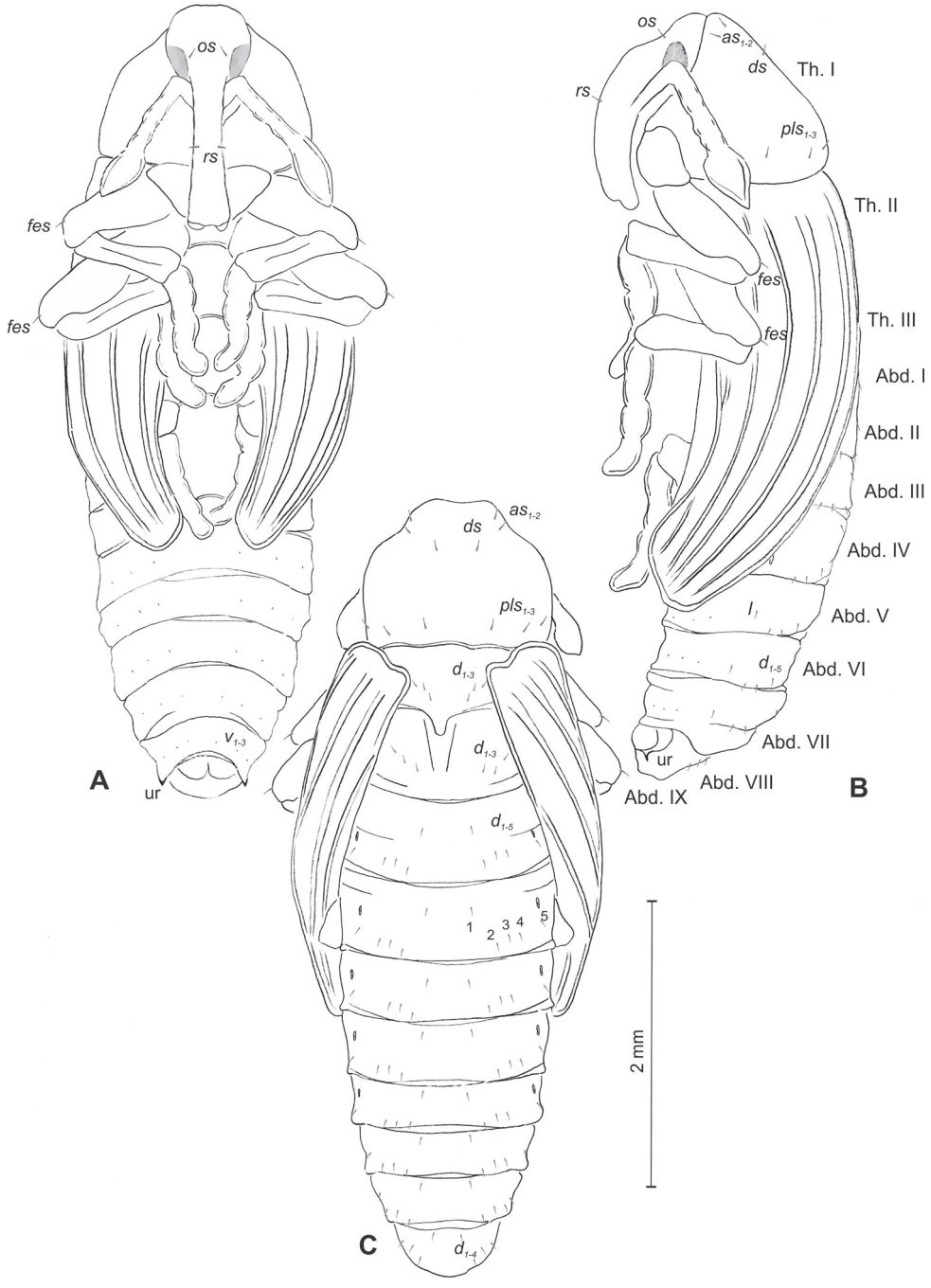

Figure 30. *Mecinus heydenii* pupa habitus and chaetotaxy **A** ventral view **B** lateral view **C** dorsal view. Abbreviations: Th. I–III – number of thoracic segments, Abd. I–IX – number of abdominal segments, ur – urogomphi, setae: *as* – apical, *d* – dorsal, *ds* – discal, *fes* – femoral, *l*, *ls* – lateral, *os* – orbital, *pls* – posterolateral, *rs* – rostral.

tive shoot swelling and hypertrophy that leads to the formation of a pseudo-gall of the young shoot. Larval development occurs inside this pseudo-gall, and pupation takes place in larval chambers prepared very close to the stem surface. Emerged adults stay inside the stem until August, when all adults leave their host plant within a two-week period. Overwintering takes place in the soil litter near the host plant.

Remarks and comparative notes. This species is widely distributed in Europe and is the only one of its group present in northern Europe, from Germany to Sweden. The adult is distinguishable by the rostrum very strongly curved from base to apex, especially before antennal insertion, in both sexes. However, it is somewhat difficult to morphologically separate this taxon from the two cryptic species *M. peterharrisi* and *M. laeviceps*. They are well distinguishable, however, by molecular and biological data (Toševski et al. 2014).

The study of the immatures allowed us to add numerous other interesting differences: larvae of *M. heydenii* differ from those of *M. laeviceps* by the pronotum with eight *prns* (instead of nine), the thoracic segments with three *pds* (instead of two), each pedal lobe with four *pda* (instead of three), *pds* of abdominal segments I–VIII distinctly smaller, and the head with four *pes* (instead of one). Both species differ from *M. peterharrisi* by fs_1 and fs_2 absent and the antennae with two *sb* (instead of four).

The pupae of the three species are also slightly different in the presence or lack of some setae on the rostrum and pronotum (without *pas* and *ls* in *M. heydenii* and *M. peterharrisi*, respectively) and femora (with *fes* in *M. heydenii* and *M. laeviceps*), and their number in the abdominal segments.

Mecinus laeviceps Tournier, 1873

Material examined. 8 L3 larvae and 10 pupae, Serbia, Slankamen, 22.06.2017 45°08.343'N, 20°15.042'E, 177 m., ex *Linaria genistifolia*, lgt. I. Toševski. Accession numbers of sequenced specimen MN992003.

Description of mature larva (Figures 31A–D, 32A–F). ***Measurements*** (in mm). Body length: 1.67–2.67. Body width (abdominal segments I–II): 0.37–0.83. Head width: 0.30–0.40.

Body (Figure 31A–D) yellowish, slender. Chaetotaxy rather weakly developed, setae capilliform, variable in length, light yellow. Prothorax (Figure 31B) with nine *prns* of unequal length (eight relatively long, one medium); two long *ps* and one medium *eus*. Meso- and metathorax (Figure 31B) with one short *prs*, two *pds*, different in length (medium, long), one short *as*, three short *ss*, one medium *eps*, one medium *ps* and one medium *eus*. Pedal area with three *pda*, different in length. Abdominal segments I–VIII (Figure 31C, D) with one short *prs*, three *pds* of different length ($pds_{1,3}$ short, pds_2 medium; all *pds* on segment VIII very long, equal in length), arranged along the posterior margin, two short *ss*, two short *eps*, one medium *ps*, one short *lsts* and two short *eus*. Abdominal segment IX (Figure 31D) with two long *ds*, located close to posterior margin, one long *ps* and two short *sts*. Each lateral anal lobe with one minute seta.

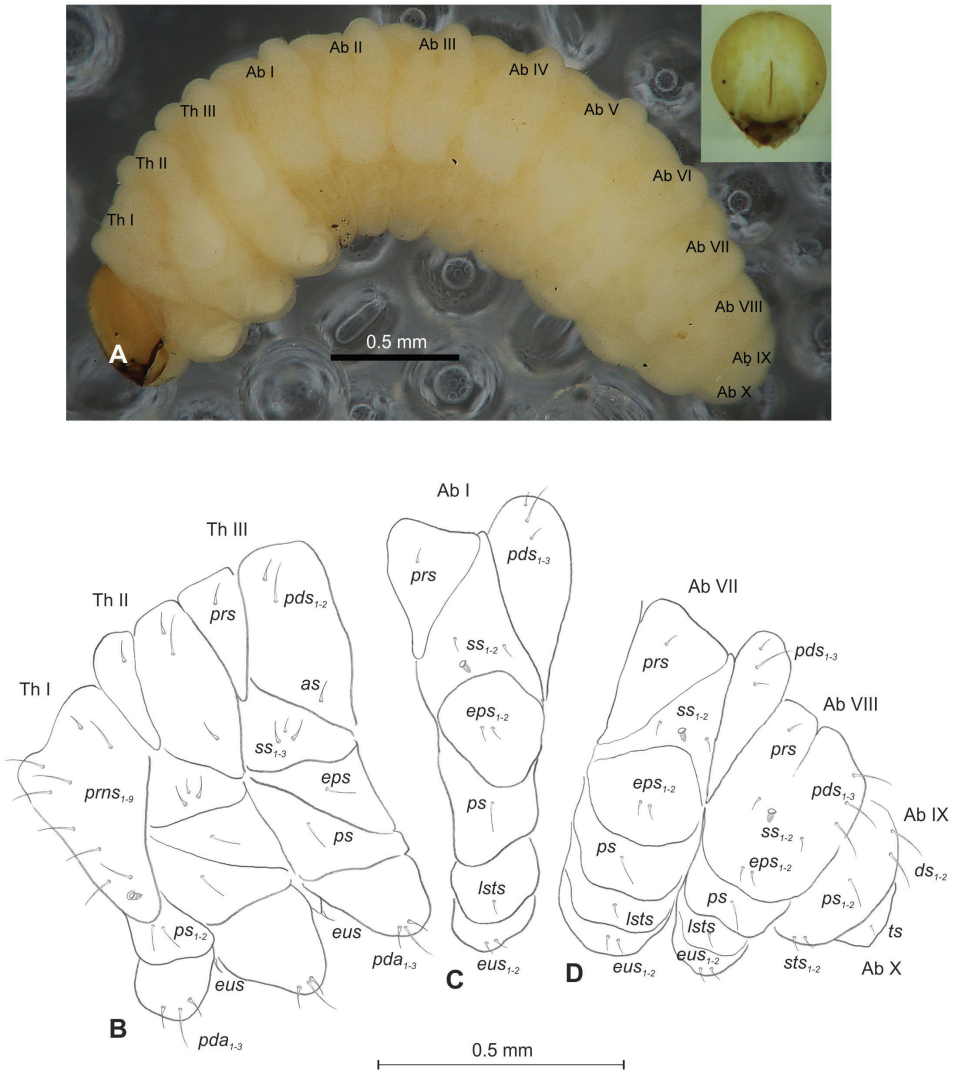

Figure 31. *Mecinus laeviceps* mature larva, habitus and chaetotaxy **A** habitus of the body and frontal view of the head **B** lateral view of thoracic segments **C** lateral view of abdominal segment I **D** lateral view of abdominal segments VII–X. Abbreviations: Th. I–III – number of thoracic segments, Abd. I–X – number of abominal segments, setae: *as* – alar, *ds* – dorsal, *eps* – epipleural, *eus* – eusternal, *lsts* – laterosternal, *pda* – pedal, *pds* – postdorsal, *prns* – pronotal, *prs* – prodorsal, *ps* – pleural, *ss* – spiracular, *sts* – sternal, *ts* – terminal.

Head capsule (Figures 31A, 32A–F) light yellow, distinctly narrowed bilaterally. $Des_{1–3,5}$ long, equal in length; des_4 very short; des_4 located in the central part of epicranium. Fs_3 short to very short, $fs_{4,5}$ long, equal in length. Les_1 and les_2 long, equal in length; two *ves* and one *pes* very short (Figure 32A). Antenna (Figure 32B) with sensorium (Se) conical, three times as long as wide, and three sensilla: one sa and two sb. Clypeus (Figure 32C) trapezium-shaped, anterior margin slightly concave; cls_2 medium; clss placed close to cls_2. Labrum (Figure 32C) almost semi-circular, anterior

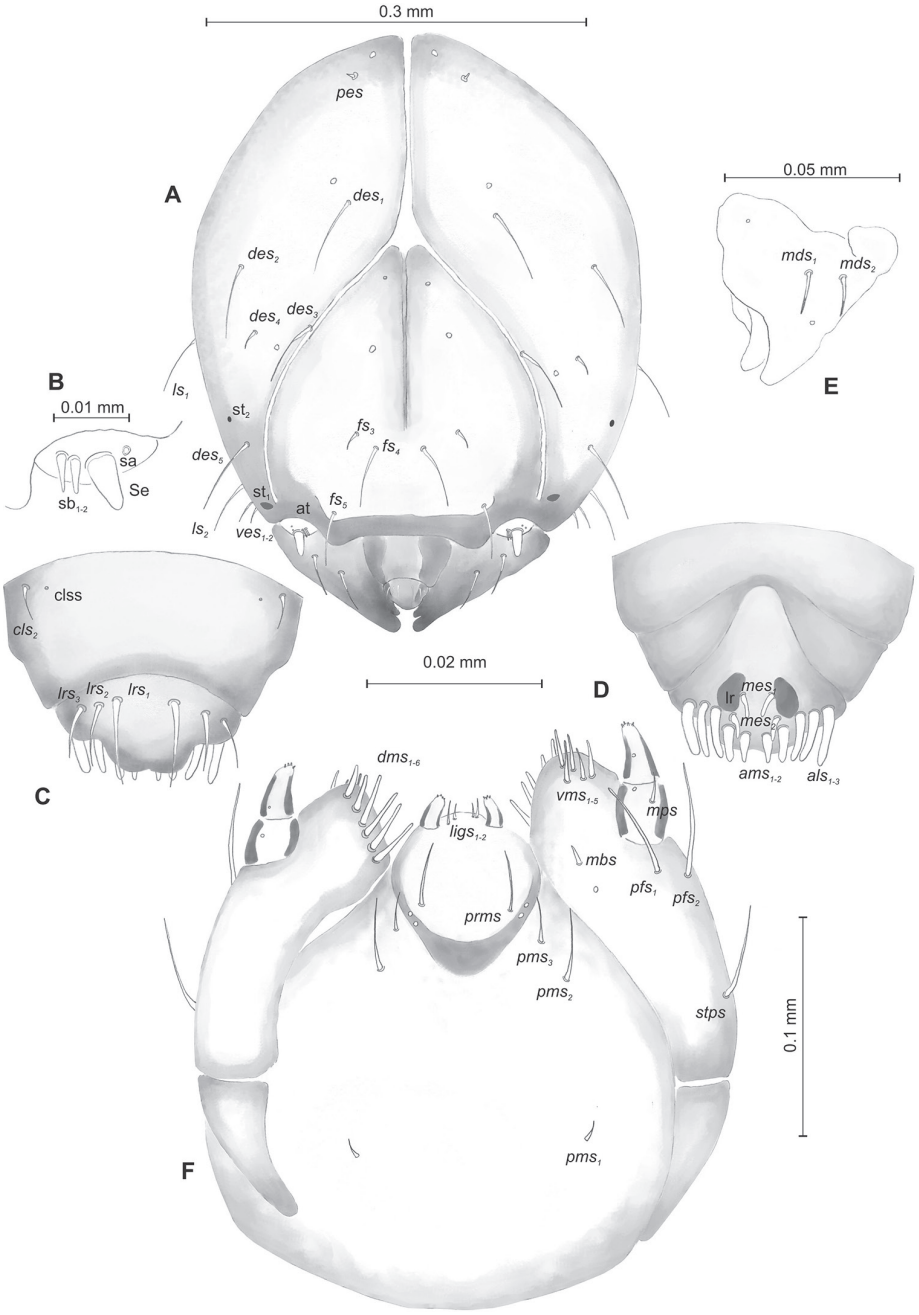

Figure 32. *Mecinus laeviceps* mature larva, head and mouth parts **A** head, frontal view **B** antenna **C** clypeus and labrum, dorsal view **D** epipharynx **E** left mandible **F** maxillolabial complex, ventral aspect. Abbreviations: at – antenna, clss – clypeal sensorium, *des* – dorsal epicranial, lr – labral rods, sa – sensillum ampullaceum, sb – sensillum basiconicum, Se – sensorium, st – stemmata, setae: *als* – anterolateral, *ams* – anteromedial, *cls* – clypeal, *dms* – dorsal malar, *fs* – frontal, *ligs* – ligular, *lrs* – labral, *ls* – lateral epicranial, *mbs* – malar basiventral, *mds* – mandibular, *mes* – median, *mxps* – maxillary palp, *pes* – postepicranial, *ves* – ventral, *pfs* – palpiferal, *pms* – postlabial, *prms* – prelabial, *stps* – stipal, *vms* – ventral malar.

margin sinuated; lrs_1 long, both lrs_2 and lrs_3 medium. Epipharynx (Figure 32D) with three finger-like *als* of almost equal length; two finger-like *ams*, both medium; two short finger-like *mes*, surface smooth; labral rods short, kidney-shaped. Mandibles (Figure 32E) conical, wide, with a small protuberance in the middle of the cutting edge; both *mds* capilliform, medium, equal in length, placed transversely. Maxilla (Figure 32F) with one *stps* and two *pfs* of equal length; *mbs* short; mala with six rod-like *dms* different in length ($dms_{1,2}$ medium, $dms_{3–6}$ long to very long), five *vms* different in length. Maxillary palpi: basal palpomere wider than distal, both of almost equal length. Prelabium (Figure 32F) oval-shaped with one long *prms*; ligula with two short *ligs*; premental sclerite clearly visible, U-shaped. Postlabium (Figure 32F) with very short pms_1, long pms_2, and medium pms_3.

Description of pupa (Figure 33A–C). ***Measurements*** (in mm). Head width: 0.35–0.40. Body width: 0.87–1.07. Body length: 2.12–2.50.

Body elongated, white. Rostrum slender, about four times as long as wide, reaching up to mesocoxae. Antennae slender and elongated. Pronotum 1.5 times as wide as long. Urogomphi (ur) very short, conical, with sclerotised apex, only slightly reaching outline of the body, directed downward (Figure 33B, C).

Chaetotaxy sparse, setae short, unequal length. Head with one *os*. Rostrum with one *rs* and one *pas*. Setae on head and rostrum straight, as long as those on prothorax (Figure 33A). Pronotum with one *as*, one *ls*, one *ds* and three *pls*. Dorsal parts of meso- and metathorax with three setae placed medially. Abdominal segments I–VIII with three very short setae ventrally, distributed in regular lines. Dorsal parts of abdominal segments I–VII with five setae (d_1 placed anteromedially, $d_{2–4}$ posteromedially, d_5 posterolaterally); segment VIII with four setae dorsally. Abdominal segment IX with two micro-setae ventrally.

Biological notes. This is a monophagous species associated with broomleaf toadflax, *Linaria genistifolia* (L.) Mill. The adults are active from early spring, following the appearance of the growing shoots of its host plant. The adults feed intensively on shoot points and apical leaves. Females oviposit batches of 3–6 eggs into the lower to middle part of the young growing shoots. Larval development usually induces stunted growth in the young shoot. The larvae develop in the central part of the stem, forming a relatively short tunnel and the formation of a pseudo-gall in which pupation takes place in the larval chamber very close to the stem surface. Like *M. heydenii*, the adults stay inside the stem until mid-August, when all adults leave their host plants. Adults overwinter in the soil close to the host plant.

Remarks and comparative notes. There are three cryptic subspecies of this species that are distinguishable by molecular and biogeographical data (Toševski et al. 2014). We studied the nominal subspecies distributed in the Czech Republic, Hungary, northern Serbia, and southern Russia; the subspecies *meridionalis* Toševski & Jović, 2014 is distributed in Serbia and Bulgaria and the subspecies *corifoliae* Toševski & Jović, 2014 is distributed in Turkey. As reported in the remarks on *M. heydenii*, several characters allow us to distinguish this last species and *M. peterharrisi* from *M. laeviceps*.

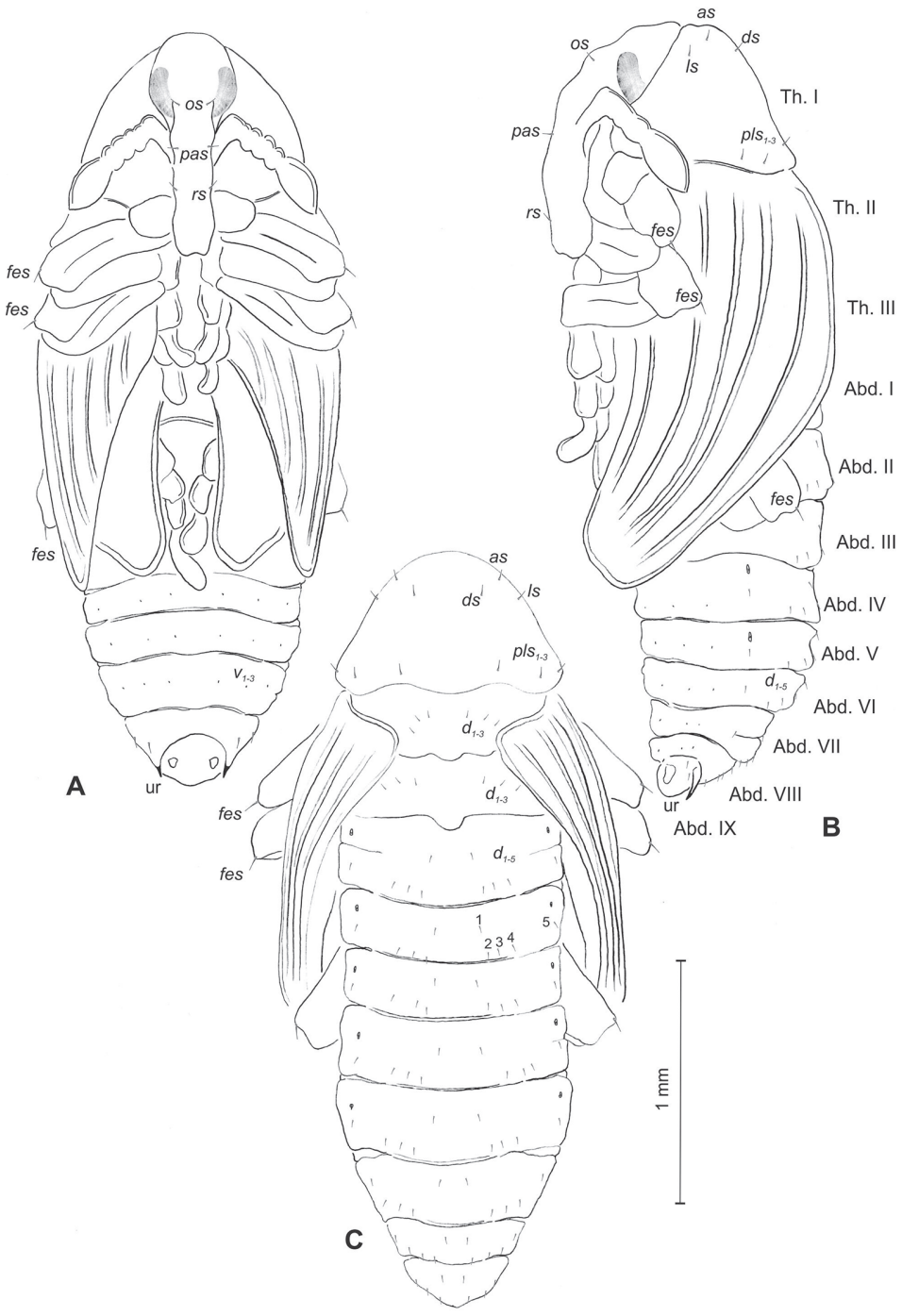

Figure 33. *Mecinus laeviceps* pupa habitus and chaetotaxy **A** ventral view **B** lateral view **C** dorsal view. Abbreviations: Th. I–III – number of thoracic segments, Abd. I–IX – number of abdominal segments, ur – urogomphi, setae: *as* – apical, *d* – dorsal, *ds* – discal, *fes* – femoral, *l*, *ls* – lateral, *os* – orbital, *pas* – postantennal, *pls* – posterolateral, *rs* – rostral.

Mecinus peterharrisi Toševski & Caldara, 2013

Material examined. 25 L3 larvae and 20 pupae, Mecedonia, Prilep, 25.07.2017, (41°17.354'N, 21°29.983'E, 618 m.) ex *Linaria dalmatica macedonica*, lgt. I. Toševski. Accession numbers of sequenced specimen MN992004.

Description of mature larva (Figures 34A–D, 35A–F). ***Measurements*** (in mm). Body length: 2.00–3.75. Body width (metathorax and abdominal segments I–II): 0.65–1.00. Head width: 0.35–0.43.

Body (Figure 34A–D) yellowish, very slender. Chaetotaxy weakly developed, setae extremely short, difficult to observe. Prothorax (Figure 34B) with nine short *prns*; two short *ps* and one short *eus*. Meso- and metathorax (Figure 34B) with one short *prs*, two short *pds*, one short *as*, three minute *ss*, one short *eps*, one short *ps* and one short *eus*. Pedal area with four short *pda.* Abdominal segments I–VIII (Figure 34C, D) with one short *prs*, three short *pds* arranged along the posterior margin, two minute *ss*, two short *eps*, one short *ps*, one short *lsts* and two short *eus*. Abdominal segment IX (Figure 34D) with two *ds* located close to the posterior margin, one short *ps* and two short *sts*. Each of anal lobe with two minute setae.

Head capsule (Figures 34A, 35A–C) pale yellow, distinctly narrowed bilaterally. Frontal suture well visible. $Des_{1–3,5}$ very long, equal in length; des_4 three times shorter than other *des*. Fs_1 as long as des_1, fs_2 and fs_3 very short, $fs_{4–5}$ long. Les_1 shorter than les_2; two *ves* and four *pes* very short (Figure 35A). Two stemmata of different size. Antennae (Figure 35B) with sensorium (Se) conical, thrice as long as wide, located medially, and three sensilla of different types: one sa and four sb. Clypeus (Figure 35C) trapezium-shaped, anterior margin slightly concave; cls_2 medium; clss clearly visible. Labrum (Figure 35C) with sinuate anterior margin; lrs_1 very long, lrs_2 shorter than lrs_1, lrs_3 three times shorter than lrs_1. Epipharynx (Figure 35D) with three relatively long, finger-shaped *als* of almost equal length; two rod-like *ams*, equal in length; two rod-like *mes* of medium length; surface smooth; labral rods short, rounded. Mandibles (Figure 35E) conical, wide, with a small protuberance in the middle of the cutting edge; both *mds* capilliform, relatively long, equal in length, placed mediolaterally. Maxilla (Figure 35F) with one *stps* and two *pfs* of equal length; *mbs* very short; mala with six finger-like *dms* different in length ($dms_{1,2}$ medium, $dms_{3–6}$ long to very long), five *vms* different in length. Maxillary palpi: basal palpomere wider than distal, both of almost equal length. Prelabium (Figure 35F) close to oval-shaped with one very long *prms*; ligula with two *ligs* of equal length; premental sclerite clearly visible, U-shaped. Postlabium (Figure 35F) with short pms_1, long pms_2, and short pms_3.

Description of pupa (Figure 36A–C). ***Measurements*** (in mm). Head width: 0.36–0.43. Body width: 0.83–1.50. Body length: 2.46–3.66.

Body elongated, slender, white. Rostrum slender, about five times as long as wide, reaching up to mesocoxae. Antennae slender and moderately elongated. Pronotum 1.1 times as wide as long. Urogomphi (ur) very short, conical, with sclerotised apex, reaching outline of the body, directed downward (Figure 36A, B).

Chaetotaxy sparse, setae very short, equal in length. Head with one *os*. Rostrum with one *rs* placed medially. Setae on head and rostrum straight, as long as those on pro-

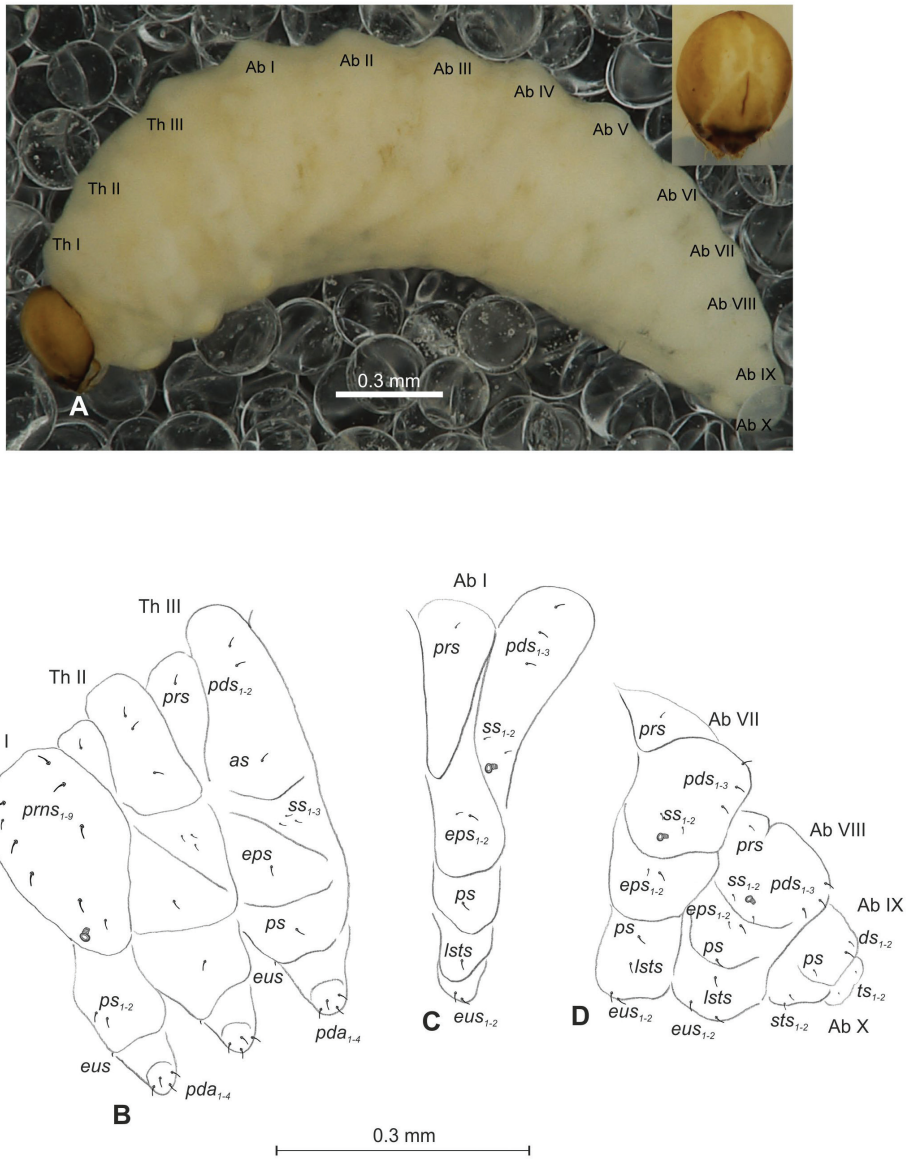

Figure 34. *Mecinus peterharrisi* mature larva, habitus and chaetotaxy **A** habitus of the body and frontal view of the head **B** lateral view of thoracic segments **C** lateral view of abdominal segment I **D** lateral view of abdominal segments VII–X. Abbreviations: Th. I–III – number of thoracic segments, Abd. I–X – number of abominal segments, setae: *as* – alar, *ds* – dorsal, *eps* – epipleural, *eus* – eusternal, *lsts* – laterosternal, *pda* – pedal, *pds* – postdorsal, *prns* – pronotal, *prs* – prodorsal, *ps* – pleural, *ss* – spiracular, *sts* – sternal, *ts* – terminal.

thorax (Figure 36A). Pronotum with one *ds*, one *sls* and three *pls*. Dorsal parts of meso- and metathorax with three setae placed medially. Abdominal segments I–VIII with one seta laterally, two very short setae ventrally and three setae dorsally, placed along posterior margin. Abdominal segment IX with two micro-setae ventrally. (Figure 36B).

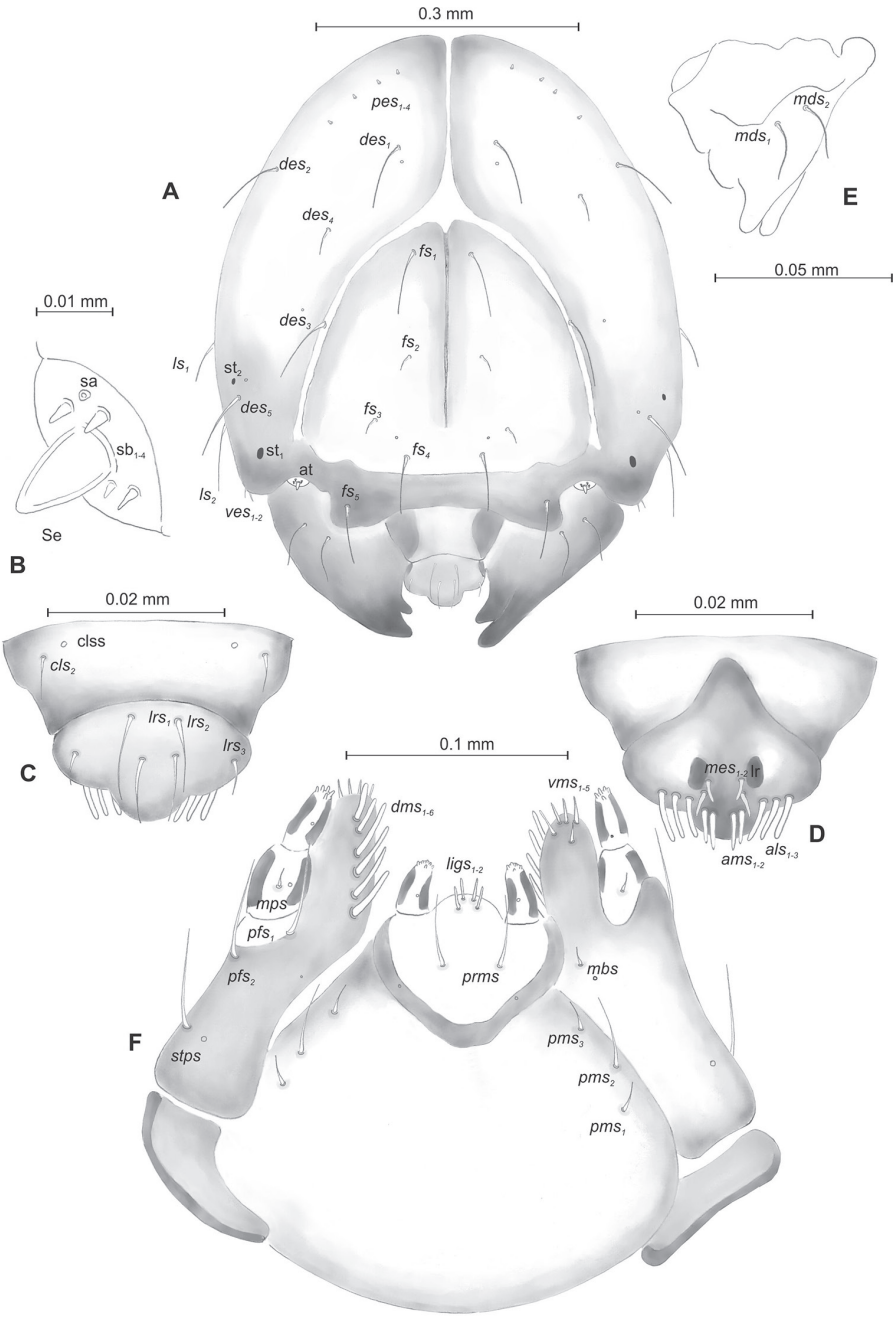

Figure 35. *Mecinus peterharrisi* mature larva, head and mouth parts **A** head, frontal view **B** antenna **C** clypeus and labrum, dorsal view **D** epipharynx **E** left mandible **F** maxillolabial complex, ventral aspect. Abbreviations: at – antenna, clss – clypeal sensorium, *des* – dorsal epicranial, lr – labral rods, sa – sensillum ampullaceum, sb – sensillum basiconicum, Se – sensorium, st – stemmata, setae: *als* – anterolateral, *ams* – anteromedial, *cls* – clypeal, *dms* – dorsal malar, *fs* – frontal, *ligs* – ligular, *lrs* – labral, *ls* – lateral epicranial, *mbs* – malar basiventral, *mds* – mandibular, *mes* – median, *mxps* – maxillary palp, *pes* – postepicranial, *ves* – ventral, *pfs* – palpiferal, *pms* – postlabial, *prms* – prelabial, *stps* – stipal, *vms* – ventral malar.

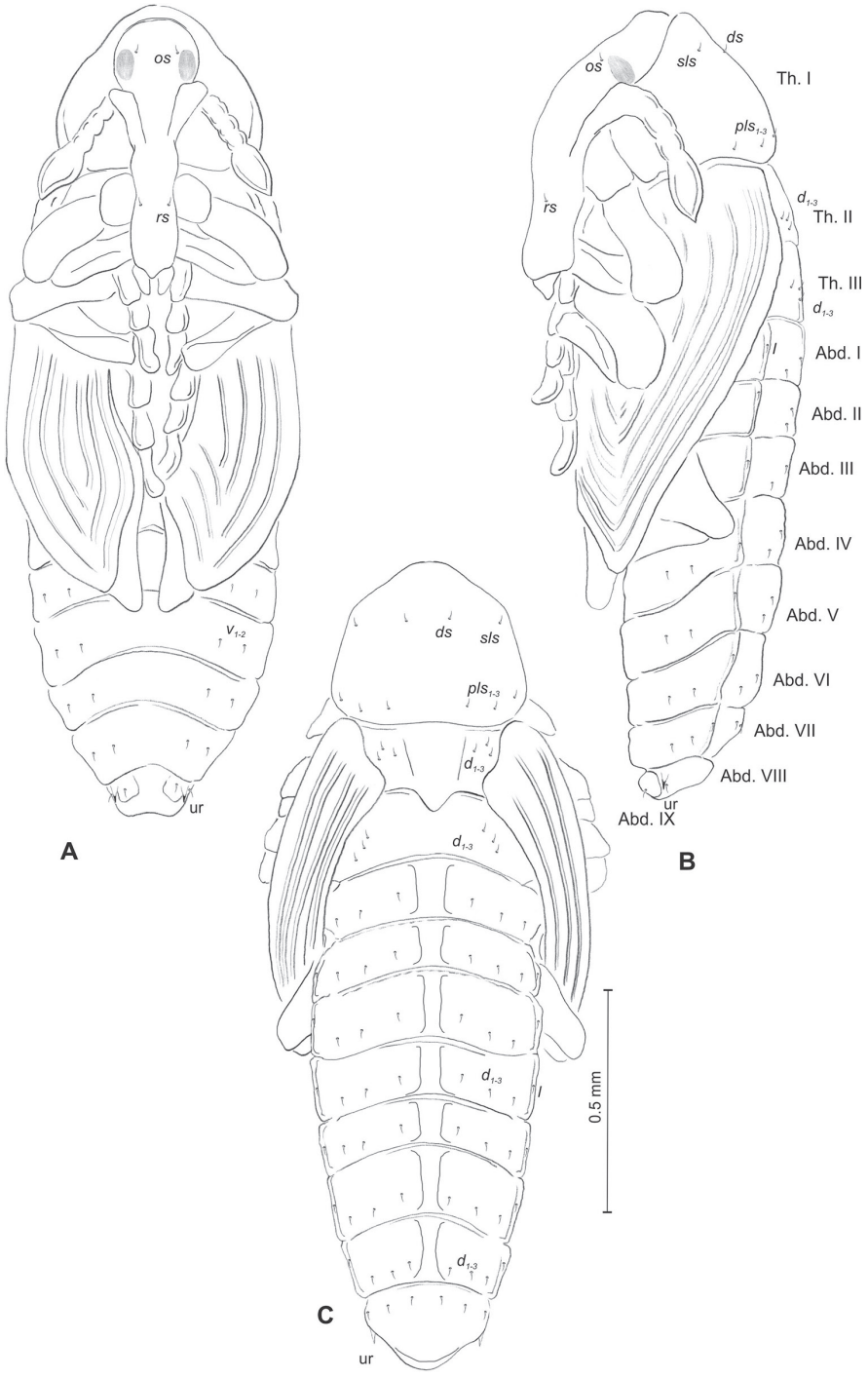

Figure 36. *Mecinus peterharrisi* pupa habitus and chaetotaxy **A** ventral view **B** lateral view **C** dorsal view. Abbreviations: Th. I–III – number of thoracic segments, Abd. I–IX – number of abdominal segments, ur – urogomphi, setae: *as* – apical, *d* – dorsal, *ds* – discal, *fes* – femoral, *l* – lateral, *os* – orbital, *pls* – posterolateral, *rs* – rostral, *sls* – superlateral.

Biological notes. This species is known only from the southwest region of North Macedonia and northwestern part of Greece following the distribution of *Linaria dalmatica macedonica* (Griseb.) D.A. Sutton, as well as from sparse populations of *L. dalmatica dalmatica* (L.) Mill. present at the Montenegrin Sea coast in the vicinity of Kotor Bay (Toševski et al. 2014). Adults appear in the field at the beginning of March and aggregate on young growing shoots, causing significant damage to the shoot points and apical leaves. Like *M. laeviceps*, the larvae develop within short larval tunnels, and the newly emerged adults remain and feed in the pupal chamber until mid-August. Adults overwinter in the soil close to the host plant.

Remarks and comparative notes. This species, found only in the Balkans (Macedonia, Greece, Montenegro) as above reported, is very similar to *M. laeviceps*, from which it differs by the body being more robust and usually longer, the integument of the pronotum more distinctly bluish, and the penis with longer tip. Moreover, the vestiture is usually formed by slightly broader scales and is therefore generally more distinct. As reported in the remarks on *M. heydenii* and in the keys, the study of the immatures has revealed other interesting differences between these three species that are very useful for their separation.

Key to known mature larvae of *Mecinus* species

The following key is based on the larvae, described in this paper, of 12 *Mecinus* species.

1 Head rounded or almost rounded, with only a single pair of stemmata. Abdominal segment X reduced to three anal lobes of equal size **2**

– Head distinctly flattened laterally, with two pairs of stemmata. Abdominal segment X reduced to three anal lobes of those lateral are the largest, and dorsal the smallest (sometimes absent) **5**

2 Head brown, only slightly narrowed bilaterally. Endocarina reaching 1/2 of the frons. Body slightly pressed dorso-ventrally. Premental sclerite, pedal lobes and spiracular area of meso- and metathorax dark pigmented. Thoracic spiracle bicameral. Cls_1 present. Labial palpi two-segmented ..... ***Mecinus collaris*** **Germar, 1821**

– Head white, rounded. Endocarina reaching 3/4 of the frons. Body rounded in cross section. Premental sclerite, pedal lobes and spiracular area of meso- and metathorax as pigmented as rest of the body. Thoracic spiracle unicameral. Cls_1 absent. Labial palpi one-segmented **3**

3 Cuticle tuberculate. Fs_1 absent. Thoracic segments with two *pds.* Abdominal segments I–VIII with three *pds*. Anterior margin of labrum almost straight. Posterior extension of premental sclerite elongated, with acute apex..... ***Mecinus pirazzolii*** **(Stierlin, 1867)**

– Cuticle smooth. Fs_1 present. Thoracic segments with three *pds*. Abdominal segments I–VIII with four *pds*. Anterior margin of labrum sinuated. Posterior

extension of premental sclerite short, with dull apex ..... **4 (*Mecinus pascuorum* group)**

4 Pronotum with 11 *prns*. Thoracic *pds* various in length (first short, second and third elongated). Thoracic *ss* various in length (first minute, second and third medium). Each pedal lobes with four *pda*. Setae on abdominal segment VIII relatively elongated. *Prms* very short. Antenna with two sb and one sa .. .. ***Mecinus labilis* (Herbst, 1795)**

– Pronotum with eight *prns*. Thoracic *pds* equal in length. Thoracic *ss* equal in length. Each pedal lobes with five *pda*. Setae on abdominal segment VIII medium size. *Prms* elongated. Antenna with three sb ....***Mecinus pascuorum* (Gyllenhal, 1813)**

5 Abdominal segments I–VIII with four *pds* and usually three *ss*. Labial palpi two-segmented. Surface of postlabium (at least partially) densely covered with asperities ..... **6 (*Mecinus janthinus* group)**

– Abdominal segments I–VIII with three *pds* and always two *ss*. Labial palpi one-segmented. Surface of postlabium smooth **8**

6 Abdominal segments I–VIII with two *ss.* Only posterior part of postlabium covered with asperities .....***Mecinus sicardi* Hustache, 1920**

– Abdominal segments I–VIII with three *ss.* Whole postlabium covered with asperities **7**

7 Pronotum with eight *prns*. *Ss* on thoracic segments various in length (two minute, one medium). Each pedal lobes with five *pda*. Head with one *ves* and four *pes*. Antenna with two sb and one sa. Mala with six *dms*. Ligula with three *ligs*..... ***Mecinus janthinus* Germar, 1821**

– Pronotum with 11 *prns*. *Ss* on thoracic segments medium, equal in length. Each pedal lobes with six *pda*. Head with two *ves* and three *pes*. Antenna with four sb. Mala with seven *dms*. Ligula with two *ligs* ....***Mecinus janthiniformis* Toševski & Caldara, 2011**

8 Thoracic spiracle bicameral. Endocarina reaching to 1/2 of the frons. Cls_1 present. Premental sclerite cup-like. All *dms* equal in length..... ..... **9 (*Mecinus circulatus* group)**

– Thoracic spiracle unicameral. Endocarina reaching to 4/5 of the frons. Cls_1 absent. Premental sclerite U-shaped. $Dms_{1,2}$ always shorter than next one .... **10 (*Mecinus heydenii* group)**

9 Pronotum with eight *prns*. Each pedal lobes with three *pda*. Anal lobes with one *ts*. Head with five *pes*. Mandible with two *mds*. Mala with four *vms*. *Prms* short ..... ***Mecinus circulatus* (Marsham, 1802)**

– Pronotum with 11 *prns*. Each pedal lobes with five *pda*. Anal lobes with two *ts*. Head with four *pes*. Mandible with one *mds*. Mala with five *vms*. *Prms* elongated ..... ***Mecinus pyraster* (Herbst, 1795)**

10 Fs_1 long, fs_2 minute. Antenna with four sb .... ***Mecinus peterharrisi* Toševski & Caldara, 2013**

– Fs_1 and fs_2 absent. Antenna with two sb..... **11**

11 Pronotum with eight *prns*. Thoracic segments with three *pds*. Each pedal lobes with four *pda*. *Pds* of abdominal segments I–VIII minute. Head with four *pes* ..... ***Mecinus heydenii* Wencker, 1866**

– Pronotum with nine *prns*. Thoracic segments with two *pds*. Each pedal lobes with three *pda*. *Pds* of abdominal segments I–VIII medium or elongated. Head with one *pes* ..... ***Mecinus laeviceps* Tournier, 1873**

Key to pupae of known *Mecinus* species

The following key is based on pupae of 12 *Mecinus* species described in this paper.

1 Body stout, length ratio at most 1.8 ..... **2**

– Body slender, length ratio at least 2.0 ..... **4**

2 Rostrum slender, very short, distinctly tapering to its top. Setae on head and pronotum extremely short, almost invisible. Abdominal segments I–VII without setae ventrally ..... ***Mecinus pirazzolii* (Stierlin, 1867)**

– Rostrum moderately elongated, linear, 2–2.5 times as long as wide. Setae on head and proonotum minute or medium. Abdominal segments I–VII with three setae ventrally **3**

3 Setae of head and pronotum medium, well visible. Pronotum with two protuberances apically ..... ***Mecinus pascuorum* (Gyllenhal, 1813)**

– Setae of head and pronotum minute, weakly visible. Pronotum without protuberances apically ..... ***Mecinus labilis* (Herbst, 1795)**

4 Abdominal segments I–IV dorsally without setae; segments V–VII with setae growing gradually ..... ***Mecinus collaris* Germar, 1821**

– Abdominal segments I–VII dorsally with setae equal in length or only slightly growing from segment I to VII **5**

5 Urogomphi short or very short, only slightly reaching outline of the body, directed downward. Setae of head and pronotum medium or short. Abdominal segments I–VII with five or less setae dorsally **6**

– Urogomphi relatively elongated, distinctly reaching outline of the body, directed outside. Setae of head and pronotum elongated. Abdominal segments I–VII with six or seven setae dorsally ..... **10 (*Mecinus janthinus* group)**

6 Body moderately slender. Head with one *vs*, one or two *sos* and one *pas*; Pronotum with two *sls* and one or two *ls*. Dorsal parts of meso- and metathorax with two setae dorsally ..... **7** (***Mecinus circulatus* group**)

– Body very slender. Head without *vs* and *sos*, and *pas* also usually absent. Pronotum without or with one *sls* and *ls*. Dorsal parts of meso- and metathorax with three setae dorsally ..... **8 (*Mecinus heydenii* group)**

7 Head with two *sos* and two *os*. Pronotum with two *as*, one *ds*, two *ls*, and three *pls*. Abdominal segments I–VII with five setae dorsally ..... ***Mecinus pyraster* (Herbst, 1795)**

– Head with one *sos* and one *os*. Pronotum with one *as*, *ds* absent, one *ls*, and two *pls*. Abdominal segments I–VII with three setae dorsally ..... ***Mecinus circulatus* (Marsham, 1802)**

8 Pronotum without *as*. Abdominal segments I–VII with three setae dorsally. Femora without *fes*..... ***Mecinus peterharrisi* Toševski & Caldara, 2013**

– Pronotum with some *as*. Abdominal segments I–VII with five setae dorsally. Femora with one *fes* **9**

9 Rostrum with one *pas*. Pronotum with one *ls*..... ***Mecinus laeviceps* Tournier, 1873**

– Rostrum without *pas*. Pronotum without *ls*..... ***Mecinus heydenii* Wencker, 1866**

10 Rostrum with one *pas* and without *rs*. Pronotum with four *pls*..... ***Mecinus sicardi* Hustache, 1920**

– Rostrum with two *pas* and one *rs*. Pronotum with three *pls*..... **11**

11 Dorsal parts of meso- and metathorax with three setae dorsally..... ***Mecinus janthiniformis* Toševski & Caldara, 2011**

– Dorsal parts of meso- and metathorax with two setae dorsally..... ***Mecinus janthinus* Germar, 1821**

Discussion

Comparison with immature stages of known Mecinini

The present detailed descriptions of the immature stages of 12 species of *Mecinus* constitute a good sample, comprising approximately 20% of the known species of this genus, allowing a comparison with other genera within the tribe Mecinini. Unfortunately, some descriptions previously published on immature stages of species belonging to other genera of Mecinini are somewhat problematic because of missing details about the chaetotaxy and/or the absence of quality drawings (see Skuhrovec et al. 2018), making such comparisons still difficult. Only the recent descriptions of six *Cleopomiarus* and three *Miarus* species (Skuhrovec et al. 2018; Szwaj et al. 2018), three *Gymnetron* species (Jiang and Zhang 2015), and two *Rhinusa* species (Gosik 2010; Ścibior and Łętowski 2018) were sufficiently complete for such a comparison. Skuhrovec et al. (2018) emphasised that the taxonomical interpretation of some characters (e.g., thoracic and abdominal dorsal setae) in the papers above is very disputable. This can cause an incorrect differential diagnosis and preclude the composition of a key to the tribe. Our new data might be able to resolve some of these uncertainties.

The number of palpomeres of the labial palpi was shown to be one of the most important morphological characters of larvae in this tribe (Skuhrovec et al. 2018). Some *Gymnetron* species have only one palpomere (May 1993; Jiang and Zhang 2015), but

the basal state in weevils is the presence of two palpomeres on labial palpi (Marvaldi 1997). *Mecinus* species can be clearly separated into two groups based on the presence of both states. Some species groups have the plesiomorphic condition, with two palpomeres on the labial palpi, but other species groups have only one palpomere, such as *Gymnetron* species. A completely different situation has been observed in some *Cleopomiarus* species (Skuhrovec et al. 2018), where there is not a distinct separation of the basal palpomere from the labium, and it can appear to be only one palpomere. This state in *Cleopomiarus* and partially in *Miarus* could be an intermediate stage in the reduction to *Gymnetron* species. This should also be compared with a higher number of *Rhinusa* species, and only then the evolutionary history of this character in the whole tribe can be discussed.

Skuhrovec et al. (2018) suggested that the number of air tubes of the thoracic and abdominal spiracles is the next crucial genus-specific character in Mecinini larvae. Larvae of *Mecinus* species have two states of this character: (1) all spiracles unicameral, as in *Gymnetron* species (Jiang and Zhang 2015), or (2) thoracic spiracle bicameral and abdominal spiracles unicameral, as in some *Rhinusa* (Anderson 1973; May 1993). A completely unique situation is seen in all known larvae of *Cleopomiarus* and *Miarus* species, which have bicameral spiracles on the thorax and abdomen.

Another disputable state is the number of epipharyngeal setae (especially *ams* and *mes*), which is not yet completely resolved in Curculionidae and was also discussed several times for different groups, e.g., Lixinae (Gosik and Skuhrovec 2011; Stejskal et al. 2014; Trnka et al. 2015). In our view, the final decision of the number of each seta is important, but not crucial, and the comparison between groups/genera should be made together for all three of these epipharyngeal setae in order to make fewer mistakes in the creation of a differential diagnosis for genera in the tribe.

The last important characteristic observed within the Mecinini tribe is the integument of the body with distinct asperities (Skuhrovec et al. 2018). This feature is very variable within each genus (*Mecinus*, *Cleopomiarus*, *Miarus*), probably due to specific environmental conditions within plant tissues. This feature may be discussed after other detailed descriptions are made within the Mecinini tribe.

Comparison of the immature stages of *Mecinus* species groups

Before this study, larvae of only four *Mecinus* species had been described – *M. pascuorum*, *M. pyraster*, *M. heydenii*, and *M. janthinus* (Emden 1938; Scherf 1964; Anderson 1973), while a description of pupae was available for only three of these species (Scherf 1964; Anderson 1973). Unfortunately, these descriptions did not include the chaetotaxy, with a few exceptions, and included only general characteristics, such as the number of teeth on the mandible or the colouration of the head and body. Therefore, a detailed description of all four species has been necessary for their incorporation into our key.

The main differential characters in larvae and pupae among known species are presented in the diagnosis of species groups and in the keys. The 12 species described here belong to five groups and one complex of the seven groups and two complexes detected

by Caldara et al. (2013) on the basis of morphological and biological apomorphies. It should be recalled that these authors defined their complexes as an assemblage of species formed by several taxa, which are mostly very similar to each other but lacking synapomorphies in contrast with the species forming the groups. Therefore, we now have the opportunity to assess whether the differences found in the immatures are able to confirm or refute the conclusions obtained after a phylogenetic study of the imagoes.

Based on several unique characters, we can confirm that all six assemblages of species obtained in the present study completely agree with those based on adult characters. Moreover, we found distinctive characters in the previously considered "complex" of *M. pascuorum*, which can now be considered a "true" group.

The main differential characters in larvae among the known species include the following: (1) the number of palpomeres of the labial palpi, (2) the number of air tubes of the thoracic and abdominal spiracles, and (3) the shape of the head and the number of stemmata on the head. The combination of the states of these three characters can easily separate all species groups. Only future studies of the whole tribe together with adult morphology and biological information may identify the values of each character and verify its effect on evolution within this tribe. Skuhrovec et al. (2018) reported that fewer genus-specific character states in larvae than in pupae, which are more conservative in chaetotaxy, were also shown in another tribe of the Curculioninae (Tychiini) with regard to the genera *Tychius* Germar, 1817 and *Sibinia* Germar, 1817 (see Skuhrovec et al. 2014, 2015; Gosik et al. 2017).

According to the two above-mentioned main characters of larvae, the groups of *Mecinus* could be assembled as follows: (1) two palpomeres on the labial palpi: *M. collaris*, *M. janthinus* groups; (2) one palpomere: *M. heydenii*, *M. pascuorum*, *M. circulatus*, *M. simus* groups; (3) all spiracles unicameral: *M. heydenii*, *M. pascuorum*, *M. simus* group; (4) thoracic spiracle bicameral and abdominal spiracles unicameral: *M. collaris*, *M. janthinus*, *M. circulatus* groups. However, if the two characters are combined, we obtain the following groupings: (1) two palpomeres on the labial palpi + thoracic spiracle bicameral and abdominal spiracles unicameral: *M. collaris* and *M. janthinus* groups; (2) one palpomere + all spiracles unicameral: *M. simus*, *M. heydenii* and *M. pascuorum* groups; (3) one palpomere + thoracic spiracle bicameral and abdominal spiracles unicameral: *M. circulatus* group.

Species of the genus *Mecinus* feed on different genera of host plants in two different tribes belonging to the family Plantaginaceae: *Plantago* (Plantagineae) and *Linaria*, *Antirrhinum* and *Anarrhinum* (Antirrhineae). The *M. heydenii* group and the *M. janthinus* group include all the species of *Mecinus* living on Antirrhineae. Until now, this ecological character was the unique putative synapomorphy that allows the assemblage of these two groups, although these species are clearly similar overall, and only these groups include species with blue elytral integument. This character is not possessed by any other Mecinini, and the other species of these groups have black elytral integument. In contrast, most species living on *Plantago*, at least in part, have reddish integument. Caldara et al. (2013) did not find other consistent synapomorphies that allow the separation of the *M. janthinus* + *M. heydenii* groups feeding on Antirrhineae from

all other species living on *Plantago*. Similarly, a molecular study did not relate these two groups which possibly evolved in parallel (I. Toševski, unpublished data).

Unfortunately, the morphology of the immatures does not seem to shed more light on this situation. In fact, the two groups living on Antirrhineae share only the following two characters in larvae: (1) head brown, distinctly narrowed bilaterally, with two pairs of stemmata and (2) endocarina reaching 4/5 of the frons. The characters of the head are also possessed by the *M. circulatus* group, which, in contrast, has the endocarina reaching only half of the frons. With regard to the pupae, the relationship of these three groups might be suggested by abdominal segments I–VII dorsally with setae. However, if the available data are assembled, one could assume that the *M. janthinus* + *M. heydenii* groups are not monophyletic sharing only a few homoplasies and suggesting that the switch from Plantaginaceae s. str. to Antirrhinae occurred independently in both the *M. heydenii* and *M. janthinus* species groups. It is noteworthy that the species of *Mecinus* that share an unusual elongated body, i.e., *M. circulatus*, *M. janthinus* and *M. heydenii*, are generally stem borers, with larval feeding and mining in the central part of the stem producing no externally visible damage or small external gall-like deformations – except for *M. dorsalis* Aubé, 1850 of the *M. heydenii* group, which produces globose galls – suggesting that the elongated body is an adaptative character for their ecological niche. At present, the only known gall-inducing species living on *Plantago* is *M. collaris*, which appears morphologically distinct from all these species.

Differences between immatures at the species level

All the studied immatures have characters that allow us to distinguish them from each other. Whereas it was expected that very characteristic species such as *M. collaris* or *M. labilis* belong to different groups on the basis of the morphology of the adult, it is also true for species within the same group. Moreover, it is even more noteworthy that cryptic species, such as *M. janthinus* and *M. janthiniformis* and *M. heydenii*, *M. peterharrisi* and *M. laeviceps*, are clearly distinguishable by the morphological characters of the immatures. Differences were found in the lack or presence and, in the latter case, the number of setae both in larvae (head, pronotum, thoracic and abdominal segments) and pupae (rostrum, pronotum, abdomen).

Biological and evolutionary considerations

It appears probable that all *Mecinus* species live on Plantaginaceae. The majority of them feed on species of *Plantago*, whereas a quarter of *Mecinus* species live on Antirrhineae, especially *Linaria* and occasionally *Antirrhinum* and *Anarrhinum*. As reported above, neither the study on adults by Caldara et al. (2013) nor ours on the immature stages have found consistent synapomorphies that allow the separation of the *M. janthinus* + *M. heydenii* groups feeding on Antirrhineae from all other species living on *Plantago*. It is noteworthy that no mecinines other than *Mecinus* live on *Plantago* (Caldara et al. 2013), whereas several species belonging to *Rhinusa*, the sister-group of

Mecinus, live on Antirrhineae (Caldara et al. 2010). These data as a whole tend to suggest that Mecinini, during their evolution, switched more than once from Plantagineae to Antirrhineae or vice versa, and that this switch could easily have occurred independently in both the *M. heydenii* and *M. janthinus* species groups.

The larvae of closely related species of *Mecinus* seem to differ in their modes of parasitism, although less significantly than *Rhinusa* larvae (see Caldara et al. 2010). Concerning the species living on *Plantago*, the apparently more primitive species belonging to the *M. pascuorum* group feed on pyxidia without producing externally visible damage. In contrast, *Mecinus circulatus* and *M. pyraster* of the *M. circulatus* group are stem borers with larval feeding and mining in the central part of the stem, producing no externally visible damage or small external gall-like deformations. At present, the only known gall-inducing species living on *Plantago* is *M. collaris*, which appears morphologically distinct from all other species. The situation of the *M. simus* group is very interesting: whereas *M. pirazzolii* feed on seeds, *M. comosus* Boheman, 1845 tunnels into the central axis of the spike of *Plantago maritima* (Prena and Caldara 2017). With regard to the species living on Antirrhineae, the same variability in biological habits is found in the *M. heydenii* group: from *M. heydenii* producing weak deformation of the stems to *M. dorsalis* producing globose galls. In contrast, in the *M. janthinus* group, there are true stem borers that produce no visible damage (*M. janthinus* and *M. barbarus*) or only small gall-like deformations (*M. janthiniformis*, *M. sicardi*). One thing seems clear: all the larvae of *Mecinus* species with elongated bodies develop along stems or, as in *M. comosus*, along spikes. It is worth noting that the genus *Mecinus* was created for these elongated species and that the other species with short bodies were described and considered *Gymnetron* for many years, until Caldara (2001) transferred them from *Gymnetron* to *Mecinus* on the basis of several synapomorphies in the male genitalia. It is also noteworthy that it was very simple to identify the species of *Mecinus* as they were formerly defined, since there are very few Curculioninae with similar elongate bodies. If we now consider the very probable polyphyly of species with long bodies on the basis of morphological, biological and molecular characters, we can speculate that the elongated body is an adaptive character for the particular ecological niche, i.e., the somewhat narrow stems of *Plantago* and *Linaria* or the spikes of *Plantago*. It is noteworthy that stems are not used as niches for the growth of larvae of other Curculioninae, except for *Rhinusa asellus* (Gravenhorst, 1807) and *R. tenuirostris* (Stierlin, 1888) (Doğanlar and Üremiş 2014), which are the more elongated species in the *R. tetra* group that usually feed on the seeds of *Verbascum* spp.

Conclusions

Our detailed descriptions of the immature stages of the Mecinini species demonstrate their importance for the taxonomy and further study of the phylogenetic relationships within the genera of the tribe Mecinini, although the number of described immatures is still low in comparison with the total number of *Mecinus* species. This is our second

paper about the Mecinini, after that of *Miarus* and *Cleopomiarus*. We are confident that the description of immatures of the genera *Rhinusa* and *Gymnetron*, which are currently under investigation, will provide an interesting final arrangement to the taxonomy of the tribe.

Acknowledgments

The study was supported by a grant from the Czech Ministry of Agriculture (Mze ČR) RO0418 to J. Skuhrovec and a grant from the Ministry of Education, Science and Technological Development of the Republic of Serbia III43001 to I Toševski. The language was corrected by the American Journal Experts company.

References

Albach DC, Jensen SR, Özkögce F, Grayer RJ (2005) *Veronica*: chemical characters for the support of phylogenetic relationships based on nuclear ribosomal and plastid DNA sequence data. Biochemical Systematics and Ecology 33: 1087–1106. https://doi.org/10.1016/j.bse.2005.06.002

Alonso-Zarazaga MA, Barrios H, Borovec R, Bouchard P, Caldara R, Colonnelli E, Gültekin L, Hlaváč P, Korotyaev B, Lyal CHC, Machado A, Meregalli M, Pierotti H, Ren L, Sánchez-Ruiz M, Sforzi A, Silfverberg H, Skuhrovec J, Trýzna M, Velázquez de Castro AJ, Yunakov NN (2017) Cooperative Catalogue of Palaearctic Coleoptera Curculionoidea. Monografías electrónicas de la Sociedad Entomológica Aragonesa 8: 1–729.

Anderson DM (1973) Keys to larvae and pupae of Gymnetrinae of America North and Mexico (Coleoptera: Curculionidae). Proceedings of the Zoological Society of Washington 75: 133–140.

APG (2016) An update of the Angiosperm Phylogeny Group classification for the orders and families of flowering plants: APG IV. Botanical Journal of the Linnean Society 181: 1–20. https://doi.org/10.1111/boj.12385

Applequist WL (2006) (1714–1715) Proposal to Reject the Names *Plantago psyllium* and *P. cynops* (Plantaginaceae). Taxon 55(1): 235–236. https://doi.org/10.2307/25065554

Caldara R (2001) Phylogenetic analysis and higher classification of the tribe Mecinini (Coleoptera: Curculionidae, Curculioninae). Koleopterologische Rundschau 71: 171–203.

Caldara R, Colonnelli E, Osella G (2009) On recently collected South African Tychiini and Mecinini, with description of seven new species (Coleoptera, Curculionidae). Fragmenta Entomologica 41: 129–167.

Caldara R, Fogato V (2013) Systematics of the weevil genus *Mecinus* Germar, 1821 (Coleoptera: Curculionidae). I. Taxonomic treatment of the species. Zootaxa 3654: 1–105. https://doi.org/10.11646/zootaxa.3654.1.1

Caldara R, Sassi D, Toševski I (2010) Phylogeny of the weevil genus *Rhinusa* Stephens based on adult morphological characters and host plant information (Coleoptera: Curculionidae). Zootaxa 2627: 39–56. https://doi.org/10.11646/zootaxa.2627.1.3

Caldara R, Sassi D, Montagna M (2013) Systematics of the weevil genus *Mecinus* Germar, 1821 (Coleoptera: Curculionidae). II. Phylogenetic analysis based on adult morphological characters and host plant information. Zootaxa 3664: 136–148. https://doi.org/10.11646/zootaxa.3664.2.2

Debinski DM, Holt RD (2000) A survey and overview of habitat fragmentation experiments. Conservation Biology 14: 342–355. https://doi.org/10.1046/j.1523-1739.2000.98081.x

De Clerck-Floate RA, Harris P (2002) *Linaria dalmatica* (L.) Miller, Dalmatian toadflax (Scrophulariaceae). In: Mason PG, Huber JT (Eds) Biological Control Programmes in Canada 1981–2000. CAB International, Wallingford, 345–362.

De Clerck-Floate RA, Miller V (2002) Overwintering mortality of and host attack by the stem-borring weevil *Mecinus janthinus* Germar on Dalmatian toadflax (*Linaria dalmatica* (L.) Miller) in western Canada. Biological Control 24: 65–74. https://doi.org/10.1016/S1049-9644(02)00010-5

Dickason EA (1968) Observations on the biology of *Gymnaetron pascuorum* (Gyll.) (Coleoptera: Curculionidae). The Coleopterists' Bulletin 22: 11–15.

Doğanlar M, Üremiş İ (2014) *Verbascum gaillardotii* Boiss. and its natural enemy complex in Hatay province, Turkey. Munis Entomology & Zoology 9: 783–791.

Dowel AB, Shipunov A (2017) (2497) Proposal to reject the name *Plantago indica* (Plantaginaceae). Taxon 66(1): 205–206. https://doi.org/10.12705/661.25

Emden FI van (1938) On the taxonomy of Rhynchophora larvae (Coleoptera). Transactions of the Royal Entomological Society of London 87: 1–37. https://doi.org/10.1111/j.1365-2311.1938.tb01800.x

Emerson BC, Oromi P, Hewitt GM (2000) Interpreting colonization of the *Calathus* (Coleoptera: Carabidae) on the Canary Islands and Madeira through the application of the parametric bootstrap. Evolution 54: 2081–2090. https://doi.org/10.1111/j.0014-3820.2000.tb01251.x

Gosik R (2010) Morphology of the mature larva and pupa of *Rhinusa bipustulata* (Rossi, 1792) (Coleoptera: Curculionidae) with some remarks on its biology. Baltic Journal of Coleopterology 10(2): 185–194.

Gosik R, Skuhrovec J (2011) Descriptions of mature larvae and pupae of the genus *Larinus* (Coleoptera: Curculionidae, Lixinae). Zootaxa 3019: 1–25. https://doi.org/10.11646/zootaxa.3019.1.1

Gosik R, Sprick P, Skuhrovec J, Derus M, Hommes M (2016) Morphology and identification of the mature larvae of several species of the genus *Otiorhynchus* (Coleoptera, Curculionidae, Entiminae) from Central Europe with an update of life history traits. Zootaxa 4108: 1–67. https://doi.org/10.11646/zootaxa.4108.1.1

Gosik R, Skuhrovec J, Toševski I, Caldara R (2017) Morphological evidence from immature stages further suggests Lignyodina being close to Tychiina (Coleoptera, Curculionidae, Curculioninae, Tychiini). Zootaxa 4320(3): 426–446. https://doi.org/10.11646/zootaxa.4320.3.2

Hoffmann A (1958) Faune de France 62 Coléoptères Curculionides (Troisième partie). Le Chevalier, Paris, 1209–1839.

Jiang C, Zhang R (2015) The genus *Gymnetron* from China with description of pre-imaginal stages of*G. miyoshii*, *G. auliense* and *G. vittipenne* (Coleoptera,Curculionidae). ZooKeys 534: 61–84. https://doi.org/10.3897/zookeys.534.5967

Marvaldi AE (1997) Higher level phylogeny of Curculionidae (Coleoptera: Curculionoidea) based mainly on larval characters, with special reference to broad-nosed weevils. Cladistics 13: 285–312. https://doi.org/10.1111/j.1096-0031.1997.tb00321.x

Marvaldi AE (1998) Larvae of South American Rhytirrhininae (Coleoptera: Curculionidae). The Coleopterists Bulletin 52(1): 71–89.

Marvaldi AE (1999) Morfología larval en Curculionidae (Insecta: Coleoptera). Acta Zoologica Lilloana 45: 7–24.

May BM (1977) Immature stages of Curculionidae: larvae of soil dwelling weevils of New Zealand. Journal of the Royal Society of New Zealand 72: 189–228. https://doi.org/10.1080/03036758.1977.10427160

May BM (1993) Fauna of New Zealand, 28. Larvae of Curculionoidea (Insecta: Coleoptera): a Systematic Overview. Manaaki Whenua Press, Lincoln, New Zealand, 226 pp.

May BM (1994) An introduction to the immature stages of Australian Curculionoidea. In: Zimmerman EC (Ed.) Australian Weevils (Coleoptera: Curculionidae) (Vol. 2). Brentidae, Eurhynchidae, Apionidae and a chapter on immature stages. CSIRO, Canberra, 365–755.

McClay AS, De Clerck-Floate RA (2002) *Linaria vulgaris* Miller. yellow toadflax (Scrophulariaceae). In: Mason PG, Huber JT (Eds) Biological Control Programmes in Canada 1981–2000. CAB International, Wallingford, 375–382. https://doi.org/10.1079/9780851995274.0375

Nieminen M, Vikberg V (2015) The insect community of *Plantago lanceolata* spikes in the Åland Islands, SW Finland. Entomologica Fennica 26: 30–52. https://doi.org/10.33338/ef.50914

O'Brien CW, Wibmer GJ (1982) Annotated checklist of the weevils (Curculionidae sensu lato) of North America, Central America, and the West Indies (Coleoptera: Curculionoidea). Memoirs of the American Entomological Institute 34: 1–382.

Olmstead RG, Depamphilis CW, Wolfe AD, Young ND, Elisons WJ, Reeves PA (2001) Disintegration of the Scrophulariaceae. American Journal of Botany 88(2): 348–361. https://doi.org/10.2307/2657024

Prena J, Caldara R (2017) First records of *Mecinus comosus* Boheman, 1845 (Coleoptera, Curculionidae, Curculioninae, Mecinini) from France. Arquivos Entomolóxicos 18: 173–174.

Scherf H (1964) Die Entwicklungsstadien der mitteleuropaischen Curculioniden (Morphologie, Bionomie, Ökologie). Abhandlungen der Senckenbergischen Naturforschenden Gesellschaft 506, 335 pp.

Ścibior R, Łętowski J (2018) The morphology of the preimaginal stages of *Rhinusa neta* (Germar, 1821) and notes on its biology (Coleoptera, Curculionidae, Mecinini). ZooKeys 807: 29–46. https://doi.org/10.3897/zookeys.807.28365

Sing SE, Peterson RKD, Weaver DK, Hansen RW, Markin GP (2005) A retrospective analysis of known and potential risks associated with exotic toadflax-feeding insects. Biological Control 35: 276–287. https://doi.org/10.1016/j.biocontrol.2005.08.004

Skuhrovec J, Bogusch P (2016) The morphology of the immature stages of *Metadonus vuillefroyanus* (Capiomont, 1868) (Coleoptera, Curculionidae, Hyperini) and notes on its biology. ZooKeys 589: 123–142. https://doi.org/10.3897/zookeys.589.7847

Skuhrovec J, Gosik R, Caldara R (2014) Immatures of Palaearctic species of the weevil genus *Tychius* (Coleoptera, Curculionidae): new descriptions and new bionomic data with an

evaluation of their value in a phylogenetic reconstruction of the genus. Zootaxa 3839(1): 1–83. https://doi.org/10.11646/zootaxa.3839.1.1

Skuhrovec J, Gosik R, Caldara R, Košťál M (2015) Immatures of Palaearctic species of the weevil genus *Sibinia* (Coleoptera, Curculionidae): new descriptions and new bionomic data with suggestions on their potential value in a phylogenetic reconstruction of the genus. Zootaxa 3955(2): 151–187. https://doi.org/10.11646/zootaxa.3955.2.1

Skuhrovec J, Gosik R, Caldara R, Toševski I, Łętowski J, Szwaj E (2018) Morphological characters of immature stages of Palaearctic species of *Cleopomiarus* and *Miarus* and their systematic value in Mecinini (Coleoptera, Curculionidae, Curculioninae). ZooKeys 808: 23–92. https://doi.org/10.3897/zookeys.808.28172

Sprick P (2001) Bericht über eine einwöchige Rüsselkäferexkursion (Col., Curculionoidea) nach Malta mit Bemerkungen zu Käfergemeinschaften und zur Ökologie einiger Wirtspflanzen. Beiträge zur Ökologie phytophager Käfer VI. Weevil News 5: 1–10.

Stejskal R, Trnka F, Skuhrovec J (2014) Biology and morphology of immature stages of *Coniocleonus nigrosuturatus* (Coleoptera: Curculionidae: Lixinae). Acta Entomologica Musei Nationalis Pragae 54: 337–354.

Szwaj E, Łętowski J, Pawlęga K (2018) The morphology of the preimaginal stages of *Cleopomiarus micros* (Germar, 1821) (Curculionidae, Coleoptera) and notes on its biology. ZooKeys 798: 45–62. https://doi.org/10.3897/zookeys.798.27173

Tamura K, Peterson D, Peterson N, Stecher G, Nei M, Kumar S (2011) MEGA5: Molecular evolutionary genetics analysis using maximum likelihood, evolutionary distance and maximum parsimony methods. Molecular Biology and Evolution 28: 2731–2739. https://doi.org/10.1093/molbev/msr121

Toševski I, Caldara R, Jović J, Hernández-Vera G, Baviera C, Gassmann A, Emerson BC (2011) Morphological, molecular and biological evidence reveal two cryptic species in *Mecinus janthinus* Germar (Coleoptera, Curculionidae), a successful biological control agent of Dalmatian toadflax, *Linaria dalmatica* (Lamiales, Plantaginaceae). Systematic Entomology 36: 741–753. https://doi.org/10.1111/j.1365-3113.2011.00593.x

Toševski I, Caldara R, Jović J, Baviera C, Hernández-Vera, G, Gassmann A, Emerson BC (2014) Revision of *Mecinus heydenii* species complex (Curculionidae): integrative taxonomy reveals multiple species exhibiting host specialization. Zoologica Scripta 43: 34–51. https://doi.org/10.1111/zsc.12037

Toševski I, Sing SE, De Clerck-Floate R, McClay A, Weaver DK, Schwarzländer M, Krstić O, Jović J, Gassmann A (2018) Twenty-five years after: post-introduction association of *Mecinus janthinus* with invasive host toadflaxes *Linaria vulgaris* and *Linaria dalmatica* in North America. Annals of Applied Biology 173: 16–34. https://doi.org/10.1111/aab.12430

Trnka F, Stejskal R, Skuhrovec J (2015) Biology and morphology of immature stages of *Adosomus roridus* (Coleoptera: Curculionidae: Lixinae). Zootaxa 4021(3): 433–446. https://doi.org/10.11646/zootaxa.4021.3.3

Vujnovic K, Wein RW (1997) The biology of Canadian weeds. *Linaria dalmatica* (L.) Mill. Canadian Journal of Plant Science 77: 483–491. https://doi.org/10.4141/P96-132

Wilson LM, Sing SE, Piper GL, Hansen RW, De Clerck-Floate R, MacKinnon DK (2005) In: Randall CB (Ed.) Biology and Biological Control of Dalamatian and Yellow Toadflax. Morgantown, WV: USDA Forest Service. FHTET-05-13. 2005,116 pp.